



الجمهورية الجزائرية الديمقراطية الشعبية
République algérienne démocratique et populaire
وزارة التعليم العالي والبحث العلمي

Ministère de l'enseignement supérieur et de la recherche scientifique

جامعة العربي التبسي - تبسة

Université Larbi Tebessi – Tébessa

معهد المناجم

Institut des mines

قسم المناجم والجيوتكنولوجيا

Département des mines et de la géotechnologie



MEMOIRE

Présenté en vue de l'obtention d'un diplôme de Master académique

Filière : Génie minier

Option : Géotechnique

A CASE STUDY ON LANDSLIDES MODELING, CAUSALITY AND EFFECTS

Présenté et soutenu par

MEZHOUDI Aissam

Devant le jury:

	Grade	Etablissement
Président : DJELLALI Adel	MCA	Université Larbi Tebessi - Tébessa
Encadreur : BERRAH Yacine	MCB	Université Larbi Tebessi - Tébessa
Examineurs : MEBROUK Faouzi	MAA	Université Larbi Tebessi - Tébessa

Promotion 2020-2021



الجمهورية الجزائرية الديمقراطية الشعبية
République algérienne démocratique et populaire
وزارة التعليم العالي والبحث العلمي

Ministère de l'enseignement supérieur et de la recherche scientifique

جامعة العربي التبسي - تبسة

Université Larbi Tebessi - Tébessa

معهد المناجم

Institut des mines

قسم المناجم والجيوتكنولوجيا

Département des mines et de la géotechnologie



MEMOIRE

Présenté en vue de l'obtention d'un diplôme de Master académique

Filière : Génie minier

Option : Géotechnique

A CASE STUDY ON LANDSLIDES MODELING, CAUSALITY AND EFFECTS

Présenté et soutenu par

MEZHOUDI Aissam

Devant le jury:

	Grade	Etablissement
Président : DJELLALI Adel	MCA	Université Larbi Tebessi - Tébessa
Encadreur : BERRAH Yacine	MCB	Université Larbi Tebessi - Tébessa
Examineurs : MEBROUK Faouzi	MAA	Université Larbi Tebessi - Tébessa



Année universitaire : 2020-2021

Tébessa le : 06/06/2021

Lettre de soutenabilité

Noms et prénoms des étudiants :

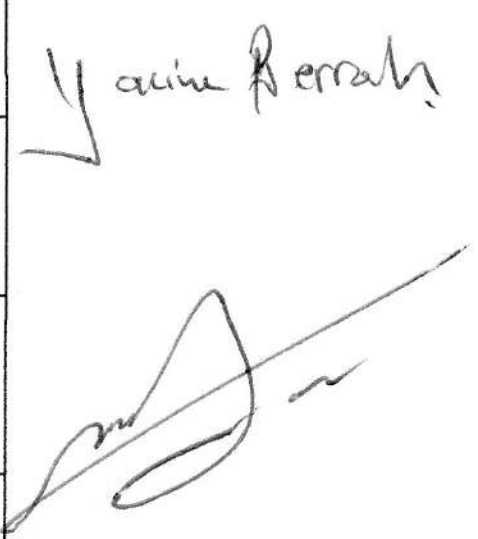
1 MEZHOUDI Aissam

Niveau : 2^{ème} année Master Option : Géotechnique

Thème :

A case study on landslides modeling, causality and effects

Nom et prénom de l'encadreur : BERRAH Yacine

Chapitres réalisés	Signature de l'encadreur
CHAPTER I: Literature Review on Landslides.	
CHAPTER II: Presentation and investigation of the study area.	
CHAPTER III: Calculations methods of slopes safety factor.	
CHAPTER IV: Slopes Safety factor investigations using statistical analysis and Design of experiments (DOE) methodology.	

مؤسسة التعليم العالي : جامعة العربي التبسي - تبسة

تصريح شرفي

خاص بالالتزام بقواعد النزاهة العلمية لانجاز بحث

أنا الممضي أدناه،

السيد (ة) مزهودي عصام

الصفة : طالب، أستاذ باحث، باحث دائم : طالب

و الصادرة بتاريخ 2016.11.30

الحامل لبطاقة التعريف الوطنية رقم : 102141373

قسم المناجم والجيوتكنولوجيا

المسجل بمعهد المناجم

و المكلف بانجاز أعمال بحث (مذكرة التخرج، مذكرة ماستر، مذكرة ماجستير، أطروحة دكتوراه)، عنوانها :

A CASE STUDY ON LANDSLIDES MODELING, CAUSALITY AND EFFECTS

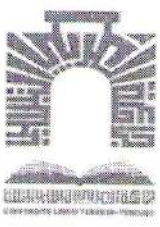
أصرح بشرفي أنني ألتزم بمراعاة المعايير العلمية و المنهجية و معايير الأخلاقيات المهنية و النزاهة إلى
المطلوبة في انجاز البحث المذكور أعلاه.

التاريخ: 2021.06.07

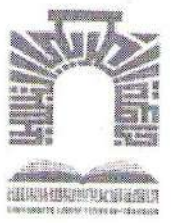
إمضاء المعني (ة)



رئيس المجلس الشعبي البلدي
و بتلويض منه رئيس مكتب الحلة المنبئية
السيد : عيسى أحسن



الجمهورية الجزائرية الديمقراطية الشعبية
وزارة التعليم العالي والبحث العلمي
جامعة العربي التبسي - تبسة



مقرر رقم: 117 مؤرخ في: 2021/05/20

يتضمن الترخيص بمناقشة مذكرة الماستر

إن مدير جامعة العربي التبسي بتبسة،

- بموجب القرار الوزاري رقم 318 و المؤرخ في 05 ماي 2021 المتضمن تعيين السيد "قواسمية عبد الكريم" مديرا لجامعة العربي التبسي - تبسة،

- وبمقتضى المرسوم التنفيذي رقم : 12-363 مؤرخ في 8 أكتوبر 2012، يعدل ويتمم المرسوم التنفيذي رقم 09 - 08 المؤرخ في: 04 جانفي 2009 والمتضمن إنشاء جامعة العربي التبسي بتبسة،

- وبمقتضى المرسوم التنفيذي رقم 08-265 المؤرخ في 17 شعبان عام 1429 الموافق 19 غشت سنة 2008 الذي يحدّد نظام الدراسات للحصول على شهادة الليسانس وشهادة الماستر وشهادة الدكتوراه، لاسيما المادة 9 منه،

- وبموجب القرار رقم 362 المؤرخ في 09 جوان 2014 الذي يحدّد كفاءات إعداد ومناقشة مذكرة الماستر، لاسيما المادة 7 منه،

- وبموجب القرار رقم 357 المؤرخ في 15 جوان 2020، المعدل للملحق القرار رقم 1080 المؤرخ في 13 أكتوبر 2015 والمتضمن تأهيل ماستر الفروع ذات التسجيل الوطني بعنوان السنة الجامعية 2015-2016 بجامعة تبسة، اختصاص جيوتقني.

وبموجب المقرر رقم 067 المؤرخ في 2021/05/19 والمتضمن تعيين لجنة مناقشة مذكرة الماستر،

وبعد الاطلاع على تقرير لجنة مناقشة مذكرة الماستر المؤرخ في

يقرر ما يأتي:

المادة الأولى: يُرخصُ للطالب (ة) عصام مزهودي ، المولود (ة) بتاريخ 1997/03/16 بئر العاتر، بمناقشة مذكرة الماستر والموسومة بـ

A case study on landslides modeling, causality and effects

المادة 2: يكلف رئيس قسم المناجم والجيوتكنولوجيا بتنفيذ هذا المقرر الذي يسلم نسخة عنه إلى الطالب المعني بالمناقشة وأعضاء لجنة المناقشة فور توقيعه، وبضمن نشره عبر فضاءات المؤسسة المادية والرقمية.

المادة 3: تُحفظ نسخة عن هذا المقرر ضمن الملفّ البيداغوجي للطالب المعني وينشر في النشرة الرسمية لجامعة العربي التبسي.

حُرر ب تبسة، في: 2021/05/20





مقرر رقم 067 مؤرخ في: 2021/05/19

يتضمن تعيين لجنة مناقشة مذكرة الماستر

إن مدير جامعة العربي التبسي بتبسة.

- بموجب القرار الوزاري رقم 318 المؤرخ في 05 ماي 2021 المتضمن تعيين السيد "قواسمية عبد الكريم" مديرا لجامعة العربي التبسي - تبسة.

- وبمقتضى المرسوم التنفيذي رقم: 12-363 مؤرخ في 8 أكتوبر 2012، يعاد ويتم المرسوم التنفيذي رقم 09-08 المؤرخ في: 04 جانفي 2009 والمتضمن إنشاء جامعة العربي التبسي بتبسة.

- وبمقتضى المرسوم التنفيذي رقم 08-265 المؤرخ في 17 شعبان عام 1429 الموافق 19 غشت سنة 2008 الذي يحدد نظام الدراسات للحصول على شهادة الليسانس وشهادة الماستر وشهادة الدكتوراه، لاسيما المادة 9 منه.

- وبموجب القرار رقم 362 المؤرخ في 09 جوان 2014 الذي يحدد كفاءات إعداد ومناقشة مذكرة الماستر، لاسيما المادتان 10 و11 منه.

- وبموجب القرار رقم 357 المؤرخ في 15 جوان 2020، المعدل لمحق القرار رقم 1080 المؤرخ في 13 أكتوبر 2015 والمتضمن تأهيل ماستر الفروع ذات التسجيل الوطني بعنوان السنة الجامعية 2015-2016 بجامعة تبسة، اختصاص جيوتقني.

- وبعد الاطلاع على محضر المجلس العلمي لمعهد المناجم المؤرخ في 2021/05/09.

يقرر ما يأتي:

المادة الأولى: تُعيّن بموجب هذا المقرر لجنة مناقشة مذكرة الماستر المحضرة من طرف الطالب (ة):

عصام مزهودي ، المولود (ة) بتاريخ 16/03/1997 بباتر العاتر.

والمسؤومة ب

A case study on landslides modeling, causality and effects

والمسجل بمعهد المناجم

المادة 2: تتشكل اللجنة المشار إليها في المادة الأولى من الأعضاء الآتي ذكرهم:

رقم	الاسم واللقب	الرتبة	مؤسسة الانتماء	الصفة
1	ياسين براح	أستاذ محاضر-ب	جامعة العربي التبسي - تبسة	مؤطرا
2	عادل جلالي	أستاذ محاضر-أ	جامعة العربي التبسي - تبسة	رئيسا
3	فوزي مبروك	أستاذ مساعد-أ	جامعة العربي التبسي - تبسة	مناقشا

المادة 3: يكلف رئيس قسم المناجم والجيوتكنولوجيا بتنفيذ هذا المقرر الذي يُسلم نسخة عنه إلى كل من الطالب المعني والمشرف على المذكرة وأعضاء لجنة المناقشة فور توقيعهم.

المادة 4: تحفظ نسخة عن هذا المقرر في الملف البيداغوجي للطالب المعني، وينشر في النشرة الرسمية لجامعة العربي التبسي.

محرر ب تبسة، في: 2021/05/19

مدير المعهد المناجم
عبد الحميد زويبي

DEDICATION

I dedicate this modest work to

To the man of my life, my eternal example, my moral support and source of joy and happiness, the one who has always sacrificed himself to see me succeed, may God guard you, and extend your age, to you my father.

for the light of my days, the source of my efforts, the flame of my heart, my life and my happiness, and every beautiful thing in my life, the one who the words do not describe her beauty, my sweet heart, mom that I adore.

To the pure soul, (Bouzned Saleh), Who died a few days ago before he saw me as an engineer, you will always remain in my memory, may God have mercy on you and place you in his vast paradise.

To the people whose presence I loved today, to my arms, my dear brothers: Hamza, Aymen, Yahia and my sister. to my uncles and my aunts specially Aicha, Fatima and all my relatives without exception.

I dedicate this work, the great pleasure of which to the people who were always by my side and who accompanied me during my path of higher study, my kind friends, study colleagues, my brothers: Mohammed, Aymene, Chiheb, Hichem, Fares, Soufa to my sisters Amani, Amina, Anfel, Assma, Hana, Khadija, Nissa and all the rest.

And specially for Jawhara

To all those who have contributed from near or far to make this project possible, and to all those who have helped me, even with a sincere invitation.

I say thank you.

Issam.....

Acknowledgment

After giving thanks to Almighty God for giving us the health and the will to start and finish this memory.

I would like to express my gratitude to my memory supervisor Mr. BERRAH Yacine, I thank him for having supervised, guided, helped and advised me.

I extend my sincere thanks to all the teachers, speakers and all the people who by their words, their writings, their advice and their criticism have guided my reflections and agreed to meet with me and answer my questions during my research.

I would also like to thank all my teachers from the beginning the beginning until now and specially Mr. Bouaoune Laid.

I would like to express my gratitude to the friends and colleagues who have provided me with moral and intellectual support throughout my process.

Finally, I also deeply thank all the people who have helped and supported us from near or far.

Summary

	Dedication	
	Acknowledgment	
	Summary	III
	Abstract	VII
	Notation	X
	List of Figures	XII
	List of tables	XVI
	General Introduction	2
Chapter I : Literature Review on Landslides.		
I.1.	Introduction	5
I.2.	Field movements	5
I.2.1.	Field Movement Definition	5
I.2.2.	Types of Field Movement	5
I.2.3.	Slow and continuous movements	6
I.2.4.	Rapid and discontinuous movements	9
I.3.	Landslide	11
I.3.1.	Types of landslides:	12
I.3.2.	The landslide process	16
I.3.3.	Classification of the landslide	16
I.3.4.	Surface slippage	17
I.4.	Hazard, Vulnerability and Risk	18
I.4.1.	Hazard	18
I.4.2.	Spatial Probability	18
I.4.3.	Temporal Probability	19
I.4.4.	Magnitude	19
I.4.5.	Vulnerability	20
I.4.6.	Risk	21
I.4.7.	Factors involved in land instability processes	22
I.4.7.1.	Action and influence of water	22
I.4.7.2.	Action of gravity	22
I.4.7.3.	The nature of the land	23
I.4.7.4.	External mechanical actions	23
I.4.7.5.	Removal of Slope Foot Stop	23
I.4.7.6.	Seismic actions	23
I.4.7.7.	Deforestation Action	24
I.4.7.8.	Anthropogenic actions	24
I.4.7.9.	Impact on People and Property (Issues)	24
I.4.8.	Examples of field movement across the world	25
I.4.8.1.	Muddy flows in Rio de Janeiro	25
I.4.8.2.	Falling Blocks	25
I.4.8.3.	Underground cavity	26
I.4.8.4.	Differential settlement	26
I.5.	Instrumentation of a landslide	27
I.5.1.	Data processing	30
I.5.2.	Main comform techniques	31
I.5.3.	Drainage devices	31

Summary

I.5.4.	Construction of reinforcements	32
I.6.	Earth Moving Systems	33
I.6.1.	Foot fill	33
I.6.2.	Lightening in the head	33
I.7.	Conclusion	34
Chapter II Presentation and investigation of the study area.		
II.1.	Introduction	36
II.2.	Geographical situation of the study area	36
II.3.	Morphology	37
II.4.	Geographical Framework	40
II.5.	Geological framework	41
II.6.	Hydrogeological framework	42
II.6.1.	The marine Miocene aquifer	42
II.6.2.	The Maastrichtian-Campanian karst aquifer	42
II.6.3.	The Turonian and Aptian aquifers	43
II.7.	Climate	43
II.8.	Seismicity of the region	44
II.8.1.	Regional seismic tectonic condition	44
II.8.2.	Classification of seismic zones in Algeria	44
II.9.	General geological overview	45
II.9.1.	The internal domain	47
II.9.2.	The flyschs domain	47
II.9.3.	The External Domain (Tablecloth Domain)	47
II.9.3.1.	Ultra tellian units S.S. (sensu-stricto)	48
II.9.3.2.	The tellian set	48
II.9.3.3.	Southern units (with nummulite limestone)	48
II.9.4.	Allochthonous or Para-Aboriginal countries	48
II.9.4.1.	The Constantinoises Neritic Series	48
II.9.4.2.	The scaly furrow of Sellaoua	48
II.9.5.	Post-Priabonian Stratigraphic Ensemble (Vila, 1980)	49
II.9.6.	The "post-water" basins	49
II.9.7.	The neo-gen magmatism	49
II.10.	Structural synthesis of the Maghrebid chain	50
II.10.1.	The finite luteceine or atlasic phase (Priabonienne)	50
II.10.2.	Miocene phases	50
II.10.2.1.	The burdigalienne phase	50
II.10.2.2.	The tortonian phase	50
II.11.	Conclusion	51
Chapter III Calculations methods of slopes safety factor		
III.1.	Introduction	53
III.	Slope stability calculation methods	53
III.2.1.	Safety Factor Calculation	53
III.2.2.	The safety factor vis-a-vis fracture	54
III.3.	Methods of fracture calculation	55
III.3.1.	Limit Equilibrium Methods	55
III.3.1.1.	Slice Method	56
III.3.1.2.	Fellenius Method (1936)	57
III.3.1.2.1.	The forces acting on a slice according to the hypothesis of	58

Summary

	Fellenius	
III.3.1.3.	Simplified BISHOP method (1954)	60
III.3.1.4.	Janbu Method (1956)	60
III.3.1.5.	Morgenstern and Price Method (1965)	62
III.3.1.6.	Reverse Analysis Method (Return to Experience)	63
III.3.2.	Finite element method:	64
III.3.2.1.	Principle of the finite element method:	65
III.3.2.2.	Current status of the finite element method:	66
III.3.2.2.1.	The practice of the finite element method:	66
III.3.2.2.2.	Difficulties in the practice of the finite element method:	67
III.3.2.2.3.	Teaching the practice of the finite element method:	67
III.3.3.	Area of use of the finite element method:	68
III.3.3.1.	Presentation of Finite element method in field	68
III.3.3.2.	Areas of use of the finite element method:	69
III.3.3.3.	Examples of applications:	69
III.3.3.3.1.	In geotechnical engineering:	69
III.4.	Conclusion:	71
Chapter IV Slopes Safety factor investigations using statistical analysis and Design of experiments (DOE) methodology		
IV.1.	Introduction	73
IV.2.	Slope stability analysis using Geostudio (geo-slope software)	73
IV.2.1.	Presentation of the geo-slope software	73
IV.2.2.	How the software works	75
IV.2.3.	Applications	76
IV.3.	Heterogeneous slope	76
IV.3.1.	For α constant	76
IV.3.2.	For α variable	82
IV.4.	Conclusion	88
IV.5.	Presentation of the statistical analysis principal component analysis (PCA) and linear regression (LR)	89
IV.5.1.	<u>Principal component analysis (PCA)</u>	90
IV.5.2.	Summary statistics on the collected samples	90
IV.5.3.	Correlation matrix	92
IV.5.4.	Eigenvalues and eigenvectors	94
IV.5.5.	Factor loadings	98
IV.5.6.	Correlations between variables and factors and the (PCA) circle	100
IV.5.7.	Contributions of variables to (PC)	104
IV.5.8.	Squared cosines of the variables	106
IV.6.	Multiple linear regression	108
IV.6.1.	Types of linear regression	109
IV.6.2.	Least-squares regression	110
IV.6.3.	Goodness of fit statistics	110
IV.6.4.	Analysis of variance (ANOVA)	112
IV.6.4.1.	Degrees of freedom (Df)	113
IV.6.4.2.	Sum of squares (SS)	114
IV.6.4.3.	Significance f (pr > f)	114
IV.6.5.	Model parameters:	115
IV.6.5.1.	P-value	117
IV.6.5.2.	Equation of the model	117
IV.6.6.	Standardized coefficients (or beta coefficients)	118

Summary

IV.6.7.	Predicted values and residuals	122
IV.7.	Conclusion	129
IV.8.	Presentation of design of experiments methodology (DOE)	130
IV.8.1.	Material and methods	132
IV.8.2.	Response surface methodology (RSM)	133
IV.8.3.	Experimental design	133
IV.8.3.	Statistical analysis	134
IV.8.4.	Results and discussion	135
IV.8.4.1.	Fitting the model	135
IV.8.4.2.	ANOVA for quadratic model	136
IV.8.4.3.	Fit statistics	136
IV.8.4.4.	Effect of independent variables on response variables	137
IV.8.4.5.	Diagnostics plots	137
IV.8.4.5.1.	Normal probability	137
IV.8.4.5.2.	Residuals vs. Predicted	139
IV.8.4.5.3.	Residuals vs. Run	140
IV.8.4.5.4.	Predicted vs. Actual	142
IV.8.4.5.5.	Box-cox plot for power transforms	143
IV.8.4.5.6.	Residuals vs. Factor	145
IV.8.5.	Modeling	146
IV.8.6.	Optimization data analysis	149
IV.9.	Conclusion	153
	General Conclusion	155
	Bibliography References	158

Abstract

In the present study, numerical modeling has been performed to investigate landslides hazard in two sectors of Souk-Ahras region using equilibrium limit by GEOSLOPE software; the results of the safety factors (Fs) varied from 0.8 to 1.7 in different conditions, it indicate clear unstable slopes. A geotechnical data was collected and analyzed using statistical methods such as principal component analysis PCA that absorbs (53,95% up to 57,10%) of the variability and family groups that affect landslides movement are classified, and geometrical slope parameters. The main factors were used to generate statistical models to predict the slope safety factor (Fs), besides in design of experiments (DOE) method response surfaces methodology (RSM) used to study and treat the solution by modeling and optimization of parameters that affect landslide phenomenon. it allows to develop models of Fs which presents the response as function with dependent or independent parameters as inputs. The obtained results show high correlations with a regression coefficient R^2 of 0.88 and 0.93 and the optimization allows to categorize the parameters with high affection of slope stability in the studied area.

Keywords: Landslides, numerical modeling, safety factor, statistical analysis, design of experiments DOE.

الملخص

في هذه الدراسة ، تم إجراء محاكاة رقمية لدراسة مخاطر الانزلاقات الأرضية في قطاعين من منطقة سوق أهراس باستخدام اتزان الميول بواسطة برنامج GEOSLOPE ؛ تباينت نتائج عوامل الأمان (Fs) من 0.8 إلى 1.7 في ظروف مختلفة ، حيث تشير إلى منحدرات واضحة غير مستقرة ؛ تم جمع البيانات الجيوتقنية وتحليلها باستخدام طرق إحصائية مثل تحليل المكون الرئيسي PCA الذي يمتص (53،95٪ حتى 57،10٪) من التباين، ومن ذلك تم الحصول على مجموعة العائلات المعيارية الجيوتقنية التي تؤثر في حركة الانزلاقات الأرضية.

تم استخدام المعايير الرئيسية لإنشاء نماذج إحصائية للتنبؤ بعامل أمان المنحدر (Fs) ، إلى جانب تطبيق طريقة تصميم التجارب (DOE) ومنهجية أسطح الاستجابة (RSM) المستخدمة لدراسة الحلول ومعالجتها عن طريق نمذجة وتحسين المعايير التي تؤثر على ظاهرة الانزلاق الأرضي. كما يسمح بتطوير نماذج الحلول (Fs) التي تمثل الاستجابة كمحصلة، مع أخذ المعايير المستقلة وغير المستقلة كعناصر مدخلة. أظهرت النتائج المتحصل عليها ارتباطات عالية بمعامل ارتباط R^2 يقدر ب (0.88 و 0.93) ويسمح التحسين بتصنيف المعايير ذات التأثير العالي لاستقرار المنحدر في المنطقة المدروسة.

الكلمات المفتاحية: الانهيارات الأرضية ، النمذجة العددية ، عامل الأمان ، التحليل الإحصائي ، تصميم التجارب (DOE).

Résumé

Dans la présente étude, une modélisation numérique a été réalisée pour étudier le risque de glissements de terrain dans deux secteurs de la région de Souk-Ahras en utilisant la méthode d'équilibre limite par le logiciel GEOSLOPE ; les résultats obtenus des facteurs de sécurité (Fs) varient entre 0,8 à 1,7 dans des différentes conditions, cela indique que les talus sont clairement instables. Des données géotechniques ont été collectées et analysées à l'aide de méthodes statistiques telles que l'analyse en composantes principales PCA qui absorbe (53,95 % jusqu'à 57,10 %) de la variabilité et permet aux groupement des familles qui affectent le mouvement des glissements de terrain sont classés, et les paramètres géométrie des talus. Les principaux paramètres ont été utilisés pour générer des modèles statistiques aide à la prédiction des facteurs de sécurité (Fs), en plus dans la méthode « DOE » plans d'expérience, l'utilisation de la méthode de réponse de surface «RSM» a été utilisé pour étudier et traiter la solution par modélisation et optimisation des paramètres qui affecte les glissements de terrain. La méthodologie des surfaces de réponse de la méthode de conception d'expériences (DOE) (RSM) utilisée pour étudier et traiter la solution par la modélisation et l'optimisation des paramètres qui affectent le glissement de terrain phénomène. Il permet de développer des modèles de Fs qui présentent la réponse en fonction des paramètres d'entrés dépendants ou indépendants. Les résultats obtenus montrent des corrélations élevées avec un coefficient de régression R^2 de 0,88 et 0,93 pour les deux cas et l'optimisation permet de catégoriser les paramètres avec une forte influence sur la stabilité des pentes dans la zone étudiée.

Mots clés : Glissements de terrain, modélisation numérique, facteur de sécurité, analyse statistique, plan d'expériences DOE.

Notation

C	kPa	Soil cohesion
ϕ	$^{\circ}$	The internal friction angle
F_s	-	The safety factor
α	%	Slope angle
w_L	%	limit of liquidity
I_p	%	plasticity index
F_f	%	the fine fraction
γ_w	Km/m ³	Water unit weight
γ_d	Km/m ³	Dry unit weight
S_r	%	Degree of saturation
PCA	-	Principal Component Analysis
DOE	-	design of experiment
RSM	-	response surface methodology
CCD	-	central composite designs
ANOVA	-	Analysis of variables
FEM	-	Finite element method
LE	-	Limit Equilibrium
CAD	-	Computer Aided Design
S	Km ²	Area
P	Km	Perimeter
H_{max}	m	Maximum altitude
H_{moy}	m	Average elevation
L	Km	Length of main Talweg
L_r	Km	Length of equivalent rectangle
I_r	Km	Width of equivalent rectangle
K_c	-	Compactness index
D_d	1/km	Drainage density
I_c	m/km	Slope index
I_g	-	Overall slope index
T_c	H	Time of concentration
V_e	m/s	Flow velocity
I_{moy}	%	Average slope of the valley
K	-	Elongation coefficient
H_{min}	m	Minimum altitude
D_s	m	Specific gradient
D	-	Drill
EC	ms/cm	The salinity of the water
S		Fracture surface
W	Km/m ³	Weight
m	-	Total number of slices
b	-	The width of the slices

Notation

α	-	The oriented angle of the radius of the circle passing through the middle of the base of the edge with the vertical
W	-	Self-weight of the slice
N	-	Stabilizing normal component
T	-	Destabilizing tangential component to the sliding circle
α_n	-	The inclination of the sliding surface in the middle of section n
U	-	Pore water pressure
θ_i		The angle formed by the resultant and the horizontal
λ		A constant that must be evaluated for the calculation of the safety factor
$f(x'_i)$		The function of variation in relation to the distance along the sliding surface
x'_i		The linear normalization of the xi coordinates
τ_f		The shear strength of the slope

Figures list

Figures list:

Figure I.01	The phenomenon of subsidence	06
Figure I.02	Types of settlements	07
Figure I.03	Landslide	07
Figure I.04	Removal –Swelling	08
Figure I.05	Creep phenomenon	08
Figure I.06	Phenomenon of Solifluxion.	09
Figure I.07	Cave-in collapses	10
Figure I.08	landslides, falls of blocks and stones	10
Figure I.09	Diagram showing a mudslide	11
Figure I.10	Coastal erosion.	11
Figure I.11	Schematic view rock fall ((Highland et al, 2008) and photo of rack fall in Samigaluh Disrtict in 2011(Eko Setya N, 2011))	12
Figure I.12	Schematic view and photo of topples in Canada (Highland et al, 2008)	13
Figure I.13	The flat sliding	14
Figure I.14	Simple rotational sliding	14
Figure I.15	Successive nested slides.	15
Figure I.16	Schematic view and photo of spread in California, USA in 1989	15
Figure I.17	Schematic view and photo of creep in UK (Highland et al, 2008)	15
Figure I.18	Solifluxion, Surface slide.	17
Figure I.19	Mudslide in the Rio region killed 205 people	25
Figure I.20	A rocky "scale" Maupas. France	26
Figure I.21	Collapse of a natural cavity by dissolution of gypsum Bargement. France [1996].	26
Figure I.22	The tower of Pisa	27
Figure I.23	Wired extensometer	28
Figure I.24	Electromagnetic geophone	28
Figure I.25	Inclinometer	28
Figure I.26	Sen Slide Distributed Architecture Mapping	29
Figure I.27	InSAR imaging deformations, red areas have undergone displacements in the order of 20mm	30
Figure I.28	Finite element modeling of a slip, color gradient represents shear deformations	31
Figure I.29	Slope drainage by barbacanes	32
Figure I.30	Nailing principle and example of realization	32
Figure I.31	Retaining wall of the RD559 in the Var, collapsed under the push of the slide	33
Figure I.32	Retaining wall in Chinon	33
Figure I.33	Principle of foot toe stop	34
Figure I.34	Principle of lightening	34
Figure II.01	Geographical location of the study area	36
Figure II.02	Topographic map of the Oued Madjerda sub-basin in Souk Ahras	39
Figure II.03	The map of the hydrographic network in Souk Ahras	40

Figures list

Figure II.04	(A) Location of Algeria in the Mediterranean basin, the blue rectangle represents the Northeast. (B) The red rectangle shows the study area.	41
Figure II.05	(C) Simplified geological and structural map of the study area with location of water points used in this study. (D) Geological section.	42
Figure II.06	(A) Gas bubbles. (B) Sulfur near the main grifón of El Demssa.	43
Figure II.07	Classification of seismic zones in Algeria 2021	45
Figure II.08	Seismicity of North Algeria	45
Figure II.09	Structural diagram of the Maghrebids	46
Figure II.10	Main structural units in North Africa	46
Figure III.01	Fracture surface (CFMS. 1995)	53
Figure III.02	Potential fracture surface (Blondeau F. 1976)	55
Figure III.03	Cutting of a bank into slices and forces acting on a slice (Bendadouche H. and al. 2013)	56
Figure III.04	The forces acting on a slice (www.pentestunnels.eu/enseignement/.../ac1_calcul_stabilite_pentes.pdf)	57
Figure III.05	Forces acting on a slice according to the Fellenius hypothesis (Fellenius, W. 1936; AHMED. A, 2012).	58
Figure III.06	The forces applied for the Janbu method (JANBU 1973)	60
Figure III.07	Variation of the correction factor as a function of depth and length (Janbu 1973).	61
Figure III.08	Representation of forces on a slice using the simplified method of Morgenstern and Price.	62
Figure III.09	Diagram of the principle of inverse analysis by reverse analytical method and by direct numerical method (b) (Colas G. & Pilot G.).	63
Figure III.10	Meshing of a domain in finite elements	66
Figure III.11	(u_i, v_i, w_i) : are the nodal displacements, $i=1...n$.	66
Figure III.12	Element (Q8)	66
Figure IV.01	The menus available on SLOPE / W software.	75
Figure IV.02	Geometry of the heterogeneous slope case 01 and case 02 (Machroha01) (GEO-SLOPE, 2012).	77
Figure IV.03	Failure area and value of F_s (case 01)	78
Figure IV.04	Slip surface and safety map (case 01)	78
Figure IV.05	Failure area and value of F_s (case 02)	79
Figure IV.06	Slip surface and safety map (case 02)	79
Figure IV.07	Geometry of the heterogeneous slope case 03 and case 04 (Zaaroria01) (GEO-SLOPE, 2012).	80
Figure IV.08	Failure area and value of F_s (case 03)	80
Figure IV.09	Slip surface and safety map (case 03)	81
Figure IV.10	Failure area and value of F_s (case 04)	81
Figure IV.11	Slip surface and safety map (case 04)	81

Figures list

Figure IV.12	Geometry of the heterogeneous slope case 05 (Machroha02) (GEO-SLOPE, 2012).	82
Figure IV.13	Geometry of the heterogeneous slope case 06 (Machroha02) (GEO-SLOPE, 2012).	82
Figure IV.14	Failure area and value of F_s (case 05)	83
Figure IV.15	Slip surface and safety map (case 05)	84
Figure IV.16	Failure area and value of F_s (case 06)	84
Figure IV.17	Slip surface and safety map (case 06)	85
Figure IV.18	Geometry of the heterogeneous slope case 07 (Zaaroria02) (GEO-SLOPE, 2012).	85
Figure IV.19	Geometry of the heterogeneous slope case 08 (Zaaroria02) (GEO-SLOPE, 2012).	86
Figure IV.20	Failure area and value of F_s (case 07)	87
Figure IV.21	Slip surface and safety map (case 07)	87
Figure IV.22	Failure area and value of F_s (case 08)	87
Figure IV.23	Slip surface and safety map (case 08)	88
Figure IV.24	PCA correlation circle (Machroha1)	101
Figure IV.25	PCA correlation circle (Machroha2)	102
Figure IV.26	PCA correlation circle (Zaaroria1)	102
Figure IV.27	PCA correlation circle (Zaaroria2)	103
Figure IV.28	F_s (Machroha1)/Standardized coefficients (95% conf. interval) plot	120
Figure IV.29	F_s (Machroha2)/Standardized coefficients (95% conf. interval) plot	121
Figure IV.30	F_s (Zaaroria1)/Standardized coefficients (95% conf. interval) plot	121
Figure IV.31	F_s (Zaaroria2)/Standardized coefficients (95% conf. interval) plot	122
Figure IV.32	F_s (Machroha1)/Standardized residuals plot	123
Figure IV.33	F_s (Machroha2)/Standardized residuals plot	123
Figure IV.34	F_s (Zaaroria1)/Standardized residuals plot	124
Figure IV.35	F_s (Zaaroria2)/Standardized residuals plot	124
Figure IV.36	Pred(F_s)/ F_s plot (Machroha1)	125
Figure IV.37	Pred(F_s)/ F_s plot (Machroha2)	126
Figure IV.38	Pred(F_s)/ F_s plot (Zaaroria1)	126
Figure IV.39	Pred(F_s)/ F_s plot (Zaaroria2)	127

Figures list

Figure IV.40	Standardized residuals /Fs (Machroha1) plot	127
Figure IV.41	Standardized residuals /Fs (Machroha2) plot	128
Figure IV.42	Standardized residuals /Fs (Zaaroria1) plot	128
Figure IV.43	Standardized residuals /Fs (Zaaroria2) plot	129
Figure IV.44	Visualization of: a DOE intent	131
Figure IV.45	Normal Plot of Residuals (Machroha02)	138
Figure IV.46	Normal Plot of Residuals (Zaaroria02)	139
Figure IV.47	Residuals vs. Predicted Residuals Plot (Machroha02)	139
Figure IV.48	Residuals vs. Predicted Residuals Plot (Zaaroria02)	140
Figure IV.49	Residuals vs. Run Plot (Machroha02)	141
Figure IV.50	Residuals vs. Run Plot (Zaaroria02)	141
Figure IV.51	Predicted vs. Actual plot (Machroha02)	142
Figure IV.52	Predicted vs. Actual plot (Zaaroria02)	143
Figure IV.53	Box-Cox Plot for Power Transforms Plot (Machroha02)	144
Figure IV.54	Box-Cox Plot for Power Transforms Plot (Zaaroria02)	144
Figure IV.55	Residuals vs. Factor Plot (Machroha02)	145
Figure IV.56	Residuals vs. Factor Plot (Zaaroria02)	146
Figure IV.57	Contour and 3D plots, (a) and (b) representing the safety factor (Fs) dependence on the dry unit weight γ_d (kN/m ³) and the wet unit weight γ_h (kN/m ³), (c) and (d) representing the safety factor (Fs) dependence on degree of saturation S_r (%) and water content w (%) (machroha02)	147
Figure IV.58	Contour and 3D plots, (a) and (b) representing the safety factor (Fs) dependence on the dry unit weight γ_d (kN/m ³) and the wet unit weight γ_h (kN/m ³), (c) and (d) representing the safety factor (Fs) dependence on degree of saturation S_r (%) and water content w (%) (Zaaroria02)	148
Figure IV.59	The maximization of the response (a) for Machroha02, (b) for Zaaroria02	151
Figure IV.60:	The minimization of the response (a) for Machroha02, (b) for Zaaroria02	152

Tables list

Tables list:

Table I.01	The various causes of landslides (USGS, 2004)	16
Table I.02	Landslide classification.	17
Table II.01	Summary of morphometric and physical parameters of the oued medjerda sub-watershed	38
Table II.02	Climate data for Souk Ahras.	44
Table III.01	Slope balance based on theoretical safety factor values (Blondeau F. 1976).	54
Table III.02	Slope equilibrium based on experimental safety factor values (Blondeau F. 1976).	54
Table IV.01	Geotechnical parameters of the heterogeneous slope (Machroha01)	77
Table IV.02	Geotechnical parameters of the heterogeneous slope (Zaaroria01)	80
Table IV.03	Geotechnical parameters of the heterogeneous slope (Machroha02)	83
Table IV.04	Geotechnical parameters of the heterogeneous slope (Zaaroria02)	86
Table IV.05	Values of F_s and the slide circle radius for the heterogeneous slope	88
Table IV.06	Summary statistics of 99 analyzed data of the studied soil of Machroha01 (with fixed (α)) (Berrah, Y. et al 2016).	90
Table IV.07	Summary statistics of 99 analyzed data of the studied soil of Machroha2 (with (α) variable) (Berrah, Y et al 2016)	91
Table IV.08	Summary statistics of 99 analyzed data of the studied soil of Zaaroria 1 (with fixed (α)) (Berrah, Y et al 2016)	91
Table IV.09	Summary statistics of 99 analyzed data of the studied soil of Zaaroria 2 (with (α) variable) (Berrah, Y et al 2016)	92
Table IV.10	Correlation matrix (Pearson (n)) Machroha1	92
Table IV.11	Correlation matrix (Pearson (n)) Machroha2	93
Table IV.12	Correlation matrix (Pearson (n)) Zaaroria1	93
Table IV.13	Correlation matrix (Pearson (n)) Zaaroria1	93
Table IV.14	Eigenvalues of Machroha1	94
Table IV.15	Eigenvalues of Machroha2	95
Table IV.16	Eigenvalues of Zaaroria1	95
Table IV.17	Eigenvalues of Zaaroria2	95
Table IV.18	Eigenvectors of Machroha1	96
Table IV.19	Eigenvectors of Machroha2	97

Tables list

Table IV.20	Eigenvectors of Zaaroria1	97
Table IV.21	Eigenvectors of Zaaroria2	98
Table IV.22	Factor loadings of Machroha1	98
Table IV.23	Factor loadings of Machroha2	99
Table IV.24	Factor loadings of Zaaroria1	99
Table IV.25	Factor loadings of Zaaroria2	100
Table IV.26	Contribution of the variables (%) of Machroha1	104
Table IV.27	Contribution of the variables (%) of Machroha2	104
Table IV.28	Contribution of the variables (%) of Zaaroria1	105
Table IV.29	Contribution of the variables (%) of Zaaroria2	105
Table IV.30	Squared cosines of the variables of Machroha1	106
Table IV.31	Squared cosines of the variables of Machroha2	107
Table IV.32	Squared cosines of the variables of Zaaroria1	107
Table IV.33	Squared cosines of the variables of Zaaroria	107
Table IV.34	Goodness of fit statistics of Machroha1	111
Table IV.35	Goodness of fit statistics of Machroha2	111
Table IV.36	Goodness of fit statistics of Zaaroria1	111
Table IV.37	Goodness of fit statistics of Zaaroria2	112
Table IV.38	Analysis of variance of Machroha1	112
Table IV.39	Analysis of variance of Machroha2	113
Table IV.40	Analysis of variance of Zaaroria1	113
Table IV.41	Analysis of variance of Zaaroria2	113
Table IV.42	Model parameters of Machroha1	115
Table IV.43	Model parameters of Machroha2	115
Table IV.44	Model parameters of Zaaroria1	116
Table IV.45	Model parameters of Zaaroria2	116
Table IV.46	The equations of (Fs) for the four cases	117
Table IV.47	Standardized coefficients of Machroha1	118
Table IV.48	Standardized coefficients of Machroha2	118
Table IV.49	Standardized coefficients of Zaaroria1	119
Table IV.50	Standardized coefficients of Zaaroria2	119
Table IV.51	Independent variables and their corresponding levels (Machroha02) and (Zaaroria02)	134
Table IV.52	Experimental design for safety factor (Fs) with independent variables, experimental and predicted values of responses (Machroha02).	135
Table IV.53	Experimental design for safety factor (Fs) with independent variables, experimental and predicted values of responses (Zaaroria02).	135
Table IV.54	Regression statistics for adopted reduced quadratic model (Machroha02)	136

Tables list

Table IV.55	Regression statistics for adopted reduced quadratic model (Zaaroria02)	136
--------------------	---	-----

General Introduction

General introduction

Ground movements group different types such as landslides, mud flows, falling blocks etc., and their consequence are either human or material damages. It occurs when the resistance of the ground is lower than the driving forces generated by gravity and the position of the aquifer or by the geometric modification caused by development works, their dynamics naturally respond to the laws of mechanics.

Landslides are a serious geologic hazard common to almost in every sector Souk-Ahras region and can cause loss of life, destruction of infrastructure, damage to land and loss of natural resources, landslides are difficult to predict because of its intensity, suddenness and dynamic nature. A view of the general conditions that characterize the Souk-Ahras region reveals the importance of the road network which is generally affected by slope movements. This network is traced within heterogeneous geological formations, generally sedimentary, the oldest age of which is the Triassic to the Quaternary constituted by limestones, marls and alluvium. Souk Ahras represents a hinge zone between the Tellian Atlas in the North and the Saharan Atlas in the South with a simple fold's structures in the South and complex in the North by faults and fractures of mainly rocky terrain. This marks the influence of neotectonics on ground movements as for the Triassic materials, it is always responsible for certain complications by the phenomenon of diapirism. From a seismic point of view, the wilaya of Souk Ahras is classified in zone I, which is a zone of low seismicity. The hydroclimatological condition in Souk Ahras region allows to classify the region as semi-arid climate. Rain is not homogeneous over the entire surface of the area depending on latitude and altitude. During the hydrological year, the wettest month is January (99.82 mm) marking a hot season in May to October and a cold season in November to April. The high-water period is from December to April. All these variations in climatic conditions participate in the intense shaping of the surface of the territory of the wilaya by erosion and change in the mechanical characteristics of the affected soils: generally, soils with considerable fine-grained content (particularly clays) are wet with water in humid periods. and desiccated in dry periods, which prepared to move at the simple request leads to the ground instability.

The purpose of this final thesis project is to study the Souk-Ahras region where a majority of natural or urban land shows signs of geotechnical instability represented by superficial and deep landslides.

This dissertation is composed of four chapters classified as follows:

The first chapter presents a bibliographic research on land movements, typology and classification and general literature review on landslides.

The second chapter is the different investigations on the studied area, an overview and presentation of geographical, geological, geomorphological and hydrogeological conditions in the region of Souk-Ahras.

The third chapter presents the different methods of calculating and analyzing slope stability as well as the methodology for studying and modeling landslides and the concept of the safety coefficient.

The fourth chapter is devoted to the slopes safety factor investigations using statistical analysis and Design of experiments (DOE) methodology, where geotechnical parameters of different sectors of Mechrouha and Zaarouria are chosen as a case study to collect the data set used in this analysis, simulation and digital modeling using the Geo-studio software code to obtain the different safety states; besides these data can be used in the statistical study by the principal component analysis, multiples regression technique by the XLSTAT to obtain models that explain the slope stability by their safety factors and finally a presentation of the DOE method to analyze the data in different results presenting the parameters and the factors of triggering and evolution of ground movements affecting the stability of the grounds.

Finally, a general conclusion on the different parts of this thesis.

**Chapter I:
Literature Review
on Landslides.**

I.1. Introduction

Many parts of the world are confronted with natural phenomena that can cause disasters. These phenomena are of very varied origins: geophysics with the earthquake and volcanic eruptions, hydrometeorology with cyclones and storms, floods and avalanches or even geomorphological with ground movements. Their frequencies and intensities vary from one region to another.

The ground movements are natural phenomena of very diverse origin, resulting from the deformation of the rupture and the displacement of the ground. They cause the death of 800 to 1,000 people/year worldwide and cause considerable economic damage and damage. Many parameters, natural or anthropogenic, condition the appearance and development of field movements (geology, hydrogeology, urbanization, etc.). In 1979, the Commission on Field Movements of the International Association of Engineering Geology estimated that 14% of the human lives lost in natural disasters could be attributed to field movements.

I.2. Field movements

I.2.1. Field Movement Definition

A ground movement is a more or less brutal movement of the ground or the subsoil, under the effect of natural influence (erosion agent, gravity, earthquake, etc.) or anthropogenic (exploitation, deforestation, earthworks, etc.). This phenomenon includes various manifestations: slow or fast, depending on the initiating mechanisms, the materials considered and their structure (Cartier G., Delmas Ph. 1984).

I.2.2. Types of Field Movement

The terrain movement is difficult to predict and is a danger to human life because of its intensity, suddenness and dynamic nature.

Depending on the speed of travel, two sets can be distinguished:

Slow movements and fast movements. Only fast movements are directly dangerous for man. Their consequences are all the more serious as the displaced masses are large.

The consequences of slow movements are essentially socio-economic or of public interest (Cruden DM, Varnes DJ. 1996).

I.2.3. Slow and continuous movements

These movements cause a progressive deformation of the ground, not always perceptible by man. They include: sagging, settling, slipping, solifluxion, creeping, indenting, and mowing. They mainly affect property, through the cracking of constructions. These disorders can be so serious for the safety of the occupants and therefore the demolition of the buildings is necessary (Varnes, D.J., 1978; Turner, et al. 1996).

- **The subsidence**

Subsidence is a large-radius-of-curvature bowl-shaped topographic depression due to the slow and progressive deflection of the cover with or without open fractures. In some cases, it may be the harbinger of collapse of buildings.

This subsidence creates a differential settlement on the foundations which results in cracks more or less important and open, sometimes through, ranging from the degradation of the work to the ruin of the load-bearing walls, passing by the blocking of doors and windows (Plan de prévention du risque mouvements de terrain Chaville, 2005; Goyallon J, France, 2000).

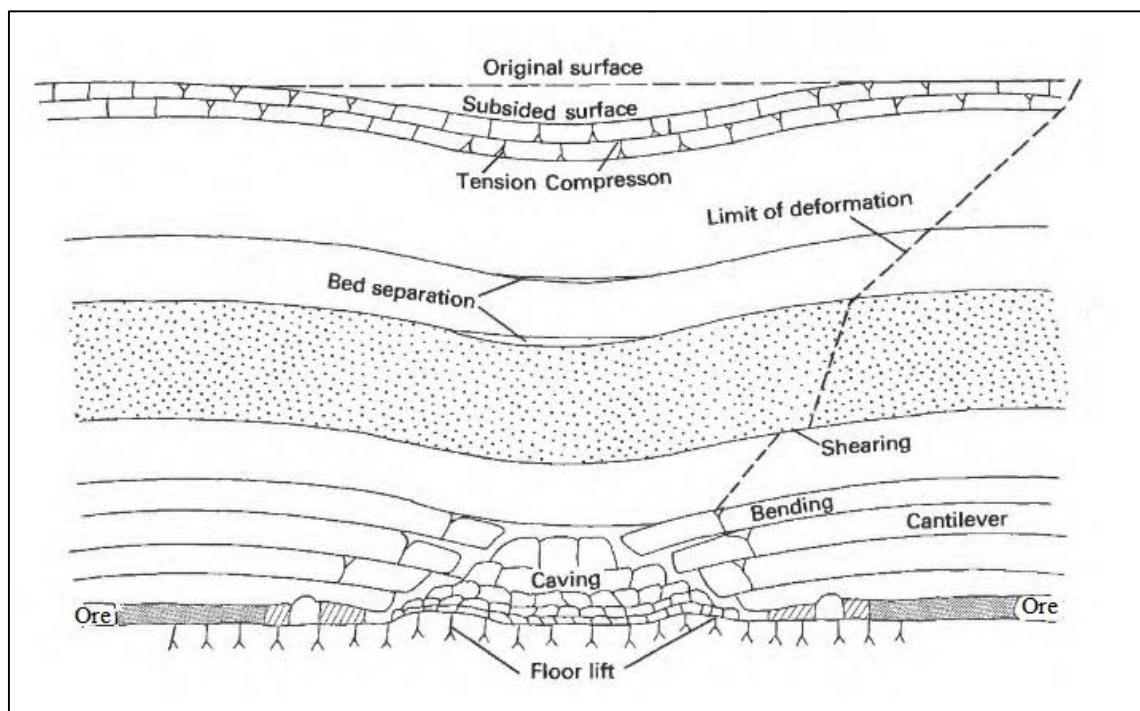


Figure I.01: The phenomenon of subsidence (www.driee.ile-de-france.developpement-durable.gouv.fr)

- **Settlement**

Settlement is a decrease in the volume of certain soils (vases, peats, clays...etc.), under the effect of applied loads and drying. This phenomenon can be of great extension and affects entire agglomerations. (Keith A., et al. 1996).

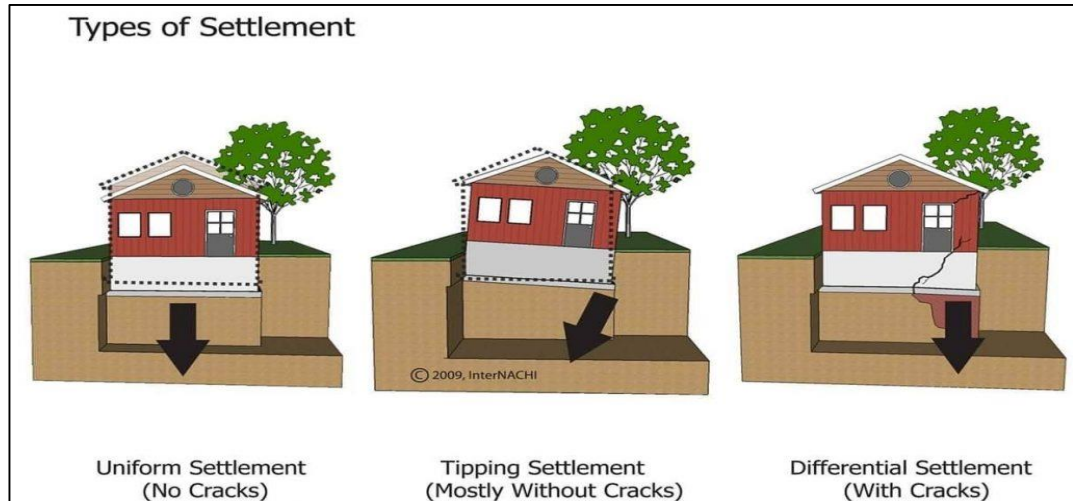


Figure I.02: Types of Settlement

- **The landslide**

This is the slow movement of a consistent ground mass along a fracture surface. This surface has a depth that varies from the order of a meter to a few tens of meters in exceptional cases. The volumes of land involved are considerable, the speeds of advance of the ground can vary up to a few decimeters per year.

*Typically occur in situations of high soil water saturation.

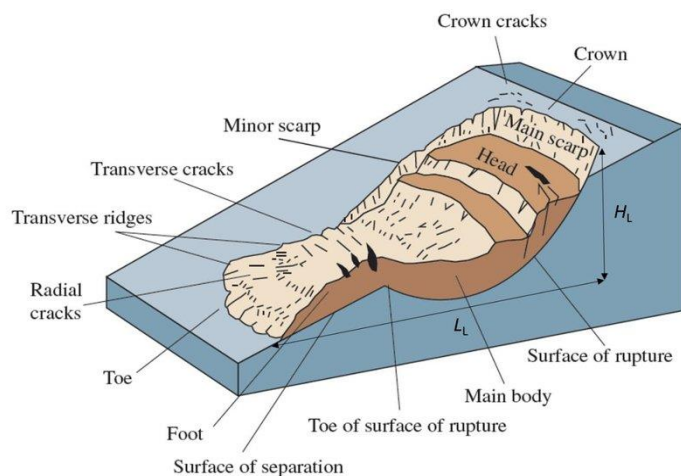


Figure I.03: Landslide

- **The removal-swelling**

Removal-swelling occurs in clay soils, it is related to variations in water in the soil. During periods of drought, the lack of water causes an irregular settlement of the surface soil (shrinkage). On the other hand, a new supply of water to these sites produces a phenomenon of swelling (Bulletin de liaison n° 16, 2005).

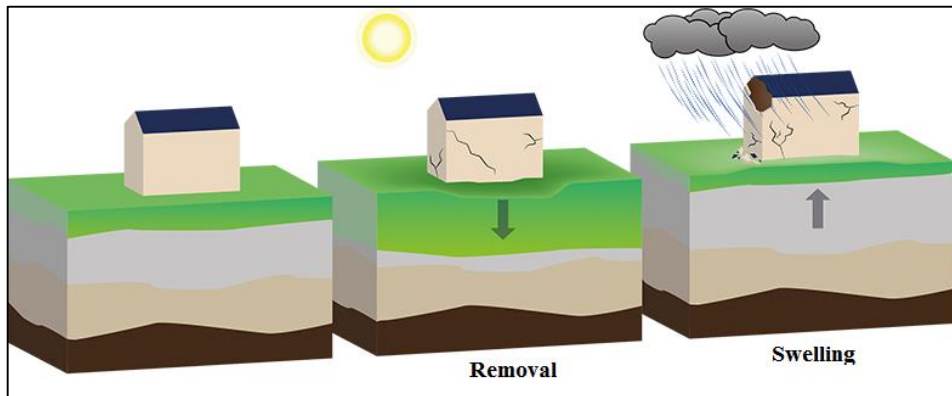


Figure I.04: Removal –Swelling

- **Creep**

Creep is characterized by slow and continuous movements, but at low speeds. In the case of creep, it is difficult to identify a fracture surface.

The movement usually occurs without modification of the applied forces (unlike the slips): in fact, the material is stressed in a state close to the rupture. This type of movement can either stabilize or evolve into a break.

The following figure shows the mechanism of the creep phenomenon

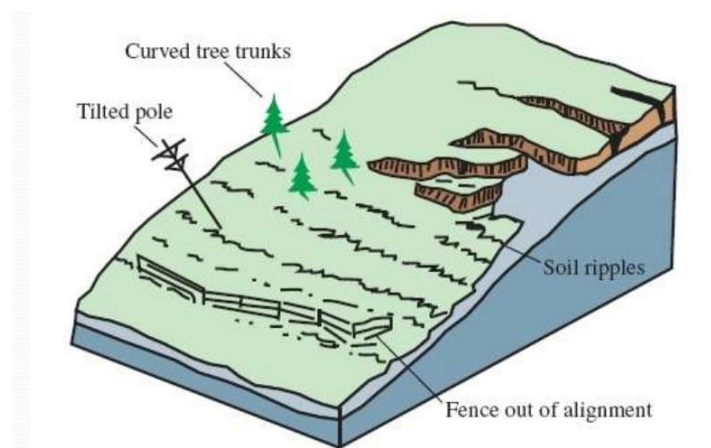


Figure I.05: Creep phenomenon

- **Solifluxion**

Solifluxion is a phenomenon of surface soil flow on very low slopes. It corresponds to a surface mass movement that is triggered when the water load exceeds the plasticity threshold of the material. The soil can then flow down the slope on a water-saturated surface.

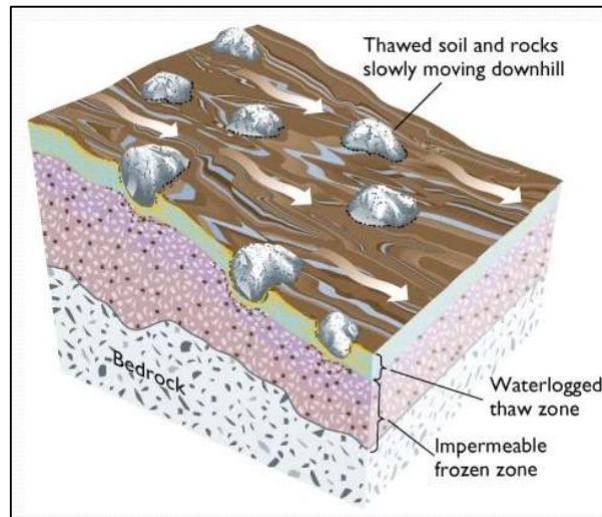


Figure I.06: Phenomenon of Solifluxion.

I.2.4. Rapid and discontinuous movements

They spread suddenly and brutally. They include collapse, rock and block falls, landslide and muddy flows.

Rapid movements mainly affect people, with often dramatic consequences. These movements have an impact on infrastructure (buildings, communication routes, etc.), ranging from degradation to total ruin (Hamasaki, E., A. Sasaki 2004).

- **Collapses of underground cavities**

They result from the rupture of the supports or the roof of an underground cavity, a rupture which propagates to the surface in a more or less brutal manner, and which determines the opening of a coarsely cylindrical excavation.

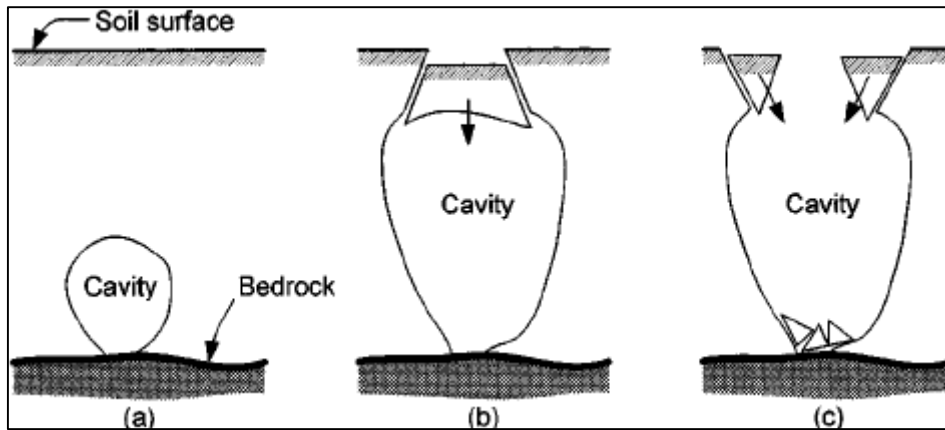


Figure I.07: Cave-in collapses

- **Landslide, falling blocks and stones**

The evolution of cliffs and rock slopes leads to rock falls (volume < 1 dm³), rock falls (volume > 1 dm³), or mass collapses (volume up to several million m³) (Marc-André Brideau, Nicholas J. Roberts 2015).

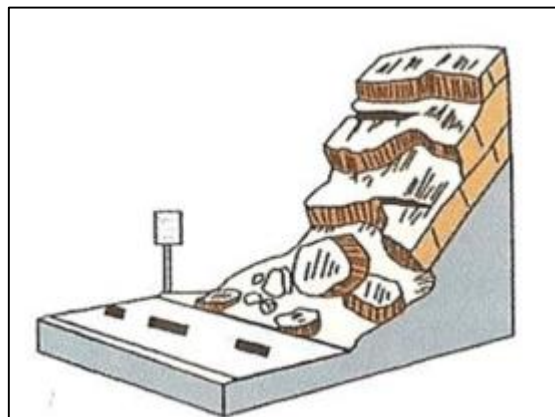


Figure I.08: landslides, falls of blocks and stones

- **Sludge flows and mudflow**

It is a rapid movement of a mass of reworked materials with a high water content and a more or less viscous consistency. These sludge flows frequently originate in the downstream part of a landslide.

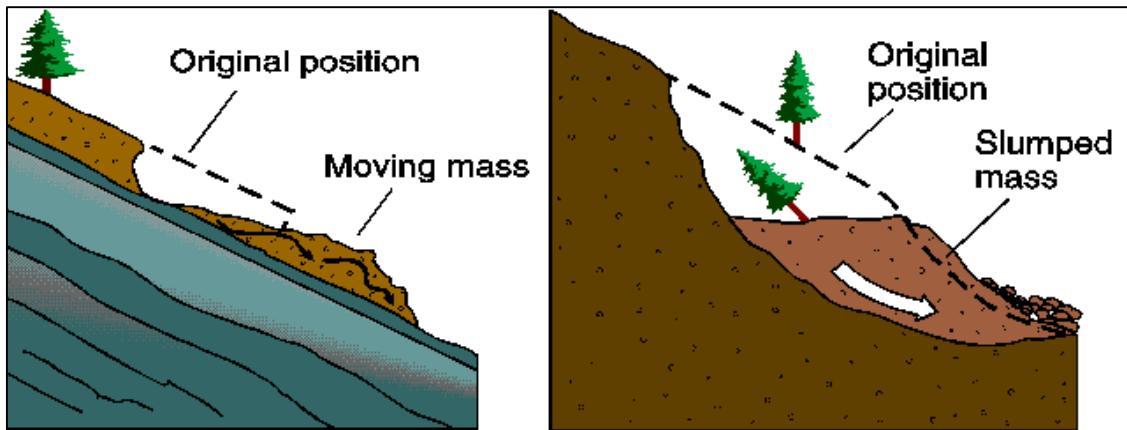


Figure I.09: Diagram showing a mudslide

- Coastal erosion

Coastal areas are subject to a generalized retreat: landslides or collapses in the case of coasts with cliffs, erosions in the case of sandy low coasts.

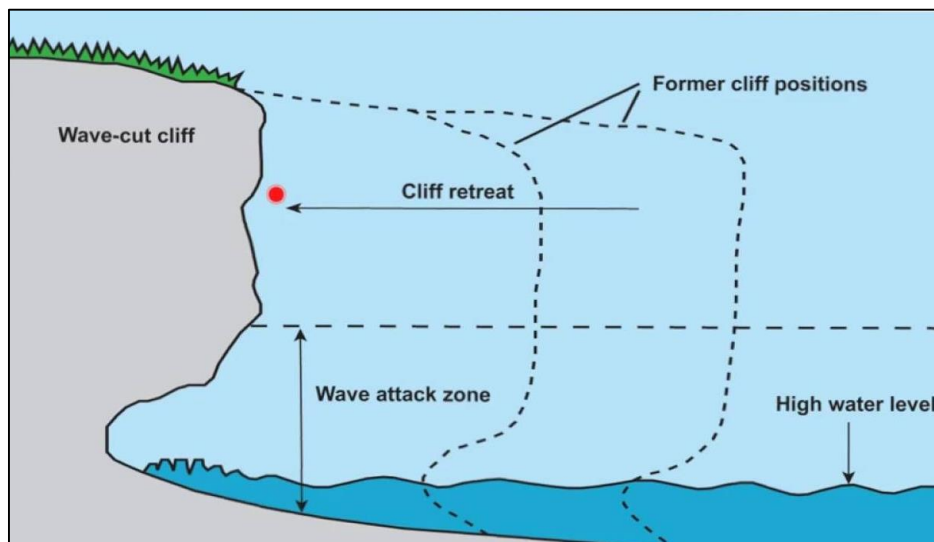


Figure I.10: Coastal erosion.

I.3. Landslide

Landslide is mass movement on slope involving rock fall, debris flow, topples, and sliding (Vernes et al, 1984). Gravity is the main driving force behind mass wasting processes. Gravity will pull on material and force to downhill (Kusky, 2008). Those two definitions stated that landslide deal with mass movement which includes rock fall, topples, debris flow and sliding. It which occurs on slope is influenced by gravitation. Landslide occurs as result of the presence of saturated clay materials on the impermeable

layer on steep slopes (Arsyad, 1989). The presence of soil moisture leads the increasing of the pore water pressure and lessens the material stability.

Landslide is one of the most natural disasters occurring in the mountainous area in the wet tropics and climate. Damage is caused by the movement not only direct damage, but also the indirect damage that cripples economic activity and development (Hardiyatmo, 2006). This definition stated that landslide frequently occurs in tropic zone in which high both of quantity and quality of rainfall deal with the increasing of landslide events. Besides that, landslide causes several damages which include direct damage and indirect damage (impact).

I.3.1. Types of landslides:

According to (Highland et al, 2008), there are 5 (five) main types of landslides, namely:

- **Falls**

It is the movement of rock or soil or both of them on a very steep slope to ramp slope, or the free fall movement of rock or soil with little contact on the surface.

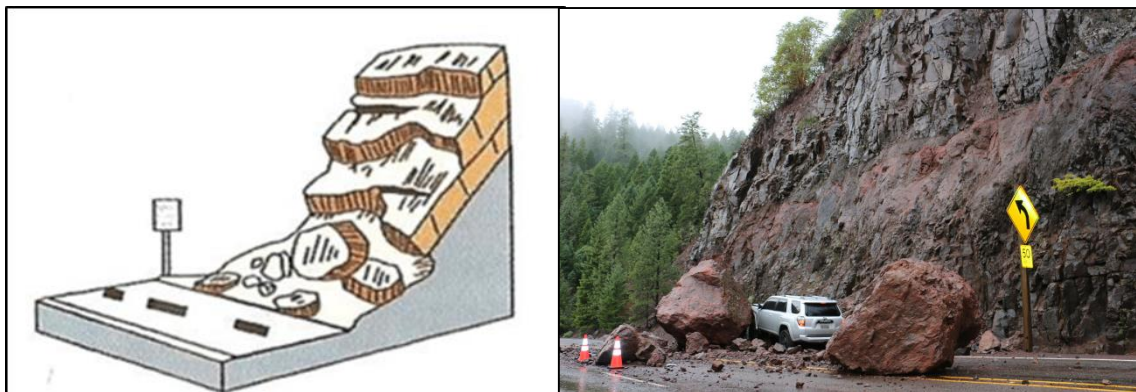


Figure I.11: Schematic view rock fall ((Highland et al, 2008) and photo of rock fall in Oregon Columbia in 2011(Eko Setya N, 2011))

Landslide fall type has a very fast motion and free fall. The material moves generally in the form of rocks, boulders and rock fragments. Characteristics that appear on the type of fall are a large rock slid down the slope, the bottom of the rock slide is a material which is less compact or easily decomposed (Figure I.11).

- **Topples**

It is the movement of rock or soil or both of them, on a very steep slope to ramps slope, or rock or soil movement in free fall with a major mass movement that involves the rotation to the front of the rock mass.

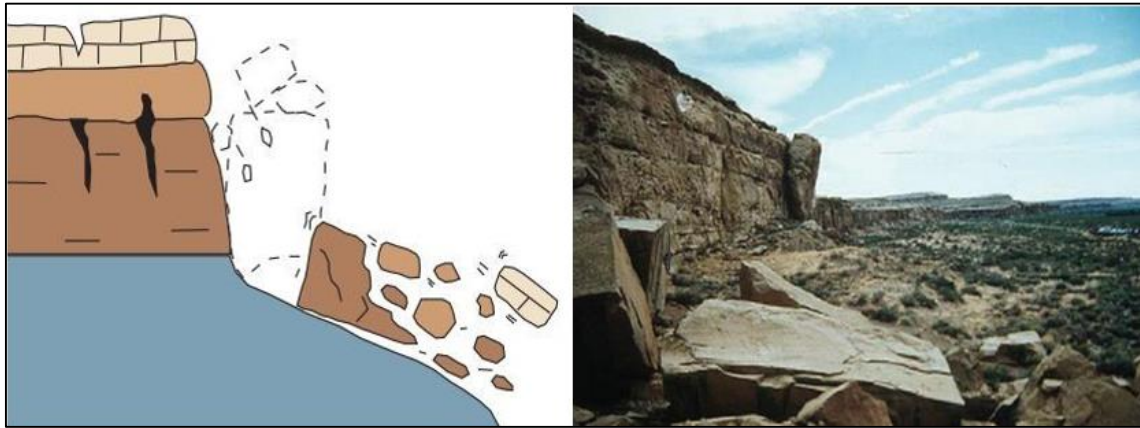


Figure I.12: Schematic view and photo of topples in Chaco Canyon, New Mexico
(Highland et al, 2008)

Topples has the same type with the type of fall that has very fast movement, but topples has fall rotation. The material moves generally in the form of rocks, boulders and rock fragments. Characteristics which appear on the type of fall are a large rock slid down the slope, the bottom of the rock slide is a material which is less compact or easily decomposed (Figure I.12).

- **Slide**

This type represents ground movement, debris, or rock which move very fast, so that there is soil or rock mass transfer along the surface. Type of slide is divided into two categories:

- a. The flat sliding:**

The line of rupture is generally flat. It is constituted by a thin layer of bad characteristics called "soap layer". In this case, the slide is accelerated by the action of water.

During trans-rational landslides, the ground layers or sets of stratified layers slide on an existing zone of weakness (often stratigraphic dip, stratigraphic discontinuity, schistosity, crack or rupture plane). In plan, the size of such slides is very variable and can include areas ranging from a few square meters to several square kilometers. The thickness of the moving masses

frequently reaches several tens of meters. The flysch zones, the marl-limestone schists or the metamorphic schists are the formations most prone to this kind of slide (Hungri et al. 2014).

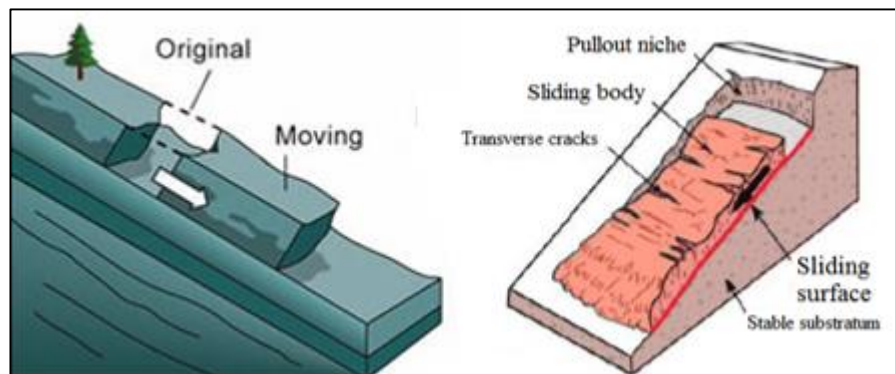


Figure I.13: The flat sliding

b. The rotational sliding:

- Simple rotational sliding:

They are generally of limited volume. They occur mainly in homogeneous loose soils, especially clay and silty soils. In a vertical section, the sliding surface is circular and plunges almost vertically into the pull-out niche. As a rule, the sliding mechanism causes only slight internal reworking of the sliding material.

Depressions with open crevices and tensile cracks are often visible in the upper half of the landslide, whereas the slid mass tends to spread and disintegrate at the front of the landslide, where mud flows (earthflows) can form if the mass is saturated with water.

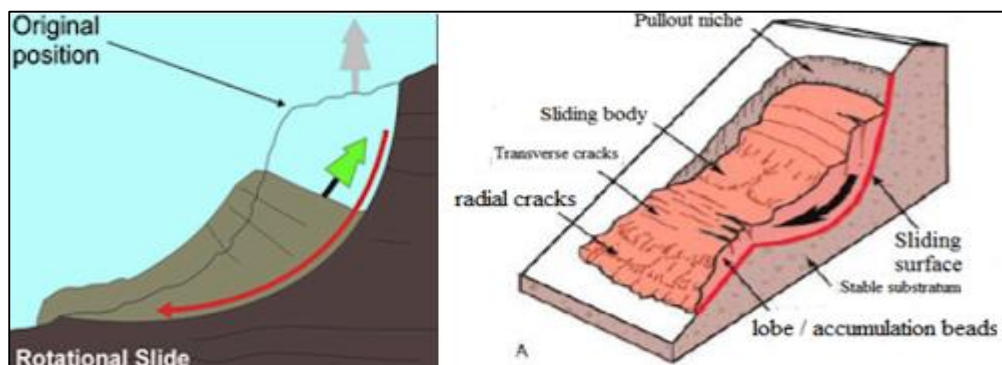


Figure I.14: Simple rotational sliding

- The complex rotational sliding:

These are multiple successive slips nested within each other as shown in the figure below

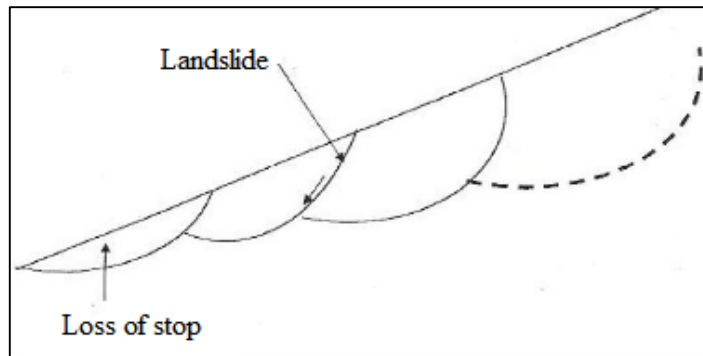


Figure I.15: Successive nested slides.

- **Spread**

It is the mass movement of soil or rock caused by the saturation of material below (Figure I.16).



Figure I.16: Schematic view and photo of spread in California, USA in 1989 (Highland et al, 2008)

- **Creep**

The movement of soil or rock material down to a slope that is very slow and difficult to identify. Characteristics for this creep type are the emergence of cracks in the construction of roads or houses, railway embankments, destroyed bridges on the road or railroad embankments (Figure I.17).

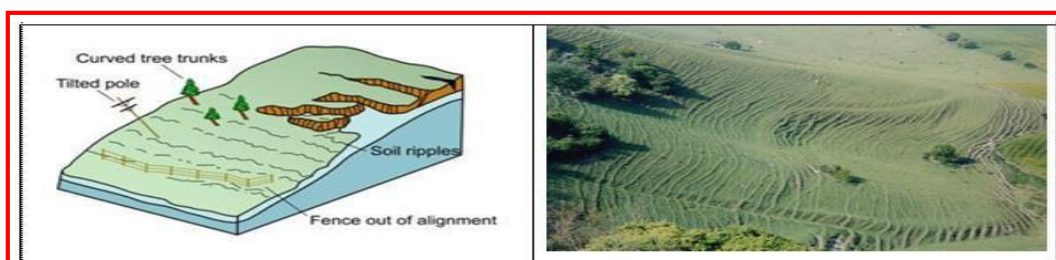


Figure I.17: Schematic view and photo of creep in UK (Highland et al, 2008)

Chapter I: Literature Review on Landslides.

Many factors, such as geological and hydrological conditions, topography, climate and weather changes, may affect the stability of the slope in a landslide. Landslide occurs rarely for one reason alone. The causes of landslides were categorized into geological causes, morphological causes and human causes by (USGS, 2004) in (Table 2.1):

Table I.01: The various causes of landslides (USGS, 2004)

Geological Causes	Morphological Causes	Human Causes
1	2	3
<ul style="list-style-type: none"> a. Weak or sensitive materials. b. Weathered materials. c. Sheared, jointed, or fissured materials. d. Adversely oriented discontinuity (bedding, schistosity, fault, unconformity, contact, and so forth). e. Contrast in permeability and/or stiffness of materials 	<ul style="list-style-type: none"> a. Tectonic or volcanic uplift. b. Glacial rebound. c. Fluvial, wave, or glacial erosion of slope toe or lateral margins. d. Subterranean erosion (solution, piping). e. Deposition loading slope or its crest. f. Vegetation removal (by fire, drought). g. Thawing. h. Freeze-and-thaw weathering. i. Shrink-and-swell weathering 	<ul style="list-style-type: none"> a. Excavation of slope or its toe b. Loading of slope or its crest. c. Drawdown (of reservoirs). d. Deforestation. e. Irrigation. f. Mining. g. Artificial vibration. h. Water leakage from utilities

Source: USGS, 2004

I.3.2. The landslide process

Landslides can occur on moderate to steep slopes of 10° to 40° and differ depending on the nature of the soil and the influence of the water; Terrain movements vary in speed and shape (Cruden. DM, Varnes. DJ 1996).

I.3.3. Classification of the landslide

Landslides can be classified according to the depth of their sliding surface and the average speed of movement (Hamza-Cherif Riad 2009).

Table I.02: Landslide classification.

Source: Federal Office for the Environment Hazard Prevention Division;2009

Classification according to the depth of the sliding surface (in m below the ground surface)		Classification according to activity (according to the average sliding speed in cm per year in the long term)	
Sliding	Sliding surface	Sliding	Sliding speed
Superficial	0 – 2 m	Sub-stability, very slow	0 – 2 cm/an
Semi-deep	2 – 10 m	Not very active, slow	2 – 10 cm/an
Deep	10 – 30 m	Active (or slow with rapid phases)	> 10 cm/an
Very deep	> 30 m		

I.3.4. Surface slippage

In slopes where the surface layer is in a state of limit equilibrium, a temporary degradation of soil quality, particularly by saturation during rains, results in either flows without net limits (solifluxion), or slips with superficial tears exposing the surface. The theoretical limit depth allowed between deep and shallow slip is 2 m.

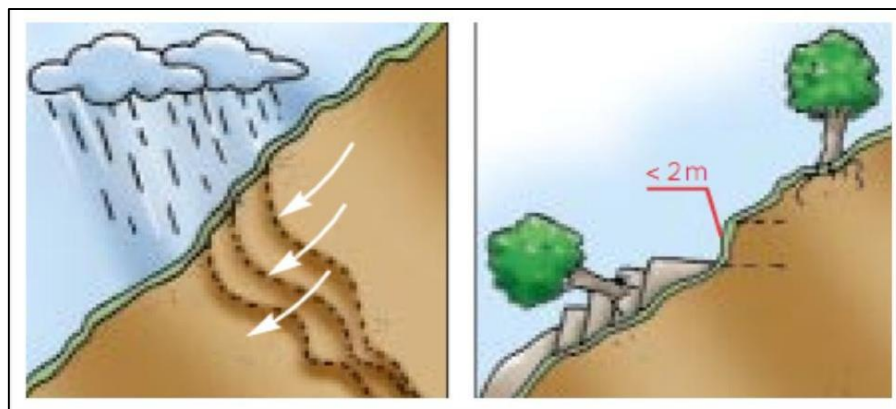


Figure I.18: Solifluxion, Surface slide

Surface slippage may be active or slightly active. A superficial slide is active when it shows a movement greater than 10 cm/year. Recall that the classification used makes the state of the situation during the topographic survey on the ground and that an active slide can stabilize (by gradual reduction of the slope and colonization by vegetation for example) Moreover, a little active slide, can at times enter a rapid phase (sudden rupture).

- **Deep Slide**

The deep slip is characterized by the presence of ripping niches, usually multiple, well-marked, with a displacement of a mass of loose or rocky materials along one or more deep sliding surfaces and of less resistance.

I.4. Hazard, vulnerability and risk

I.4.1. Hazard

Hazard is a potentially physical damage, human activity which can cause death or injury and damage of property, social, economic, and environmental. This event has an occurrence probability in a specified period and in certain areas, and intensity (Van Westen et al, 2009; Coppola, 2007) stated hazard is a source of potential damage to a community which includes population, private & public property, infrastructure, environment and businesses. These definitions stated that hazard is a threat to people and the things value (property, infrastructure, facilities etc). In this study, roads were categorized as infrastructure and the landslide hazard threaten the existence of road. In this case, the landslide hazard arises from human activity which cut the contour to build roads. This activity can cause the reducing of slope stability. Hazard has 3 components which are probability within specified period (temporal probability), probability within certain areas (spatial probability), and an intensity (magnitude). In other definition, (Chakraborty, 2008) stated hazard includes parameters which are location related to question “where”, time related to “when” and the size to “how”. This definition explains that spatial probability (location) can answer the place of occurrence (where?), temporal probability (time) is used in order to answer the time of occurrence (when?) and magnitude (size) can answer (how?). According to (Varnes, 1984) landslide hazard consists of two major elements, namely landslide spatial probability and landslide temporal probability which is related to the magnitude, return period of the triggering event and the occurrence of landslides

I.4.2. Spatial Probability

Chakraborty, 2008 distinguished the landslide spatial probability methods which were classified as direct method and indirect method. The direct method uses geomorphological mapping deal with past and present landslide events and then zonation is created in area in which failure frequently occur (Chakraborty, 2008). Otherwise,

indirect method can be divided as two methods, namely heuristic method (knowledge driven) and statistic method (data driven). Heuristic method considers landslide influencing factor such as, slope, rock type, landform and landuse and then is ranked or weighted based on the influence of causing mass movement. In statistical method, spatial probability is determined based on the relationship with the past/present landslide distribution (Carara et.al, 1991). To compose landslide hazard map in Menoreh Limestone was used five parameter maps, namely slope map, landuse map, geological map, soil map and landform map (Hadmoko et al, 2010). In this study, author uses heuristic method and considers several factors to create mapping unit, namely; slope, and land use in which those factors will influence landslide event.

I.4.3. Temporal Probability

Temporal probability is the probability of occurrence of landslide event in a particular time steps (Chakraborty, 2008). Temporal probability can be derived from several methods (Jaiswal et al, 2009) distinguished temporal probability method which are physically threshold based model and empirical rainfall threshold methods. In the physical threshold-based model, it uses certain features of the local terrain (e.g. slope, gradient, soil depth, lithology) based on a dynamic hydrological model where the most important variable is rainfall. Otherwise, empirical rainfall threshold method is method to measure temporal probability based on the calculation of rainfall threshold causing landslides. The other method is gumbel extreme value distribution which uses maximum annual rainfall. By using this method, it can be known the relationship between the temporal probability and time periods. This method was used by (Wahono, 2010) to determine landslide temporal probability in Wadaslintang, Central Java. Temporal probability can be determined by using poisson probability model, this method was used by (Chakraborty, 2008) and (Nayak, 2010) to calculate temporal probability of landslide in India. The poisson probability model is a continuous-time model consisting of random-point events that occur independently in ordinary time, which is considered naturally continuous (Nayak, 2010)

I.4.4. Magnitude

Magnitude deal with the amount of energy released during the hazardous event, or it shows the hazard size. By using a scale, consisting of classes, and related to a (logarithmic) increase of energy, magnitude can be indicated (Van Westen et al, 2009).

Landslides magnitude which is as a factor to determine the amount of damage on each element in the risk of landslides within a specified time is the most important element in assessing the risk of landslides. Magnitude can be determined by several methods. One of the methods was proposed by (Malamud et al, 2004). He calculated magnitude based on some equation which used several variables (events number, total volume of landslide, and landslide total area). The other method was proposed by Jaiswal, (Nayak, 2010). In this method, he tried to quantify landslide magnitude for each types of landslide which was used to determine landslide magnitude on road corridor. The magnitude class was classified based on volume, type and characteristics of landslides (location, potential for damage, human perception and field investigations).

I.4.5. Vulnerability

Vulnerability is the degree of loss of certain elements at risk which is caused by the natural phenomena of a given certain size (magnitude) and shown in a scale from 0 (= no damage) to 1 (= total loss) UNDR0 (Thywissen, 2006). This definition tries to quantify vulnerability by giving scale from 0 to 1 based on the level of damage (Coppala, 2007), stated transportation systems (roads, highway, railroad, public transportation) which are affected by hazard, can be categorized as physical vulnerability. According to (Dai et al 2002) landslide vulnerability concept mainly depends on run out distance, volume of landslide, sliding velocity, the element at risk, the nature of the element at risk type and proximity to a slide. This concept explains several factors that influence landslide vulnerability. Based on (Berdica, 2002), the vulnerability of the road transport system relates to the incident, which may reduce the functionality of the road network. This means the failure of the service function road in operating

Condition at given time (non-reliability). This definition stated road transport vulnerability is associated with decreased the road service function because of certain incident.

Several methods were used to determine road vulnerability, (Abella, 2008) used vulnerability values from 0.5 to 1 which were assigned to each road type. These values represent a financial loss when a landslide hit the road. This means that the high cost of road construction (such as high way) have a vulnerability value of 0.5, because these roads will have a stronger construction to protect landslide event. In other hand, the low cost road construction (such as trail, path) have vulnerability value 1, because both of the

road type have worst construction to face landslide. AGSO 2001 make vulnerability scale from 0.3 to 1 based on slope. High vulnerability (score 1), if road lies on slope $> 25^{\circ}$. And low vulnerability (score 0.3), if road lies on slope $< 25^{\circ}$. This concept based on previous research in Cairn, Queensland that roads on slope $> 25^{\circ}$ will totally damage due to landslide event given score 1. Otherwise, roads on slope $< 25^{\circ}$ show that every 5 km road length will damage 1-2 km due to landslide and given value 0.3 (Ebta, 2008).

I.4.6. Risk

Risk which consists of three elements, namely, vulnerability, hazard and exposure is the possibility of damage or loss. Element of risk associated with each other, when one of the elements increases, the risk will increase, and vice versa (Thywissen, 2006; Coppola, 2007) stated risk is the likelihood of an event multiplied by the consequence of that event. The term of “likelihood” can be given as a probability or a frequency (Vernes et al, 1984). explained risk is the expected degree of loss which can be caused particular natural phenomenon. It is showed by the product of hazard times vulnerability. These definitions above explain risk elements, which will influence the risk value.

Several methods propose to determine landslide risk (Abella, 2008) distinguished risk based on the level of quantification; there are the landslide risk assessment methods in qualitative, semi quantitative and quantitative. Qualitative methods based on risk classes which are categorized by expert judgment. Risk classes: high, moderate and low; Semi-quantitative based on ranking weighted by given criteria. Risk index: ranked value (0-1, 0-10 or 0-100); Quantitative based on probabilities or percentage of losses expected. Risk value: probabilistic values (0-1) over certain amount of monetary or human loss. According to (Coppala, 2007) qualitative analysis uses definition to describe and determine risk. Quantitative analysis uses mathematical and/or statistical data to calculate risk (Van Westen, 2006) explained some expert have made consensus about classification of landslide risk approach, there are four approaches which are landslide inventory-based probabilistic approach, heuristic approach, statistical and deterministic approach. Landslide inventory-based probabilistic approach, it can be determined by using landslide historical events which can be used as the main input in hazard assessment. Heuristic approach can be divided into 2 methods, namely: direct method based on the experience of experts by considering geomorphologic mapping, and indirect methods using combination with a heuristic approach. Statistical approach can be divided into 2 methods

which are bivariate statistical analysis based on weights of evidence modeling by testing the factors of landslide susceptibility, and multivariate statistics. Deterministic approach based on slope stability models which can be used to determine safety factors.

I.4.7. Factors involved in land instability processes

The transition from stable to unstable is linked to numerous and varied causes that add to the initial conditions, intrinsic to the terrain. There are several factors that influence the phenomenon of field movement.

-They correspond to the natural or anthropogenic action required to trigger a landslide. This triggering action can be linked to one or more external stimuli (intense rain, earthquake, etc.) (Cruden & Varnes 1996).

I.4.7.1. Action and influence of water.

The variation of hydraulic conditions is one of the main causes of landslides and its action in the breakdown of equilibrium manifests itself through several ways and at different stages. It is mainly rainfall that the authors agree is the most influential factor, and more particularly, they show an occurrence between high-intensity movements and rains (Cartier and Delmas, 1984). Water from man-made structures: almost all receiving or transporting water can cause landslides. The action of water on different type of soil, but especially for fine and clay soils, the water supply leads to a decrease in resistance of the medium.

I.4.7.2. Action of gravity

The action of gravity is the main motor of the movement. The stability of a block is given by the ratio of stabilizing forces to destabilizing forces. We are talking about the safety factor (F). If it is less than 1, there is a break in the balance, and if it is greater than 1, there is a conservation of the balance. If the weight of a block or a portion of land is increased, the destabilizing forces will increase and the F ratio will decrease until the limit equilibrium threshold is reached. The action of gravity, as a factor of motion, is intimately linked to anthropogenic action, because man most often changes the conditions of the medium towards and sometimes beyond the limit of rupture, either by overload, or by the suppression of the foot stop (Besson, 1996).

I.4.7.3. The nature of the land

The nature of the land is one of the main factors in the occurrence of this phenomenon, as is water and slope. The vast majority of landslides occur in clay soils or in grainy formations sufficiently laden with clay for this material to impose its behaviour. The predisposition to the landslide of fine and clay soils is first of all the role that water in its various forms can play.

I.4.7.4. External mechanical actions

Slope, excavation and scouring at the foot of the slope, site deforestation, and overload on a slope can affect the stability of the terrain.

I.4.7.5. Removal of Slope Foot Stop

The removal of the foot stop can have several origins:

- By earthmoving
- Scour or regressive erosion: example Bardo
- Dredging: underwater excavation.
- Implementation of overloads on a slope

It can be an embankment (road, terrace...etc.), a building based superficially, a retaining wall, a landfill, a storage, a large construction site equipment... etc. When placed high or halfway up a slope, overloads are frequently the cause of a landslide.

Conversely, the slope foot overloads, by the stabilizing torque they provide, almost always increase the stability of the site.

I.4.7.6. Seismic actions

Earthquakes, by the vibration of ground elements and the modification of gravity conditions can be the cause of the destabilization of the masses in place.

We have also seen in saturated furniture environments, an earthquake giving rise to an interstitial pressure that can lead to instantaneous, partial or total liquefaction of the medium.

I.4.7.7. Deforestation Action

The deforestation of a slope frequently leads to the appearance of landslides. It disturbs the ground in depth and then promotes the penetration of water into the mass. The stabilizing role of trees is due to several factors:

- Anchoring by the roots
- Drainage by evapotranspiration
- Retention of rainwater: water retained by leaves and the covering of the undergrowth.
- Protection against erosion.

I.4.7.8. Anthropogenic actions

Anthropogenic actions that affect hazard: during construction sites, earthworks operations may result in the removal of a stabilizing foot stop from a land mass, or increase the slope of a slope composed of materials that are not consistent enough for this new topography. The backfill creates an overload that can trigger or aggravate a slip.

I.4.7.9. Impact on People and Property (Issues)

As the large movements on the ground are often slow, the victims are, fortunately, few. On the other hand, these phenomena are often very destructive, because human settlements are very sensitive and damage to property is considerable and often irreversible. The buildings, if they can withstand small displacements, undergo intense cracking in case of displacements of only a few centimeters. Disorders can quickly be such that occupant safety can no longer be guaranteed and demolition remains the only solution.

Rapid and discontinuous ground movements (collapse of underground cavities, collapse and fall of boulders, muddy flows), by their sudden character, increase the vulnerability of people. These land movements have consequences on infrastructure (buildings, communication routes, etc.), ranging from degradation to total ruin; they may cause induced pollution when they concern a chemical plant, a sewage treatment plant, etc.

Landslides and falls of boulders can lead to landscape reshaping; for example, the obstruction of a valley by displaced materials creating a water reservoir that can suddenly

break and cause a surge in the valley. For slow movements, there is no direct human risk and their consequences are essentially socio-economic or public interest. These are very serious structural damages that lead to ruin or frequent orders of peril and evacuation (total or partial destruction of construction works: housing, road infrastructure, etc.).

Indirectly, these are disruptions in activity and significant financial losses.

I.4.8. Examples of field movement across the world

I.4.8.1. Muddy flows in Rio de Janeiro

Also called "liquid landslides" which are very often the consequence of deforestation. The surface layer of the soil, subjected to heavy precipitation, stalls and slides in a viscous mass along the slope.



Figure I.19: Mudslide in the Rio region killed 205 people

Source: www.zone-ufo.com

Favelas (slums) that grow like mushrooms on the hills around Rio de Janeiro are particularly exposed. The flows are characterized by the transport of materials in more or less fluid form, on the slopes or in the bed of the torrents (thalweg).

Often fast and extremely dangerous, flows are triggered by excess water (exceptional rains, melting snow or a glacier, etc.) (Ladghem Chikouche 2009).

I.4.8.2. Falling Blocks

Boulder falls result from the degradation of a cliff or rocky slope



Figure I.20: A rocky "scale" Maupas. France

Source : [Laboratoire centrale de pont et chaussée (1996)]

I.4.8.3. Underground cavity

It is a natural cavity slowly eroded by water for millennia or an underground quarry used to extract ore and building materials, it is obviously more dangerous to live above a hole than next to it.



Figure I.21: Collapse of a natural cavity by dissolution of gypsum Bargement. France [1996]. Source: Ladghem Chicouche Fadila.

I.4.8.4. Differential settlement

The earth's subsoil is full of rivers, underground lakes and groundwater that are actively involved in the water cycle. In wet areas (marshes, swamps, lagoons, etc.), some clay or peat soils can swell and settle under the effect of water or, on the contrary, drought. In both cases, this has serious consequences for construction if it is not taken into account. The Leaning Tower is an example of a building built on compressible ground that has posed problems for generations of architects (Goyallon J, 2000).



Figure I.22: The tower of Pisa [Italy 2021]

Source : Rapport du bureau des recherches géologiques et minières

I.5. Instrumentation of a landslide

The identification of risk areas is the preliminary of the quantification of the risk, the monitoring of the danger area is the corollaries. The slide instrumentation provides real-time remote monitoring and alerts to populations in the event of an imminent trip. Instrumenting a slip is done to be able to follow its movements, but also its internal variations.

The movements can be followed by extensometers (Figure I.23) operating on the length variation of a cable: the measuring device is placed in a stable position (not included in the moving mass), a cable is pulled between the stable position and the unstable position to be monitored. The variation of the length of the cable informs the movements of the slip, even if they are of the order of the millimeter. The measurement of seismic vibration displacement rates in the ground can be performed by geophones (Figure I.24) allowing a real-time view of the slide geometry. These measures make it possible to extrapolate movement of the slide, or actively serve, by retrieving the profile of a wave emitted on the surface to extract information about the subsoil of the slide. Variations of a slope can also be assessed via an inclinometer measuring the angle to the horizontal.

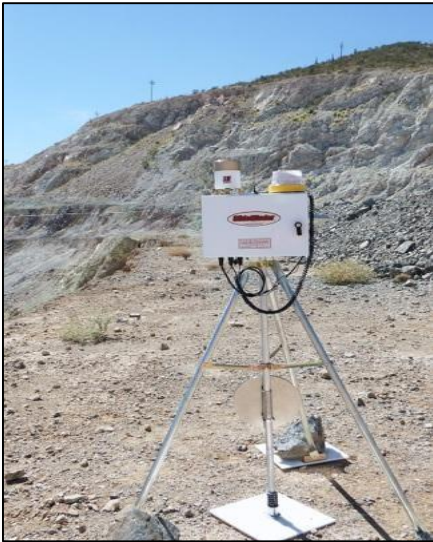


Figure I.23: Wired extensometer, Picture of Wikipédia



Figure I.24: Electromagnetic geophone, Picture of Wikipédia



Figure I.25: Inclinometer, www.solexperts.com

To complete the vision of the glide, knowledge of the internal dimensions on the ground is necessary. Inclinometer (Figure I.25), is a sensor used to measure angles in relation to the horizon (or horizontal) line. Where the spirit level (or level) makes it possible to detect precisely where the horizontal is located, the inclinometer also determines the angle of inclination with respect to this horizontal line.

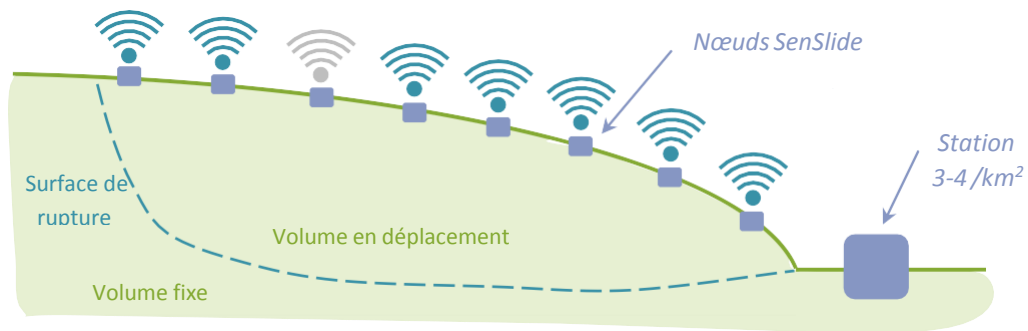


Figure I.26: Sen Slide Distributed Architecture Mapping

A new distributed tracking architecture such as SenSlide (Anmol Sheth et al. 2007) does not require continuous support and provides an overview of a sector. This system proposes to use many inexpensive sensors that are likely to fail without affecting the predictive capacity of the system (up to 800 sensors per square kilometer), rather than using a dozen very expensive but very reliable devices. Each stand-alone node communicates with others via radio waves (Figure I.26) from near to near, until reaching a station (up to five per square kilometer) equipped with a longer range transmitter and digital storage capabilities. The difficulty is then shifted on the design of inter-node communication protocols, to ensure that everyone can reach the station, without consuming too much energy, and on the processing of the data obtained, often very noisy.

A slip is logically unstable, and the installation of instruments must not disturb it. Sometimes inaccessible it is then impossible to use it properly for technical, financial or temporal reasons. The possibility of powering all these devices and repatriating the data is not always assured. Remote monitoring from air or space is always possible.

LiDAR7 systems on aircraft scan the ground with tens of thousands of laser pulses per second, getting three-dimensional visualization of slopes, even through dense forest cover. The identification of slips is done by comparison of several surveys showing the evolution of the geometry of the slope. InSAR8 imaging systems, based on satellite interferometry, can measure soil displacements very accurately (Figure I.27). InSAR systems are based on the transmission and reception of the same radio pulse, deformed by the ground; each satellite can follow areas of several thousand square kilometers. During the passage of the satellite, the gates of the received waves are compared, the phase difference makes it possible to extrapolate the movements of the ground with an

accuracy of the order of the tenth of a millimeter. Unlike LiDAR, this pulse can penetrate cloud layers, so measurement can be done at any time.

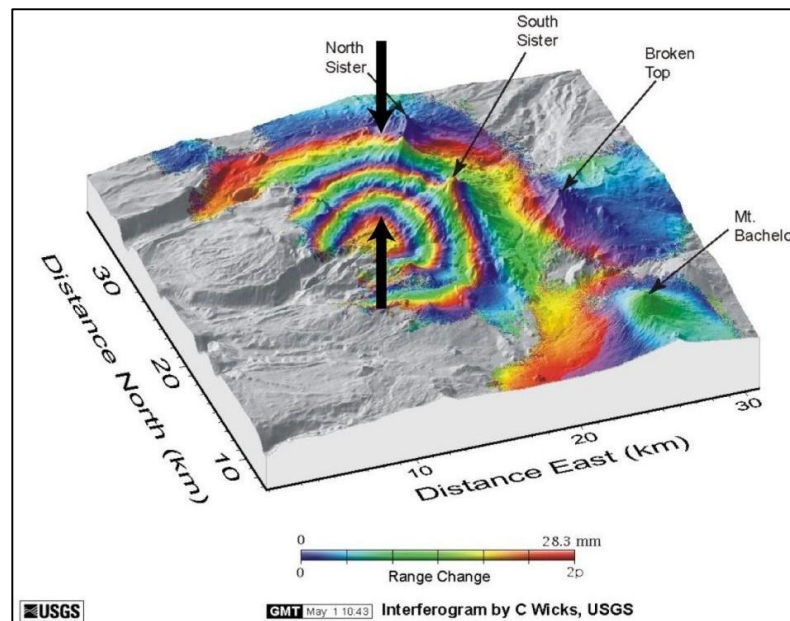


Figure I.27: InSAR imaging deformations, red areas have undergone displacements in the order of 20mm, C Wicks image, USGS

I.5.1. Data processing

The data obtained are most often processed by geologists, systems that can assist them. The finite element method is an additional tool for risk assessment and requires the combination of map information and shifting geometry variations. By aggregating all the data, it is possible to populate relatively accurate finite element models of the shifts (Figure I.28). Advances in the quantification of large deformations in heterogeneous areas and the increase in available computing power now allow reliable and usable models. Indeed, these finite element models can work with complex fracture surface geometries, very close to reality. The results obtained by these simulations provide an assurance of the existence of a risk. The modification of the parameters makes it possible to simulate future possibilities: consequences of a loss of a greater volume of water from an upstream glacier, consequences of the construction of an upstream highway, etc.

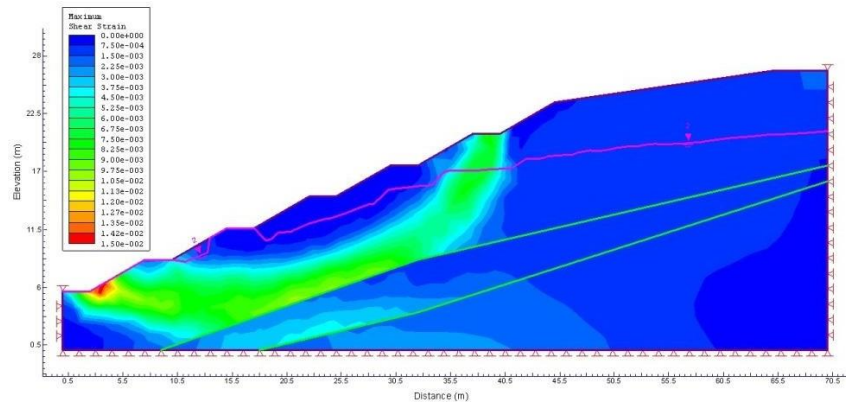


Figure I.28: Finite element modeling of a slip, color gradient represents shear deformations, image Scientific Academic Publishing.

Prevention still relies on the expertise of geologists in the analysis of map data obtained in the field or at a distance. The day before, costly, requires significant human resources. Today, a large part of landslide research is devoted to the development of innovative monitoring methods, minimizing human intervention and thus the means available to combat land movements.

I.5.2. Main comfort techniques

It is sometimes possible to deploy countermeasures, which neutralize the advance of the movement or limit its impact when it is triggered. These countermeasures are varied, some of which are presented in this resource. To consolidate a glide requires to know not only its dimensions but also its origin (loading, water flow, soil alteration, singular runoff): the choice of the method of comfort depends on it.

I.5.3. Drainage devices

Water frequently plays a driving role in landslides, the purpose of drainage is to control the water content of the soil and reduce pore pressures at the fracture surface. Drainage can drain water from the area (Figure I.29) or avoid water supply to the area by collecting and channeling surface water.



Figure I.29: Slope drainage by barbicanes, image (University of Illinois at Urbana-Champaign, Department of Geology)

I.5.4. Construction of reinforcements

The role of these systems is to arm the earth and limit its movement.

- **Nailing:** This device transfers the forces of the moving volume to the fixed volume through a nailing system (piles, nails) (Figure I.30)

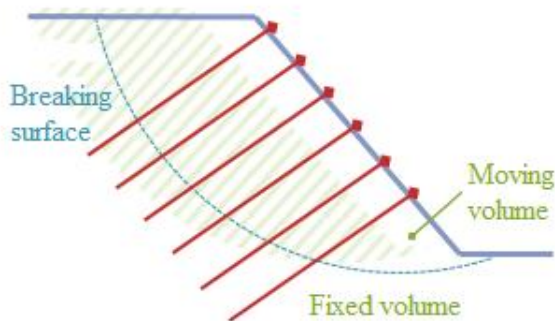


Figure I.30. Nailing principle and example of realization, SIMPRO image

- **Supports:** It is a rigid or flexible screen that blocks the volume in motion. Rigid, the forces involved are significant and can lead to failure (Figure I.31).



Figure I.31: Retaining wall of the RD559 in the Var, collapsed under the push of the slide, image A.Woimant

I.6. Earth moving systems



Figure I.32: Retaining wall in Chinon, Image Pinon SA.

I.6.1. Foot fill: The foot load of the slide counterbalances the driving forces of the moving volume (Figure I.33).

I.6.2. Lightening in the head: Moving the head of the glide lightens the mass of the moving volume, and thus reduces the driving forces (Figure I.34).

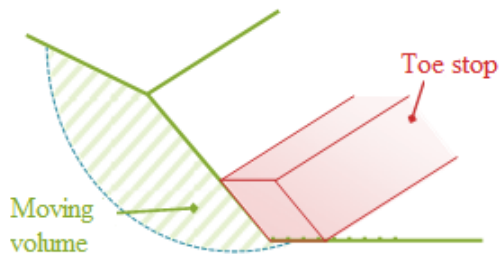


Figure I.33: Principle of foot toe stop

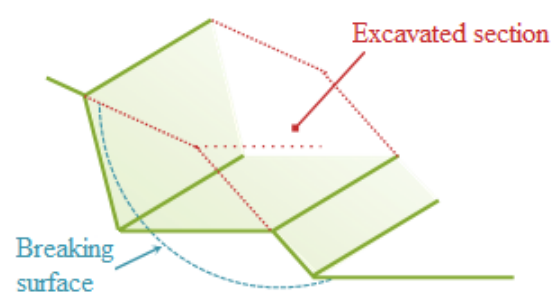


Figure I.34. Principle of lightening

Sometimes it is possible to trigger a slide early to better control it, or to build infrastructure to ensure that it does not trigger catastrophic consequences. The problem is that, most often, the establishment of a response to a risk of movement takes months and requires the knowledge of dozens of engineers; the financial cost is therefore very important. There is currently no general solution to the control of landslides.

I.7. Conclusion

The study of field movements is particularly complex and has since many laboratories and universities. Throughout this work we have focused on grouping together almost all the theories developed that deal with the landslide phenomenon and all that results from it in a predefined. In the first stage, the problem of landslide and in the second stage all types of slip have been identified and differentiated, with an identification of several types of supports and supports possible depending on the constraints of the sites studied and the feasibility of the reinforcement works.

Landslides are caused by numerous geological, geomorphological, and anthropogenic factors but are generally triggered by rainfall and earthquake vibrations. In the tectonically active mountainous terrains, earthquake is one of the major triggering factors for the occurrence of landslides, and many a time, it has been noticed that the destruction caused due to the earthquake-induced landslides is much greater than the destruction caused by direct ground shaking of an earthquake

**Chapter II:
Presentation and
investigation of the
study area.**

II.1. Introduction

The first geological investigations on the scale of the Medjerda mountains were initiated by Powel (1888), before the first regional monographs on the East of Constantine appear (Blayac, 1912), followed by the work of Flandrin (1934) which produces the first geological map at 1: 50,000 Souk Ahras.

David (1956) then undertook a detailed geological survey of the Medjerda Mountains, establishing several geological sections and a 1/200,000 geological sketch. From 1985 to 1986, the geological works of Kriviakin, Kovalenko and Vnouchkov led in 1989 to the edition of the geological map at 1: 50,000 of the sheet of Taoura, by the Geological Service of Algeria, on the basis of the geological works of David (1956).

Recent work has included work in the region, notably in Vila (1970, 1971, 1972, 1977, 1978, 1980), and Chouabbi (1987).

II.2. Geographical situation of the study area

The wilaya of Souk Ahras is located in the East of Algeria (figure II.01), it is limited by Tunisia to the East, the wilaya of Taref and Guelma to the North and North-West, and the wilayates of Tébessa and Oum El Baoughi to the South and South-West. The total area of the Wilaya is 4350 Km². The population of Wilaya reached 374,940 Inhabitants in 1998 which represents a density of 76 inhabitants per km² spread over 26 communes and 10 dairates.

The main urban centres of the wilaya of Souk Ahras are: Souk Ahras (W), M'daourouche, Sedrata, Taoura, Mechroha.

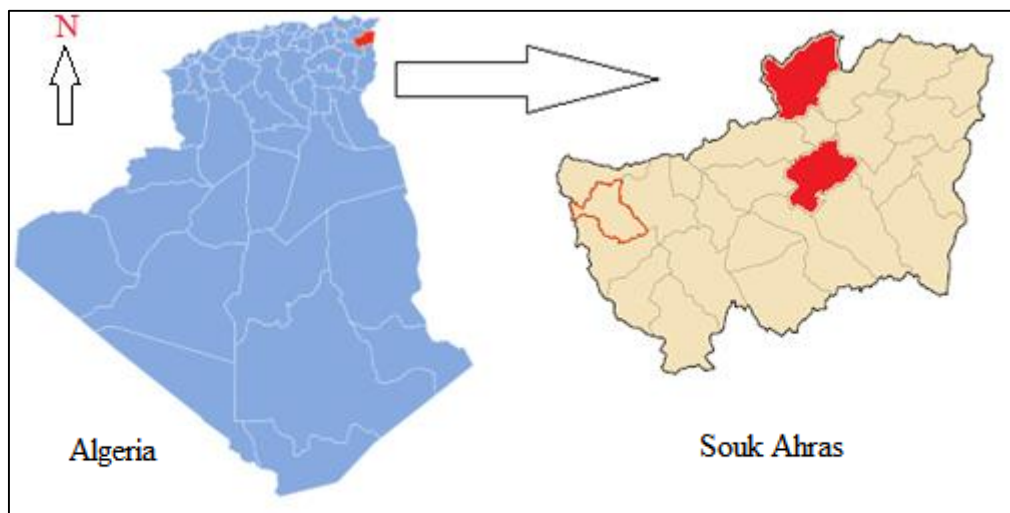


Figure II.01: Geographical location of the study area

Between 1950 and 1955, LOUIS DAVID undertook extensive work on the region of Souk Ahras, Oued Megras, Taoura and Hammam Tassa; this region of eastern Algeria is known as the high basin mountains of Medjerda, it comprises an important mountain range, SW-NE management complex that extends far west of the Algerian-Tunisian border.

- The reliefs:

Are uneven with mainly the geological formations of the Triassic, Cretaceous and Quaternary, generally composed of marls and sandstones.

- The vegetation:

It is closely linked to the nature of the soil and the climate and offers in mountainous areas forests mainly of Aleppo pines, sometimes forming difficult to penetrate maquis. Elsewhere, where only rare vegetation grows, quaternary glacia and plains almost devoid of trees are sometimes delivered to sheep farming and cereal cultivation.

- The ruins:

The Roman ruins, almost completely destroyed, are abundant. The most beautiful remains are located in the region of Souk Ahras and its surroundings (Museum of St. Augustine, Khemissa and Tifech).

II.3. Morphology

The region of Souk Ahras is part of the Upper Medjerda Mountains, the latter of which was the subject of a study established by the geologist (David. L) in 1956. The High Medjerda Mountains of Eastern Algeria represent a great geological interest, it is the area of contact between the two largest units of Eastern Berberia: The Tellian Atlas and the Saharan Atlas. It has a large mountain range going south – west, north – east that extends far west of the Algerian – Tunisian border, where the Medjerda River and its tributaries run. The river widens its valley and winds through important alluvial formations. The topographical surface of the Wilaya Souk Ahras is very irregular and marks a rugged terrain with an average altitude of 1000 m in the North and 650 m in the South. Drainage conditions are also complicated by overlapping three major watersheds within the Wilaya boundary:

CHAPTER II Presentation and investigation of the study area.

- The Medjerda watershed is represented in its northern part by mountain ranges and coasts ranging from 700 to 1400 m. In the southern part, the coasts do not exceed 600 m. The valley of Oued Medjerda is characterized by a form of meander. They are essentially syncline and anticline (syncline of Dréa, Taoura, Merahna and Bordj.Mraou) whose flans are formed by limestones of the Cretaceous while the basins are formed by the sandstones of the miocene.
- The Seybouse watershed is represented by a mountainous relief to the north (DJ. El Meida: 1423 m, DJ.El Moudia: 1271 m, DJ.Zouabi: 1164 m) as for the southern part of the basin, it is the immense extent of the Terreguelt ditch drained by Oued Trough with the coasts ranging from 600 m to 700 m.
- The Mellègue catchment area has an average altitude of 600m.

The morphometric study of a sub-basin belonging to the great basin of Oued Medjerda downstream of which the dam of Ain Dalia was located, allowed the calculation of the parameters of shape (Table 1) within these limits, the territory of the Wilaya of Souk Ahras (Figure II.02) is characterized by an average altitude of 900m, it has a low vegetation cover, which promotes the increase of the effect of erosion. The surface area is 193 km², the perimeter is 600km and the compactness index is 1.20 characterizing an elongated watershed, which increases the time of concentration of water at the outlet (9h 14mn). Thus, the terrain parameters indicate that this basin is characterized by moderate terrain.

The drainage characteristics of the basin (Figure II.03) show a low drainage density (0.95 1/Km) and a flow rate of 1.25 m/s.

Nevertheless, due to the vastness of the study area, the complexity and diversity of the geological and geomorphological environment, an assessment study will be made at the level of two sectors most threatened by the danger of slippage and where the communications voices are in condition, already, altered; the first sector of Mechroha is located north of the wilaya of Souk Ahras, the second of Zaarouria in the center of the wilaya the details on the geological and mechanical study in these two areas will be envisaged in subsequent chapters.

CHAPTER II Presentation and investigation of the study area.

Table II.01: Summary of morphometric and physical parameters of the oued medjerda sub-watershed

Parameter	Symbol	Value	Unit
Area	S	193	Km ²
Perimeter	P	60	Km
Maximum altitude	H _{max}	1317	m
Average elevation	H _{moy}	900	m
Length of main talweg	L	41,5	Km
Length of equivalent rectangle	Lr	22,18	Km
Width of equivalent rectangle	Ir	8,69	Km
Compactness index	Kc	1,20	-
Drainage density	Dd	0,95	1/km
Slope index	Ic	10,76	m/km
Overall slope index	Ig	13,34	-
Time of concentration	Tc	9h14mn	h
Flow velocity	Ve	1,25	m/s
Average slope of the valley	I _{moy}	3,05	%
Elongation coefficient	K	18,65	-
Minimum altitude	H _{min}	640	m
Specific gradient	Ds	185,32	m

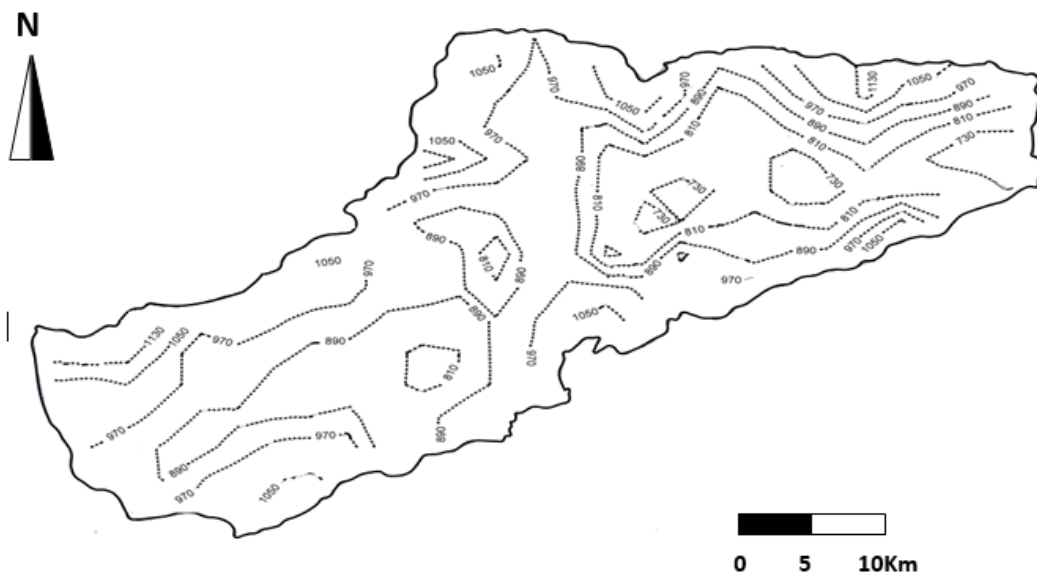


Figure II.02: Topographic map of the Oued Madjerda sub-basin in Souk Ahras.

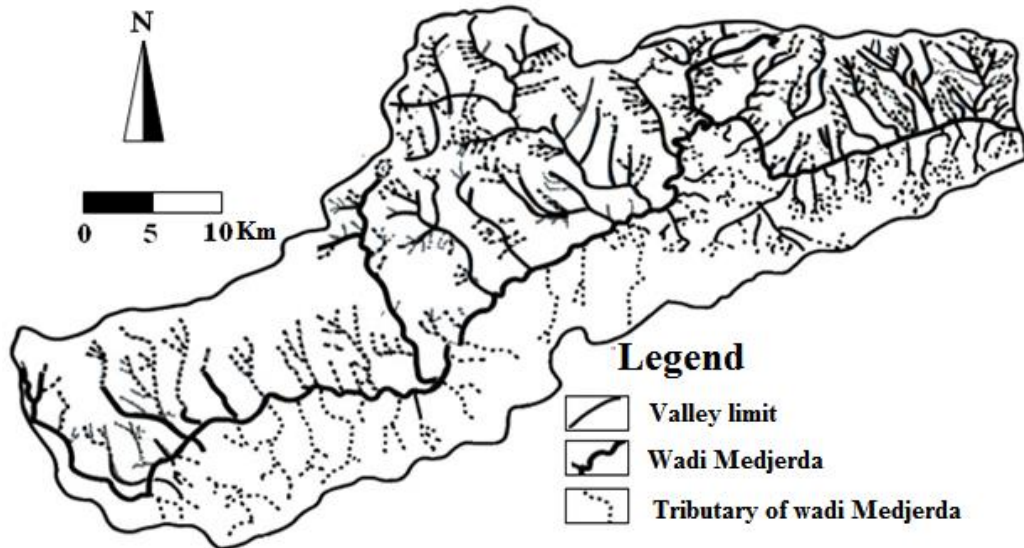


Figure II.03: The map of the hydrographic network in Souk Ahras.

II.4. Geographical framework

Constituting the northern part of the zone of the Diapirs, the area of study of surface of more than 1700km², is 80 km south of the Mediterranean Sea, to the borders Algerian-Tunisians This region belongs to the zone of transition between the Tellian atlas and the Saharan atlas. The climate is sub-humid in the northern part and clearly semi-arid to arid in its southern part, it is characterized by irregular precipitation (on average 550 mm.an-1) (ANRH 1993), the average temperature of the air is nearly 15°C with a high evaporating power (74%). Two wadis characterize the area; Medjerda in the North and Mellegue in the South, they continue to Tunisia to constitute a single river that finally leads to the Mediterranean Sea (ABH. 2005). The forest cover is very dense in the North on the northern massifs called: mountains of Medjerda and strongly degraded as one progresses towards the South.

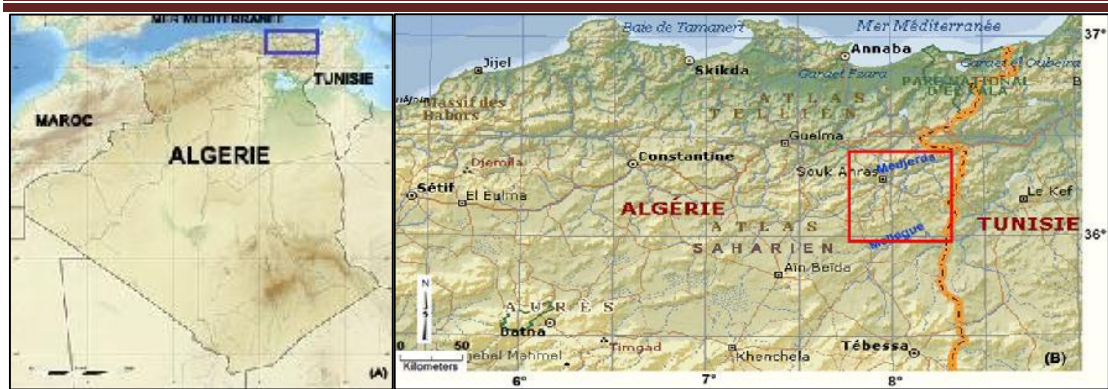


Figure II.04 :(A) Location of Algeria in the Mediterranean basin, the blue rectangle represents the Northeast. (B) The red rectangle shows the study area.

II.5. Geological framework

The region of Souk Ahras is located in the northern border of Atlasica and in contact with the Tellian domain of the Maghrebi chain (Durand M. 1969). The Saharan atlas is characterized by thick Mesozoic formations (about 2500m) (David L. 1956) folded and fractured, having the peculiarity of a stratigraphic gap of the Jurassic, and large outcrops triassic masses arranged parallel to the chain, The Tellian atlas is made up of a pile-up of charriages from different paleographic domains (Vila J M. 1980). In the Algerian-Tunisian confines, the units of the Numidian Flysch and the formations of the external domain of the Maghrebid chain outcrop. The units of the Numidian Flysch are thick series of sandstones arranged in abnormal contact on the Tellian and paraaboriginal allochthonous series of the Atlasic foreland (Vila J M. 1980). The southern region belongs to a large subsident synclinorial zone that extends from Ain Beïda to Merahna to the Algerian-Tunisian borders (Figure II.04 A and B). The northern part is the southern flank of the Medjerda mountains (David L. 1956). The formations of the native are: the Triassic, composed of evaporatites with various fragments and blocks of rocks; the Cretaceous formations (2500m) are predominantly carbonate intercalated of marls; the Paleogene is essentially marly to rare limestone past (200m) ; the neogenous sediments of variable thicknesses are very heterogeneous but mainly of marine type, the continental Miocene is made up of puffins, red and gray clays, lake limestone, it occupies the heart of the collapse ditch of Taoura. The Quartenaire is made of gravel, sand, silt, breccia, travertine.

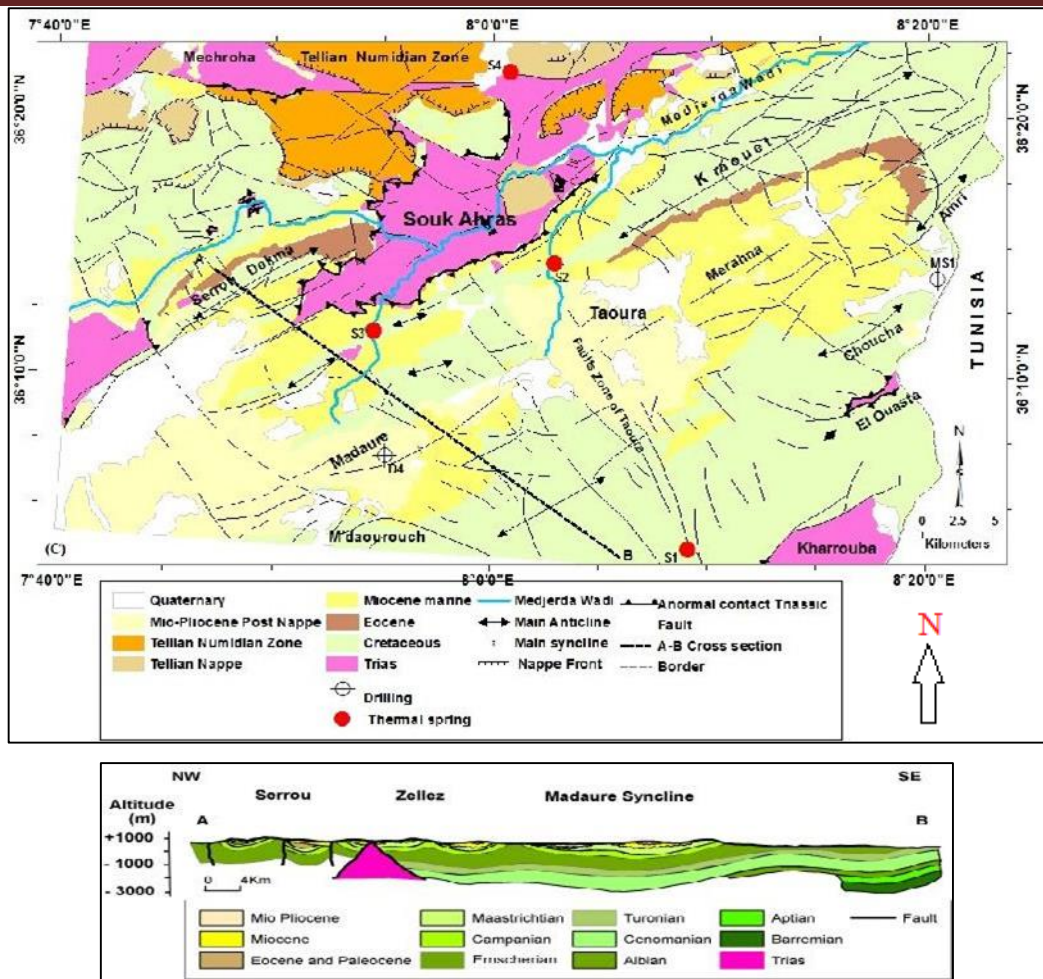


Figure II.05: (C) Simplified geological and structural map of the study area with location of water points used in this study. (D) Geological section.

II.6. Hydrogeological framework

The Souk Ahras aquifer complex is a multi-layered system (Bouroubi Y. 2012) The main hydrogeological reservoirs are:

II.6.1. The marine Miocene aquifer:

The Drill (D4) captures the Miocene sandstone aquifer (0 to 95m) from there, there was no rise in cuttings, it was stopped at (146m) (Strojexport 1977) The autochthonous Eocene aquifer has a few cold springs (<02 L. s-1) at high altitude, they are directly influenced by water from precipitation and snow.

II.6.2. The Maastrichtian-Campanian karst aquifer:

Presents a highly developed aquifer in chalky limestones. It updates several sources with a flow (<15L. S-1) (Bouroubi Y 2011) this aquifer is exploited by boreholes reaching a depth between (150 to 350m).

II.6.3. The Turonian and Aptian aquifers:

To the South and South-East of Taoura, around ten hydrogeological reconnaissance boreholes were abandoned because of the salinity of the water ($EC = 7.2\text{ms / cm}$). They reach the Turonian and especially the Aptian aquifers to a depth ($<250\text{m}$). In the southern part of the study basin, these carbonate formations outcrop at the surface. In 1996, surveys carried out by the Office of Geological and Mining Research - Algeria in the region of El Ouasta (Figure II.05) intersected these formations (327.4 - 562.1m). Some intervals show polymetallic mineralization linked to small cracks characterized by sphalerite (ZnS), galena (PbS), chalcopyrite (CuFeS₂), gray copper, pyrite (FeS₂), barite (BaSO₄) and calcite (CaCO₃). These minerals are often associated with small veinlets filled with bitumen (Haddouche O. 2003). The contact between Aptian and Triassic is characterized by a ferro-barite zone in Celestine.

The deep aquifer: updates thermal springs which all spring up through deep accidents affecting different geological formations. are characterized by a very marked smell of sulfur. In the northern part of the diapirs area there are four main hot springs, each with at least three griffins.

Note that the Miocene sandstone aquifer and the Maastrichtian-Campanian karst aquifer are exploited for drinking water supply, irrigation of cultivated land and some industrial needs. All the productive boreholes cross very karstified zones.

(During their achievements, total losses of drilling mud were reported).



Figure II.06: (A) Gas bubbles. (B) Sulfur near the main grifón of El Demssa.

(Photos: Bouroubi Y. September 2014).

II.7. Climate

The climate of Souk Ahras is influenced by factors that give it specific characteristics. Distant of 80 km from the Mediterranean Sea, the penetration of the marine and wet currents is easy. The town of Souk Ahras is located in a basin

CHAPTER II Presentation and investigation of the study area.

surrounded by mountainous terrain. As a result, the city is characterized by a semi-humid climate. Souk-Ahras is distinguished by a warm summer and a cold and humid winter and rainfall reaches an average of 800 mm per year (www.weatherreports.com).

Table II.02: Climate data for Souk Ahras.

Source: Weather Reports, statistics for 121 years.

Months	Jan.	feb.	mars	April	may	June	Jull.	Aug.	Sep.	Oct.	Nov.	Dec.	Years
Mean minimum Temperature (°C)	3,9	3,9	5,6	6,7	10,6	13,9	16,7	17,8	15,6	11,7	7,8	5	10
Mean Temperature (°C)	8,9	10	11,7	13,9	17,8	21,7	25,6	26,7	22,8	18,9	13,9	10	16,7
Mean maximum Temperature (°C)	13,9	15	17,8	20,6	25	30	35	35	30,6	25,6	20	15	22,8
Precipitations (mm)	111,76	81,28	101,6	71,12	45,72	22,86	2,54	10,16	45,72	104,14	109,22	137,16	840,74

II.8. Seismicity of the region

II.8.1. Regional seismic tectonic condition

The distribution of seismic areas in Algeria is shown on (Figure II.07), this map shows that seismic activity areas are concentrated in northern and northeastern Algeria along the coastal chain between Oran and Annaba, and in the Hodna and Aures region. A third area of activity is found in the Atlas, passing through Gabes in Tunisia, Biskra and Laghouat in Algeria and Agadir in Morocco.

II.8.2. Classification of seismic zones in Algeria

The Algerian Seismic Regulation (version 2003) divides the national territory into five (05) areas of increasing seismicity, defined as follows:

- Zone 0: Negligible seismicity
- Zone I: low seismicity
- Zone (II a – II b): average seismicity
- Zone III: high seismicity

The map of the seismic zones of Algeria and the overall zoning of the different Wilaya is shown on (Figure n°04).

CHAPTER II Presentation and investigation of the study area.

Thus, the consultation of documents and seismic-tectonic maps of the region shows that the epicenters of the tremors are located close to the major and adjacent tectonic discordances to the many small masses of Triassic outcrops in the region. The majority of earthquakes recorded in the Souk Ahras region do not exceed a magnitude of five (05) on the Richter scale.

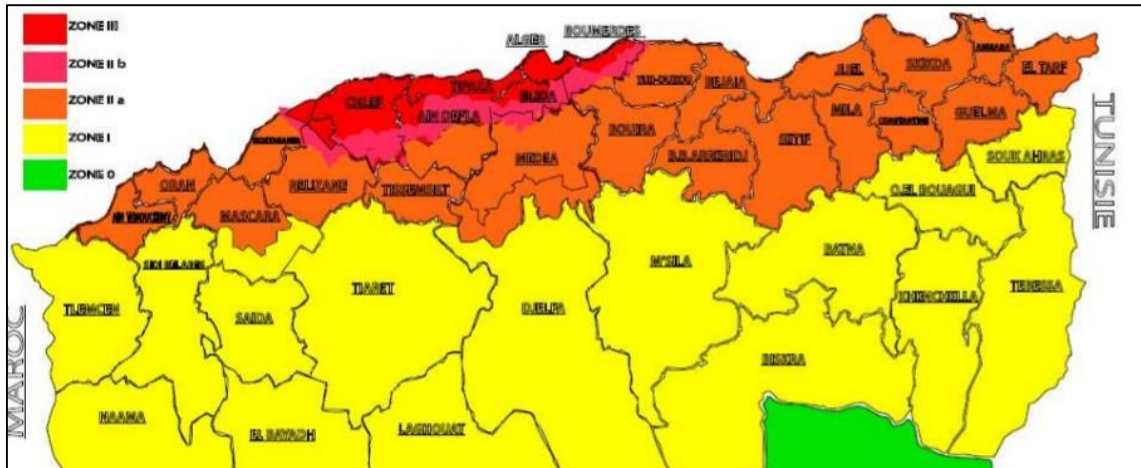


Figure II.07: Classification of seismic zones in Algeria 2021

March 18, 2021(Elkhabar Newspaper 18/03/2021)

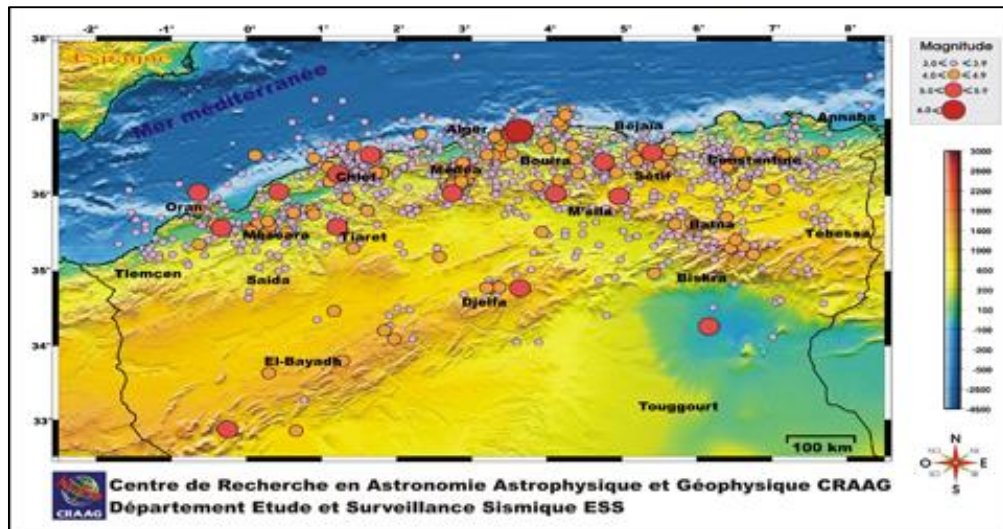


Figure II.08: Seismicity of North Algeria

II.9. General geological overview

The general geology of northern Algeria is marked by two chains going from north to south: The Alpine chain known as the Maghrebids and the Atlasic chain.

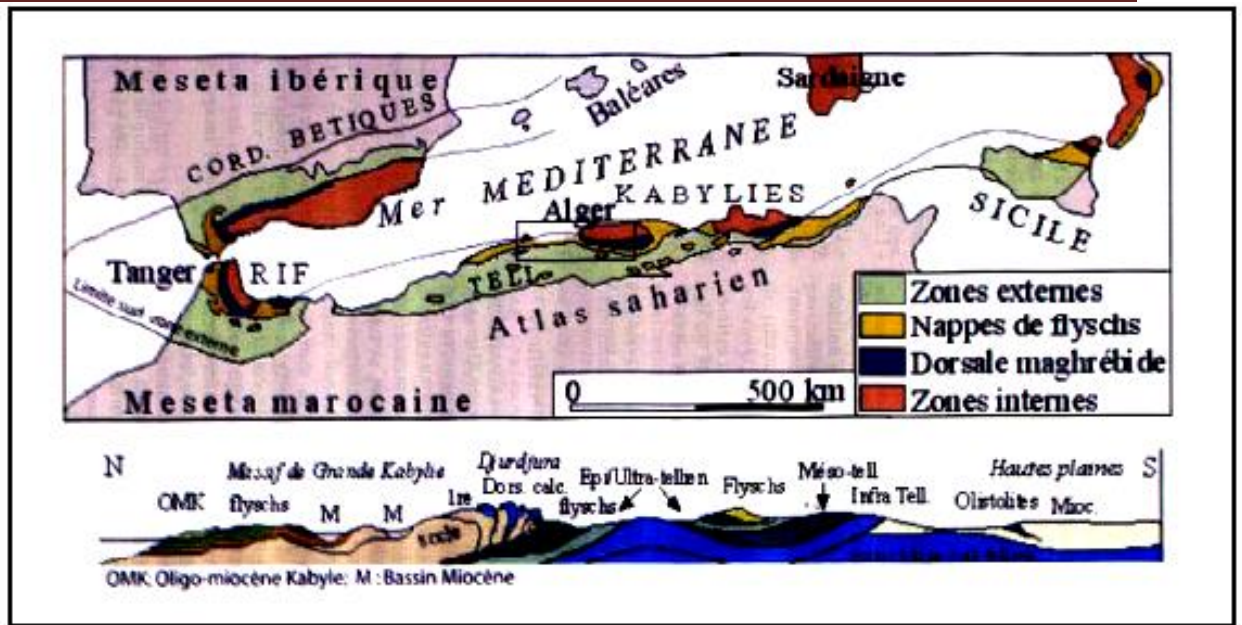


Figure II.09 : Structural diagram of the Maghrebids
(based on M.Durand-Delga and J. M. Fontboté, 1980)

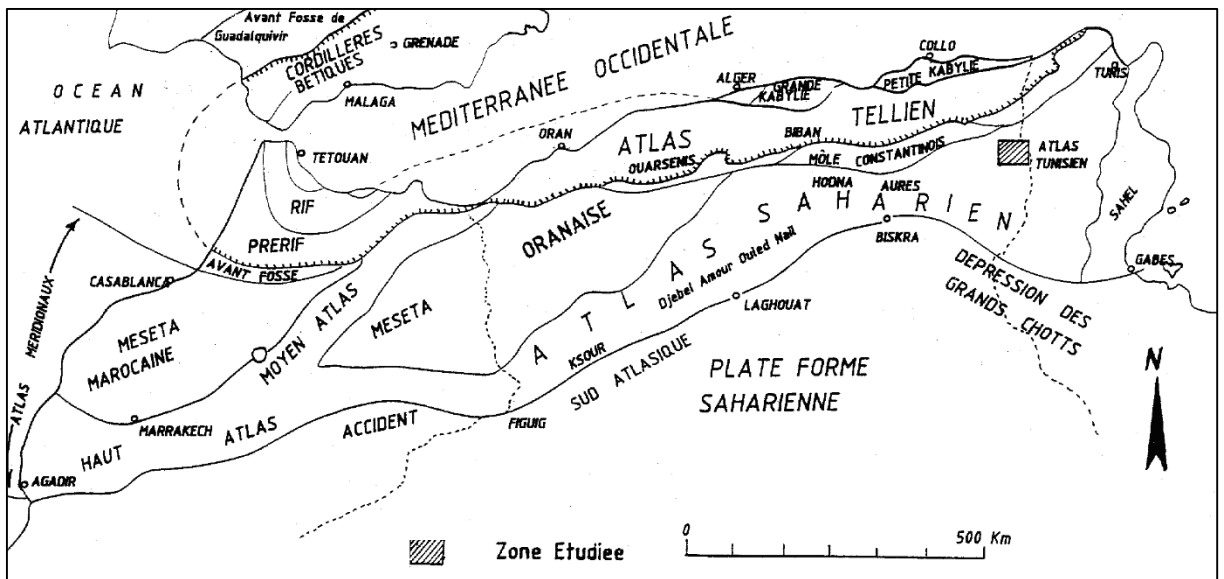


Figure II.10 : Main structural units in North Africa
(after Cairo, 1967)

The study area is part of the Maghrebi Chain (figure II.09 and II.10) which extends from the Strait of Gibraltar to the North of Calabria (Italy) over a length of more than 1,000 km, passing through the Moroccan Rif, the Tell littoral of Algeria (Kabylie and Tell), Tunisia (Kroumirie and Nefza) Sicily and finally Calabria. This chain is caught between the plate Africa in the south and the plate Europe in the north, it is characterized by a tectonic stacking of layers.

CHAPTER II Presentation and investigation of the study area.

Its country front is complex, it comprises: basins of chain front, slightly deformed areas (high plateaux), another orogenic building: The atlasic system (Atlas saharien, Aurès), and more to the south, the Saharan platform stable.

From North to South, the Maghrebid chain consists of three main groups:

The internal domain, the flyschs domain and the external domain.

II.9.1. The internal domain

It consists of ancient crystallographic sites of varied nature (Kabyle base) surmounted by a little metamorphic paleozoic. Many authors admit that the various internal massifs of the Maghrebid chain (internal Betico-Rifaine zones, Kabylies, Péloritain massif of Sicily, Calabrian base) were initially grouped into a single block, called the AlKaPeCa (Bouillin, 1986). This complex, probably emerging during part of the Mesozoic and up to the Oligocene, was bordered to the south by a continental margin Jurassic and Cretaceous whose sections rifains, kabyles and Péloritains of the Maghrebid limestone chain are witnesses.

II.9.2. The flyschs domain

It is made up of a set of rubbish sheets, which have an external character in relation to the dorsal (Raoult, 1974). These are flyschs-type deposits ranging from the Lower Cretaceous to the Oligo-Miocene. From the North to the South of the basin, we distinguish flyschs: Mauritanian flyschs and flyschs massyliens, different from each other by their primitive position and by their diet.

The ensemble is surmounted by the Numidian of Oligocene age at Lower Burdigalien. The latter filled a depression that was the heir to the Cretaceous-paleogenic flyschs basin.

II.9.3. The External Domain (Tablecloth Domain)

The Tellian units form a complex pile-up of southerly vergence aquifers that surmount the pre-Saharan native high plains (high and rigid areas that separate the coastal chains of the Saharan Atlas) to the south.

Tellian allochthone results from the detachment and cleavage of the mesozoic–cenozoic sedimentary cover deposited on the northern margin of the Africa plate. In eastern Algeria and the Algerian-Tunisian borders, we distinguish from north to south:

II.9.3.1. Ultra tellian units S.S. (sensu-stricto)

They were defined in Djebel Bou-Sba, north of Guelma, by Vila (1986) and north of kef Sidi Driss by Raoult (1968). They have a marl-limestone character (clear face of a high background) and they appear everywhere inverted (Cretaceous age - infra lutetian).

II.9.3.2. The tellian set

This is a complex pile-up of carbonate layers. These units are likely deposited in the deep reaches of the Tellian trench. In the field of study, this set is represented by series marl limestone of paleogenic age, it is the Suesonian of the authors, with a Ypresian very rich in Globigerins.

II.9.3.3. Southern units (with nummulite limestone)

These units are composed, on the one hand, of the southern Settifian layers, and on the other, on the East, of the shavings of Djebel Bardou, and of the southern slope of Zouara, of the klippen of Dekma and Djebel Bou Kebch. The Cretaceous is absent in these units in favor of the limestone Eocene (Lower Ypresian-Lutetian) rich in nummulites and the marly Eocene (Upper Lutetian) to oysters.

II.9.4. Allochthonous or Para-Aboriginal countries

II.9.4.1. The Constantinoises Neritic Series

The necritical series appeared at the level of Constantine, Ain M'lila, Hammam Debagh and Guelma. These formations appear over 160 km E-W and 80 km from North to South. For Vila (1980), this domain would have emerged at the end of the Cretaceous period and would have subsequently undergone a slight displacement to the south (Constantinese neric tablecloths).

II.9.4.2. The scaly furrow of Sellaoua

These formations were deposited in a wide path of direction NE-SW, located between the Atlasic platform in the South and the alpine domain in the North. They do not outcrop at the foot of the necritical series, they are found in the regions of Ain M'lila, Ain Babouche, Ain Fakroun, Chebket Sellaoua and they spread widely from Ksar Sbihi to Souk Ahras. It is a powerful and monotonous marl and marl limestone ensemble dominated by the Cretaceous.

CHAPTER II Presentation and investigation of the study area.

Chadi (1993) believes that Constantine's nephritics and the Sellaoua series come from the same field.

II.9.5. Post-Priabonian Stratigraphic Ensemble (Vila, 1980)

These are syntectonic detritic formations, linked to the tangential phase priabonine and subsequent to it, this ensemble brings together the transgressive detritic series of the Oligo Miocene kabyle, the Numidian, the mixed series, Tellian Oligo-Miocene and post-layer series such as continental Miocene.

II.9.6. The "post-water" basins

Discordant basins, posterior to the great overlaps of the internal zones, flysch and tellian layers formed on the whole of the chain from the Langhien. Such basins are found in the internal areas of Petite and Grande Kabylie. They are little deformed but have nevertheless recorded, by fracturing, a succession of tectonic episodes. Other basins extend over the external zones: basins of Constantine, Soummam, Chélif and Guelma and Hammam N'bails. They underwent Miocene to Quaternary age deformations (folds, small overlaps, fracturing) greater than those of the basins of the internal zones.

II.9.7. The neo-gen magmatism

Finally, magmatic phenomena developed along the Algerian coast. They are particularly developed in Petite Kabylie, where granitoid massifs were established from 16 Ma, but volcanic episodes of various ages affect the entire coastal zone, from Langhien to Pliocene-Pleistocene.

This calco-alkaline magmatism (Semroud, 1980) occurs in the following regions:

Bejaia-Amizour (Diorites, microgranites, granodiorites and volcanic complex), El Aouana (diorites and microdiorites associated with volcanic rocks), Kabylie de Collo (granites, microgranites, monzonites, gabbro and rhyolites), Dj Filfila (Granites) and Cap de Fer and Edough (diorites, andesites, rhyolites and microgranites). This magmatism is most often accompanied by hydrothermal phenomena to which are linked most of the polymetallic mineralization of the northern part of North East Algeria (Aissa, 1996; Graine, 1999; Benali, 1993; Laouar, 2002).

II.10. Structural synthesis of the maghrebid chain

The Triassic period was followed by the tertiary tectonic phases during which the Maghrebid were structured.

II.10.1. The finite lutevine or atlasic phase (Priabonienne)

Marks the end of the sedimentary cycle. This phase began in the upper trias with local tectonic manifestations of low sedimentation impact (Obert and Leiken, 1974; Chadi, 2004). This compressive phase is explained by the closure of the Western Tethys during the rotation of Africa around a pole located west of Tangier, leading to the collision between the eastern part of the Alboran and the Tellian African margin.

- This phase is associated with vertical NE-SW steering accidents.

II.10.2. Miocene phases

These phases mark the end of the building of the tell by a generalized compression of the structures

II.10.2.1. The burdigalienne phase

It marks the beginning of the north-south shortening. The western part of the Alboran lake continues its westward migration, colliding with the Rifaine margin of Africa. This migration contributes to the opening of the northern Algerian basin. The tectonic effects are:

- advancing the numidin tablecloth southward and forming kabyle olistostomes in a northern depression;
- a bulge at the level of the southern kabyle edge or had previously piled up the units of flyschs on the Tellian layers at Priabonien;
- folded structures in the south of the kabyle domain.

II.10.2.2. The tortonian phase

In the late Lower Miocene and early Middle Miocene, inlets invade gulfs in the northern part of the Algerian chains. In the Babord, the first post-water-table marine sediments were deposited. In addition to this transgression, there was an alkaline volcanic phase and a plutonism that set up granitic intrusions in large kabylia, in Babor

CHAPTER II Presentation and investigation of the study area.

and small kabylia. The radon metric datations indicate ages 12 to 16 MA, corresponding to the basal Langhien-Tortonien (Benabbes 2006).

In the upper basal Miocene, the tortonian phase continues with a vast north-south shortening and the crushing of the structures by approximation of the borders, these tectonics has had the effects of overlapping southward of the southern units,

South Sestifian and Sellaoua scales, involving posterior formations to the upper Burdigalien. In far eastern Algeria, this tangential phase has caused scaling and drop-head structures.

- The post-tectogenic Plio- Quaternary period

The post-tectonic period extends from the upper Miocene to the Plio–Quaternary and is the subject of neotectonic history referring globally to the movements of plates (Iberia, Africa) and the opening of the Alboran Sea.

In the framework of this work, one will be limited, on a point scale, to the effects, such as compressive and distensive movements and the rejuvenation of the large structures causing collapses.

II.11. Conclusion

Overall, the structures of the front country are quite complex. For example, at the approaches to the Tunisian border, in the southern part of the Souk Ahras region, are individualized reliefs composed of syncline plains cloistered by anticline, and compartmentalized by faults and accidents. This set of structures constitutes globally vast folds quite singular.

On a regional scale, the region of Souk Ahras, which belongs to the domain of the high plains, is located in the forepit of the tello-rifaine chain. Mesozoic carbonate marl intercalation sites of varying thicknesses were extensively fractured and deeply folded. Synclinals thus constitute vast depressions filled with essentially heterogeneous tertiary sediments of continental type.

The geological framework indicates, in hydrogeological context, that the synclinal of the Taoura would constitute a hydrogeological unit, with aquifers developed in the cracked mesozoic carbonates and in the coenozoic continental formations. Due to the intensity of fracturing, with varying sizes, this aquifer assembly could exhibit systemic functioning.

**Chapter III:
Calculations
methods of slopes
safety factor.**

III.1. Introduction

The purpose of the slope stability calculation is to look for the minimum value of the safety factor, and to repair the most likely fracture surface corresponding to that value.

There are two main methods of calculating slope stability:

- Methods based on limit equilibrium
- Finite element methods.

III.2. Slope stability calculation methods

Ground stability calculation methods are based on the following observation: When there is a landslide, a ground mass is separated from the rest of the terrain and the landslide occurs following a fracture surface. Having defined a fracture surface "S", we study the stability of the mass (1) mobile relative to the mass (2) which is fixed (Figure III.1).

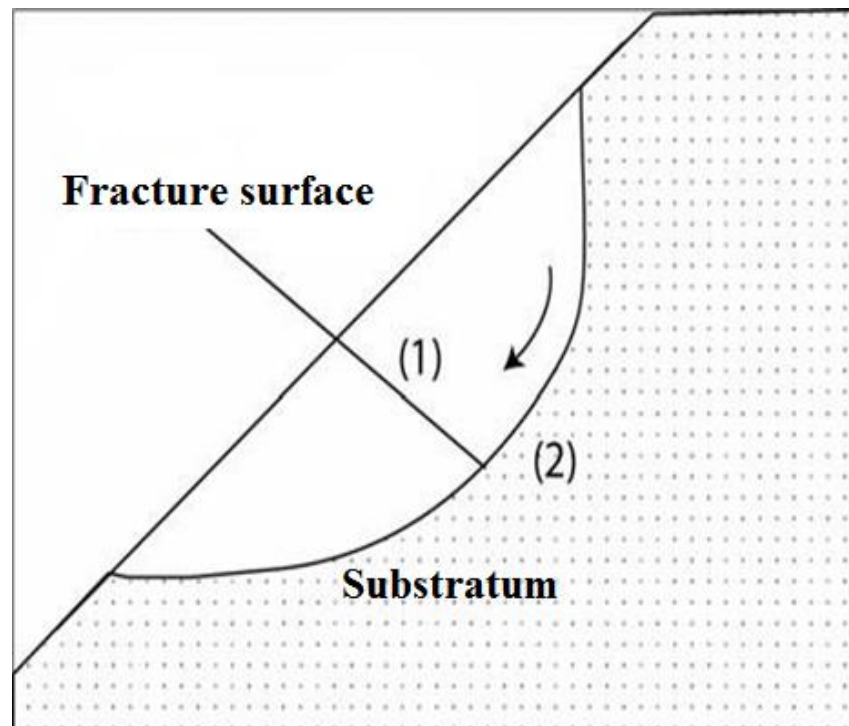


Figure III.01: Fracture surface (CFMS. 1995).

III.2.1. Safety Factor Calculation

The calculation of slope stability is generally estimated using a factor called safety factor (Fs). This factor is defined as the relationship between the driving force and the resistant force. The stability of the slope can be assessed by reference to the safety factor values as shown in Table III.1 below (Blondeau F. 1976).

Table III.01: Slope balance based on theoretical safety factor values

Chapter III Calculations methods of slopes safety factor

(Blondeau F. 1976).

Safety factor F_s	State of the work.
$F_s < 1$	Danger.
$F_s = 1$	Limit stability
$F_s \in] 1, 1.25 [$	Questionable security.
$F_s \in] 1.25, 1.40 [$	Satisfactory safety for minor works but by Against this is questionable security for the slopes of open quarries.
$F_s > 1.4$	Satisfactory security

At the end of the experiments a classification was proposed by the International Society of Rock Mechanics in Table III.02 below:

Table III.02: Slope equilibrium based on experimental safety factor values

(Blondeau F. 1976).

$F_s < 1$	Unstable slope.
$1 < F_s < 1.5$	Possible slippage.
$F_s > 1.5$	Generally stable.

III.2.2. The safety factor vis-a-vis fracture

The most common methods used to assess the stability status of a slope are called "slice-by-slice" fracture calculation methods.

They consist in considering the forces which tend to retain a certain volume of rock delimited by the free faces of the slope and a potential fracture surface, and the forces which tend to set it in motion.

The calculations are made for a large number of possible sliding surfaces in order to find the minimum safety factor corresponding to the most critical sliding surface (Blondeau F. 1976).

Note: A value of the safety factor between 1,1 and 1,3 is generally considered as an acceptable criterion for with regard to large-mass slippage is ensured to the extent that the mechanical and hydraulic behavior of the rock is checked, (F_s) between 1.1 and 1.3 is low compared to the values adopted for road embankments or dams, for obvious economic reasons.

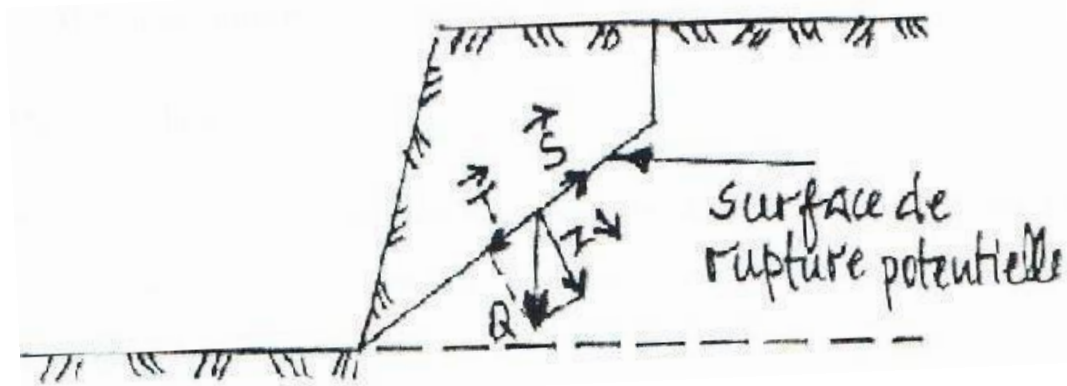


Figure III.02: Potential fracture surface (Blondeau F. 1976).

III.3. Methods of fracture calculation

The analysis of the stability of earthworks is traditionally carried out by means of methods of calculation at break which give by safety factor(F_s) The main methods of calculation of slope stability are:

- Methods based on limit equilibrium;
- Geometric (or stereographic) method;
- Finite element methods;
- The methods of the abacus.

III.3.1. Limit Equilibrium Methods

In routine geotechnical analysis, the use of limit equilibrium (LE) methods with a Mohre Coulomb failure criterion tends to be the preferred option to examine the failure initiation of slopes using a 2D approximation that corresponds as closely as possible to the worst credible scenario, and there are various commercial software packages available to do this.

The advantage of the (LE) approach is twofold:

- First, the analysis is simple and parametric studies can easily be undertaken.
- Second, the Mohre Coulomb strength parameters are relatively easy to obtain: by back analysis of a known failure (i.e. By varying the material strength and/or pore pressures and setting the factor of safety to unity); by material strength testing in a shear box, triaxial test, or ring shear; or by carrying out index testing (e.g., Atterberg plastic and liquid limits for clay) and using published correlations of these indices with shear strength (Mitchell and Soga, 2005; Muir Wood, 1990). With known parameters, the factor

Chapter III Calculations methods of slopes safety factor

of safety, defined as the ratio of resisting forces to driving forces within the slope may be determined, and this is easily communicated as a concept to non-specialists.

The disadvantages of (LE) methods are that pre-failure deformations are notable to be modeled, that the user must specify the failure mode (rotational, planar, or wedge-type) and then which method to use to analyze the failure (e.g., Bishop's or Spencer's methods of slices for rotational failures; Janbu or Sarma's method for non-rotational failures), and that resisting forces provided by retaining structures or reinforcing elements may not be modeled well. Neither are three-dimensional situations easily dealt with.

The equation of the problem of the equilibrium of a soil mass can be made by breaking down the slope into slices whose individual equilibrium is first studied before globalizing the result by involving certain simplifying hypotheses. This is the "Slice Method" (Bendadouche.H et al. 2013).

III.3.1.1. Slice Method

This method consists of considering the forces that tend to retain a certain volume of land, delimited by the free forces of the slope and a potential fracture surface, and those that tend to set it in motion (Ahmed. A, 2012).

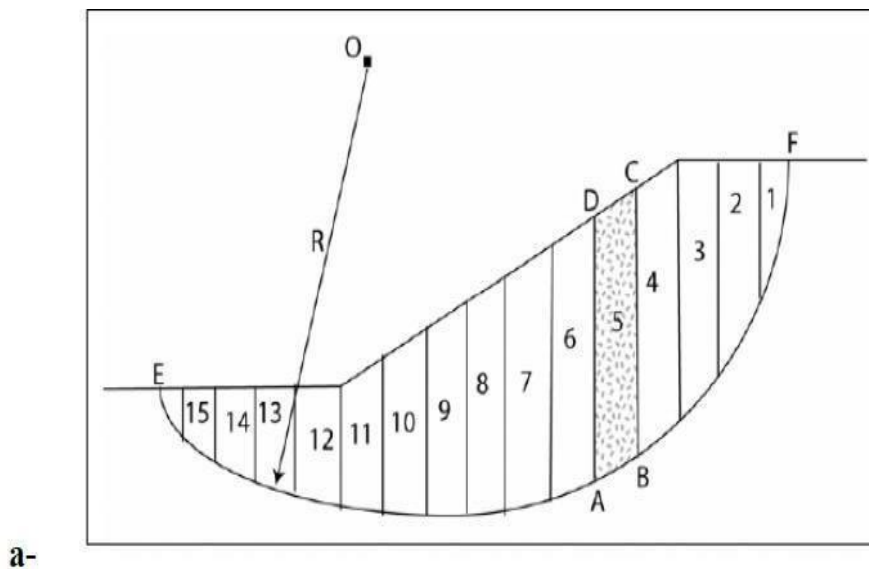


Figure III.03: Cutting of a bank into slices and forces acting on a slice (Bendadouche.H and al. 2013).

III.3.1.2. Fellenius Method (1936)

Also known as the Swedish method, it is considered that:

Chapter III Calculations methods of slopes safety factor

- The sliding line is circular in shape;
- There is a total neglect of inter-tranche efforts;

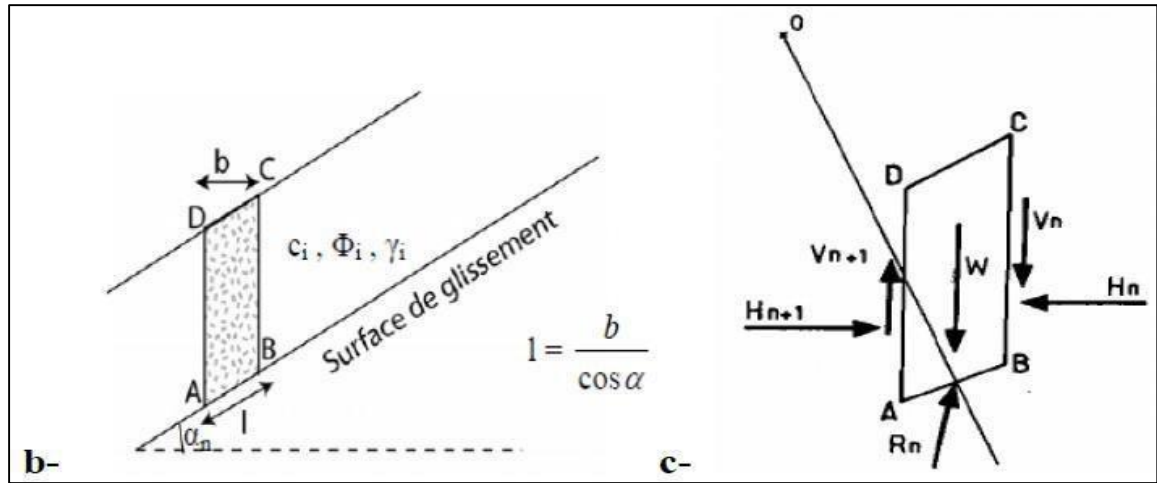


Figure II.04: The forces acting on a slice

(www.pentestunnels.eu/enseignement/.../ac1_calcul_stabilité_pentes.pdf)

- The only force acting on the arc AB is the weight W. Relative to the center O, one can define:
- The driving moment as that of the weight of the terrain W tending to cause the slip; The maximum strength moment provided by the maximum value that can take the tangential component of R (Figure III.05).

According to Coulomb's law:

$$R_n = c_n \cdot AB + N_n \cdot \tan \Phi_n \quad (1)$$

In addition: $N_n = W_n \cos \alpha_n$ (2)

Therefore: $R_n = c_n AB + W_n \cos \alpha_n \tan \Phi_n$ (3)

Furthermore: $AB = l_n = bn / \cos \alpha_n$ (4)

The sum of the maximum resistance moments is thus written:

$$\sum Rm_1 * (c_i \cdot b_n / \cos \alpha_n + W_n \cos \alpha_n \tan \Phi_i) \quad (5)$$

Where: m = total number of slices.

C_i, ϕ_i = mechanical characteristics of the layer in which the arc AB is located.

The driving moment is due to T and equal to $T_n \cdot R_n$.

Moreover: $T_n = W_n \sin \alpha_n$ (06)

By replacing (05) and (06) in the formula of F_s , we obtain the expression of the factor

Chapter III Calculations methods of slopes safety factor

of security:

$$FS = \frac{\sum_{n=1}^m (c_i \frac{b_n}{\cos \alpha_n} + W_n \cos \alpha_n \tan \Phi_i)}{\sum_{n=1}^m W_n \sin \alpha_n} \quad (07)$$

Or:

- b, the width of the slices.
- α , the oriented angle of the radius of the circle passing through the middle of the base of the edge with the vertical.
- the height of the slice for the calculation of the weight W.

This method shows that it is a direct method of calculating (Fs) by checking only the equilibrium of moments with respect to a center O of the sliding circle (Ahmed. A, 2012; Fellenius, W. 1936).

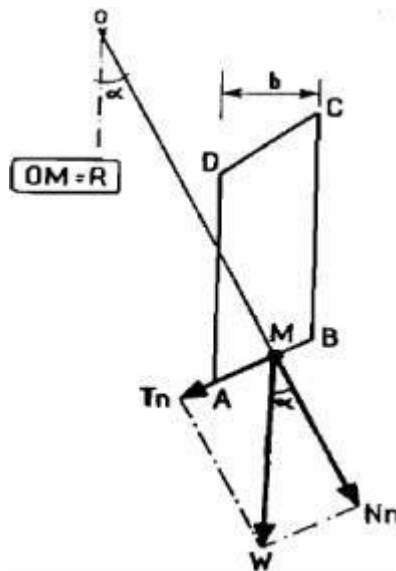


Figure III.05: Forces acting on a slice according to the Fellenius hypothesis (Fellenius, W. 1936; AHMED. A, 2012).

III.3.1.2.1. The forces acting on a slice according to the hypothesis of fellenius

- **Force of gravity (self-weight of the slice)**

The force of gravity is applied to the center of gravity for each slice. It is given by the following formula:

$$W = b \sum (\gamma_i h_i) \quad (08)$$

With:

W: self-weight of the slice

b: width of a slice

Chapter III Calculations methods of slopes safety factor

h_i : slice heights

The weight « W » being a force which has two components:

$$N = W \cos \alpha \quad \text{and} \quad T = W \sin \alpha \quad (09)$$

N: stabilizing normal component

T: destabilizing tangential component to the sliding circle.

- **Cohesion force**

$$F_C = C \cdot AB \quad (10)$$

with:

$$AB = \frac{b}{\cos \alpha_i} \quad (11)$$

C: cohesion of the soil considered.

α : the oriented angle made by the radius of the circle passing through the middle of the base of the slice with the vertical

b: the width of the slices

AB: length of the arc delimiting the base of the slice.

- **Friction force**

$$F_f = (N - U_i \cdot AB) \tan \varphi = (W \cos \alpha - U_i \cdot AB) \tan \varphi \quad (12)$$

- **Water force**

$$U_i = \gamma_w \cdot h \cdot AB \quad (13)$$

- **Seismic force**

$$T = a \cdot W \quad (14)$$

With:

W: slice weight

a: coefficient of acceleration of seismic zone.

The expression of the safety factor:

$$Fs(\text{without earthquake}) = \frac{\sum_1^n \left(C_i \frac{b}{\cos \alpha_i} + (W \cos \alpha_i - U_i) \tan \Phi_i \right)}{\sum_1^n W \sin \alpha_i} \quad (15)$$

$$Fs(\text{with earthquake}) = \frac{\sum_1^n \left(C_i \frac{b}{\cos \alpha_i} + (W \cos \alpha_i - U_i) \tan \Phi_i \right)}{\sum_1^n W \sin \alpha_i + \frac{1}{R} \sum (W \cdot a \cdot dn_i)} \quad (16)$$

dn_i : distance between the center of gravity of the slice and the center of the sliding

circle.

III.3.1.3. Simplified Bishop method (1954)

In this method it is considered that:

- The sliding line is always circular; The inter-unit vertical forces are zero

$$(V_n - V_{n+1} = 0) \quad (17)$$

- The safety factor is given by the following formula:

$$FS = \frac{\sum_{n=1}^m (C_i b_n + W_n \tan \varphi_i)}{m \alpha \sum_{n=1}^m W_n \sin \alpha_n} \quad (18)$$

Where

$$m_\alpha = \cos \alpha_n [1 + \tan \alpha_n \tan \varphi_i / FS] \quad (19)$$

To determine FS , it is necessary to proceed by successive iterations. The first iteration is made by adopting, as a value FS , the safety factor obtained by the Fellenius method. It is therefore an indirect (or iterative) method and it only checks the equilibrium of moments, just like the Fellenius method (does not check the equilibrium of forces) (Bishop, A.W. 1955).

III.3.1.4. Janbu Method (1956)

The generalized Janbu method (Janbu 1973) considers the two inter-unit forces and assumes a push line in order to determine an inter-unit force relationship. Therefore, the safety factor becomes a complex function:

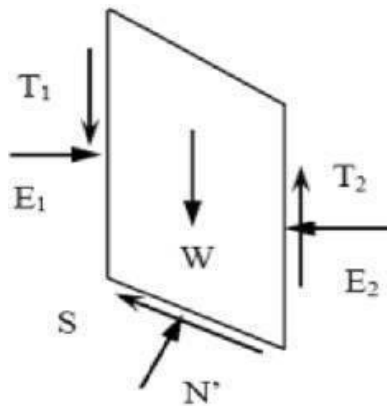


Figure III.06: The forces applied for the Janbu method (JANBU 1973).

$$F_{S_0} = \frac{\sum_{n=1}^m \left(b_n \tan \varphi_i \left(c_i + \left(\frac{W_n}{b_n} - U \right) \right) / n \alpha \right)}{\sum_{n=1}^m W_n \tan \alpha_n} \quad (20)$$

with

$$N\alpha = \cos^2 \left(1 + \tan \alpha_n \frac{\tan \varphi_i}{F_{S_0}} \right) \quad (21)$$

- $\frac{W_n}{b_n}$: is the total vertical stress
- b_n : is the width of slice n;
- α_n : the inclination of the sliding surface in the middle of section n;
- U: pore water pressure.

It can be noted that the Janbu method satisfies the equilibrium of forces and considers the normal inter-slice forces E. It is an indirect method (iterative, since F_{S_0} is on both sides of the equation). It is generally used for a compound shear surface (general sliding surface; (Figure II.06).

Janbu introduced a correction factor (F_0) in the original safety factor to compensate for the effects of inter-slice shear forces. With this change, the Janbu method gives more important safety factor values F_s , such as:

$$F_s = f_0 F_{S_0} \quad (22)$$

The correction factor depends on the depth-to-length ratio of the fracture surface (d/L) (Figure I.07). The factor of safety, with this correction factor, can increase by 5 to 12%, giving a lower margin in the case of friction alone (Janbu 1973).

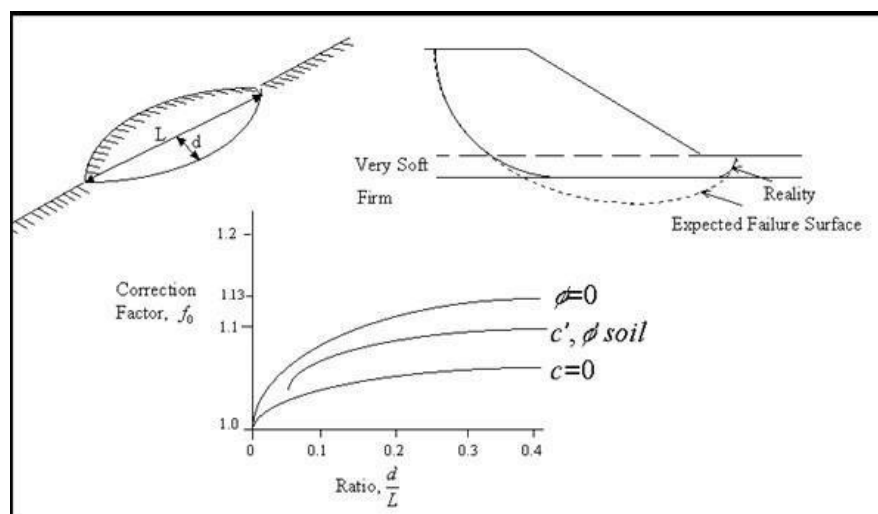


Figure III.07: Variation of the correction factor as a function of depth and length (Janbu 1973).

III.3.1.5. Morgenstern and Price Method (1965)

Morgenstern and Price define a function giving the inclination of the inter-unit forces, this method introduces an arbitrary mathematical function to represent the variation of the direction of the forces between the units:

$$\tan \theta_i = X/E = \lambda \cdot f(x'_i) \quad (23)$$

Where:

θ_i : is the angle formed by the resultant and the horizontal, it varies systematically from one slice to another along the sliding surface;

λ : is a constant that must be evaluated for the calculation of the safety factor;

$f(x'_i)$: is the function of variation in relation to the distance along the sliding surface;

x'_i : is the linear normalization of the xi coordinates, with the values of the two ends of the fracture surface equal to zero and π .

This method satisfies all the static equilibrium conditions for each slice, as well as the equilibrium of moments and the equilibrium of forces in the horizontal direction, for the whole mass that slides along a circular or non-circular fracture surface (Morgenstern, N. R. & Price, V. E. 1965).

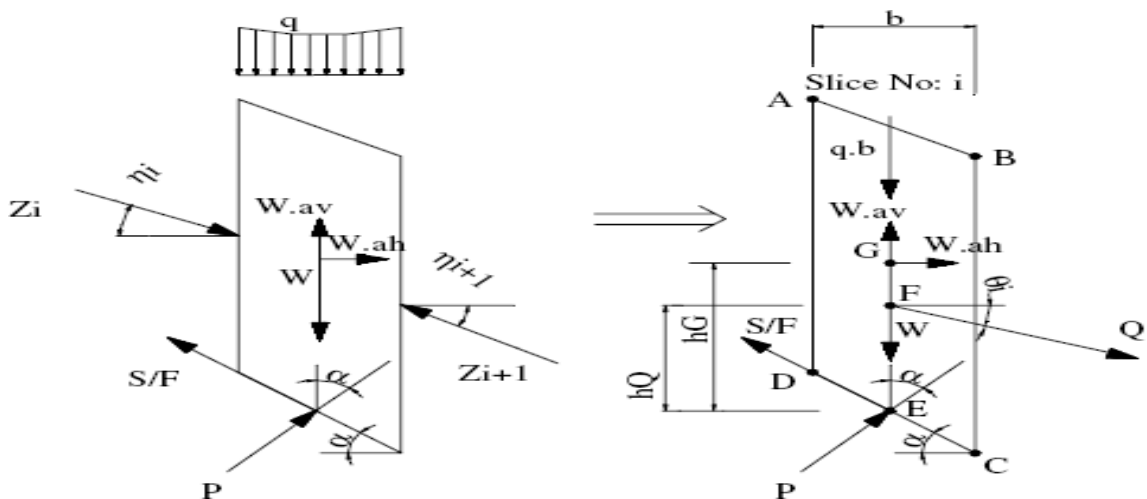


Figure III.08: Representation of forces on a slice using the simplified method of Morgenstern and Price.

III.3.1.6. Reverse Analysis Method (Return to Experience)

Parker and Sant amarina introduced the concept of reverse analysis for geophysics and geotechnical engineering. They describe two types of approaches to solving inverse problems

- The reverse analysis approach by reverse analytical method, schematized in Figure (III.09 (a));
- The reverse analysis approach by direct numerical method, shown in Figure (III.09 (b)).

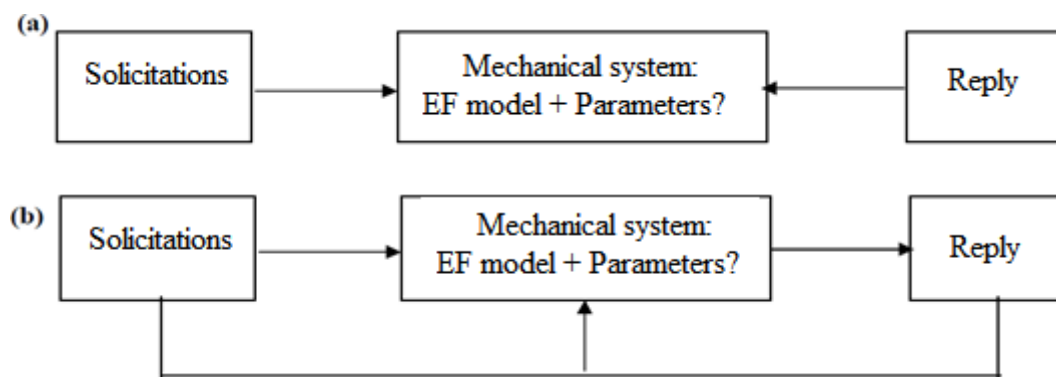


Figure III.09: Diagram of the principle of inverse analysis by reverse analytical method and by direct numerical method (b) (Colas G. & Pilot G.).

Typically, a problem is said to be well established if the stresses, boundary conditions and soil parameters are known. If the system is stable, then the response of the model is unique. The opposite problem can then be solved analytically in figure (III.09 (a)) (Colas G. & Pilot G.).

The analytical inversion of the problem is a method that can be used in geotechnics. Geomechanical systems and associated models are complex and strongly non-linear. Behavioral equations are irreversible. All of this makes the inverse solution not unique, if not non-existent, when an exact solution is sought.

Moreover, the parameters that must be introduced in geotechnical calculations are often poorly known. To this are added the uncertainties about the stresses and the conditions at the limits as well as the error that can introduce the hypotheses and approximations of the mechanical model used, so finding an analytical solution becomes difficult. The solution is sensitive to data and data errors. Maier and Gioda show that a resolution by direct minimization between in situ measurements and corresponding

numerical quantities is preferable since it avoids the inversion of stress analysis equations (Colas G. & Pilot G.).

III.3.2. Finite element method

The method of calculation by finite elements has known a very important development essentially through its application to the calculation of structures, it is considered as one of the tools of resolution of the equations with the partial derivatives of the mathematical physics. Moreover, the progress of data processing and its democratization make that today the numerical simulation is not any more the business of the large industrial groups but concerns more and more the small and medium-sized companies.

Thus, the digital tools become within the economic and technical reach of the latter and often constitute a major asset, even unavoidable for their development. This generalization of simulation methods currently affects a wide range of scientific disciplines and many technical or technological sectors.

The finite element method is one of the most widely used numerical simulation methods today. It consists in using a simple approximation of the geometry and of the variables describing the physical phenomenon such as displacement, temperature... in order to reduce the continuous problem with an infinite number of unknowns to an algebraic system with a finite number of degrees of freedom. It calls upon the following three domains:

- Engineering sciences for the mathematical formulation of the physical problem, often described by a system of partial differential equations.
- Numerical and functional analysis methods for the construction of the algebraic system to solve.
- Computer techniques for the execution of the simulation calculations.

The use of the finite element method has been developed for about sixty years through the analysis of structures via assemblies of bars or beams whose behavior was dictated by the assumptions of the strength of materials. The emergence of computer science and industrial needs led to a rapid development of the method through a reformulation based on energy considerations on the one hand, and the creation of elements of high geometric and physical precision on the other hand.

Since 1960, the finite element method has been recognized as a general tool for solving linear or non-linear, stationary or non-stationary physical problems not only in

the field of structures but also in other fields such as soil mechanics, fluid mechanics, thermic, electromagnetism.... The use of this method has thus spread, during the last decades, in various industrial sectors such as aeronautics, shipbuilding, automotive industry and in fields related, among others, to the mechanics of materials and structures.

In structural design, the use of the finite element method contributes efficiently to the optimization of structures subjected to static or dynamic loads.

III.3.2.1. Principle of the finite element method

The finite element method is a nodal approximation method based on the discretization of the domain into subdomains or elements. The method is a set of consecutive approximations of the geometry, the physical variable and the mathematical integration on the domain (Dhath.G & Touzot.G 1984).

- The geometric approximation which consists in the discretization of the domain (mesh) in small elements of well-defined geometry.
- The approximation of the physical variable (nodal approximation) in the element by the values of this variable in the nodes of the element.
- The mathematical approximation by considering that the integration on the domain is equal to the sum of the integrals on the elements and by using numerical integration (Gauss for example).

All these approximations can be summarized in the following steps:

- Define the nodes and elements (create the mesh).
- For each element, establish the elementary stiffness matrix R_e relating the nodal degrees of freedom (displacements) u_e and the forces f_e applied to the nodes:

$$R_e u_e = f_e \quad (24)$$

- Assemble the matrices and elementary vectors into a global system $RU = F$ so as to satisfy the equilibrium conditions at the nodes.
- Modify the global system taking into account the boundary conditions.
- Solve the system $R U = F$ and obtain the displacements U at the nodes.
- Calculate the gradients (heat fluxes, strains and stresses) in the elements and the reactions at the nodes on which the boundary conditions are imposed (Zhi-Qiang F. et al. 1999).

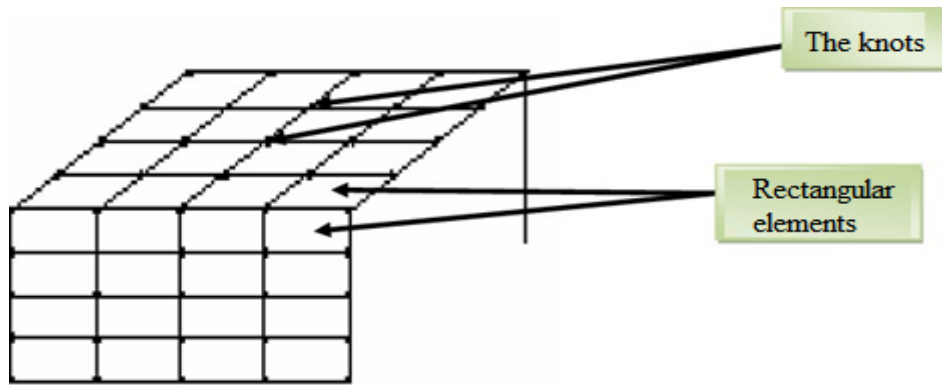


Figure III.10: Meshing of a domain in finite elements

It is useful if the unknowns are physical parameters. This is why we choose the displacement components of the nodes (nodal displacements). For example: (u_i, v_i, w_i) for node i

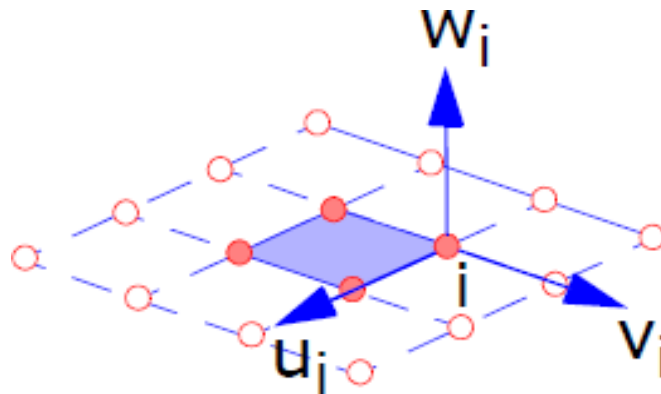


Figure III.11: (u_i, v_i, w_i) are the nodal displacements, $i=1 \dots n$.

The structure to be studied is replaced by a set of elements supposedly linked to each other at a finite number of points called "nodes". These nodes are located at the corners of the elements or all along their border; as shown by

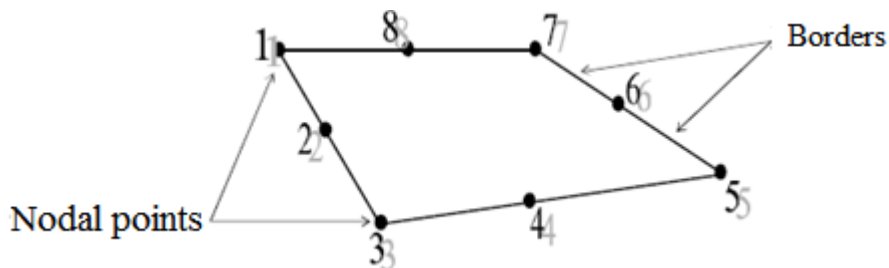


Figure III.12: Element (Q8)

III.3.2.2. Current status of the finite element method

III.3.2.2.1. The practice of the finite element method

(FEM) is based on complex theoretical foundations and uses fairly high-level

mathematics. At the same time, at the practical level, (FEM) is nowadays well implemented in many commercial (CAD) (Computer Aided Design) software and modern engineering processes use it intensively for the calculation of all kinds of structures. The integration of (FEM) into engineering processes affects all phases of the product development cycle (preliminary engineering, solution finding, detailed engineering, preparation for manufacturing, etc.). In particular, this integration has a very important impact on the context in which physical prototyping is used. On the other hand, the important research efforts in the field of (CAD) during the years 1990-2000 have made it possible to implement interfaces which, at first sight, make the use of this kind of technology increasingly easy, even for non-specialists. On this subject, we can mention in particular the extremely important progress made in recent years in the field of automatic meshing (automatic cutting of (CAD) geometry into finite elements) and in the field of error estimators (procedures that allow the estimation of the order of magnitude of the error of a (FE) calculation with respect to the exact solution). Thanks to these advances, it is now possible to perform some (FE) calculations from a 3D (CAD) model in a few minutes whereas the same operation would have taken several days a few years ago (Jean-Cristophe G. 2011).

III.3.2.2.2. Difficulties in the practice of the finite element method

These appearances are nevertheless deceptive because the method relies, as mentioned above, on complex theoretical bases that must be mastered in order to carry out calculations in an enlightened manner and thus obtain realistic calculation results. Moreover, the increasingly frequent use of this type of technology by non-specialists or inadequately trained personnel is beginning to be a source of very serious concern, given the underlying safety issues. In general, using any software to solve an engineering problem without understanding how it works is very dangerous and this book is mainly aimed at acquiring basic knowledge, allowing an informed use of (FE) calculation software to solve practical problems of dimensioning and calculation of mechanical resistance of parts, assemblies and structures. On the other hand, the very rapid evolution of technology means that analysts and engineers themselves are faced with a large number of computational tools which they must learn to use effectively, in order to make the right choices according to the types of problems they have to solve in a practical way (Jean-Cristophe G. 2011).

III.3.2.2.3. Teaching the practice of the finite element method

Historically, (FEM) has been taught exclusively at the graduate level, due to the

fact that it is based on quite complex mathematical foundations, but also due to the fact that it was considered to be a cutting-edge technology, associated with high-tech industries. Over time, advances in computer systems and research have led to a democratization of (CAD/CAM) technologies in general and the practical use of (FEM) in particular. This phenomenon has a very important effect on the evolution of professional practice in mechanical engineering. Today, with the increasing use of this type of technology in many industrial fields, there is a need to train engineers who are able to effectively use commercial (FE) tools. The pedagogical challenges encountered in teaching this course at the undergraduate level in mechanical engineering are numerous, and some engineering programs only introduce this course at the graduate level or as an undergraduate elective, which is a weakness given the evolution of professional practice.

Thus, in the historical context mentioned above, the literature on (FEM) is very abundant but is generally aimed at an audience of researchers or graduate students interested in developing advanced knowledge in this area. As a result, the existing literature is very focused on the theoretical side of the method and does not specifically the practical use of software tools in the context of an engineer's work. The present book is an introductory work that is specifically intended for engineers and students in mechanical engineering at the undergraduate level. The theoretical basis of the method is covered with the specific goal of effective use of the software and informed exploitation of the results.

Indeed, to perform good (FE) calculations in mechanical resistance, it is first necessary to have a good understanding of the phenomena involved in the in-service operation of a part, which requires a solid knowledge of theoretical mechanics (statics, dynamics, elasticity, etc.). Then, it is necessary to have a basic knowledge of (FEM), in order to use it adequately to obtain accurate and realistic results with respect to the real operation of the simulated parts and assemblies. Finally, it is necessary to develop a knowledge of the most modern software tools, in order to obtain these results in a fast and efficient way (Jean-Cristophe G. 2011).

III.3.3. Area of use of the finite element method

III.3.3.1. Presentation of Finite element method in field

In the field of mechanical industry, aeronautics and geotechnical engineering, the optimization of the resistance of the construction on the one hand, and the saving of material and money on the other hand, are the main goals of the constructors. For this reason, the knowledge of the behavior of a structure when it is subjected to a static or

dynamic load is of great importance in order to ensure a good dimensioning and to avoid their cracking, their rupture and their disaster due to external conditions during their operation and thus to increase their life span. In fact, the knowledge of the different loads makes the calculation of the stress distribution in the most solicited part possible, which once done, represents the basis for a rigorous and optimum design.

In general, discrete structures are the structures most often encountered in the automotive industry (bodies, chassis, etc....); aerospace (space structures), aeronautics (fuselages, aircraft wings and ailerons, etc.) and geotechnical engineering structures (buildings, bridges, steel structures, etc.).

III.3.3.2. Areas of use of the finite element method

The method of elements it is usable in several fields of engineering, and among these fields are:

- mechanical engineering
- geotechnical engineering
- civil engineering
- transportation
- aeronautics
- space
- nuclear
- energy
- military

III.3.3.3. Examples of applications

The analysis of structures by the finite element method is a current topic that is the subject of much research in various sectors such as geotechnical engineering, civil engineering, mechanics, automotive, aeronautics, aerospace, shipbuilding, nuclear, and even medicine where the finite element method has been introduced in the modeling of human body organs to better target the areas to be treated.

III.3.3.3.1. In geotechnical engineering

Stability analysis using the FEM strength reduction method

Compared with the traditional LA method, the finite element method (FEM) performs better with the advantage of considering much complex boundary conditions, as well as the non-homogeneity of the soil and rock mass. Another advantage of the FEM method is that the stress and deformation field can be also obtained. The FEM strength reduction method has been proposed and applied in the analysis of slope stability (Zienkiewicz, O.

Chapter III Calculations methods of slopes safety factor

C. et al. 1975; Duncan, J. M. 1996). It regarded the safety factor FS as the reduction degree of shear strength of the soil material when the slope reaches the limit state. The safety factor FS can be redefined as $F_s = c/c_f$ or $F_s = \tan\phi/\tan\phi_f$, where c and ϕ are the initially-input shear strength parameters, while c_f and ϕ_f are the output shear strength parameters in the limit state after reduction, respectively.

The definition of the safety factor mentioned above is consistent with the definition introduced by Bishop (Bishop, A.W. 1955)., that the safety factor F_s is expressed as bellow,

$$F_s = \frac{\tau_f}{\tau} = \frac{\int_0^1 (c + \sigma \tan\phi) dl}{\int_0^1 \tau f} \quad (25)$$

where, τf represents the shear strength of the slope and can be calculated by the Mohr-Coulomb model with the cohesion and internal friction angle. τ denotes the actual shear stress of slope. Equation (25) can be transformed as follow,

$$\frac{F_s}{F_s} = \frac{\int_0^1 (\frac{c}{F_s} + \sigma \frac{\tan\phi}{F_s}) dl}{\int_0^1 \tau dl} = \frac{\int_0^1 (c' + \sigma \tan\phi') dl}{\int_0^1 \tau dl} = 1 \quad (26)$$

Equation (26) means that the slope will reach the limit state with the $c' = c/F_s$ and $\tan\phi' = \tan\phi/F_s$, which is the same with the definition mentioned above. Therefore, in our study, the reduction equations of shear strength are expressed as bellow, deducing with the assumption of the constant external load,

$$c' = \frac{c}{R}, \phi' = \arctan\left(\frac{\phi}{R}\right) \quad (27)$$

where R denotes the reduction coefficient with an initiate value of $R = 1.0$. In each iteration step, R increases with the stress and deformation analysis based on FEM implemented. The Mohr-Coulomb model is introduced to describe the constitutive relationship of the landslide mass. Commonly, the vertical boundary of the model is fixed in the horizontal direction, while the bottom boundary is constrained in both horizontal and vertical directions. The iteration of simulation breaks until the slope reaches the limit state. The value of the variable R under the limit state is regarded as the safety factor F_s for the selected landslide profile.

III.4. Conclusion

Chapter III Calculations methods of slopes safety factor

The stabilization of a landslide is a complex and delicate operation, and for this there are several valuable methods that have been proposed by different authors for the calculation of the stability and the safety factor of a landslide, and that still remain approaches.

Currently there are several methods of calculating landslides, such as the limit equilibrium method of forces and the finite element method, in this chapter We have seen that the limit equilibrium method divides the medium into a number of slices, these slices are subjected to driving forces and forces resisting the slope is considered to be stable if the driving forces are greater than the resistant forces.

The finite element method is a mathematical technique in which the studied body is considered as a continuous medium. this body will be discretized and transformed into a number of finite elements (mesh). each element is subjected to stresses and loads resulting from deformations and displacements.

For the best calculation method, another important choice, which depends on the means that can be implemented, must be made between a method modeling the entire mass of soil (finite element method) and a kinematic method, defining a failure surface for example (method equilibrium limit) However, with the possibilities of analyzing a large number of potential failure curves, the two approaches come together. In the case of a method involving the whole mass, the calculation will directly provide the most probable failure zone, while a method based on a previously defined curve will be repeated a large number of times for a similar result. This choice must be made by examining the means available, the overall behavior of the slope, but also by ensuring the possibility of obtaining the calculation parameters corresponding to the model.

The finite element method is used more for measuring the stability of the masses and structures, while the limit equilibrium method is better used to calculate the safety factor of slopes, failure area and slip radius, so for calculating the safety factor of a slope, the best method is the limit equilibrium, which we're going to use it in our study in the next chapter.

**Chapter IV: Slopes
Safety factor
investigations using
statistical analysis and
Design of experiments
(DOE) methodology.**

IV.1. Introduction

After an overview on geotechnical description of soil parameters, the laboratory and fields obtained parameters can help in modeling and analyses the stability with finite elements methods, some different soil parameters and their integration in slope stability analysis was developed by the GEO-SLOPE software, which will be defined later. the numerical modeling process provides the final state description of the slope stability.

In this study it is focus on comparing four (04) cases of landslides hazards in Souk-Ahras region (Machroha sector 01 and 02 and Zaaroria sector 01 and 02); the slope cases have been treated and analysis to get the best correlation between the soil parameters and the safety factor, this compose the first part of the present work.

In the second part, two slope cases were treated taking into account the angle of the slope α constant and variable. The obtained data base is composed of final results of the stability described by the Fs in the two cases. A second matrix data base composed of Fs as output factor and a maximum of physical and mechanical and geometrical soil parameters as input affecting stability factors such as (wet density (γ_h), dry density (γ_d), water content (w) plasticity index (I_p), degree of saturation (S_r), the fine fraction (ff), liquidity limit (WL), cohesion strength (C), the angle of internal friction (ϕ) and the angle of the studied slope (α)). The methods used in the present work to analyze the obtained data set is called Principal Component Analysis (PCA) combined with the Linear Regression (LR) in the aim to generate the best describing model for the stability safety factor.

Finally, the Design of experiments method (DOE) has been used to find the accurate and sophisticate best fit models that describe the correlation of the different geotechnical parameters to the output safety factor Fs. As the Response surface methodology and the central composite design (RSM and CCD) allow to the optimization step of the final (DOE) models; at this level of screening it is suitable to optimize by maximization or minimization the output response Fs to obtain the best accurate model that describe the stability of slopes in the studied region.

IV.2. Slope stability analysis using Geostudio (Geo-slope software)

IV.2.1. Presentation of the geo-slope software

GEO-SLOPE is a slope stability calculation program that allows to model geotechnical and geo-environmental problems. This computer-aided design program allows the use of the slice method to determine the safety factor of sloping masses made up of one or more layers of one or more layers of soil, with or without the presence of a water table or suction, etc. In its global architecture, this program is composed of eight distinct modules.

Here is a brief presentation of these different modules:

- **SLOPE / W:** calculation of the safety factors of a slope using classical analysis methods (Bishop, Janbu, Spencer, Morgenstern-Price...).
- **SEEP / W:** calculation, analysis and evaluation, thanks to a finite element model, of the pore water pressures.
- **QUAKE / W:** finite element modeling of the behavior of the ground under earthquake.
- **SIGMA / W:** finite element analysis of stress - strain problems.
- **TEMP / W:** analysis of geothermal soil problems.
- **CTRAN / W:** modeling the movement of contamination in porous materials.
- **AIR / W:** analysis of the interactions between water and soil air in porous materials.
- **VADOSE / W:** flux analysis below the soil surface, in the unsaturated dose VA and which join the water regime in the soil.

Once the geometric model of the slope is defined, the main characteristics of the soil are characteristics are integrated and a limit equilibrium analysis is performed for the calculation of the safety factor. The possibility to integrate the effect of suction allows the analysis of the stability of unsaturated slopes.

In this work, the SLOPE / W module makes it possible to describe the problem geometry, the stratigraphy of the site, the soil resistance parameters. besides modeling the unsaturated soil. This module allows interaction between them by using the results of one to make an analysis in the other and vice versa. These combinations, limit equilibrium methods and finite element methods, make it possible to overcome the serious limitations of the limit equilibrium method of slices which only satisfy the equations of the statics and which do not take into account the compatibility between the deformation and

displacement. The methodology applied with these two modules for the modeling of sliding must be developed during this chapter (Jean, BJ, 2012).

IV.2.2. How the software works

This software, like all other calculation programs, is used to provide results from a defined number of parameters, so it is necessary to follow the following steps to complete the calculation operation:

- 1) **Define:** This step is very important because we will define the problem and introduce the different data specific to the current problem:
 - **Set:** Used for the delimitation of the work surface; the definition of the scale; the definition of networks; determination of the zoom; he fixing of axes.
 - **Keyln:** Used for specification of analysis methods; Specification of analysis options; The definition of soil properties.
 - **Draw:** Used for drawing of the points; Line drawing; determination of the piezometric line; drawing of the radius of the fracture surface; the drawing of the networks of the fracture surface.
 - **Sketch:** Used for carrying out the sketch of the problem; soil labeling; addition of a title identifying the problem; clear the darkness of identification.
 - **Modify:** This instruction allows users to add, eliminate, delete and modify objects in the problem.
 - **Tools:** using this icon you can check all the data of this problem and facilitate access for its resolution.
 - **Saving:** As soon as the problem definition process is completed, this data must be saved in the form of a file.
- 2) **Solve:** It is the stage of resolution of the problem, using the traditional methods and the finite element method and starting from the introduced data, one determines the safety factor F_s .
- 3) **Contour:** This is the stage responsible for translating the different results into a graphic form; and display these results (Aissa Mohamed Hamza, 2011).

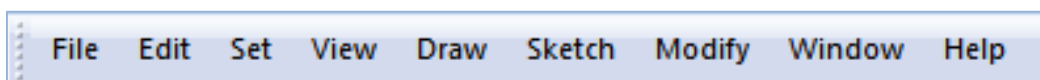


Figure IV.01: The menus available on SLOPE / W software.

IV.2.3. Applications

In this work, several calculation cases were considered using the different model for (Machroha01) and (Zaaroria01) for (α) constant, (Machroha02) and (Zaaroria02) for (α) variable in the whole modeling steps. the geological cross section of the Machroha slope contain two layers (in general the domination is for altered marl with 11 m altitude for the first layer (substratum) and 10 m for the second one (from 11 m to 21 m) with 45 m length, the slop of sector 01 is 30,39% (constant), for sector 02 the slop varied between [18,55% to 30%] (variable). Also Zaaroria case have two layers, the first (substratum) is 4 m as an altitude and the second is 16 m (from 4 m to 20 m) with 45 m length, the slop of sector 01 is 23,56% (constant), for sector 02 the slop varied between [24,94% to 30,38%] (variable).

- A first case in which the stability of a heterogeneous model (two layers) is studied for Machroha and Zaaroria where we keep the angle of slope constant and we only change the soil parameters in the layers (γ_h , ϕ , C).
- A second case in which the stability of a heterogeneous model (two layers) under the same conditions as the first case is studied but with changing the angle of slope in each time.

IV.3. Heterogeneous slope

IV.3.1. For α constant

Examples of Machroha ($\alpha=30,39\%$)

Figure IV.02 show two different studied slopes, geometry and geotechnical characteristics are given in Table IV.01.

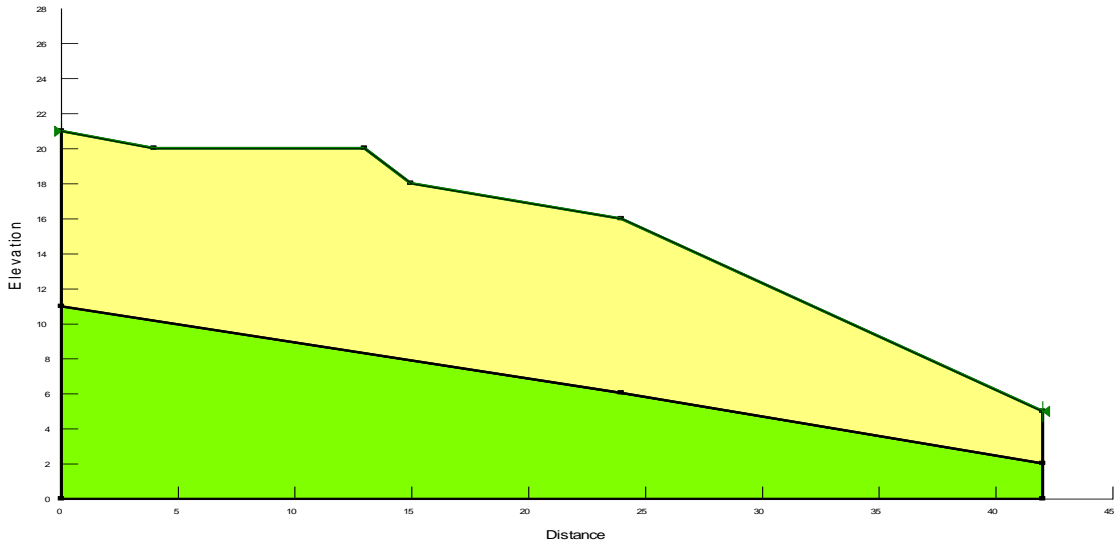


Figure IV.02: Geometry of the heterogeneous slope case 01 and case 02 (Machroha01)
(GEO-SLOPE, 2012).

TABLE IV.01: Geotechnical parameters of the heterogeneous slope (Machroha01)

Cases	Layers	γ_h (kN/m ³)	C(kPa)	ϕ (°)
01	Layer 01	19.6	4	19
	Layer 02	21.4	45	16
02	Layer 01	20.3	7	22
	Layer 02	21.4	45	16

Figures IV.03, IV.04, IV.05 and IV.06 below show the results obtained by using Mohr coulomb's model for the clays and marls materials, the slide circle

we can see the slide circle clearly with water table, entry and exit lines, and safety factor value.

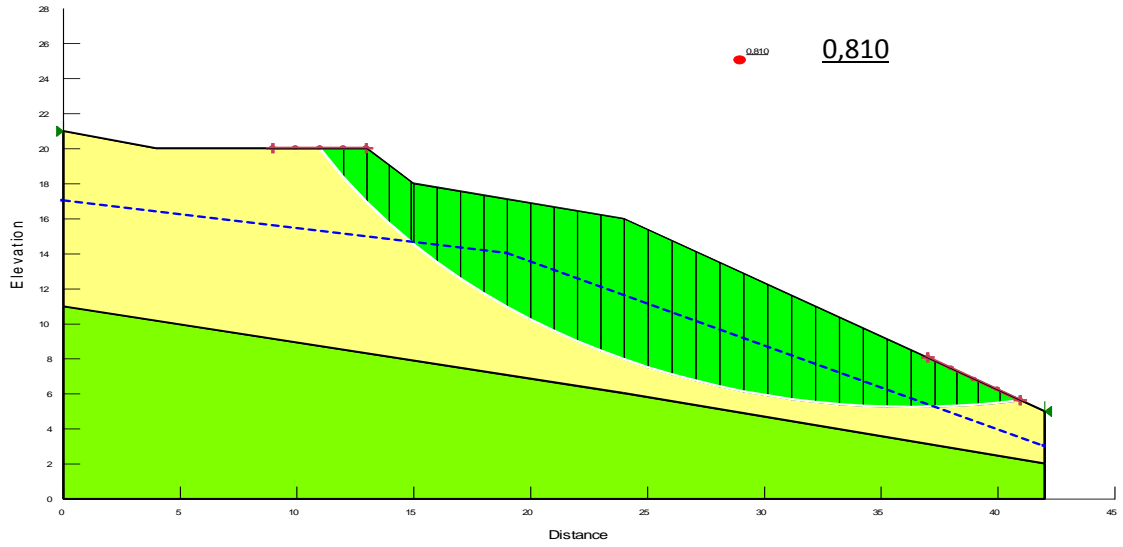


Figure IV.03: Failure area and value of F_s (case 01)

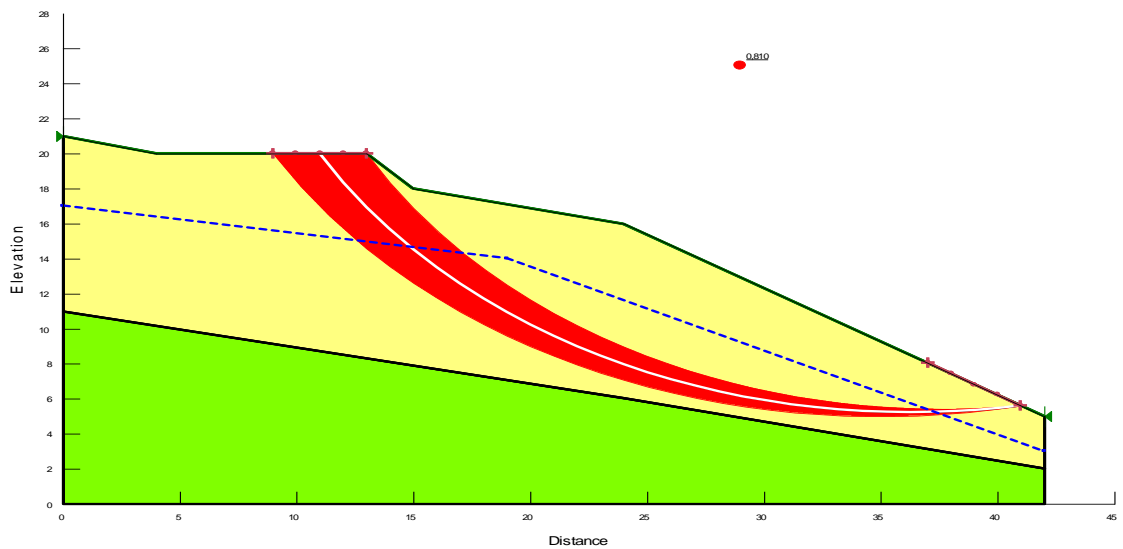


Figure IV.04: Slip surface and safety map (case 01)

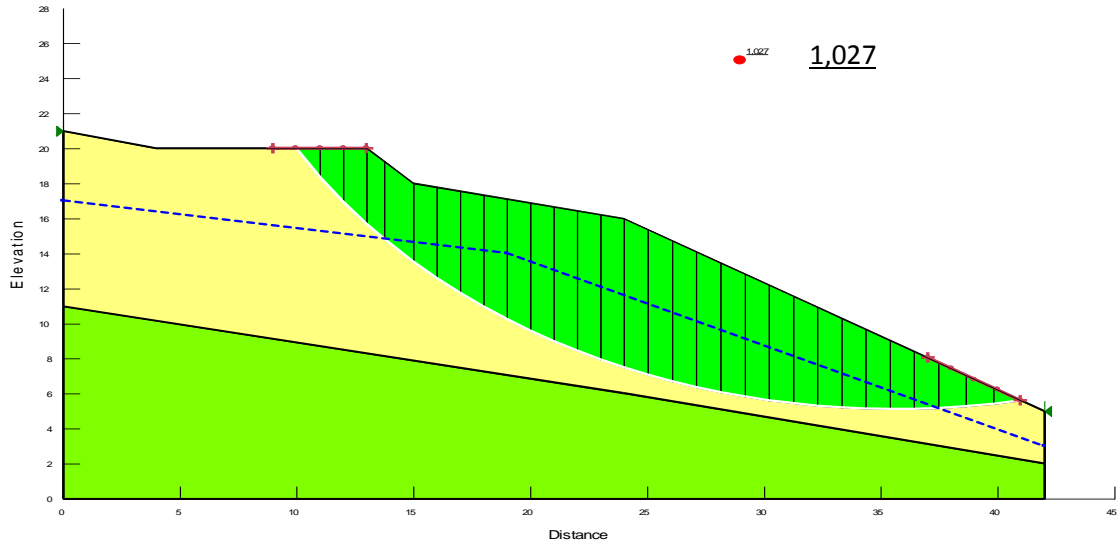


Figure IV.05: Failure area and value of F_s (case 02)

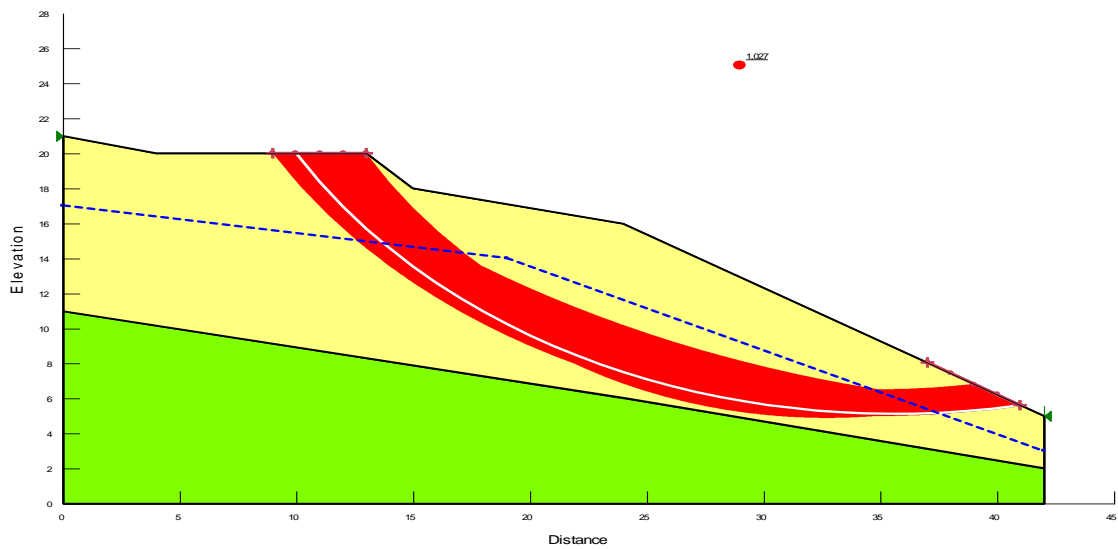


Figure IV.06: Slip surface and safety map (case 02)

Examples of Zaaroria ($\alpha=23,56\%$)

Figures IV.07 and Table IV.02 give the geometry and geotechnical characteristics of the treated example using Mohr-Coulomb's model.

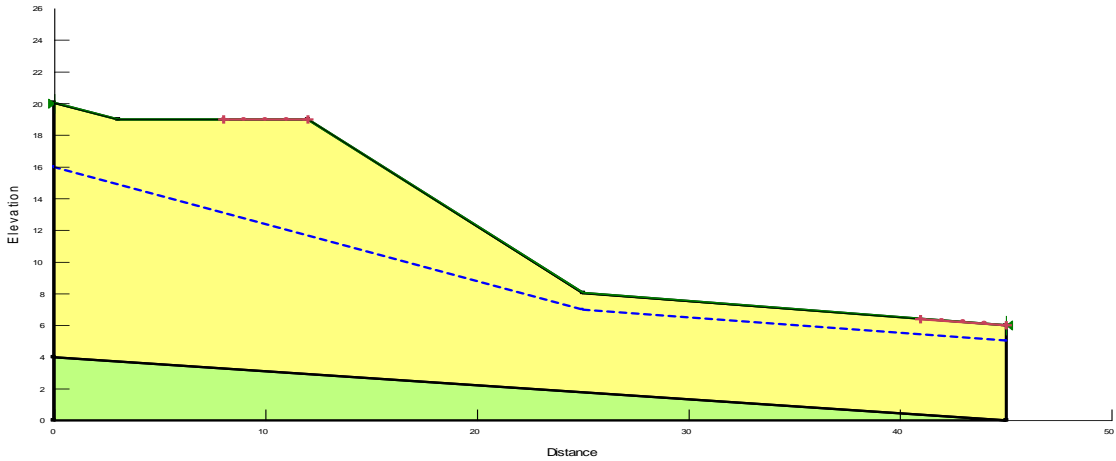


Figure IV.07: Geometry of the heterogeneous slope case 03 and case 04 (Zaaroria01) (GEO-SLOPE, 2012).

TABLE IV.02: Geotechnical parameters of the heterogeneous slope (Zaaroria01)

Cases	Layers	γ_h (kN/m ³)	C(KPa)	phi(°)
03	Layer 01	20.4	7	26
	Layer 02	20	50	30
04	Layer 01	21	7.1	12
	Layer 02	20	50	30

Figures below show the results obtained.

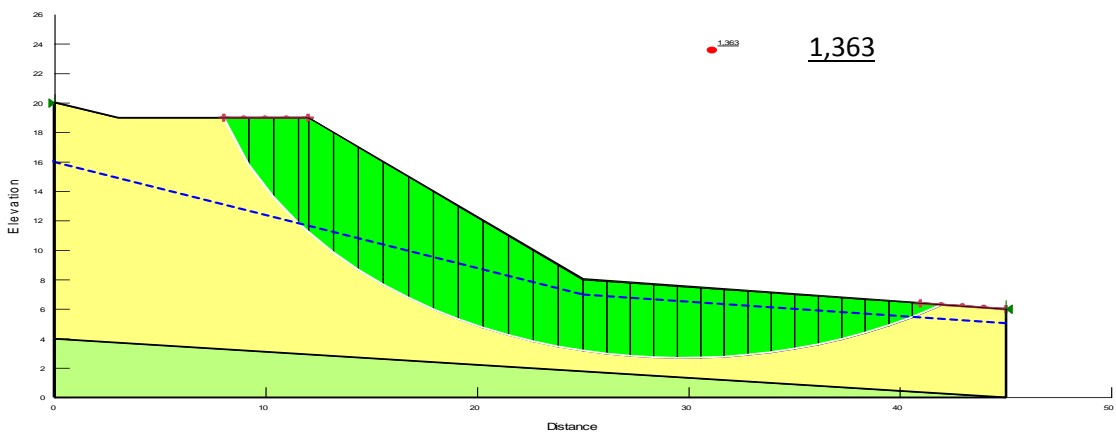


Figure IV.08: Failure area and value of F_s (case 03)

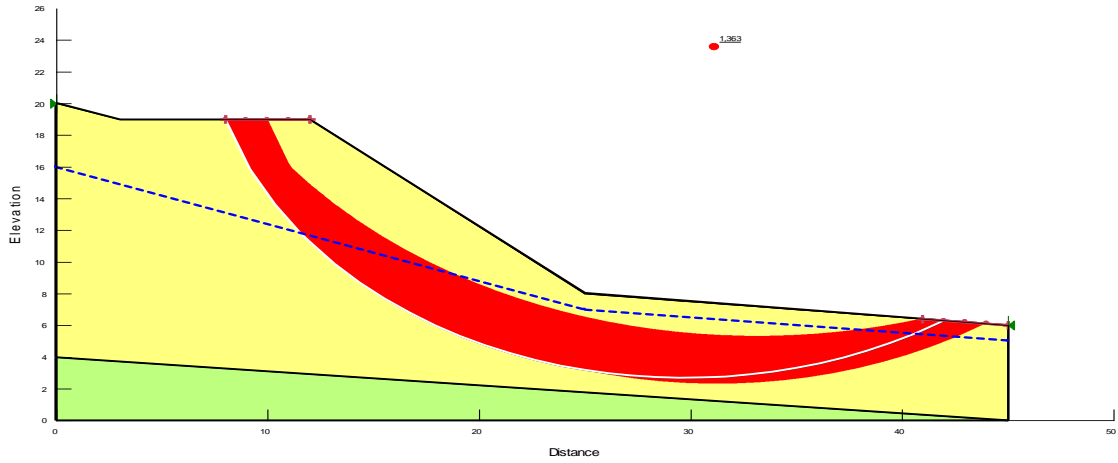


Figure IV.09: Slip surface and safety map (case 03)

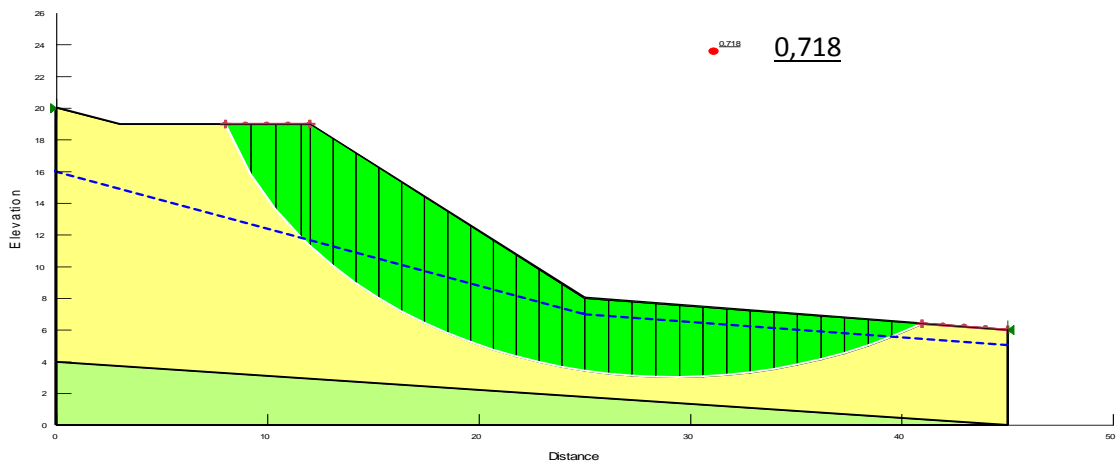


Figure IV.10: Failure area and value of F_s (case 04)

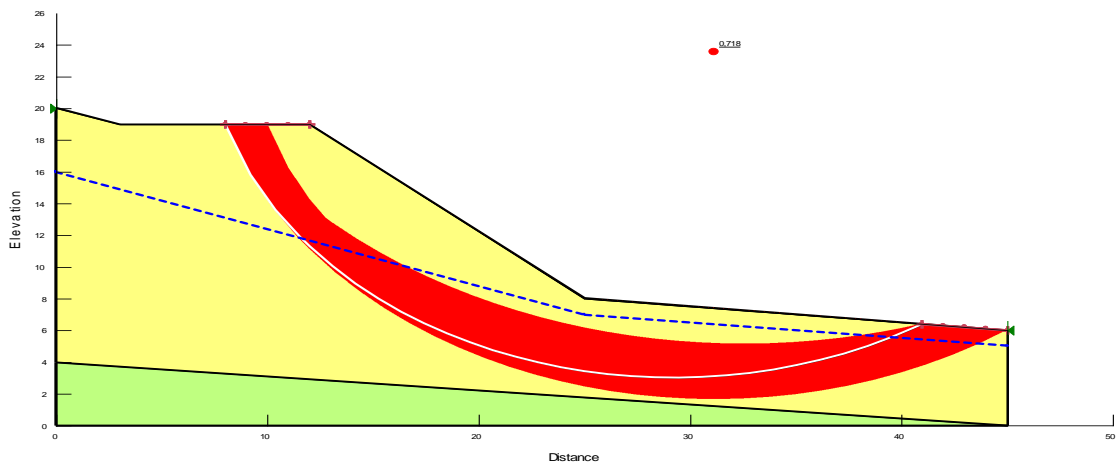


Figure IV.11: Slip surface and safety map (case 04)

IV.3.2. For α variable

Examples of Machroha

Figures IV.12, 13 show two different treated slopes and Table IV.02 gives their geometry and geotechnical characteristics, using Mohr-Coulomb's model.

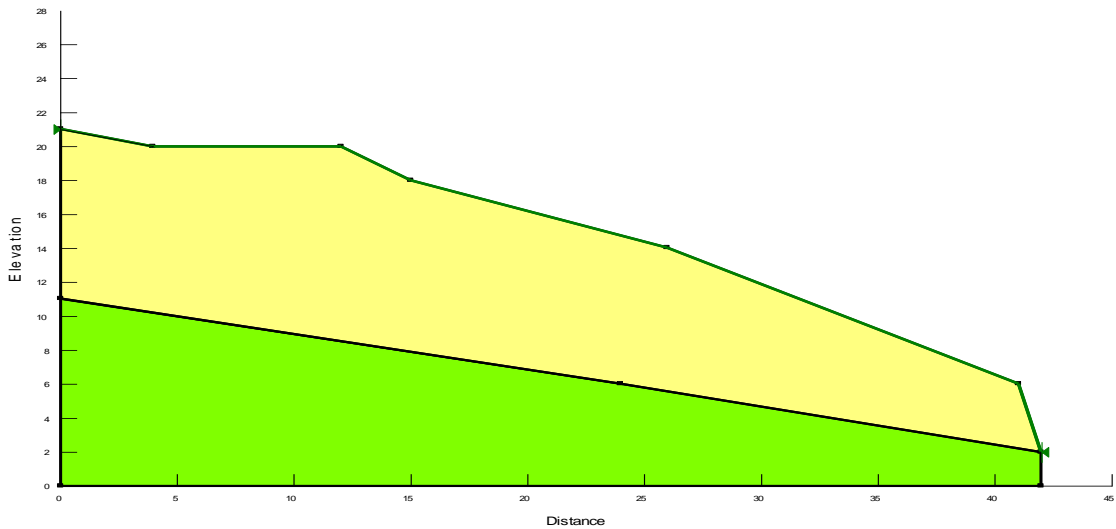


Figure IV.12: Geometry of the heterogeneous slope case 05 (Machroha02)

(GEO-SLOPE, 2012).

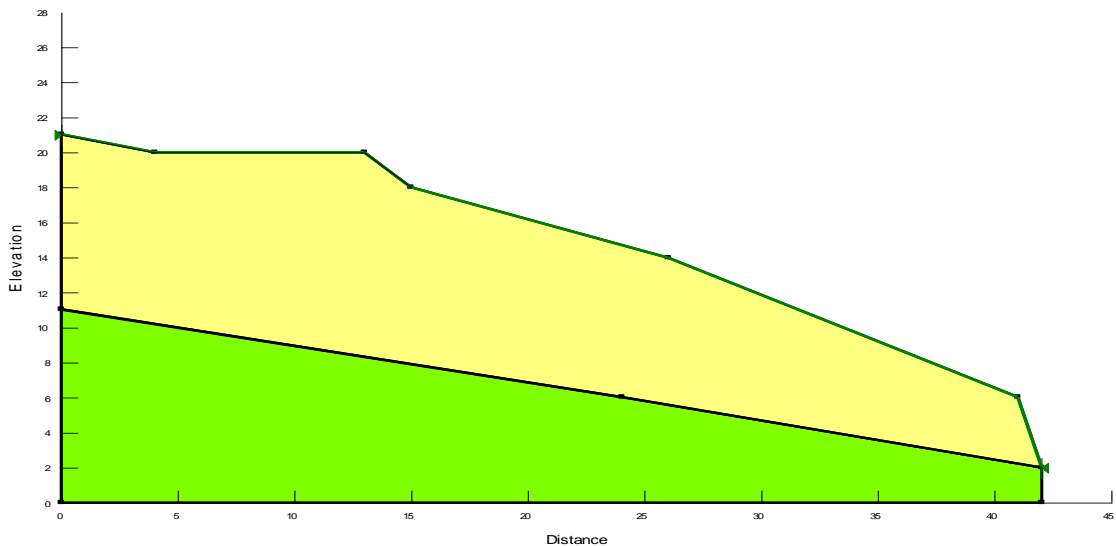


Figure IV.13: Geometry of the heterogeneous slope case 06 (Machroha02)

(GEO-SLOPE, 2012).

Table IV.03: Geotechnical parameters of the heterogeneous slope (Machroha02)

Cases	Angle α (%)	Layers	γ_h (kN/m ³)	C(KPa)	ϕ (°)
05	29,52	Layer 01	19.2	33,8	10
		Layer 02	21.4	45	16
06	30	Layer 01	20,9	52,9	10
		Layer 02	21.4	45	16

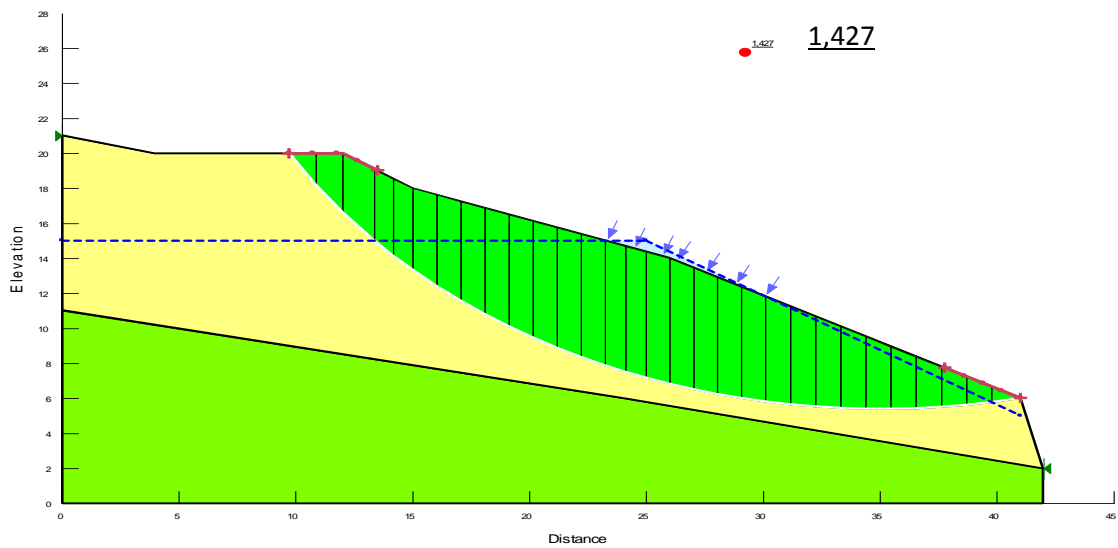


Figure IV.14: Failure area and value of F_s (case 05)

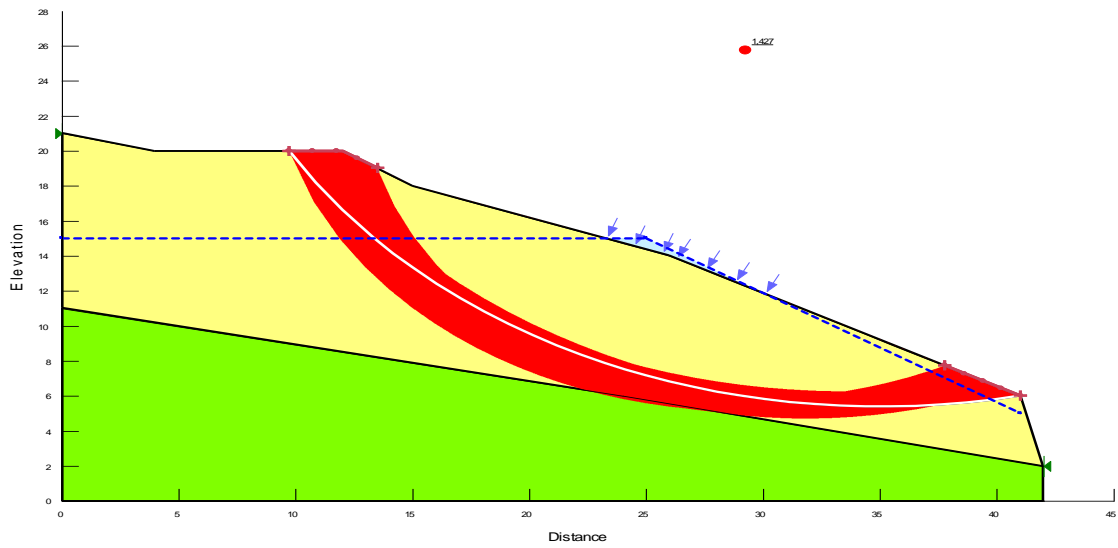


Figure IV.15: Slip surface and safety map (case 05)

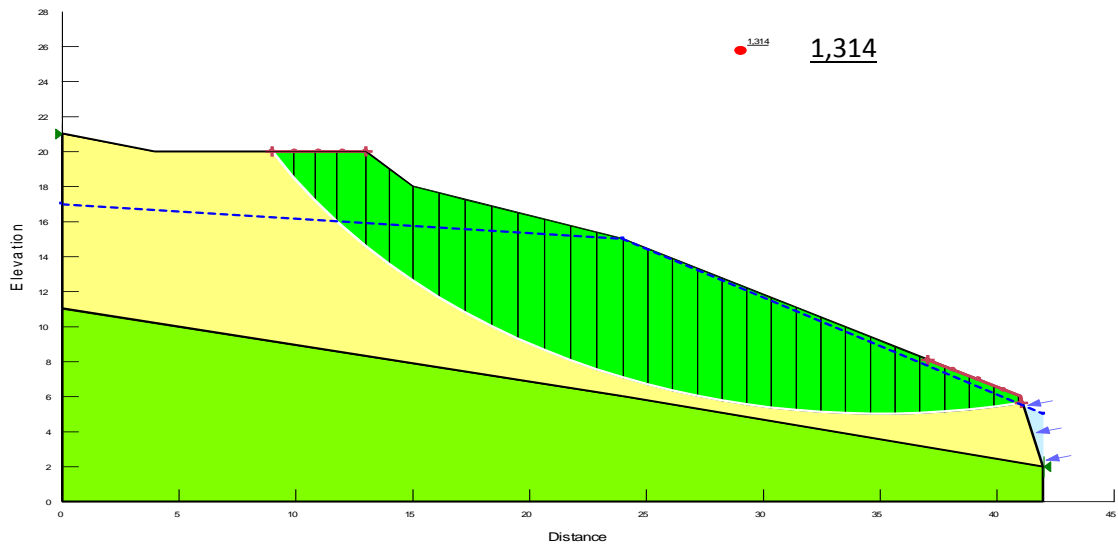


Figure IV.16: Failure area and value of F_s (case 06)

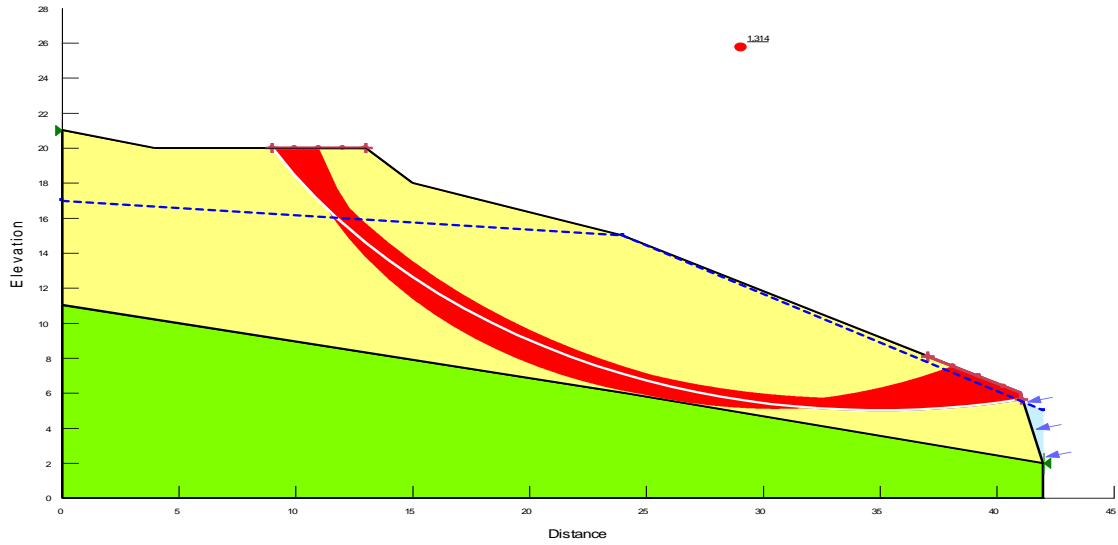


Figure IV.17: Slip surface and safety map (case 06)

Examples of Zaaroria

Figures 15, 16 and Table IV.02 give the geometry and geotechnical characteristics of the treated example using Mohr-Coulomb's model.

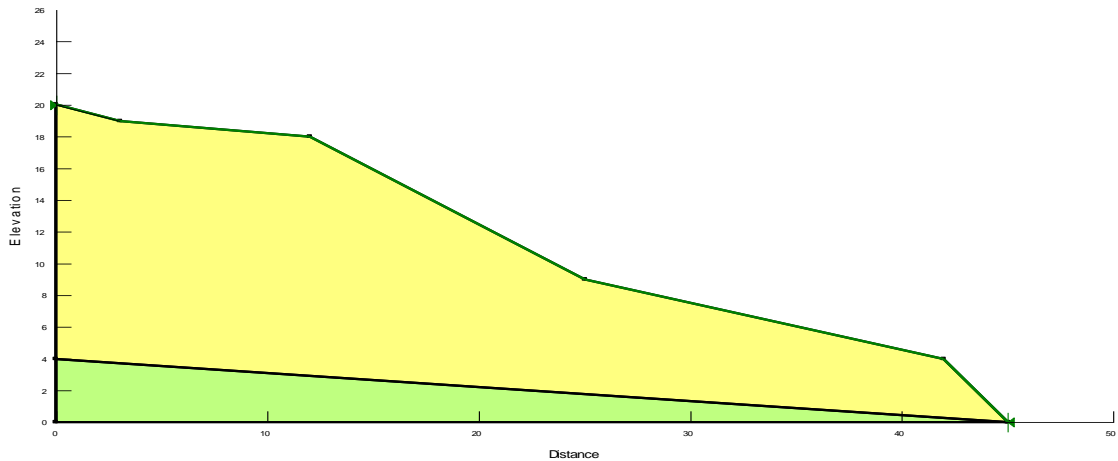


Figure IV.18: Geometry of the heterogeneous slope case 07 (Zaaroria02)

(GEO-SLOPE, 2012).

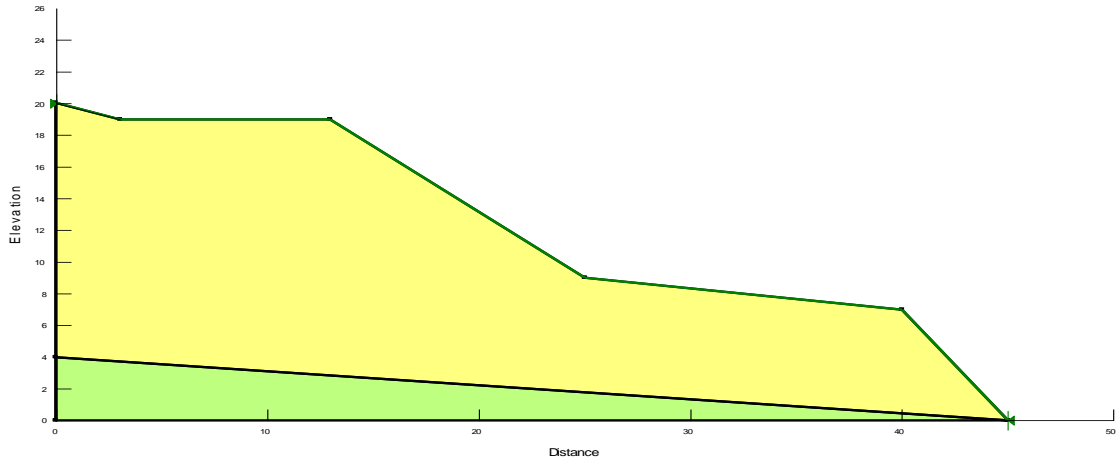


Figure IV.19: Geometry of the heterogeneous slope case 08 (Zaaroria02)

(GEO-SLOPE, 2012).

Table IV.04: Geotechnical parameters of the heterogeneous slope (Zaaroria02)

Cases	Angle α (%)	Layers	γh (kN/m ³)	C(KPa)	ϕ (°)
07	28,74	Layer 01	19,8	7,4	22
		Layer 02	20	50	30
08	26,25	Layer 01	19,7	7,3	23
		Layer 02	20	50	30

Figures 17 and 18 below show the results obtained by using Mohr coulomb's model, we can see the slide circle clearly with water table, entry and exit lines, and safety factor value.

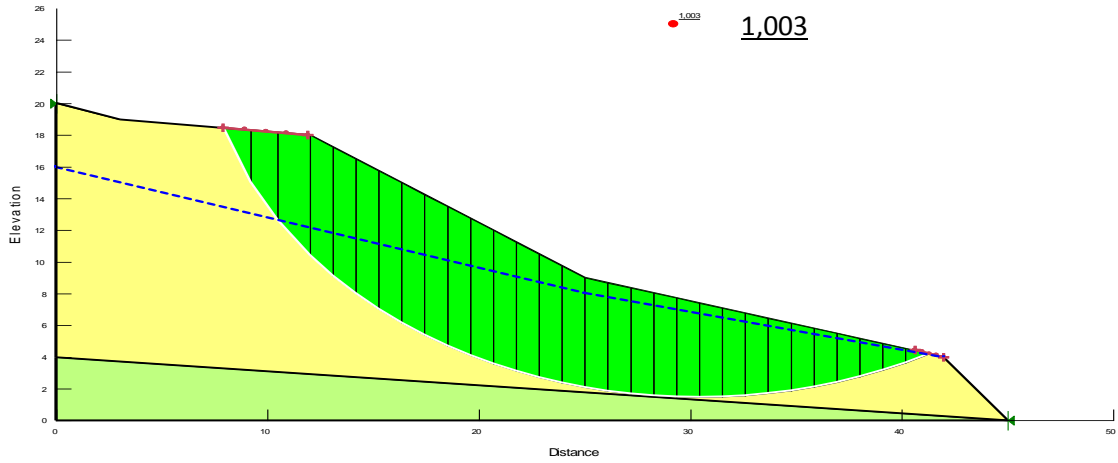


Figure IV.20: Failure area and value of F_s (case 07)

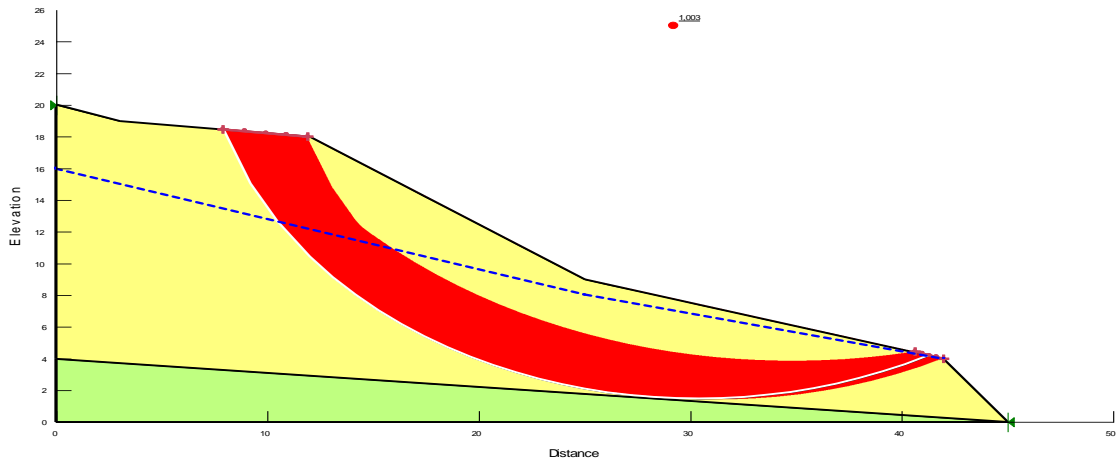


Figure IV.21: Slip surface and safety map (case 07)

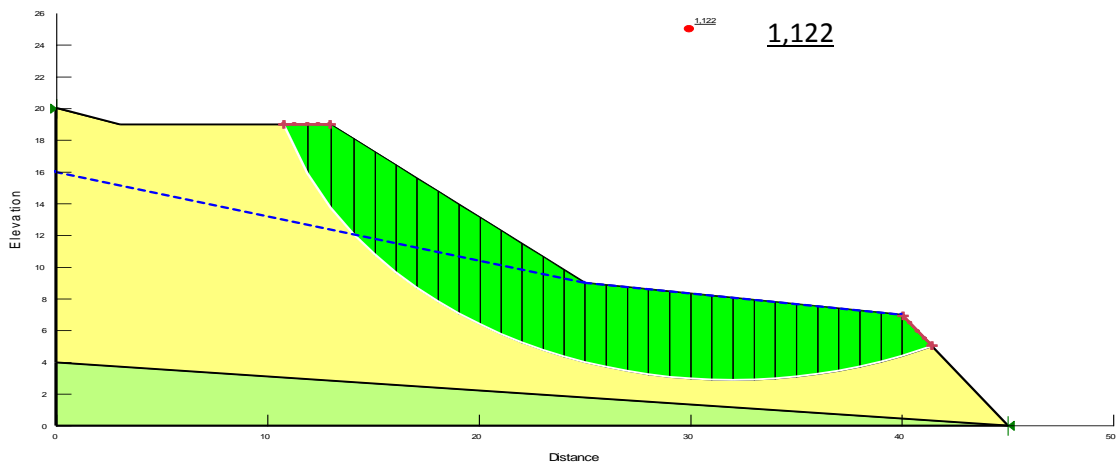


Figure IV.22: Failure area and value of F_s (case 08)

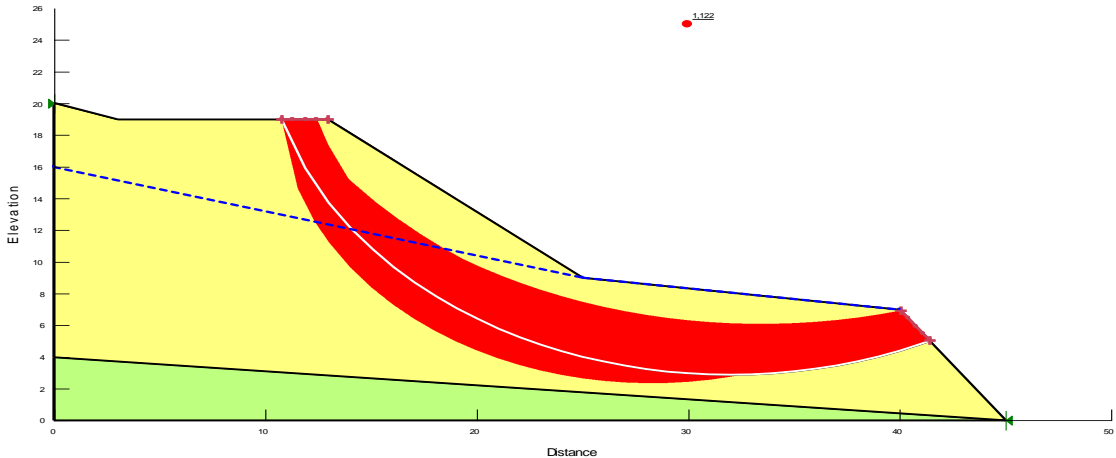


Figure IV.23: Slip surface and safety map (case 08)

The table below shows the safety factor values for the eight (08) studied cases and the slide circle radius in each one, we can see right away that there is a relation between the input variables and the (Fs), when the wet weight (γh), the cohesion (C) and the internal friction angle (φ) increase the (Fs) increase, the slope angle (α) have a strongly effect on the (Fs), it's an inverse relationship, when (α) decrease, the slope will be more stable.

The (Fs) values varied between 0,718 and 1,363, the cases 01 and 02 are not stable (Fs<1), other cases are stable (Fs>1)

Table IV.05: Values of Fs and the slide circle radius for the heterogeneous slope (with α constant and variable) for Mohr-Coulomb's model used in SLOPE / W.

Cases	01	02	03	04	05	06	07	08
Fs value	0.810	1,027	1.363	0.718	1.427	1.314	1,003	1.122
Slide circle radius (m)	17,541	17,336	18,623	17,274	19,230	19,445	17,901	18,085

IV.4. Conclusion

This chapter has been the subject of the analysis of the stability of some examples of sloping terrain with (α) constant and variable.

This study made it possible to give some conclusions:

- The increasing of cohesion value increases the value of F_s .
- The three soil parameters (γh , C , ϕ) are the inputs according to Mohr-coulomb model.
- The angle of the slop plays an important role, the more the angle of the slop increase, the less the stability.

IV.5. Presentation of the statistical analysis principal component analysis (PCA) and linear regression (LR)

The multiplicity of mechanical and physical properties of soil taken through laboratory experiments or in the field. The large number of data for each variable makes it difficult to choose the optimal variable that has a greater impact on the safety factor. (PCA) was originally proposed by K. Pearson and independently developed by Hotelling (Hotelling, 1936). The goals of (PCA) are to extract the most important information from the available data, compress the size of the dataset by retaining only this important information, simplify the description of the dataset, and analyze the structure of observations and variables. The selection of tools in the agricultural area is made from a wide range (Voicu Gh et al., 2008). Usually the choice is not based on all features, but on a set of characteristics. In the first stage, for each device, the largest possible number of features are taken into account. (PCA) is the standard technique for minimizing multivariate data sets in a subspace of small dimensions, systematically in two or three dimensions. The purpose of pre-processing is to attempt to convert data into a form that is most appropriate for the main purpose of this research. object (individual) with its attributes, and each column is an attribute (property, variable). The number of attributes gives the dimension of the initial representation space of the objects. Anyway it is considered an m-dimensional coordinate system, each coordinate being an attribute. Instead of actual attributes the (PCA) uses new factors, but only a few, which are artificial ones.

As with correlation, regression is used to analyze the relation between two continuous (scale) variables, Regression analysis is a statistical technique for investigating and modeling the relationship between variables. Applications of regression

are numerous and occur in almost every field, including engineering. In fact, regression analysis may be the most widely used statistical technique.

However, regression is better suited for studying functional dependencies between factors. The term functional dependency implies that X [partially] determines the level of Y.

In addition, regression is better suited than correlation for studying samples in which the investigator fixes the distribution of X (Biometrica).

IV.5.1. Principal Component Analysis (PCA)

(PCA) is a technique that is useful for the compression and classification of data. The purpose is to reduce the dimensionality of a data set (sample) by finding a new set of variables, smaller than the original set of variables, that nonetheless retains most of the sample's information.

By information we mean the variation present in the sample, given by the correlations between the original variables. The new variables, called principal components (PCs), are uncorrelated, and are ordered by the fraction of the total information each retains (Connolly et al. 1995; Dressler, et al. 1987; Jolliffe IT. 2002; Kherif, Ferath et al 2020; Lever 2017).

IV.5.2. Summary statistics on the collected samples:

As mentioned in the Table IV.1, the 99 collected samples has been:

Table IV.06: Summary statistics of 99 analyzed data of the studied soil of Machroha01 (with fixed (α)) (Berrah, Y. et al 2016).

Variable	Observations	Obs. with missing data	Obs. without missing data	Minimum	Maximum	Mean	Std. deviation
γ_d (kN/m ³)	99	0	99	13,200	18,800	16,855	1,168
γ_h kN/m ³	99	0	99	17,000	22,000	20,190	0,882
W %	99	0	99	12,500	38,800	20,102	4,669
Sr%	99	0	99	62,000	100,000	89,220	10,410
Ff	99	0	99	22,480	100,000	84,494	16,645
WL %	99	0	99	29,000	72,790	49,207	11,601
IP%	99	0	99	10,000	39,000	24,870	7,609
C(KPa)	99	0	99	3,000	140,000	37,717	33,299
ϕ (°)	99	0	99	10,000	43,000	18,598	6,779

α % (Mc)	99	0	99	30,390	30,390	30,390	0,000
Fs(M)	99	0	99	0,454	3,946	1,538	0,831

Table IV.07: Summary statistics of 99 analyzed data of the studied soil of Machroha2 (with (α) variable) (Berrah, Y et al 2016)

Variable	Observations	Obs. with missing data	Obs. without missing data	Minimum	Maximum	Mean	Std. deviation
γ_d (kN/m ³)	99	0	99	13,200	18,800	16,855	1,168
γ_h kN/m ³	99	0	99	17,000	22,000	20,190	0,882
W %	99	0	99	12,500	38,800	20,102	4,669
Sr%	99	0	99	62,000	100,000	89,220	10,410
Ff	99	0	99	22,480	100,000	84,494	16,645
WL %	99	0	99	29,000	72,790	49,207	11,601
IP%	99	0	99	10,000	39,000	24,870	7,609
C(KPa)	99	0	99	3,000	140,000	37,717	33,299
ϕ (°)	99	0	99	10,000	43,000	18,598	6,779
α % (Mv)	99	0	99	18,550	30,000	27,890	3,181
Fs(M')	99	0	99	0,538	3,953	1,600	0,775

Table IV.08: Summary statistics of 99 analyzed data of the studied soil of Zaaroria 1 (with fixed (α)) (Berrah, Y et al 2016)

Variable	Observations	Obs. with missing data	Obs. without missing data	Minimum	Maximum	Mean	Std. deviation
γ_d (kN/m ³)	99	0	99	13,200	18,800	16,855	1,168
γ_h kN/m ³	99	0	99	17,000	22,000	20,189	0,882
W %	99	0	99	12,500	38,800	20,102	4,669
Sr%	99	0	99	62,000	100,000	89,222	10,410
Ff	99	0	99	22,480	100,000	84,494	16,645
WL %	99	0	99	29,000	72,790	49,208	11,600
IP%	99	0	99	10,000	39,000	24,870	7,609
C(KPa)	99	0	99	3,000	140,000	37,716	33,300
ϕ (°)	99	0	99	10,000	43,000	18,608	6,785
α % (Zc)	99	0	99	23,560	23,560	23,560	0,000
Fs(Z)	99	0	99	0,718	4,920	2,057	1,084

Table IV.09: Summary statistics of 99 analyzed data of the studied soil of Zaaroria 2 (with (α) variable) (Berrah, Y et al 2016)

Variable	Observations	Obs. with missing data	Obs. without missing data	Minimum	Maximum	Mean	Std. deviation
γ_d (kN/m ³)	99	0	99	13,200	18,800	16,855	1,168
γ_h kN/m ³	99	0	99	17,000	22,000	20,190	0,882
W %	99	0	99	12,500	38,800	20,102	4,669
Sr%	99	0	99	62,000	100,000	89,220	10,410
Ff	99	0	99	22,480	100,000	84,494	16,645
WL %	99	0	99	29,000	72,790	49,207	11,601
IP%	99	0	99	10,000	39,000	24,870	7,609
C(KPa)	99	0	99	3,000	140,000	37,717	33,299
ϕ (°)	99	0	99	10,000	43,000	18,598	6,779
α % (Zv)	99	0	99	24,940	30,380	29,178	1,306
Fs(Z')	99	0	99	0,580	4,720	1,696	0,911

As a first step, statistical tests were performed to take an overview and examine as far as the known parameters have any relationships with the safety factor (Fs) for different types of soil and the difference between the results of the four types of slopes (Machroha and Zaaroria with fixed or variable α). These variables are chosen as independent variables as wet density (γ_h), dry density (γ_d), water content (w) plasticity index (I_P), degree of saturation (Sr), the fine fraction (ff), liquidity limit (WL), cohesion strength (C), the angle of internal friction (ϕ) and the angle of the studied slope (α).

IV.5.3. Correlation matrix

Table IV.10: Correlation matrix (Pearson (n)) Machrohal

Variables	γ_d (kN/m ³)	γ_h (kN/m ³)	W %	Sr%	Ff	WL %	IP%	C(KPa)	ϕ (°)	Fs(M)
γ_d (kN/m ³)	1	0,879	-0,844	0,048	0,469	-0,145	-0,182	0,222	0,143	0,217
γ_h (kN/m ³)	0,879	1	-0,498	0,456	0,462	0,001	-0,026	0,327	0,226	0,322
W %	-0,844	-0,498	1	0,440	-0,351	0,269	0,307	-0,037	-0,001	-0,035
Sr%	0,048	0,456	0,440	1	0,169	0,285	0,294	0,243	0,249	0,270
Ff	0,469	0,462	-0,351	0,169	1	0,459	0,422	0,158	0,016	0,194
WL %	-0,145	0,001	0,269	0,285	0,459	1	0,985	-0,060	-0,013	0,027
IP%	-0,182	-0,026	0,307	0,294	0,422	0,985	1	-0,050	-0,036	0,011
C(KPa)	0,222	0,327	-0,037	0,243	0,158	-0,060	-0,050	1	-0,107	0,873

ϕ (°)	0,143	0,226	-0,001	0,249	0,016	-0,013	-0,036	-0,107	1	0,063
Fs(M)	0,217	0,322	-0,035	0,270	0,194	0,027	0,011	0,873	0,063	1

Table IV.11: Correlation matrix (Pearson (n)) Machroha2

Variables	γ_d (kN/m ³)	γ_h (kN/m ³)	W %	Sr%	Ff	WL %	IP%	C(KPa)	ϕ (°)	α % (Mv)	Fs(M')
γ_d (kN/m ³)	1	0,879	-0,844	0,048	0,469	-0,145	-0,182	0,222	0,143	0,209	0,241
γ_h (kN/m ³)	0,879	1	-0,498	0,456	0,462	0,001	-0,026	0,327	0,226	0,246	0,338
W %	-0,844	-0,498	1	0,440	-0,351	0,269	0,307	-0,037	-0,001	-0,090	-0,061
Sr%	0,048	0,456	0,440	1	0,169	0,285	0,294	0,243	0,249	0,202	0,241
Ff	0,469	0,462	-0,351	0,169	1	0,459	0,422	0,158	0,016	0,208	0,182
WL %	-0,145	0,001	0,269	0,285	0,459	1	0,985	-0,060	-0,013	0,053	0,000
IP%	-0,182	-0,026	0,307	0,294	0,422	0,985	1	-0,050	-0,036	0,043	-0,017
C(KPa)	0,222	0,327	-0,037	0,243	0,158	-0,060	-0,050	1	-0,107	0,564	0,862
ϕ (°)	0,143	0,226	-0,001	0,249	0,016	-0,013	-0,036	-0,107	1	0,119	0,071
α % (Mv)	0,209	0,246	-0,090	0,202	0,208	0,053	0,043	0,564	0,119	1	0,600
Fs(M')	0,241	0,338	-0,061	0,241	0,182	0,000	-0,017	0,862	0,071	0,600	1

Table IV.12: Correlation matrix (Pearson (n)) Zaarorial

Variables	γ_d (kN/m ³)	γ_h kN/m ³	W %	Sr%	Ff	WL %	IP%	C(KPa)	ϕ (°)	Fs(Z)
γ_d (kN/m ³)	1	0,879	-0,844	0,048	0,469	-0,145	-0,182	0,222	0,142	0,218
γ_h kN/m ³	0,879	1	-0,498	0,455	0,461	0,002	-0,025	0,328	0,224	0,336
W %	-0,844	-0,498	1	0,440	-0,351	0,269	0,307	-0,037	-0,001	-0,019
Sr%	0,048	0,455	0,440	1	0,169	0,285	0,294	0,243	0,248	0,283
Ff	0,469	0,461	-0,351	0,169	1	0,460	0,422	0,158	0,017	0,172
WL %	-0,145	0,002	0,269	0,285	0,460	1	0,985	-0,060	-0,014	-0,024
IP%	-0,182	-0,025	0,307	0,294	0,422	0,985	1	-0,050	-0,038	-0,030
C(KPa)	0,222	0,328	-0,037	0,243	0,158	-0,060	-0,050	1	-0,108	0,945
ϕ (°)	0,142	0,224	-0,001	0,248	0,017	-0,014	-0,038	-0,108	1	0,099
Fs(Z)	0,218	0,336	-0,019	0,283	0,172	-0,024	-0,030	0,945	0,099	1

Table IV.13: Correlation matrix (Pearson (n)) Zaarorial

Variables	γ_d (kN/m ³)	γ_h kN/m ³	W %	Sr%	Ff	WL %	IP%	C(KPa)	ϕ (°)	α % (Zv)	Fs(Z')
γ_d (kN/m ³)	1	0,879	-0,844	0,048	0,469	-0,145	-0,182	0,222	0,143	0,088	0,241
γ_h kN/m ³	0,879	1	-0,498	0,456	0,462	0,001	-0,026	0,327	0,226	0,252	0,340

W %	-0,844	-0,498	1	0,440	-0,351	0,269	0,307	-0,037	-0,001	0,113	-0,054
Sr%	0,048	0,456	0,440	1	0,169	0,285	0,294	0,243	0,249	0,289	0,273
Ff	0,469	0,462	-0,351	0,169	1	0,459	0,422	0,158	0,016	0,179	0,191
WL %	-0,145	0,001	0,269	0,285	0,459	1	0,985	-0,060	-0,013	0,148	0,027
IP%	-0,182	-0,026	0,307	0,294	0,422	0,985	1	-0,050	-0,036	0,157	0,030
C(KPa)	0,222	0,327	-0,037	0,243	0,158	-0,060	-0,050	1	-0,107	0,384	0,848
φ (°)	0,143	0,226	-0,001	0,249	0,016	-0,013	-0,036	-0,107	1	0,142	0,115
α % (Zv)	0,088	0,252	0,113	0,289	0,179	0,148	0,157	0,384	0,142	1	0,373
Fs(Z')	0,241	0,340	-0,054	0,273	0,191	0,027	0,030	0,848	0,115	0,373	1

Firstable the main result is the correlation matrix. We can see right away that γd has an important contribution regression with γh ($R^2 = 0,88$) almost same thing with the regression between C and Fs [Machroha1 $R^2 = 0,87$, Machroha2 $R^2 = 0,86$, Zaaroria1 $R^2 = 0,95$, Zaaroria2 $R^2 = 0,85$) where we notice that the C is most effecting parameters to Fs, also they are negatively correlated with some parameters like water content w, and the fine fraction (ff), the angle of internal friction (ϕ), and the angle of the studied slope (α), but we can also see that has a low correlation with the rest of parameter (wl, ip, Sr), These latter variables could have been removed without effect on the quality of the results.

IV.5.4. Eigenvalues and Eigenvectors:

The eigenvectors and eigenvalues of the covariance (or correlation) matrix represent the "core" of (PCA): the eigenvectors (principal components) determine the directions of the new feature space, and the eigenvalues determine their magnitude. In other words, eigenvalues explain the variance of data along the axes of new features. Projection quality reflects from the N-dimensional initial Table IV.14 (N = 11 in this example) to a smaller number of dimensions.

Table IV.14: Eigenvalues of Machroha1

	F1	F2	F3	F4	F5	F6	F7	F8	F9	F10
Eigenvalue	3,121	2,583	1,759	1,279	0,704	0,363	0,109	0,065	0,013	0,004
Variability (%)	31,214	25,827	17,589	12,795	7,040	3,627	1,094	0,647	0,127	0,041
Cumulative (%)	31,214	57,040	74,629	87,424	94,464	98,091	99,185	99,831	99,959	100,000

Table IV.15: Eigenvalues of Machroha2

	F1	F2	F3	F4	F5	F6	F7	F8	F9	F10	F11
Eigenvalue	3,388	2,594	1,916	1,293	0,800	0,448	0,363	0,116	0,064	0,013	0,004
Variability (%)	30,804	23,585	17,420	11,753	7,273	4,076	3,295	1,055	0,583	0,117	0,037
Cumulative (%)	30,804	54,390	71,810	83,563	90,836	94,913	98,208	99,263	99,846	99,963	100,000

Table IV.16: Eigenvalues of Zaaroria1

	F1	F2	F3	F4	F5	F6	F7	F8	F9	F10
Eigenvalue	3,137	2,573	1,836	1,267	0,708	0,363	0,068	0,032	0,012	0,004
Variability (%)	31,369	25,734	18,358	12,671	7,079	3,630	0,675	0,321	0,123	0,041
Cumulative (%)	31,369	57,103	75,460	88,131	95,210	98,840	99,515	99,836	99,959	100,000

Table IV.17: Eigenvalues of Zaaroria2

	F1	F2	F3	F4	F5	F6	F7	F8	F9	F10	F11
Eigenvalue	3,265	2,670	1,830	1,259	0,756	0,659	0,364	0,117	0,063	0,014	0,004
Variability (%)	29,679	24,269	16,635	11,449	6,875	5,992	3,309	1,060	0,569	0,125	0,038
Cumulative (%)	29,679	53,948	70,583	82,032	88,908	94,900	98,208	99,268	99,837	99,962	100,000

We can see that the first eigenvalue for all examples is roughly equal (mean=3,228) and represents (mean=30,77%) of the total variance. This means that if we represented the data on only one axis, we would still be able to see (%)of the total variance of the data.

Every eigenvalue corresponds to a factor, and every factor has one dimension. A factor is a linear combination of prime variables, and all factors are unrelated ($r = 0$). The eigenvalues and their corresponding factors are sorted in descending order for the amount of elemental variance they represent (converted to%).

We can notice, that the first two or three eigenvalues have a high percentage of variance, that is, the maps based on the first two or three factors are a good quality projection of the elementary multi-dimensional table.

In these examples, the first two factors account for (55,08%) of the initial data variance. This is an acceptable result as long as it is greater than (50%), but some information may be hidden in other factors, and this must be taken into account when interpreting maps.

We can observe four components with eigenvalues greater than or equal to 1.0 and together they account for (mean=84,75%) of the variance of the original data

We can work with only two components, the first and second components are the result of the linear summation of the eleven variables studied and both are (mean=30,77%) and (mean=24,85%) clearer of variance, respectively. Other components as shown in Table IV.4, the values written in bold for each variable correspond to the factor in which the square cosine is largest.

When comparing the four examples, we will find that the results obtained from Zaarorial are the highest among them (50,10%) but with a very small difference that can be neglected.

Table IV.18: Eigenvectors of Machrohal

	F1	F2	F3	F4	F5	F6	F7	F8	F9	F10
γd (kN/m3)	0,508	-0,174	-0,220	0,047	-0,102	-0,229	-0,010	-0,029	0,018	0,773
γh kN/m3	0,511	0,011	-0,059	0,234	-0,312	-0,204	0,120	0,575	-0,024	-0,442
W %	-0,359	0,335	0,345	0,187	-0,163	0,180	0,140	0,566	0,013	0,453
Sr%	0,160	0,362	0,256	0,458	-0,495	0,113	-0,181	-0,526	0,014	-0,034
Ff	0,346	0,254	-0,309	-0,182	0,077	0,822	0,028	0,064	-0,024	0,010
WL %	0,003	0,564	-0,248	-0,127	0,135	-0,287	-0,045	0,005	0,708	-0,023
IP%	-0,017	0,568	-0,228	-0,132	0,103	-0,313	0,102	-0,059	-0,696	0,018
C(KPa)	0,308	0,076	0,538	-0,306	0,106	-0,034	0,678	-0,197	0,082	-0,010
φ (°)	0,104	0,027	0,000	0,701	0,686	0,035	0,153	-0,030	-0,003	-0,003
α %(Mc)	0,000	0,000	0,000	0,000	0,000	0,000	0,000	0,000	0,000	0,000
Fs(M)	0,317	0,120	0,515	-0,215	0,323	-0,046	-0,661	0,155	-0,079	0,007

Table IV.19: Eigenvectors of Machroha2

	F1	F2	F3	F4	F5	F6	F7	F8	F9	F10	F11
γ_d (kN/m³)	0,441	-0,232	-0,299	0,047	-0,093	0,013	-0,231	0,008	-0,026	0,020	0,773
γ_h (kN/m³)	0,462	-0,047	-0,189	0,262	-0,311	0,023	-0,206	0,023	0,585	-0,016	-0,446
W %	-0,289	0,377	0,345	0,218	-0,171	0,031	0,179	0,027	0,585	0,021	0,449
Sr%	0,181	0,345	0,129	0,510	-0,456	0,225	0,085	-0,102	-0,542	0,005	-0,031
Ff	0,317	0,208	-0,360	-0,196	0,054	0,024	0,825	-0,007	0,063	-0,025	0,010
WL %	0,024	0,552	-0,257	-0,150	0,123	-0,101	-0,278	-0,037	-0,016	0,708	-0,023
IP%	0,006	0,559	-0,236	-0,152	0,093	-0,090	-0,304	0,104	-0,031	-0,698	0,019
C(KPa)	0,352	0,063	0,450	-0,228	-0,122	-0,312	0,024	0,699	-0,102	0,074	-0,009
ϕ (°)	0,102	0,018	-0,030	0,671	0,648	-0,292	0,072	0,163	-0,016	-0,003	-0,002
α % (Mv)	0,322	0,101	0,320	-0,117	0,432	0,754	-0,093	0,010	0,070	-0,001	-0,009
Fs(M')	0,371	0,083	0,427	-0,147	0,093	-0,420	-0,015	-0,679	0,012	-0,071	0,011

Table IV.20: Eigenvectors of Zaaroria1

	F1	F2	F3	F4	F5	F6	F7	F8	F9	F10
γ_d (kN/m³)	0,504	-0,160	-0,240	0,047	-0,104	-0,225	-0,030	0,001	0,024	0,773
γ_h (kN/m³)	0,509	0,026	-0,079	0,228	-0,316	-0,204	0,581	-0,087	-0,032	-0,442
W %	-0,355	0,326	0,358	0,180	-0,166	0,179	0,583	-0,057	0,020	0,451
Sr%	0,159	0,367	0,246	0,449	-0,507	0,124	-0,550	0,039	0,010	-0,033
Ff	0,333	0,264	-0,311	-0,185	0,100	0,820	0,076	0,016	-0,021	0,008
WL %	-0,014	0,566	-0,238	-0,128	0,140	-0,289	-0,032	-0,188	0,683	-0,027
IP%	-0,033	0,570	-0,215	-0,136	0,112	-0,317	-0,010	0,210	-0,672	0,024
C(KPa)	0,321	0,079	0,523	-0,325	0,110	-0,056	0,052	0,672	0,203	-0,018
ϕ (°)	0,108	0,032	0,013	0,707	0,679	0,022	0,026	0,158	0,027	-0,005
α % (Zc)	0,000	0,000	0,000	0,000	0,000	0,000	0,000	0,000	0,000	0,000
Fs(Z)	0,330	0,104	0,524	-0,194	0,300	-0,033	-0,093	-0,656	-0,194	0,014

Table IV.21: Eigenvectors of Zaaroria2

	F1	F2	F3	F4	F5	F6	F7	F8	F9	F10	F11
γ_d (kN/m ³)	0,444	-0,290	-0,233	0,059	0,083	0,049	-0,231	0,002	-0,029	0,007	0,773
γ_h (kN/m ³)	0,487	-0,100	-0,095	0,227	0,292	0,139	-0,211	0,097	0,579	-0,011	-0,445
W %	-0,268	0,423	0,327	0,156	0,188	0,046	0,178	0,094	0,581	0,013	0,451
Sr%	0,222	0,328	0,190	0,420	0,552	0,104	0,108	-0,153	-0,527	0,009	-0,032
Ff	0,350	0,147	-0,377	-0,160	-0,068	-0,005	0,823	-0,010	0,075	-0,027	0,009
WL %	0,077	0,519	-0,326	-0,110	-0,083	-0,124	-0,278	0,052	-0,021	0,709	-0,013
IP%	0,062	0,530	-0,300	-0,121	-0,068	-0,107	-0,308	0,049	-0,030	-0,704	0,009
C(KPa)	0,332	0,044	0,455	-0,370	0,048	-0,188	0,013	0,695	-0,148	0,006	-0,005
ϕ (°)	0,120	0,015	0,046	0,706	-0,507	-0,428	0,064	0,200	-0,022	-0,018	-0,003
α % (Zv)	0,246	0,196	0,267	0,027	-0,526	0,737	-0,047	-0,065	-0,053	0,008	0,004
Fs(Z')	0,356	0,080	0,418	-0,238	-0,121	-0,420	-0,053	-0,652	0,129	0,002	0,000

IV.5.5. Factor loadings:

Depending to Factor Loadings Correlations between variables and factors, and the Eigenvalue vectors the variables with negative contribution are on the factors F1, F2 respectively, (w , γ_d) in all four examples, the other factors represented by (Ff, α , ϕ , C, Fs, Sr) have a positive contribution in this analysis, but (IP, WL, γ_h) are sometimes positive or negative.

It is important to note the high and strong correlation between the parameter (γ_h , γ_d), also the good correlation between (Ff) and (w , C, Fs), this is because this method take into account neither the position of points in space, neither the degrees of similarity between the parameters.

Table IV.22: Factor loadings of Machrohal

	F1	F2	F3	F4	F5	F6	F7	F8	F9	F10
γ_d (kN/m ³)	0,897	-0,279	-0,292	0,053	-0,086	-0,138	-0,003	-0,007	0,002	0,050
γ_h (kN/m ³)	0,903	0,018	-0,078	0,265	-0,261	-0,123	0,040	0,146	-0,003	-0,028

W %	-0,634	0,538	0,458	0,212	-0,137	0,109	0,046	0,144	0,001	0,029
Sr%	0,284	0,581	0,339	0,518	-0,415	0,068	-0,060	-0,134	0,002	-0,002
Ff	0,611	0,408	-0,410	-0,206	0,065	0,495	0,009	0,016	-0,003	0,001
WL %	0,006	0,907	-0,329	-0,144	0,113	-0,173	-0,015	0,001	0,080	-0,001
IP%	-0,030	0,914	-0,303	-0,149	0,086	-0,189	0,034	-0,015	-0,078	0,001
C(KPa)	0,544	0,122	0,713	-0,346	0,089	-0,020	0,224	-0,050	0,009	-0,001
φ (°)	0,184	0,043	-0,001	0,793	0,576	0,021	0,050	-0,008	0,000	0,000
α % (Mc)	0,000	0,000	0,000	0,000	0,000	0,000	0,000	0,000	0,000	0,000
Fs(M)	0,560	0,193	0,683	-0,243	0,271	-0,028	-0,219	0,039	-0,009	0,000

Table IV.23: Factor loadings of Machroha2

	F1	F2	F3	F4	F5	F6	F7	F8	F9	F10	F11
γd (kN/m³)	0,811	-0,373	-0,414	0,053	-0,083	0,009	-0,139	0,003	-0,006	0,002	0,049
γh (kN/m³)	0,850	-0,075	-0,261	0,297	-0,278	0,015	-0,124	0,008	0,148	-0,002	-0,029
W %	-0,532	0,608	0,478	0,248	-0,153	0,021	0,108	0,009	0,148	0,002	0,029
Sr%	0,333	0,556	0,178	0,580	-0,408	0,150	0,051	-0,035	-0,137	0,001	-0,002
Ff	0,584	0,335	-0,498	-0,223	0,048	0,016	0,496	-0,002	0,016	-0,003	0,001
WL %	0,044	0,890	-0,355	-0,171	0,110	-0,067	-0,168	-0,013	-0,004	0,080	-0,001
IP%	0,012	0,901	-0,327	-0,173	0,083	-0,060	-0,183	0,036	-0,008	-0,079	0,001
C(KPa)	0,649	0,102	0,623	-0,259	-0,109	-0,209	0,014	0,238	-0,026	0,008	-0,001
φ (°)	0,188	0,029	-0,041	0,763	0,580	-0,196	0,043	0,055	-0,004	0,000	0,000
α % (Mv)	0,593	0,162	0,443	-0,133	0,387	0,505	-0,056	0,003	0,018	0,000	-0,001
Fs(M')	0,682	0,134	0,591	-0,167	0,083	-0,282	-0,009	-0,231	0,003	-0,008	0,001

Table IV.24: Factor loadings of Zaarorial

	F1	F2	F3	F4	F5	F6	F7	F8	F9	F10
γd (kN/m³)	0,893	-0,256	-0,325	0,053	-0,087	-0,135	-0,008	0,000	0,003	0,049
γh (kN/m³)	0,901	0,042	-0,107	0,256	-0,266	-0,123	0,151	-0,016	-0,004	-0,028
W %	-0,628	0,523	0,486	0,203	-0,139	0,108	0,152	-0,010	0,002	0,029

Sr%	0,282	0,589	0,333	0,505	-0,427	0,075	-0,143	0,007	0,001	-0,002
Ff	0,590	0,424	-0,422	-0,208	0,084	0,494	0,020	0,003	-0,002	0,000
WL %	-0,025	0,908	-0,322	-0,144	0,118	-0,174	-0,008	-0,034	0,076	-0,002
IP%	-0,058	0,914	-0,291	-0,153	0,095	-0,191	-0,002	0,038	-0,075	0,002
C(KPa)	0,569	0,126	0,708	-0,366	0,092	-0,034	0,013	0,120	0,023	-0,001
φ (°)	0,191	0,052	0,017	0,796	0,571	0,013	0,007	0,028	0,003	0,000
α % (Zc)	0,000	0,000	0,000	0,000	0,000	0,000	0,000	0,000	0,000	0,000
Fs(Z)	0,585	0,167	0,710	-0,218	0,252	-0,020	-0,024	-0,118	-0,022	0,001

Table IV.25: Factor loadings of Zaaroria2

	F1	F2	F3	F4	F5	F6	F7	F8	F9	F10	F11
γd (kN/m³)	0,802	-0,473	-0,316	0,066	0,072	0,040	-0,139	0,001	-0,007	0,001	0,050
γh (kN/m³)	0,881	-0,163	-0,129	0,254	0,254	0,113	-0,127	0,033	0,145	-0,001	-0,029
W %	-0,484	0,691	0,442	0,175	0,164	0,038	0,107	0,032	0,145	0,002	0,029
Sr%	0,402	0,536	0,257	0,472	0,480	0,085	0,065	-0,052	-0,132	0,001	-0,002
Ff	0,633	0,240	-0,510	-0,179	-0,059	-0,004	0,496	-0,003	0,019	-0,003	0,001
WL %	0,139	0,848	-0,441	-0,124	-0,072	-0,100	-0,168	0,018	-0,005	0,083	-0,001
IP%	0,113	0,867	-0,406	-0,136	-0,059	-0,087	-0,186	0,017	-0,008	-0,083	0,001
C(KPa)	0,600	0,072	0,616	-0,415	0,042	-0,153	0,008	0,237	-0,037	0,001	0,000
φ (°)	0,217	0,025	0,063	0,792	-0,441	-0,348	0,038	0,068	-0,005	-0,002	0,000
α % (Zv)	0,444	0,321	0,361	0,030	-0,458	0,598	-0,028	-0,022	-0,013	0,001	0,000
Fs(Z')	0,643	0,131	0,565	-0,267	-0,105	-0,341	-0,032	-0,223	0,032	0,000	0,000

IV.5.6. Correlations between variables and factors and the (PCA) circle:

(PCA) reveals that 50.04% (case of machroha1) of the variance in our dataset can be represented in a 2-dimensional space. The dimension with the most explained variance is called F1 and plotted on the horizontal axes, the second-most explanatory dimension is

called F2 and placed on the vertical axis. Inside this 2-dimensional circle the original 11 variables are projected in red onto this 2-dimensional factor space.

The angle between the red vectors is an approximation of the correlation between the variables. A small angle indicates the variables are positively correlated, an angle of 90 degrees indicates the variables are not correlated, and an angle close to 180 degrees indicates the variables are negatively correlated.

The length of the line and its closeness to the circle indicate how well the variable is represented in the plot. It is therefore unwise to make inferences about relationships involving variables that are poorly represented.

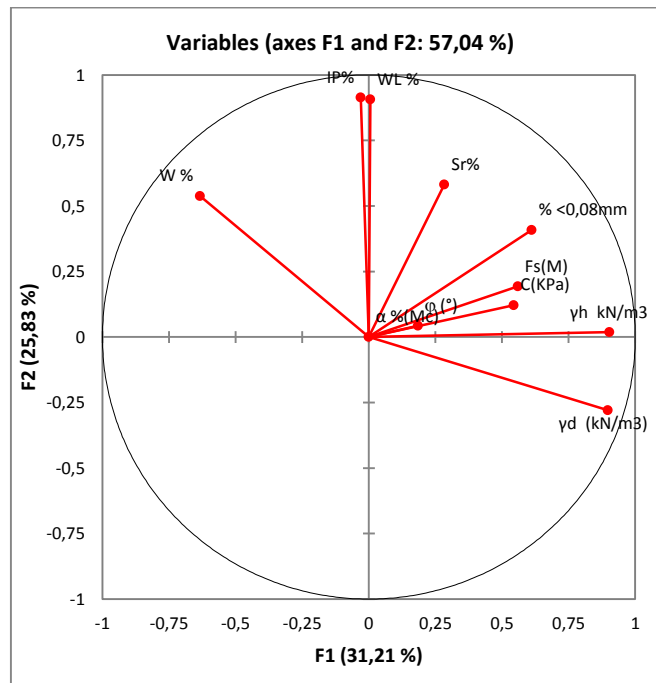


Figure IV.24: (PCA) correlation circle (Machroha1)

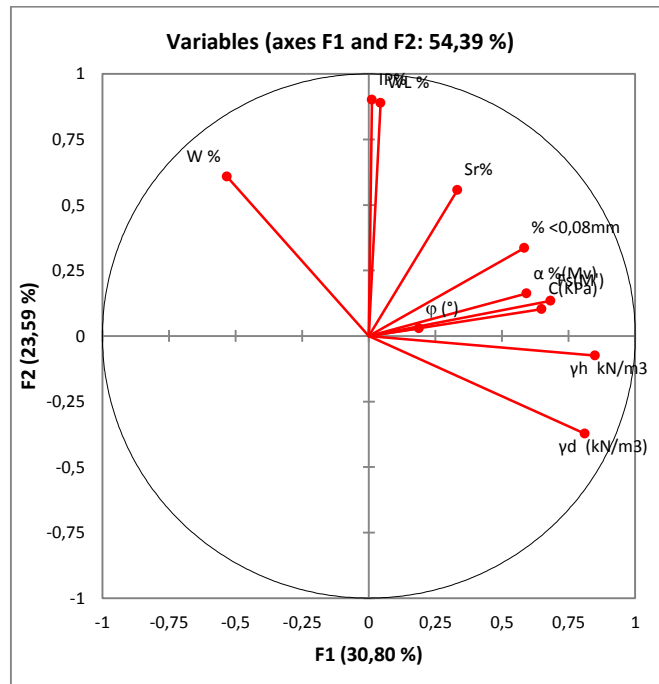


Figure IV.25: (PCA) correlation circle (Machroha2)

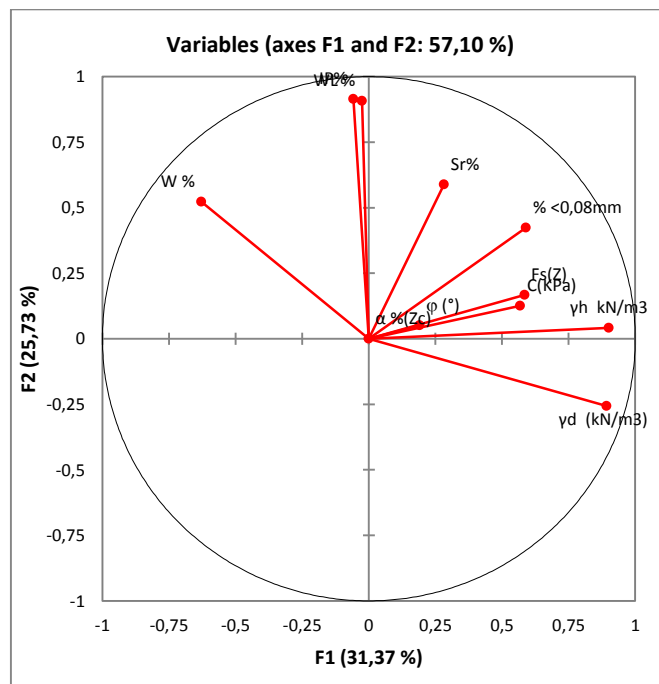


Figure IV. 26: (PCA) correlation circle (Zaaroria1)

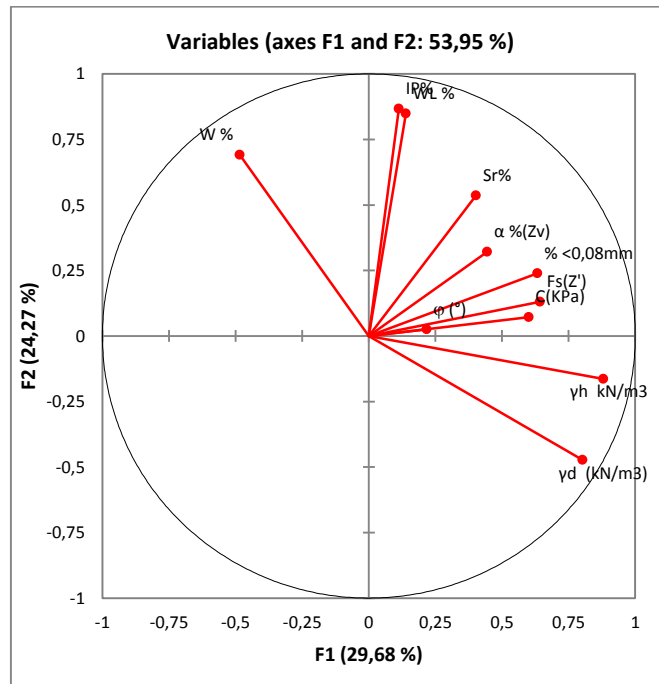


Figure IV.27: (PCA) correlation circle (Zaaroria2)

The four cases are almost identical and have the same correlation, except for the highly observed variable (α), whose position can be distinguished between all the cases, the other variables, for example, we find that (γ_d) and (w) are negatively related and this is logical, there is also a positive correlation between (γ_d) and (γ_h) and another strongly positive between (IP) and (WL).

The other variables (F_f , S_r , ϕ) are difficult to confirm that there is a correlation between them or other variables, but there are two variables that are important to us, namely (F_s) and (C) the angle between them is very small, which means that their correlation is positive, but they are not close enough to the line, so we cannot establish a relationship between them by 100%.

Furthermore, geotechnical soil properties, such as water content, plasticity index, angle of internal friction, and cohesion, can play a significant role when trying to understand and predict slope soil failure mechanisms (Martino, S.; Mazzanti, 2014, Epada, P.D et al 2012; Wouatong, A.S.L et al 2017).

IV.5.7. Contributions of variables to (PC)

The contributions of variables in accounting for the variability in a given principal component are expressed in percentage.

Variables that are correlated with (PC1) (i.e., F1) and (PC2) (i.e., F2) are the most important in explaining the variability in the data set.

Variables that do not correlated with any (PC) or correlated with the last dimensions are variables with low contribution and might be removed to simplify the overall analysis (Abdi, et al. 2010; Husson, et al. 2017; Jolliffe, I.T. 2002; Kaiser, 1961; Peres-Neto et al. 2005).

Table IV.26: Contribution of the variables (%) of Machroha1

	F1	F2	F3	F4	F5	F6	F7	F8	F9	F10
γ_d (kN/m³)	25,791	3,011	4,861	0,221	1,046	5,234	0,009	0,086	0,032	59,709
γ_h (kN/m³)	26,145	0,013	0,347	5,496	9,703	4,153	1,449	33,078	0,060	19,556
W %	12,869	11,220	11,911	3,498	2,660	3,255	1,970	32,089	0,016	20,512
Sr%	2,575	13,076	6,543	20,971	24,489	1,268	3,294	27,649	0,019	0,115
Ff	11,960	6,450	9,557	3,308	0,599	67,572	0,080	0,404	0,059	0,009
WL %	0,001	31,821	6,153	1,611	1,812	8,260	0,203	0,003	50,086	0,051
IP%	0,028	32,319	5,216	1,732	1,059	9,803	1,036	0,342	48,434	0,031
C(KPa)	9,484	0,574	28,908	9,346	1,121	0,115	45,904	3,863	0,674	0,011
ϕ (°)	1,090	0,072	0,000	49,204	47,092	0,124	2,328	0,089	0,001	0,001
α % (Mc)	0,000	0,000	0,000	0,000	0,000	0,000	0,000	0,000	0,000	0,000
Fs(M)	10,057	1,445	26,503	4,613	10,420	0,216	43,726	2,396	0,619	0,005

Table IV.27: Contribution of the variables (%) of Machroha2

	F1	F2	F3	F4	F5	F6	F7	F8	F9	F10	F11
γ_d (kN/m³)	19,406	5,365	8,952	0,217	0,866	0,017	5,355	0,006	0,065	0,038	59,713
γ_h kN/m³	21,309	0,218	3,554	6,845	9,664	0,053	4,230	0,054	34,166	0,025	19,881
W %	8,349	14,231	11,909	4,747	2,923	0,096	3,205	0,074	34,240	0,042	20,185
Sr%	3,271	11,927	1,660	25,995	20,815	5,043	0,730	1,035	29,430	0,003	0,093
Ff	10,050	4,330	12,938	3,855	0,292	0,060	67,996	0,005	0,401	0,063	0,010
WL %	0,057	30,510	6,583	2,250	1,505	1,013	7,754	0,138	0,026	50,110	0,054
IP%	0,004	31,278	5,573	2,314	0,861	0,813	9,265	1,087	0,098	48,671	0,036

C(KPa)	12,420	0,402	20,267	5,196	1,485	9,748	0,058	48,826	1,046	0,545	0,007
φ (°)	1,044	0,032	0,088	45,059	42,029	8,550	0,516	2,653	0,026	0,001	0,001
α %(Mv)	10,363	1,011	10,259	1,373	18,693	56,926	0,869	0,010	0,489	0,000	0,007
Fs(M')	13,729	0,696	18,217	2,148	0,867	17,681	0,022	46,114	0,013	0,500	0,012

Table IV.28: Contribution of the variables (%) of Zaaroria1

	F1	F2	F3	F4	F5	F6	F7	F8	F9	F10
γd (kN/m³)	25,420	2,551	5,755	0,223	1,079	5,055	0,093	0,000	0,058	59,767
γh (kN/m³)	25,875	0,068	0,618	5,188	9,973	4,148	33,708	0,752	0,100	19,569
W %	12,588	10,618	12,842	3,244	2,744	3,217	34,016	0,329	0,041	20,360
Sr%	2,535	13,464	6,028	20,125	25,744	1,536	30,297	0,149	0,010	0,112
Ff	11,080	6,995	9,692	3,406	1,004	67,176	0,574	0,024	0,043	0,006
WL %	0,020	32,006	5,645	1,647	1,973	8,355	0,100	3,548	46,633	0,074
IP%	0,109	32,486	4,628	1,836	1,265	10,040	0,009	4,417	45,152	0,058
C(KPa)	10,310	0,621	27,332	10,574	1,205	0,315	0,267	45,222	4,124	0,031
φ (°)	1,165	0,104	0,016	50,002	46,038	0,049	0,068	2,482	0,074	0,003
α %(Zc)	0,000	0,000	0,000	0,000	0,000	0,000	0,000	0,000	0,000	0,000
Fs(Z)	10,897	1,088	27,443	3,754	8,976	0,109	0,869	43,076	3,767	0,021

Table IV.29: Contribution of the variables (%) of Zaaroria2

	F1	F2	F3	F4	F5	F6	F7	F8	F9	F10	F11
γd (kN/m³)	19,705	8,391	5,443	0,343	0,686	0,244	5,340	0,000	0,084	0,005	59,759
γh (kN/m³)	23,754	0,999	0,906	5,141	8,553	1,920	4,460	0,950	33,504	0,012	19,799
W %	7,173	17,884	10,661	2,426	3,547	0,214	3,170	0,880	33,730	0,017	20,299
Sr%	4,950	10,780	3,611	17,654	30,495	1,091	1,176	2,341	27,793	0,008	0,103
Ff	12,257	2,149	14,209	2,551	0,461	0,003	67,720	0,010	0,562	0,070	0,008
WL %	0,593	26,960	10,645	1,219	0,692	1,532	7,739	0,274	0,045	50,283	0,018
IP%	0,389	28,132	9,024	1,466	0,460	1,146	9,475	0,245	0,092	49,564	0,008
C(KPa)	11,042	0,193	20,725	13,673	0,234	3,543	0,016	48,366	2,202	0,003	0,003
φ (°)	1,440	0,023	0,214	49,792	25,697	18,336	0,406	4,012	0,047	0,032	0,001
α %(Zv)	6,047	3,850	7,108	0,071	27,705	54,290	0,219	0,419	0,281	0,007	0,002
Fs(Z')	12,650	0,639	17,454	5,664	1,469	17,682	0,278	42,503	1,660	0,000	0,000

We can note (depending on the variable contribution tables) the following:

- There is similarity in the results between the annotated cases 1 and Hawthorne 1 and the annotated and Hawthorne cases.

The factor strongly influencing the results is the degree of propensity.

- In the case of Machroha1 and Zaaroria1, the variables (γ_d , γ_h) are the most contributing to the first factor, then the variables (Fs, C, Ff, W) in an average manner, while the variables (Sr, WL, IP, ϕ , α) have no significant contribution and can be ignored. Regarding the second factor, the most contributing variables are (WL, IP), followed by (W, Sr) and (Ff), while the other variables do not contribute nearly all.

- In the case of Machroha2 and Zaaroria2, we can notice the contribution of the two variables (γ_d , γ_h) to the first factor and its absence to the two variables (WL, IP) where the degree of contribution to the other variables varies, and on the second factor, the most contributing ones are (WL, IP) and the contribution of the other variables is almost non-existent.

IV.5.8. Squared cosines of the variables:

Squared cosines reflect the representation quality of a variable on a (PCA) axis. As in other factor methods, squared cosine analysis is used to avoid interpretation errors due to projection effects. If the squared cosines of a variable associated to an axis is low, the position of the variable on this axis should not be interpreted (XLstat site).

Table IV.30: Squared cosines of the variables of Machroha1

	F1	F2	F3	F4	F5	F6	F7	F8	F9	F10
γ_d (kN/m ³)	0,805	0,078	0,085	0,003	0,007	0,019	0,000	0,000	0,000	0,002
γ_h (kN/m ³)	0,816	0,000	0,006	0,070	0,068	0,015	0,002	0,021	0,000	0,001
W %	0,402	0,290	0,210	0,045	0,019	0,012	0,002	0,021	0,000	0,001
Sr%	0,080	0,338	0,115	0,268	0,172	0,005	0,004	0,018	0,000	0,000
Ff	0,373	0,167	0,168	0,042	0,004	0,245	0,000	0,000	0,000	0,000
WL %	0,000	0,822	0,108	0,021	0,013	0,030	0,000	0,000	0,006	0,000
IP%	0,001	0,835	0,092	0,022	0,007	0,036	0,001	0,000	0,006	0,000
C(KPa)	0,296	0,015	0,508	0,120	0,008	0,000	0,050	0,002	0,000	0,000
ϕ (°)	0,034	0,002	0,000	0,630	0,332	0,000	0,003	0,000	0,000	0,000
α %(Mc)	0,000	0,000	0,000	0,000	0,000	0,000	0,000	0,000	0,000	0,000
Fs(M)	0,314	0,037	0,466	0,059	0,073	0,001	0,048	0,002	0,000	0,000

Table IV.31: Squared cosines of the variables of Machroha2

	F1	F2	F3	F4	F5	F6	F7	F8	F9	F10	F11
γ_d (kN/m ³)	0,658	0,139	0,172	0,003	0,007	0,000	0,019	0,000	0,000	0,000	0,002
γ_h (kN/m ³)	0,722	0,006	0,068	0,088	0,077	0,000	0,015	0,000	0,022	0,000	0,001
W %	0,283	0,369	0,228	0,061	0,023	0,000	0,012	0,000	0,022	0,000	0,001
Sr%	0,111	0,309	0,032	0,336	0,167	0,023	0,003	0,001	0,019	0,000	0,000
Ff	0,341	0,112	0,248	0,050	0,002	0,000	0,246	0,000	0,000	0,000	0,000
WL %	0,002	0,792	0,126	0,029	0,012	0,005	0,028	0,000	0,000	0,006	0,000
IP%	0,000	0,811	0,107	0,030	0,007	0,004	0,034	0,001	0,000	0,006	0,000
C(KPa)	0,421	0,010	0,388	0,067	0,012	0,044	0,000	0,057	0,001	0,000	0,000
ϕ (°)	0,035	0,001	0,002	0,583	0,336	0,038	0,002	0,003	0,000	0,000	0,000
α % (Mv)	0,351	0,026	0,197	0,018	0,150	0,255	0,003	0,000	0,000	0,000	0,000
Fs(M')	0,465	0,018	0,349	0,028	0,007	0,079	0,000	0,054	0,000	0,000	0,000

Table IV.32: Squared cosines of the variables of Zaaroria1

	F1	F2	F3	F4	F5	F6	F7	F8	F9	F10
γ_d (kN/m ³)	0,797	0,066	0,106	0,003	0,008	0,018	0,000	0,000	0,000	0,002
γ_h (kN/m ³)	0,812	0,002	0,011	0,066	0,071	0,015	0,023	0,000	0,000	0,001
W %	0,395	0,273	0,236	0,041	0,019	0,012	0,023	0,000	0,000	0,001
Sr%	0,080	0,346	0,111	0,255	0,182	0,006	0,020	0,000	0,000	0,000
Ff	0,348	0,180	0,178	0,043	0,007	0,244	0,000	0,000	0,000	0,000
WL %	0,001	0,824	0,104	0,021	0,014	0,030	0,000	0,001	0,006	0,000
IP%	0,003	0,836	0,085	0,023	0,009	0,036	0,000	0,001	0,006	0,000
C(KPa)	0,323	0,016	0,502	0,134	0,009	0,001	0,000	0,015	0,001	0,000
ϕ (°)	0,037	0,003	0,000	0,634	0,326	0,000	0,000	0,001	0,000	0,000
α % (Zc)	0,000	0,000	0,000	0,000	0,000	0,000	0,000	0,000	0,000	0,000
Fs(Z)	0,342	0,028	0,504	0,048	0,064	0,000	0,001	0,014	0,000	0,000

Table IV.33: Squared cosines of the variables of Zaaroria

	F1	F2	F3	F4	F5	F6	F7	F8	F9	F10	F11
γ_d (kN/m ³)	0,643	0,224	0,100	0,004	0,005	0,002	0,019	0,000	0,000	0,000	0,002
γ_h (kN/m ³)	0,776	0,027	0,017	0,065	0,065	0,013	0,016	0,001	0,021	0,000	0,001
W %	0,234	0,477	0,195	0,031	0,027	0,001	0,012	0,001	0,021	0,000	0,001
Sr%	0,162	0,288	0,066	0,222	0,231	0,007	0,004	0,003	0,017	0,000	0,000
Ff	0,400	0,057	0,260	0,032	0,003	0,000	0,246	0,000	0,000	0,000	0,000

WL %	0,019	0,720	0,195	0,015	0,005	0,010	0,028	0,000	0,000	0,007	0,000
IP%	0,013	0,751	0,165	0,018	0,003	0,008	0,034	0,000	0,000	0,007	0,000
C(KPa)	0,360	0,005	0,379	0,172	0,002	0,023	0,000	0,056	0,001	0,000	0,000
φ (°)	0,047	0,001	0,004	0,627	0,194	0,121	0,001	0,005	0,000	0,000	0,000
α % (Zv)	0,197	0,103	0,130	0,001	0,210	0,358	0,001	0,000	0,000	0,000	0,000
Fs(Z')	0,413	0,017	0,319	0,071	0,011	0,117	0,001	0,050	0,001	0,000	0,000

To confirm that a variable is well linked with an axis, we a look at the squared cosines table: the greater the squared cosine, the greater is the link with the corresponding axis. The closer the squared cosine of a given variable is to zero, the more careful you have to be when interpreting the results in terms of trends on the corresponding axis. Looking at Table IV.1 and 2 it may be noticed that the (PC) F1 covers four of the variables (γ_d , γ_h , W, Ff), and F2 explains three (Sr, WL, IP), while F3 an F4 explain the last three (the variable (α) is always zero).

Otherwise at Table IV.3 the (PC) F1 covers six variables (γ_d , γ_h , Ff, C, α , Fs) F2 three variables, and F4 last two of them. For Table IV.4 the (PC) F1 covers four variables (γ_d , γ_h , $\alpha < 0,08\text{mm}$, Fs) as same as F2 (W, Sr, WL, IP), and the others go with F3 F4 and F6.as a note (α) has a value in tables 3 and 4 because it is not constant in cases machroha2 and zaaroria2.

IV.6. Multiple linear regression

Linear regression is a basic and commonly used type of predictive analysis. The general idea of regression is to examine two things:

Regression estimates are used to explain the relationship between one dependent variable and one or more independent variables. The linear regression analysis uses the mathematical equation, i.e., $y = mx + c$, that describes the line of best fit for the relationship between y (dependent variable) and x (independent variable). The regression coefficient, i.e., r^2 implies the degree of variability of y due to x.

Naming the variables. There are many names for the dependent variable. It may be called an outcome variable, criterion variable, internal variable, or regression. The independent variables can be called the exogenous variables, expectancy variables, or the variables

In correlation analysis, the correlation coefficient “r” is a dimensionless number whose value ranges from -1 to $+1$. A value toward -1 indicates inverse or negative relationship, whereas towards $+1$ indicate a positive relation. When there is a normal distribution, the Pearson’s correlation is used, whereas, in nonnormally distributed data, Spearman’s rank correlation is used.

Three main uses of regression analysis are resumed to the determination of the strength of predictors, the impact prediction and the trend predicting. In the first one, regression can be used to determine the strength of the influence of the independent variable (s) on the dependent variable, in the second, it can be used to predict the effects or impact of changes. That is, regression analysis helps us understand the extent to which the dependent variable has changed with the change of one or more independent variables, finally regression analysis predicts future trends and values. Regression analysis can be used to obtain point estimates (Aiken, et al. 2012; Alpar. R, 2003, Büyükoztürk. Ş. 2002; Schmidt, et al 2018).

IV.6.1. Types of Linear Regression

- Simple linear regression
1 dependent variable (interval or ratio), 1 independent variable (interval or ratio or dichotomous)
- Multiple linear regression
1 dependent variable (interval or ratio), 2+ independent variables (interval or ratio or dichotomous)
- Logistic regression
1 dependent variable (dichotomous), 2+ independent variable(s) (interval or ratio or dichotomous)
- Ordinal regression
1 dependent variable (ordinal), 1+ independent variable(s) (nominal or dichotomous)
- Multinomial regression
1 dependent variable (nominal), 1+ independent variable(s) (interval or ratio or dichotomous)
- Discriminant analysis

1 dependent variable (nominal), 1+ independent variable(s) (interval or ratio).

When selecting the model for the analysis, an important consideration is model fitting. Adding independent variables to a linear regression model will always increase the explained variance of the model (typically expressed as R^2). However, overfitting can occur by adding too many variables to the model, which reduces model generalizability. Occam's razor describes the problem extremely well – a simple model is usually preferable to a more complex model. Statistically, if a model includes a large number of variables, some of the variables will be statistically significant due to chance alone (Schneider A, et al 2010; Elazar JP. 1982).

IV.6.2. Least-Squares Regression

The most common method for fitting a regression line is the method of least-squares. This method calculates the best-fitting line for the observed data by minimizing the sum of the squares of the vertical deviations from each data point to the line (if a point lies on the fitted line exactly, then its vertical deviation is 0). Because the deviations are first squared, then summed, there are no cancellations between positive and negative values.

IV.6.3. Goodness of fit statistics:

The most important value for the quality of the fit statistics is R^2 , which is a statistical measure of how close the data are to the fitted regression line. It is also known as the coefficient of determination, or the coefficient of multiple determination for multiple regression.

The definition of R-squared is fairly straight-forward; it is the percentage of the response variable variation that is explained by a linear model. Or:

R-squared = Explained variation / Total variation

R-squared is always between 0 and 100%:

- 0% indicates that the model explains none of the variability of the response data around its mean.
- 100% indicates that the model explains all the variability of the response data around its mean.

In general, the higher the R-squared, the better the model fits your data.

Table IV.34: Goodness of fit statistics of Machrohal

Observations	99,000
Sum of weights	99,000
DF	89,000
R²	0,809
Adjusted R²	0,790
MSE	0,145
RMSE	0,381
MAPE	18,334
DW	1,437
Cp	10,000
AIC	-181,708
SBC	-155,757
PC	0,233

Table IV.35: Goodness of fit statistics of Machroha2

Observations	99,000
Sum of weights	99,000
DF	88,000
R²	0,798
Adjusted R²	0,775
MSE	0,135
RMSE	0,367
MAPE	15,783
DW	1,563
Cp	11,000
AIC	-187,961
SBC	-159,415
PC	0,252

Table IV.36: Goodness of fit statistics of Zaarorial

Observations	99,000
Sum of weights	99,000
DF	89,000
R²	0,941
Adjusted R²	0,935
MSE	0,076

RMSE	0,276
MAPE	6,389
DW	2,310
Cp	10,000
AIC	-245,647
SBC	-219,696
PC	0,072

Table IV.37: Goodness of fit statistics of Zaaroria2

Observations	99,000
Sum of weights	99,000
DF	88,000
R²	0,772
Adjusted R²	0,746
MSE	0,211
RMSE	0,459
MAPE	12,844
DW	2,016
Cp	11,000
AIC	-143,832
SBC	-115,286
PC	0,285

So in the first case (Machroha1) $R^2 = 0.809$ and this is very good also the second case (Zaaroria1) R^2 is very high equal to 0.941 and this is close to perfect which means that 80.9% to 94.1% of the data fits into the regression model.

In the other two cases, $R^2 = 0.789$ in (Machroha2) and $R^2 = 0.778$ in (Zaaroria2). Therefore, 78.9% to 77.8% of the data fit the regression model. We notice that the value of R^2 decreases because (α) is variable, which means that it is a factor affecting the results.

IV.6.4. Analysis of Variance (ANOVA)

Table IV.38: Analysis of variance of Machroha1

Source	DF	Sum of squares	Mean squares	F	Pr > F
Model	9	54,788	6,088	41,981	< 0,0001
Error	89	12,906	0,145		
Corrected Total	98	67,694			

Table IV.39: Analysis of variance of Machroha2

Source	DF	Sum of squares	Mean squares	F	Pr > F
Model	10	46,982	4,698	34,821	< 0,0001
Error	88	11,873	0,135		
Corrected Total	98	58,856			

Table IV.40: Analysis of variance of Zaaroria1

Source	DF	Sum of squares	Mean squares	F	Pr > F
Model	9	108,378	12,042	158,415	< 0,0001
Error	89	6,765	0,076		
Corrected Total	98	115,143			

Table IV.41: Analysis of variance of Zaaroria2

Source	DF	Sum of squares	Mean squares	F	Pr > F
Model	10	62,838	6,284	29,822	< 0,0001
Error	88	18,542	0,211		
Corrected Total	98	81,380			

IV.6.4.1. Degrees of freedom (df)

- **Model df** is the number of independent variables in our regression model. Since we consider 10 variables (we ignore the value of (α) when it is constant does not affect the results), so it is 9 in Machroha1 and Zaaroria1 and 10 in Machroha2 and Zaaroria2.
- **Error df** is the total number of observations (rows) of the dataset subtracted by the number of variables being estimated. In this examples, the Fs is estimated.
Error df = 99 - 10 = 89 in Machroha1 and Zaaroria1.
Error df = 99 - 11 = 88 in Machroha2 and Zaaroria2.
- **Corrected df** is the sum of the regression and residual degrees of freedom, which equals the size of the dataset minus 1.

IV.6.4.2. Sum of Squares (SS)

Regression SS is the total variation in the dependent variable that is explained by the regression model. It is the sum of the square of the difference between the predicted value and mean of the value of all the data points.

$$\sum (\hat{y} - \bar{y})^2$$

From the ANOVA:

Machroha1 table, the Model SS is 54,788 and the Corrected SS is 67,694, which means the regression model explains about 54,788/67,694 (around 80,9%) of all the variability in the dataset.

Zaaroria1 table, the Model SS is 108,378 and the Corrected SS is 115.143, which means the regression model explains about 108,378/115.143 (around 94.1%) of all the variability in the dataset.

Machroha2 table, the Model SS is 46,982 and the Corrected SS is 58,856, which means the regression model explains about 46,982/58,856 (around 79,8%) of all the variability in the dataset.

Zaaroria2 table, the Model SS is 62,838 and the Corrected SS is 81,38, which means the regression model explains about 62,838/81.38 (around 77,2%) of all the variability in the dataset.

This results are the confirmation of R^2 .

IV.6.4.3. Significance F ($Pr > F$)

The simplest way to understand the significance F is to think of it as the probability that our regression model is wrong and needs to be discarded!! The significance F gives you the probability that the model is wrong. We want the significance F or the probability of being wrong to be as small as possible.

Significance F: Smaller is better....

in our cases Significance F is always close to zero (Significance F < **0.0001**) that means it is a very strong regression and the results are so good.

IV.6.5. Model parameters:

Each variable value represents the change in the mean response F_s , per unit increase in the associated predictor variable when all the other predictors are held constant.

Table IV.42: Model parameters of Machroha1

Source	Value	Standard error	t	Pr > t	Lower bound (95%)	Upper bound (95%)
Intercept	1,980	2,439	0,812	0,419	-2,867	6,826
γ_d (kN/m ³)	-0,153	0,396	-0,386	0,701	-0,938	0,633
γ_h (kN/m ³)	0,011	0,317	0,035	0,972	-0,619	0,641
W %	-0,039	0,061	-0,634	0,528	-0,160	0,082
Sr%	0,008	0,009	0,907	0,367	-0,009	0,025
Ff	-0,001	0,003	-0,182	0,856	-0,007	0,006
WL %	0,055	0,020	2,757	0,007	0,015	0,095
IP%	-0,076	0,030	-2,498	0,014	-0,137	-0,016
C(KPa)	0,023	0,001	17,633	< 0,0001	0,020	0,025
ϕ (°)	0,018	0,006	2,958	0,004	0,006	0,030
α %(Mc)	0,000	0,000				

Table IV.43: Model parameters of Machroha2

Source	Value	Standard error	t	Pr > t	Lower bound (95%)	Upper bound (95%)
Intercept	-0,077	2,403	-0,032	0,975	-4,852	4,699
γ_d (kN/m ³)	-0,249	0,383	-0,651	0,517	-1,011	0,512
γ_h (kN/m ³)	0,214	0,309	0,692	0,491	-0,400	0,828
W %	-0,034	0,059	-0,576	0,566	-0,151	0,083
Sr%	-0,002	0,008	-0,218	0,828	-0,019	0,015
Ff	-0,001	0,003	-0,434	0,665	-0,008	0,005
WL %	0,049	0,019	2,531	0,013	0,011	0,088
IP%	-0,069	0,029	-2,360	0,021	-0,128	-0,011
C(KPa)	0,019	0,002	12,668	< 0,0001	0,016	0,022
ϕ (°)	0,015	0,006	2,540	0,013	0,003	0,027
α %(Mv)	0,029	0,015	1,954	0,054	-0,001	0,059

Table IV.44: Model parameters of Zaaroria1

Source	Value	Standard error	t	Pr > t	Lower bound (95%)	Upper bound (95%)
Intercept	1,671	1,770	0,944	0,348	-1,845	5,188
γ_d (kN/m ³)	-0,126	0,289	-0,438	0,663	-0,700	0,447
γ_h kN/m ³	0,015	0,231	0,064	0,949	-0,444	0,474
W %	-0,022	0,044	-0,493	0,623	-0,110	0,066
Sr%	0,003	0,006	0,485	0,629	-0,009	0,015
Ff	0,000	0,002	0,179	0,858	-0,004	0,005
WL %	0,038	0,015	2,602	0,011	0,009	0,067
IP%	-0,054	0,022	-2,449	0,016	-0,098	-0,010
C(KPa)	0,032	0,001	34,296	< 0,0001	0,030	0,034
ϕ (°)	0,033	0,004	7,409	< 0,0001	0,024	0,042
α % (Zc)	0,000	0,000				

Table IV.45: Model parameters of Zaaroria2

Source	Value	Standard error	t	Pr > t	Lower bound (95%)	Upper bound (95%)
Intercept	1,867	3,040	0,614	0,541	-4,174	7,908
γ_d (kN/m ³)	0,015	0,478	0,031	0,975	-0,934	0,964
γ_h kN/m ³	-0,121	0,385	-0,314	0,754	-0,886	0,644
W %	-0,028	0,073	-0,380	0,705	-0,174	0,118
Sr%	0,008	0,010	0,765	0,446	-0,013	0,029
Ff	-0,001	0,004	-0,272	0,786	-0,009	0,007
WL %	0,003	0,024	0,107	0,915	-0,046	0,051
IP%	0,009	0,037	0,242	0,809	-0,064	0,082
C(KPa)	0,024	0,002	14,624	< 0,0001	0,021	0,027
ϕ (°)	0,029	0,008	3,793	0,000	0,014	0,043
α % (Zv)	0,006	0,041	0,140	0,889	-0,076	0,088

For example, in Machrohal when $\gamma_d = -0.153$ we would say we expect (Fs) to decrease by 0.153 if we were to increase gamma d by one unit and keep other parameters fixed.

or in Zaaroria2 when $\gamma d=0.015$ we would say we expect (Fs) to increase by 0.015 if we were to increase gamma d by one unit and keep other parameters fixed.

same thing for all the rest.

The intercept term value, represents the estimated mean response, (Fs), when all the predictors (parameters) are all zero (which may or may not have any practical meaning).

IV.6.5.1. p-value

The other important item is the p-value this is a test of whether this coefficients (these slopes) are too close to zero because zero slope means that it has no effect, so if the p-value is smaller than 0.5 we normally would say that these coefficients are have an effect on Fs.

In the four cases the smallest p-values are writing in **bold**, more than 2 or 3 values in each Table IV.but we can see clearly that the value C is always the smallest one so it's the most affecting coefficient in Fs.

IV.6.5.2. Equation of the model

The calculations in model parameters are explained by the following equation:

Table IV.46: The equations of (Fs) for the four cases

Cases	The equation of (Fs)
Machroha1	$F_s = 1,98 - 0,15\gamma d + 0,01\gamma h - 0,038W + 0,007Sr - 0,0006Ff + 0,005WL - 0,08IP + 0,02C + 0,01\varphi$
Zaaroria1	$F_s = 1,67 - 0,13\gamma d + 0,015\gamma h - 0,02W + 0,003Sr + 0,0004Ff + 0,04WL - 0,05IP + 0,03C + 0,03\varphi$
Machroha2	$F_s = -0,08 - 0,249\gamma d + 0,21\gamma h - 0,03W - 0,002Sr - 0,001Ff + 0,05WL - 0,07IP + 0,02C + 0,02\varphi + 0,03\alpha$
Zaaroria2	$F_s = 1,87 + 0,01\gamma d - 0,12\gamma h - 0,03W + 0,008Sr - 0,001Ff + 0,003WL + 0,009IP + 0,02C + 0,03\varphi + 0,006\alpha$

IV.6.6. Standardized coefficients (or Beta Coefficients)

The beta coefficients can be negative or positive, and have a t-value and significance of the t-value associated with each. The beta coefficient is the degree of change in the outcome variable for every 1-unit of change in the predictor variable. The t-test assesses whether the beta coefficient is significantly different from zero. If the beta coefficient is not statistically significant (i.e., the t-value is not significant), the variable does not significantly predict the outcome. If the beta coefficient is significant, examine the sign of the beta. If the beta coefficient is positive, the interpretation is that for every 1-unit increase in the predictor variable, the outcome variable will increase by the beta coefficient value. If the beta coefficient is negative, the interpretation is that for every 1-unit increase in the predictor variable, the outcome variable will decrease by the beta coefficient value (Lindstrom, D. 2010; Roth, P.L., et al. 2018).

Table IV.47: Standardized coefficients of Machroha1

Source	Value	Standard error	t	Pr > t	Lower bound (95%)	Upper bound (95%)
γ_d (kN/m ³)	-0,214	0,556	-0,386	0,701	-1,318	0,890
γ_h (kN/m ³)	0,012	0,336	0,035	0,972	-0,657	0,680
W %	-0,217	0,342	-0,634	0,528	-0,897	0,463
Sr%	0,098	0,108	0,907	0,367	-0,117	0,313
Ff	-0,012	0,068	-0,182	0,856	-0,147	0,123
WL %	0,774	0,281	2,757	0,007	0,216	1,333
IP%	-0,696	0,279	-2,498	0,014	-1,250	-0,142
C(KPa)	0,914	0,052	17,633	< 0,0001	0,811	1,017
ϕ (°)	0,148	0,050	2,958	0,004	0,049	0,248
α % (Mc)	0,000	0,000				

Table IV.48: Standardized coefficients of Machroha2

Source	Value	Standard error	t	Pr > t	Lower bound (95%)	Upper bound (95%)
γ_d (kN/m ³)	-0,376	0,577	-0,651	0,517	-1,523	0,771
γ_h (kN/m ³)	0,243	0,352	0,692	0,491	-0,455	0,942
W %	-0,204	0,354	-0,576	0,566	-0,908	0,500

Sr%	-0,025	0,113	-0,218	0,828	-0,249	0,200
Ff	-0,031	0,070	-0,434	0,665	-0,170	0,109
WL %	0,737	0,291	2,531	0,013	0,158	1,316
IP%	-0,681	0,289	-2,360	0,021	-1,254	-0,107
C(KPa)	0,826	0,065	12,668	< 0,0001	0,696	0,956
φ (°)	0,135	0,053	2,540	0,013	0,029	0,240
α %(Mv)	0,120	0,061	1,954	0,054	-0,002	0,242

Table IV.49: Standardized coefficients of Zaaroria1

Source	Value	Standard error	t	Pr > t	Lower bound (95%)	Upper bound (95%)
γd (kN/m³)	-0,136	0,311	-0,438	0,663	-0,754	0,482
γh (kN/m³)	0,012	0,188	0,064	0,949	-0,362	0,386
W %	-0,094	0,191	-0,493	0,623	-0,473	0,285
Sr%	0,029	0,060	0,485	0,629	-0,090	0,148
Ff	0,007	0,038	0,179	0,858	-0,068	0,082
WL %	0,406	0,156	2,602	0,011	0,096	0,715
IP%	-0,379	0,155	-2,449	0,016	-0,686	-0,071
C(KPa)	0,988	0,029	34,296	< 0,0001	0,930	1,045
φ (°)	0,206	0,028	7,409	< 0,0001	0,151	0,262
α %(Zc)	0,000	0,000				

Table IV.50: Standardized coefficients of Zaaroria2

Source	Value	Standard error	t	Pr > t	Lower bound (95%)	Upper bound (95%)
γd (kN/m³)	0,019	0,612	0,031	0,975	-1,197	1,235
γh (kN/m³)	-0,117	0,372	-0,314	0,754	-0,857	0,623
W %	-0,143	0,376	-0,380	0,705	-0,891	0,605
Sr%	0,092	0,120	0,765	0,446	-0,146	0,329
Ff	-0,020	0,075	-0,272	0,786	-0,169	0,129
WL %	0,033	0,309	0,107	0,915	-0,581	0,648
IP%	0,074	0,307	0,242	0,809	-0,536	0,684
C(KPa)	0,882	0,060	14,624	< 0,0001	0,763	1,002

φ (°)	0,212	0,056	3,793	0,000	0,101	0,323
α % (Zv)	0,008	0,059	0,140	0,889	-0,110	0,126

So we can see that in all cases the C value is bigger than 0.82 so the variable C significantly predict the outcome, then there is the variables WL and IP in machroha1 and zaaroria1 (IP is always negative), where in zaaroria2 all other variables are close to zero.

(Ff) is almost zero in all cases we can say it's not important in our study.

The data of the previous Table IV.is shown in the following plot:

Where it shows us the value of each variable and its sign, we notice C as the largest value on the positive side for all cases compared to the other values, And IP is the largest on the negative side, except in the case of Zaaroria2.

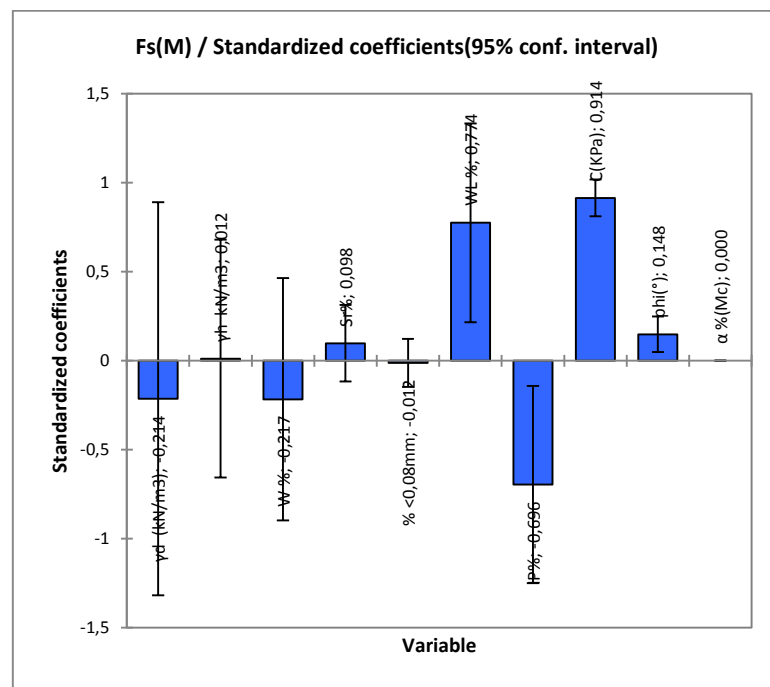


Figure IV.28: Fs(Machroha1)/Standardized coefficients (95% conf. interval) plot

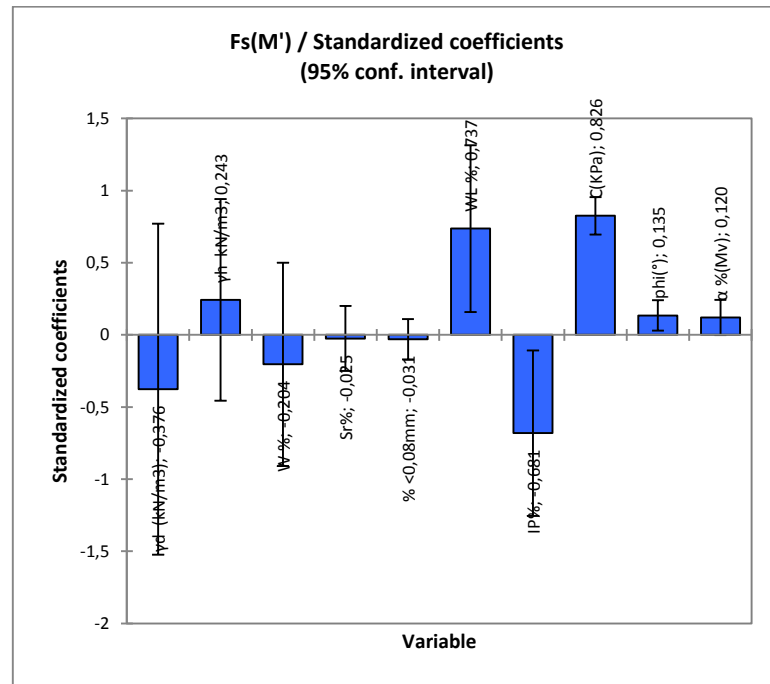


Figure IV.29: Fs(Machroha2)/Standardized coefficients (95% conf. interval) plot

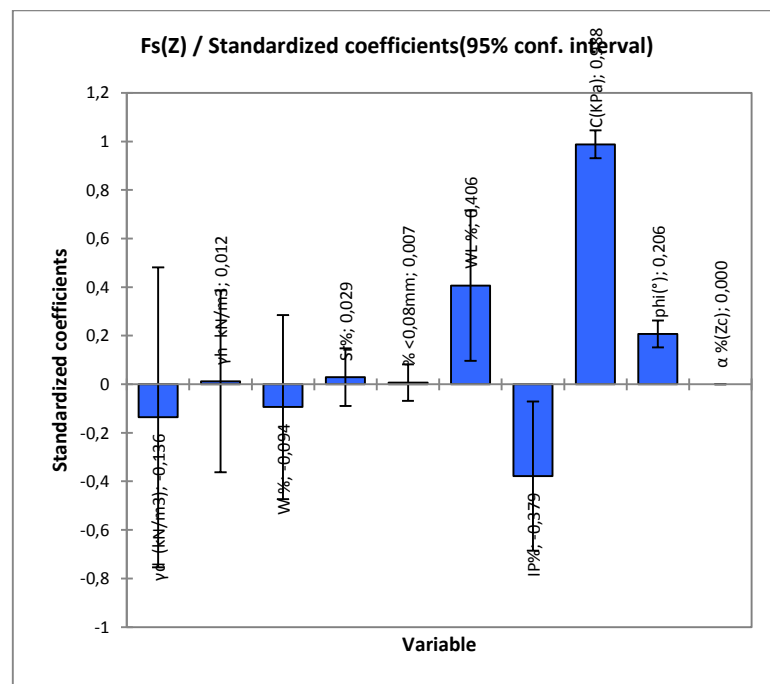


Figure IV.30: Fs(Zaaroria1)/Standardized coefficients (95% conf. interval) plot

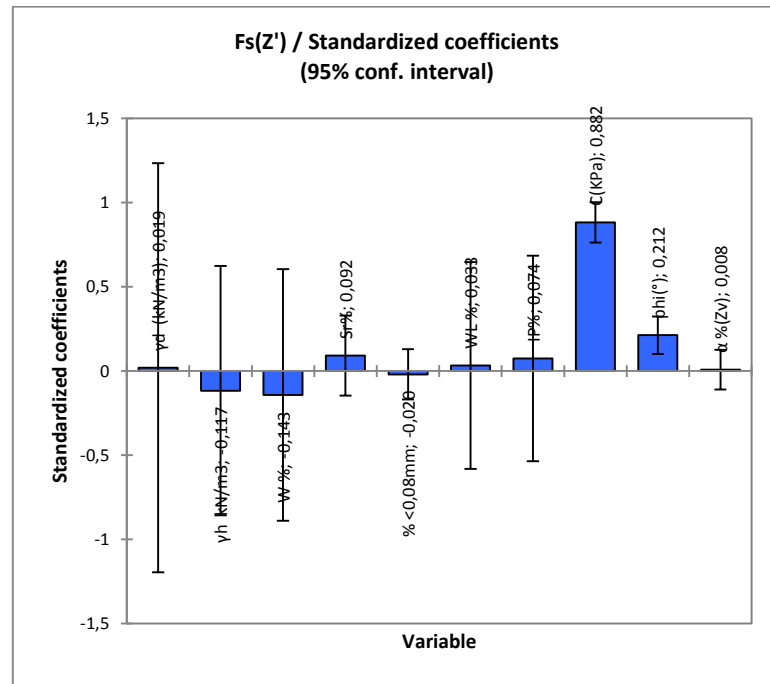


Figure IV.31: Fs(Zaatoria2)/Standardized coefficients (95% conf. interval) plot

IV.6.7. Predicted Values and Residuals:

- The predicted value is defined by the regression equation.
- The residual is the error that is not explained by the regression equation.

“Fs/standardized residuals” plot allows us to visualize the standardized residuals versus the Fs. It is not the case here, but when plotting the residuals against the explanatory variable, if a trend is identified, this indicates that the model is not correct or there is an autocorrelation in the residuals, which is contrary to one of the assumptions of parametric linear regression.

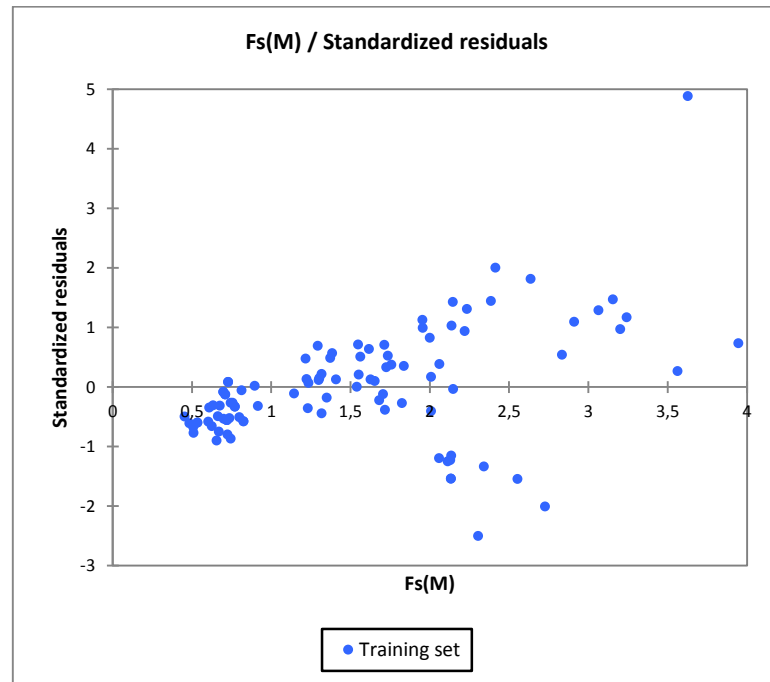


Figure IV.32: Fs(Machroha1)/Standardized residuals plot

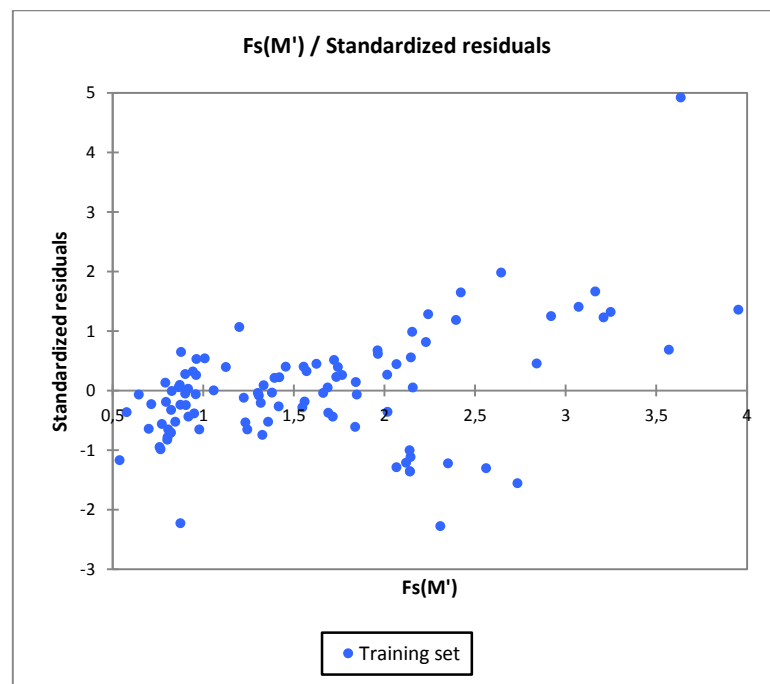


Figure IV.33: Fs(Machroha2)/Standardized residuals plot

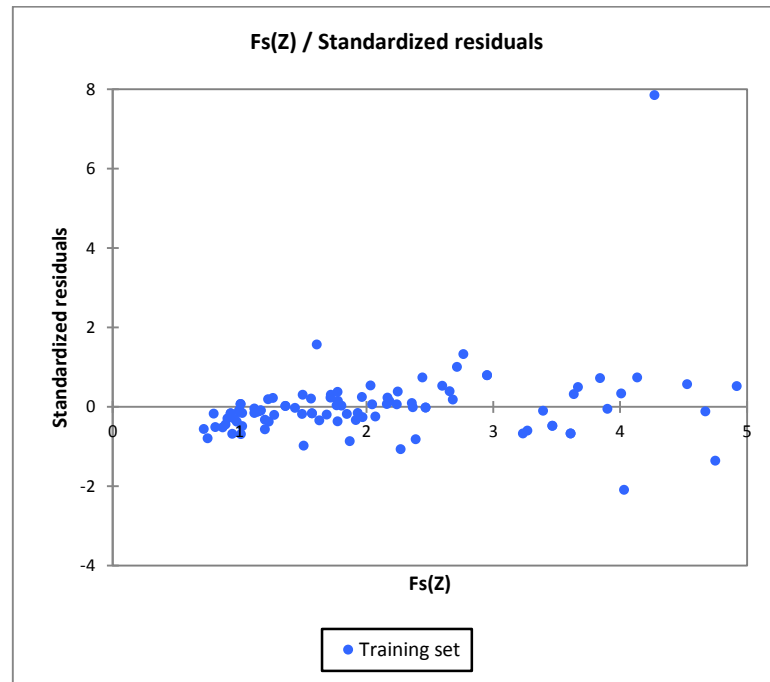


Figure IV.34: Fs(Zaaroria1)/Standardized residuals plot

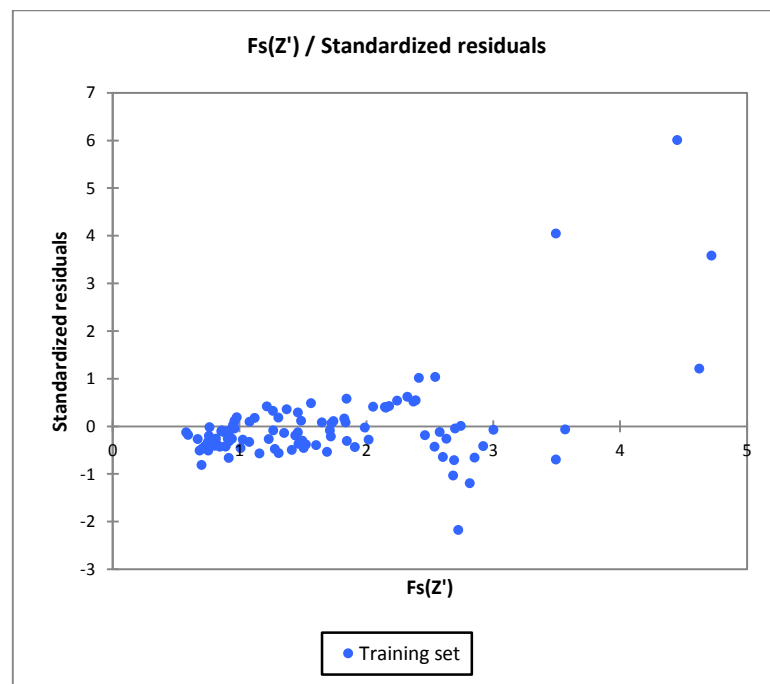


Figure IV.35: Fs(Zaaroria2)/Standardized residuals plot

“**Pred(Fs)/(Fs)**” plot allows to compare the predictions to the observed values. The confidence limits or the range allow, as with the regression plot displayed above, to identify outliers.

These residuals, given the assumptions of the linear regression model, should be normally distributed, meaning that 95% of the residuals should be in the interval. All values outside this interval are potential outliers, or might suggest that the normality assumption is wrong.

Out of 99, we can identify 1 to 3 residuals are out of the range, which makes 1% to 3% instead of 5%. 1% or 3% is a very low value which means that more than 97% of the predicted variables are explained by the regression equation.

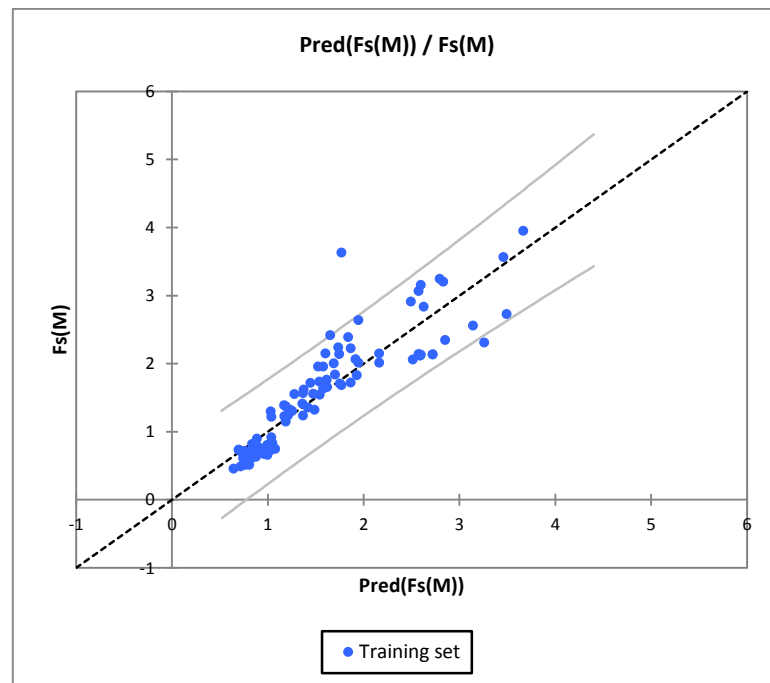


Figure IV.36: Pred(Fs)/Fs plot (Machrohal)

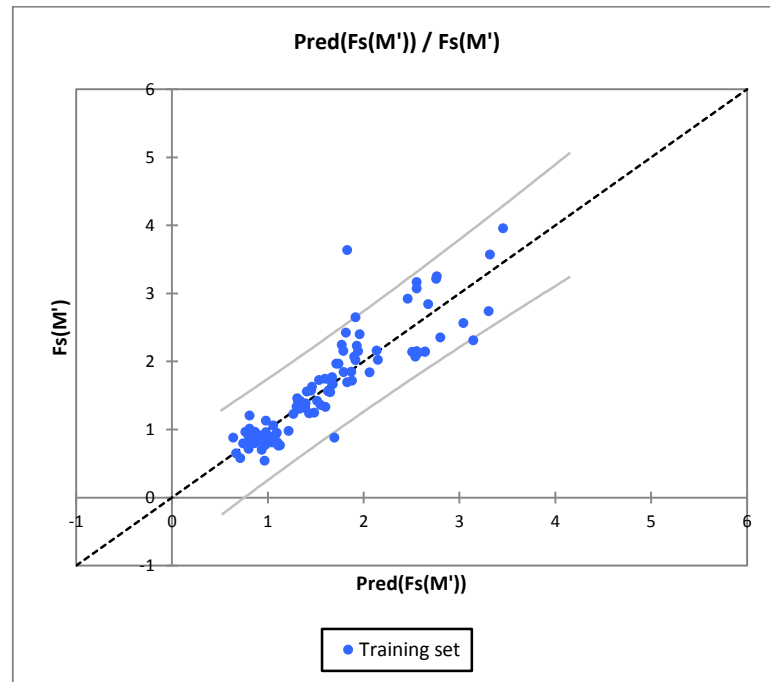


Figure IV.37: Pred(Fs)/Fs plot (Machroha2)

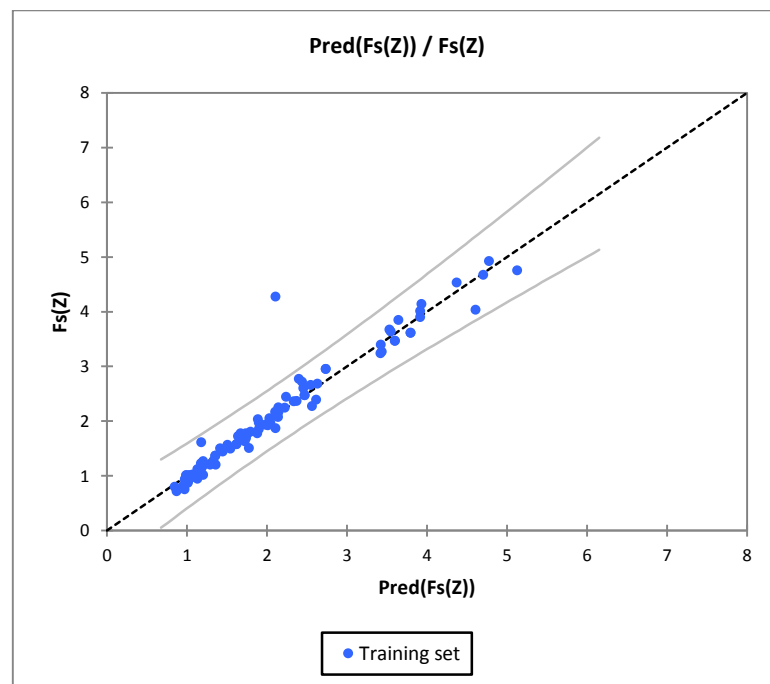


Figure IV.38: Pred(Fs)/Fs plot (Zaaroria1)

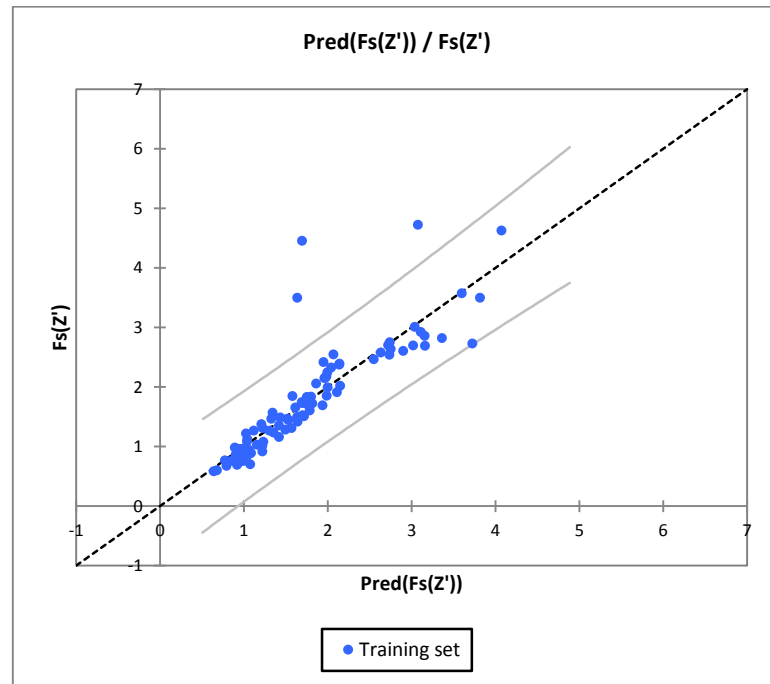


Figure IV.39: Pred(Fs)/Fs plot (Zaaroria2)

The histogram of the residuals enables us to quickly visualize the residuals that are out of the range.

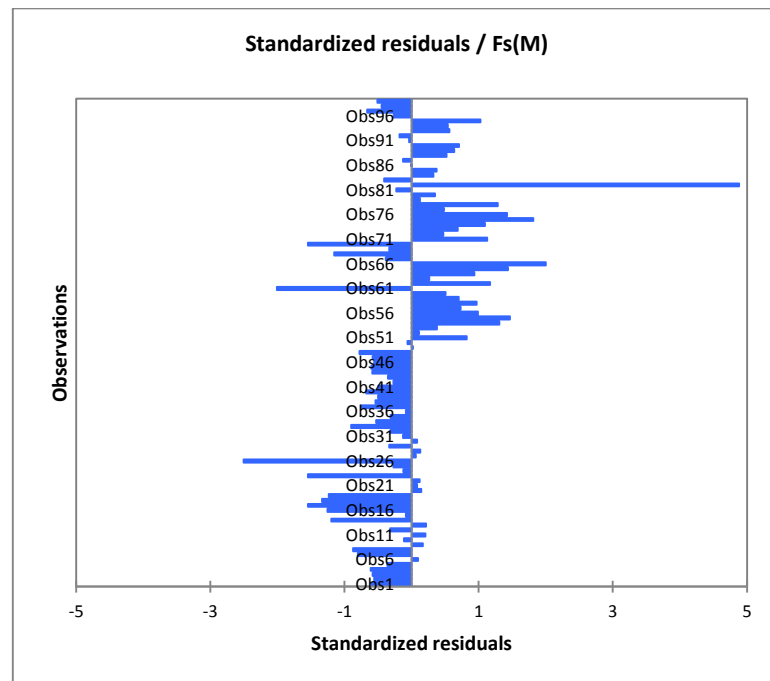


Figure IV.40: Standardized residuals /Fs (Machroha1) plot

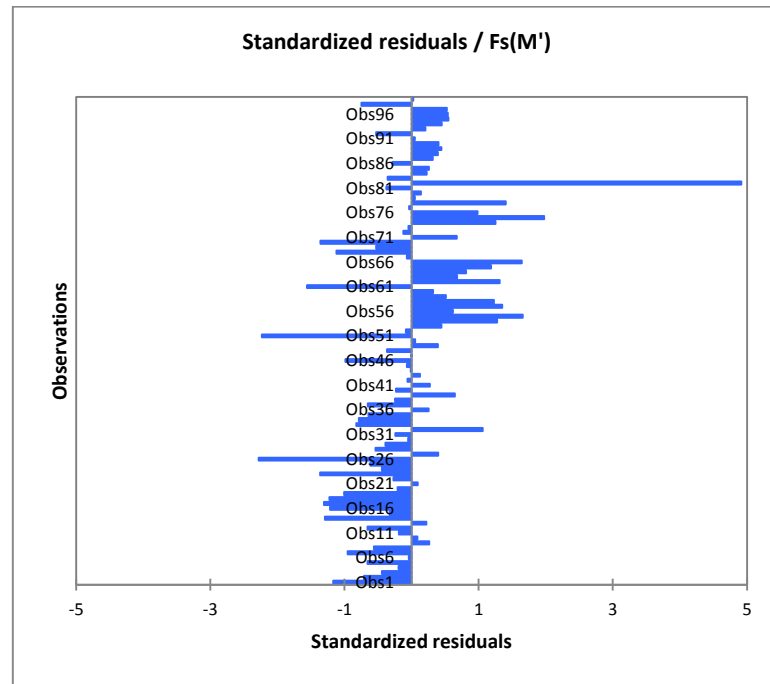


Figure IV.41: Standardized residuals /Fs (Machroha2) plot

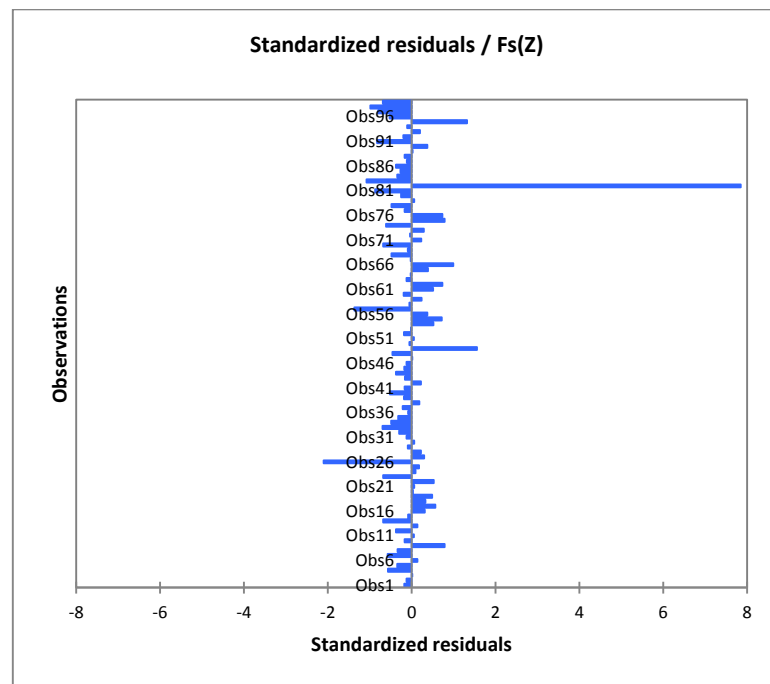


Figure IV.42: Standardized residuals /Fs (Zaaroria1) plot

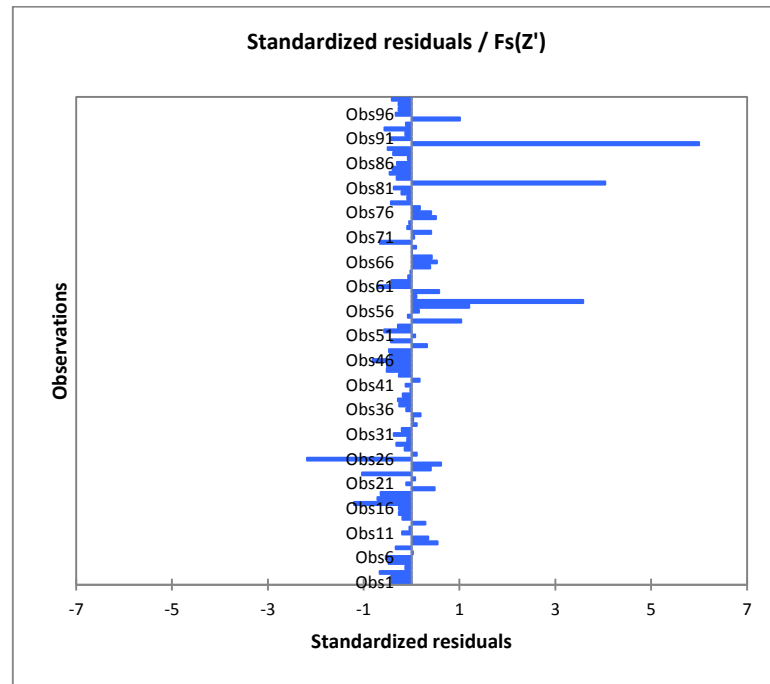


Figure IV.43: Standardized residuals /Fs (Zaaria2) plot

IV.7. Conclusion

(PCA) is indeed a useful statistical method to abstract special features from a data set with a high number of attributes. The ability to group features of similar kinds, and find outliers in the data set, are special characteristics of the method. The most attractive feature of (PCA) is the ability to plot the whole data set in one or more 2D plots, and by analyzing each plot one can expose all the information embedded in the data set. Having one plot that reveals groupings and outliers with the attributes that causes those is a distinguishing feature that cannot be observed in any other correlation related plots.

From (PCA) applied to analyze data measured upon 10 parameters physic and mechanic of many kind of soils in four slopes case, in this work, C is shown to exhibit a strong correlation with Factor of Safety, as eminent in (PCA) plots, also the angle (α) plays a good role in slope stability. While we found that some parameters such as (Ff) almost do not affect the safety factor in any way.

A multiple linear regression model is very effective for predicting dependent variables using independent variables. The accuracy of the prediction model depends on the accuracy of the data that are used to construct the prediction model. For example, in

this data set we were able to build prediction models for (C) data only, due to the reason that other variables do not show sufficiently good correlations with Fs.

Finally, we can reach the conclusion that although there are parameters that control the safety factor of slope stability more than others, some of them have an indirect effect because there is a relationship that links them to other parameters such as (γh) and (W) or (WL) and (IP).

IV.8. Presentation of design of experiments methodology (doe)

The Design of Experiments (DoE) method can be adapted in order to offer a practical way for studying, modeling, and characterizing the influence of the mechanical and physical soil parameters in the response of safety factor. Indeed, the DoE method has been successfully introduced in industrial systems and research and has built its principles from statistical and mathematical methods (W. Tinsson, 2010). Several domains use the DoE method as those mentioned in Refs (F. Gillon 1997; P. Dagnelie 2012). Substantially, the DoE method is used to design new industrial products based on both a set of experimental trials and a statistical analysis process (M. Michaelis, 2015) in order to optimize the settings of a manufacturing process (I. Saha, et al 2011), to improve its performances (J.A.B. Montevechi, et al. 2007), or to predict and characterize its behavioral model (F. Hannane, et al. 2013; J. Goupy 1988). Based on a few experiments in a strict closed study domain of input parameters variation, DoE appears as an alternative method for evaluating the significant factors, correlation between factors and their influence on the response of the system. The method does not require to know the physical model of the studied process. By cons, other physical methods (P. Moçotéguy et al. 2016; A. Zegaoui et al. 2011), which can vary only one parameter at a time, are not able to measure the correlation between different input parameters that influence the system response.

To overcome the shortcoming of these physical techniques, the DoE method allows to predict the self-effects as well as the interactions between the different variables involved in the experiment (M. Michaelis, C.S. Leopold 2015; F. Elkhalil 2011; A. Guenounou et al. 2016). Otherwise, to characterize and model any system, the DoE method strongly minimizes the number of experiment trials without influencing accuracy of the response (N. Lemonakis et al. 2016). To model any system, the DoE is concerned with a set of input variables that can modify a specific output variable named by a

response of the system. The DoE leads to deduce a mathematical model of factorial design of the response as a function of input factors that can vary in a bonded study domain limiting the input parameters variations (J.P. Charles et al. 2015).

In the present work, one can stand out the characterization, the predictive modeling, and the study of the behavior of safety factor F_s for a slop by using the DoE technique. We consider in our study, as input parameters of the established predictive model, the mechanical and physical soil parameters and also the geometry of the slop. For the output responses we consider the safety factor.

These variables are chosen as independent variables as wet density (γ_h), dry density (γ_d), water content (w) plasticity index (I_p), degree of saturation (S_r), the fine fraction (ff), liquidity limit (WL), cohesion strength (C), the angle of internal friction (ϕ) and the angle of the studied slope (α).

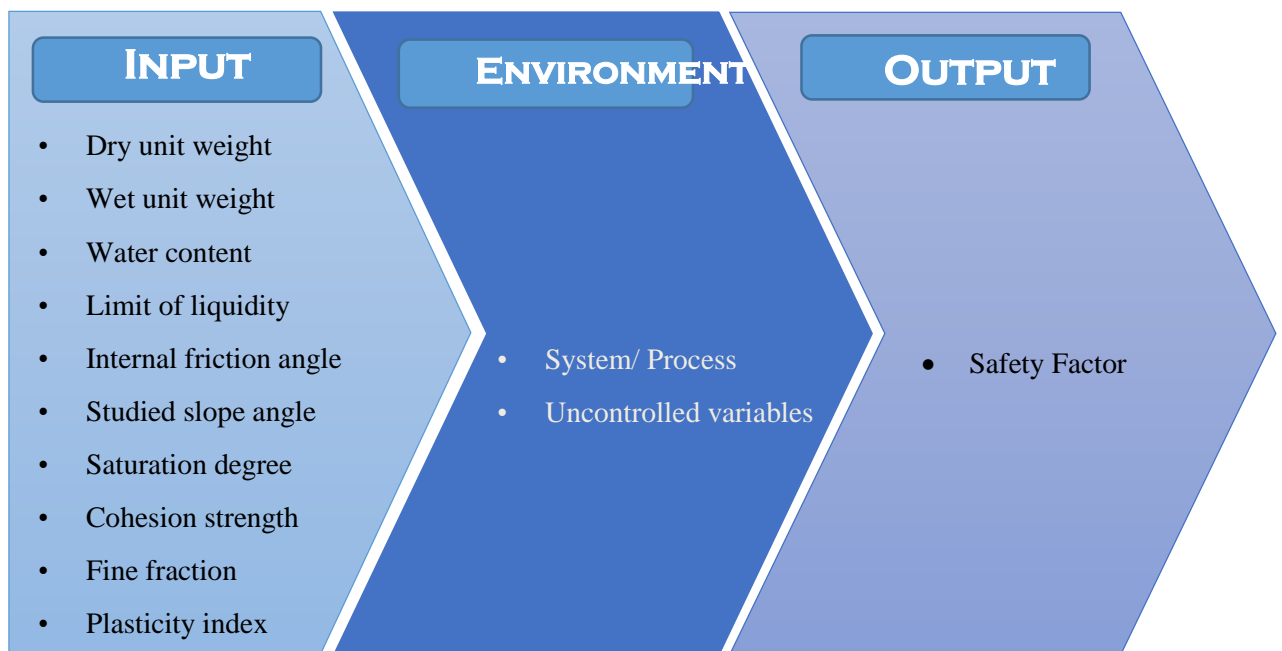


Figure IV.44: Visualization of: a DOE intent

Our cases studied is Machroha and Zaaroria, these regions are rich in clay soil, the watershed level is high, and with the presence of a layer of organic soil, all of these factors greatly affected the stability of the slopes, so the region experienced many cases of landslides.

for this part of our research the concept of Experimental Design (DOE) was introduced to study the safety factor of the slope stability. With around 99 samples collected and tested in the Soil Mechanics Laboratory (LTPE) identification.

IV.8.1. Material and Methods:

To estimate the safety factor (Fs) as a function of a different soil properties, which collected from the wilaya of Souk Ahras in the northeast of Algeria, 99 different samples are taken from Machroha and Zaaroria specifically in order to investigate their geotechnical parameters namely as wet density (γ_h), dry density (γ_d), water content (w) plasticity index (I_p), degree of saturation (Sr), the fine fraction (ff), liquidity limit (WL), cohesion strength (C), the angle of internal friction (ϕ) and the angle of the studied slope (α).

in our strategy, experiments are conducted by simultaneously varying ten factors over two levels (namely low level and high level). The two levels are so chosen that they cover the practical range of the parameters under consideration Table IV.01.

The predictive mathematical model that links the response y to the factors x_i using the DoE method is established based on the linear regression as follows (F. Hannane, 2013; J.P. Charles, 2014; J. Goupy, 2013; F. Rabier, 2007).

$$y = a_0 + \sum_{i=1}^k a_i x_i + \sum_{\substack{i,j=1 \\ i < j}}^k a_{ij} x_i x_j + \sum_{i=1}^k a_{ii} x_i^2 \quad (1)$$

where x_i and x_j are the levels of the factors i and j ($i, j = 1, 2, \dots, k$: number of factors) are the reduced centered values of factors, they are determined without error.

a_0, a_i, a_{ij}, a_{ii} denote, respectively, the constant coefficient, the coefficients relative to the principal effect of the factors, the coefficients representing the interactions between several factors, and the coefficients of the second degree terms. These coefficients must be calculated from the measurements of trials using our developed code under Matlab.

The matrix form of equation 1 is:

$$Y = X \cdot a \quad (2)$$

with y representing the individual response recorded for the n trials in the study domain, a is the vector of the n corresponding coefficients to be calculated, and X is the design matrix that must be a square matrix.

From Eq. 2, the coefficients of the model can be estimated:

$$a = X^{-1}y \quad (3)$$

Solving equation 3 using a script developed under Matlab software allows to obtain the needed coefficients.

IV.8.2. Response surface methodology (RSM)

In statistics, response surface methodology (RSM) explores the relationships between several explanatory variables and one or more response variables. The method was introduced by George E. P. Box and K. B. Wilson in 1951. The main idea of RSM is to use a sequence of designed experiments to obtain an optimal response. Box and Wilson suggest using a second-degree polynomial model to do this. They acknowledge that this model is only an approximation, but they use it because such a model is easy to estimate and apply, even when little is known about the process (Box et al. 1951).

Statistical approaches such as RSM can be employed to maximize the production of a special substance by optimization of operational factors. Of late, for formulation optimization, the RSM, using proper design of experiments (DoE), has become extensively used. (Karmoker, J.R et al. 2019) In contrast to conventional methods, the interaction among process variables can be determined by statistical techniques.

IV.8.3. Experimental design

Response surface methodology "RSM" was used to investigate the effect of independent variables, including (wet density (γ_h), dry density (γ_d), water content (w) plasticity index (I_P), degree of saturation (Sr), the fine fraction (ff), liquidity limit (WL), cohesion (C), the angle of internal friction (ϕ) and the angle of slope (α)) on the response which is the safety factor (Fs). RSM design along with coded and uncoded two levels from maximum to minimum is presented in Table IV.1. Central composite design (Five levels) and quadratic model has been suggested in the analysis step using ANOVA method to design

this experiment. 99 treatments (Runs), including 76 non-center points, 23 center points were randomly performed according to CCD.

Table IV.51: Independent variables and their corresponding levels (Machroha02) and (Zaaroria02)

Factor	Name	Units	Min.	Max.	Coded low		Coded high	Mean	Std. Dev.
A	γ_d	(kN/m ³)	13,20	18,80	-1	\leftrightarrow	+1 \leftrightarrow 18,80	16,85	1,17
B	γ_h	(kN/m ³)	17,00	22,00	-1	\leftrightarrow	+1 \leftrightarrow 22,00	20,19	0,8820
C	W	%	12,50	38,80	-1	\leftrightarrow	+1 \leftrightarrow 38,80	20,10	4,67
D	Sr	%	62,00	100,00	-1	\leftrightarrow	+1 \leftrightarrow 100,00	89,22	10,41
E	Ff	%	22,48	100,00	-1	\leftrightarrow	+1 \leftrightarrow 100,00	84,49	16,65
F	WL	%	29,00	72,79	-1	\leftrightarrow	+1 \leftrightarrow 72,79	49,21	11,60
G	IP	%	10,00	39,00	-1	\leftrightarrow	+1 \leftrightarrow 39,00	24,87	7,61
H	ϕ	°	10,00	43,00	-1	\leftrightarrow	+1 \leftrightarrow 43,00	18,60	6,78
J	$\alpha(M02)$	%	18,55	30,00	-1	\leftrightarrow	+1 \leftrightarrow 30,00	27,89	3,18
J	$\alpha(Z02)$	%	24,94	30,38	-1	\leftrightarrow	+1 \leftrightarrow 30,38	29,18	1,31
K	C	KPA	3,00	140,00	-1 \leftrightarrow 3,00		+1 \leftrightarrow 140,00	37,72	33,30

The standard deviation is a measure of the amount of variation or dispersion of a set of values (Bland et al. 1996). A low standard deviation indicates that the values tend to be close to the mean (also called the expected value) of the set, while a high standard deviation indicates that the values are spread out over a wider range.

IV.8.3. Statistical analysis

Experimental data were statistically analyzed using Design Expert Software (version 13.0.1.0). Numerous statistical parameters (lack-of-fit, predicted and adjusted multiple correlation coefficients and coefficient of variation) of different polynomial models were compared to select the best fitting polynomial model.

IV.8.4. Results and discussion

IV.8.4.1. Fitting the model

Response surface methodology (RSM) is a statistical, theoretical and mathematical technique for model building in order to optimize the level of independent variables (Homayoonfal et al. 2015). The effect of independent variables (γ_d , γ_h , W, Sr, Ff<0,08mm, WL, IP, ϕ , α , C) on safety factor (Fs) are given in Table IV.2. Coefficients of polynomial equation were computed from experimental data to predict the values of the response variable. Regression equations for each response variable, obtained from response surface methodology are mentioned in Equations:

$$Fs = -0,08 - 0,25\gamma_d + 0,21\gamma_h - 0,034W - 0,002Sr - 0,001Ff + 0,05WL - 0,07IP + 0,02\phi + 0,029\alpha + 0,0192C$$

Table IV.52: Experimental design for safety factor (Fs) with independent variables, experimental and predicted values of responses (Machroha02).

Std	Run	F. 1 A: γ_d	F. 2 B: γ_h	F. 3 C:W	F. 4 D:Sr	F. 5 E:Ff	F. 6 F:WL	F. 7 G:IP	F. 8 H: ϕ	F. 9 J: α	F. 10 K:C	Response 1 Fs
81	1	15,4	19,6	27,27	97	50,2	57	31	19	28,68	4	0,538
43	2	17,3	20,3	17,34	84	62	47	23	22	26,25	7	0,822
53	3	16,8	20,4	21,42	95	96,8	59	31	26	25	7	0,919
50	4	17,5	21	20	79,48	100	56,77	28,16	12	21,07	7,1	0,795
27	5	16,7	19,2	14,97	68,09	100	56,42	29,59	10	29,52	33,8	1,243
64	6	17,6	20,9	18,75	97,6	100	59,03	33,52	10	30	52,9	1,663
91	7	16,2	19,8	21,6	89,62	100	39,29	16,45	22	25,77	7,4	0,76
5	8	18,2	19,7	13,09	89,82	100	39,38	16,42	23	28,56	7,3	0,772
80	9	13,2	17	28,78	74	65,5	50	27	14	30	60,9	2,015
31	10	16,4	19,8	20,73	84	89,4	38	17	18	26,84	24	1,334

Table IV.53: Experimental design for safety factor (Fs) with independent variables, experimental and predicted values of responses (Zaaroria02).

Std	Run	F. 1 A: γ_d	F. 2 B: γ_h	F. 3 C:W	F. 4 D:Sr	F. 5 E:Ff	F. 6 F:WL	F. 7 G:IP	F. 8 H: ϕ	F. 9 J: α	F. 10 K:C	Response 1 Fs
81	1	15,4	19,6	27,27	97	50,2	57	31	19	28,68	4	0,728
43	2	17,3	20,3	17,34	84	62	47	23	22	26,25	7	0,89
53	3	16,8	20,4	21,42	95	96,8	59	31	26	25	7	0,916
50	4	17,5	21	20	79,48	100	56,77	28,16	12	21,07	7,1	0,58

27	5	16,7	19,2	14,97	68,09	100	56,42	29,59	10	29,52	33,8	1,278
64	6	17,6	20,9	18,75	97,6	100	59,03	33,52	10	30	52,9	1,69
91	7	16,2	19,8	21,6	89,62	100	39,29	16,45	22	25,77	7,4	0,951
5	8	18,2	19,7	13,09	89,82	100	39,38	16,42	23	28,56	7,3	1,078
80	9	13,2	17	28,78	74	65,5	50	27	14	30	60,9	3,389
31	10	16,4	19,8	20,73	84	89,4	38	17	18	26,84	24	1,373

The above tables (10 & 11) represent 99 runs in the actual design analysis, just 10 runs are illustrated to show the response and the input variable for the both case of study.

IV.8.4.2. ANOVA for Quadratic model

Analysis of variance addresses models where the response variable Y is a function of categorical predictor variables (so called factors). We have already seen how such predictors can be applied in a linear regression model. This means that analysis of variance can be viewed as a special case of regression modeling. However, it is worthwhile to study this special case separately. Analysis of variance and linear regression can be summarized under the term linear model. Regarding design of experiments, we only cover one topic, the optimization of a response variable.

IV.8.4.3. Fit Statistics

Table IV.54 Regression statistics for adopted reduced quadratic model (Machroha02)

Std. Dev.	0,3588	R²	0,9278
Mean	1,60	Adjusted R²	0,7856
C.V. %	22,43	Predicted R²	-20,2155
		Adeq Precision	10,7631

Table IV.55: Regression statistics for adopted reduced quadratic model (Zaaroria02)

Std. Dev.	0,5248	R²	0,8883
Mean	1,70	Adjusted R²	0,6684
C.V. %	30,94	Predicted R²	-5,9054
		Adeq Precision	9,3555

Statistical analysis (ANOVA) results revealed that the experimental data could be represented well with a quadratic polynomial model with coefficient of determination (R²) values for (Machroha02) being 0,9278 and 0,8883 for (Zaaroria02) (Table 4). The Lack of Fit F-value of 0,09 implies the Lack of Fit is not significant relative to the pure

error. There is a 100,00% chance that a Lack of Fit F-value this large could occur due to noise, "Non-significant lack of fit is good" we want the model to fit. Lack of fit was non-significant ($p \leq 0.05$) relative to pure error for all variables, which indicates that our model is statistically accurate. If the value of R^2 is closer to unity, then it is the indication of better model fitting to actual data. On the other end, lower values of R^2 indicate that response variables were not appropriate to explain the variation in behavior (Myers et al. 2016). In our study, proximity to unity R^2 demonstrates that the influence of the variables on response variable could be adequately described through a quadratic polynomial model. Significance level for coefficients of the quadratic polynomial model were determined through analysis of variance (ANOVA). Smaller P-value and larger F-value is the indication of a highly significant effect of any term on the response variable (Quanhong & Caili, 2005).

IV.8.4.4. Effect of independent variables on response variables:

The safety factor (Fs) was successfully measured by using the geo-slope program with (γ_h , C, ϕ) as inputs and (α) for the geometry. The effect of independent variables on safety factor are given in Tables (IV.52. & IV.53.), Regression coefficients for independent variables are summarized in Tables (IV.54. & IV.55.)

IV.8.4.5. Diagnostics Plots

Externally Studentized residuals are the default with Internally Studentized and raw residuals as options. Unless the leverages of all the runs in a design are identical, the standard errors of the residuals are different. This means that each raw residual belongs to different populations (one for each different standard error). Therefore, raw residuals should not be used for checking the regression assumptions. Studentizing the residuals maps all the different normal distributions to a single standard normal distribution.

Externally Studentized residuals based on a deletion method are the default due to being more sensitive for finding problems with the analysis. Internally Studentized residuals are also available but are less sensitive to finding such problems.

IV.8.4.5.1. Normal Probability: The normal probability plot indicates whether the residuals follow a normal distribution, thus follow the straight line. Expect some scatter

even with normal data. Look only for definite patterns, like an “S-shaped” curve, which indicates that a transformation of the response may provide a better analysis.

Note: The Shapiro-Wilk test for normality (used on the Half-Normal and Normal Plots of Effects) is not shown on the Residuals Normal Probability plot because this plot violates the assumption of independence by ordering the residuals. Therefore, it is not an appropriate test.

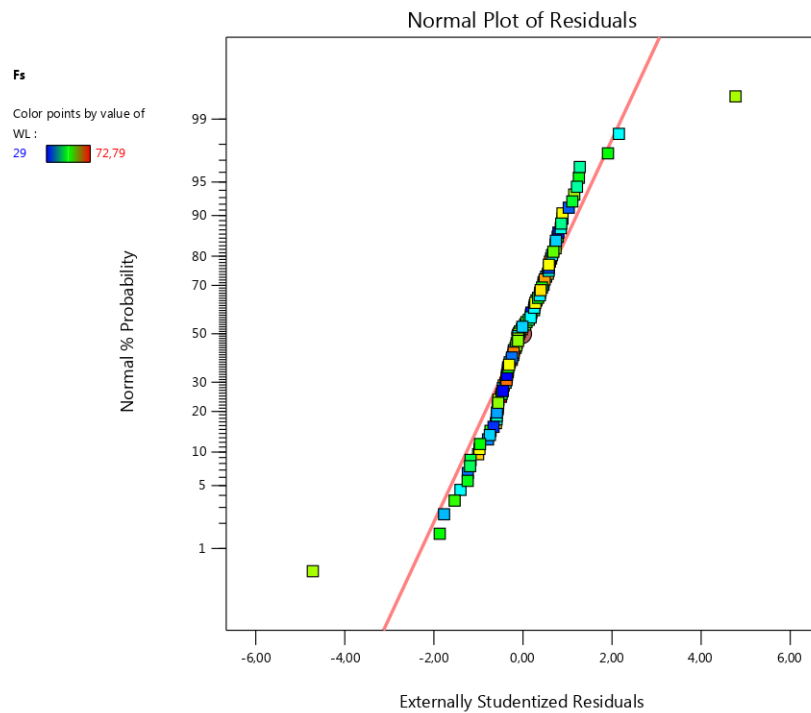


Figure IV.45: Normal Plot of Residuals (Machroha02)

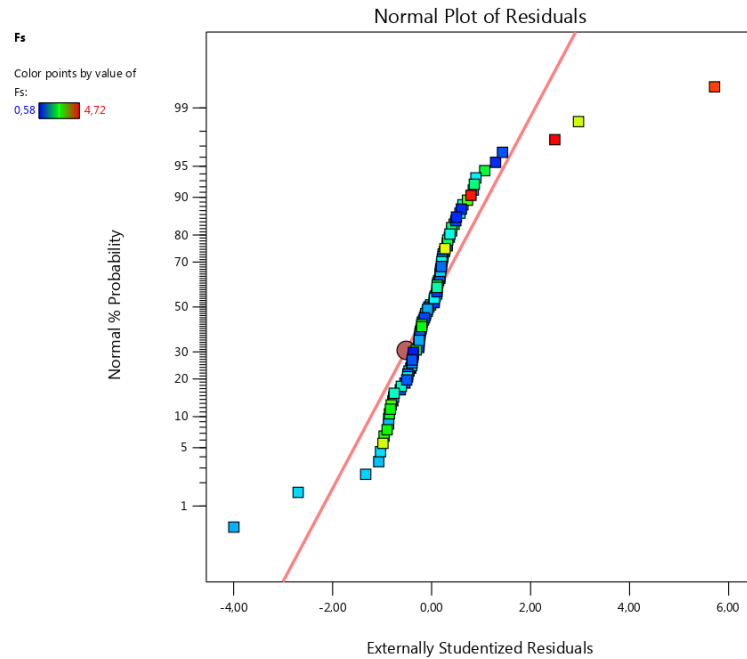


Figure IV.46: Normal Plot of Residuals (Zaaroria02)

IV.8.4.5.2. Residuals vs. Predicted: This is a plot of the residuals versus the ascending predicted response values. It tests the assumption of constant variance. The plot should be a random scatter (constant range of residuals across the graph). Expanding variance (“megaphone pattern <”) in this plot indicates the need for a transformation.

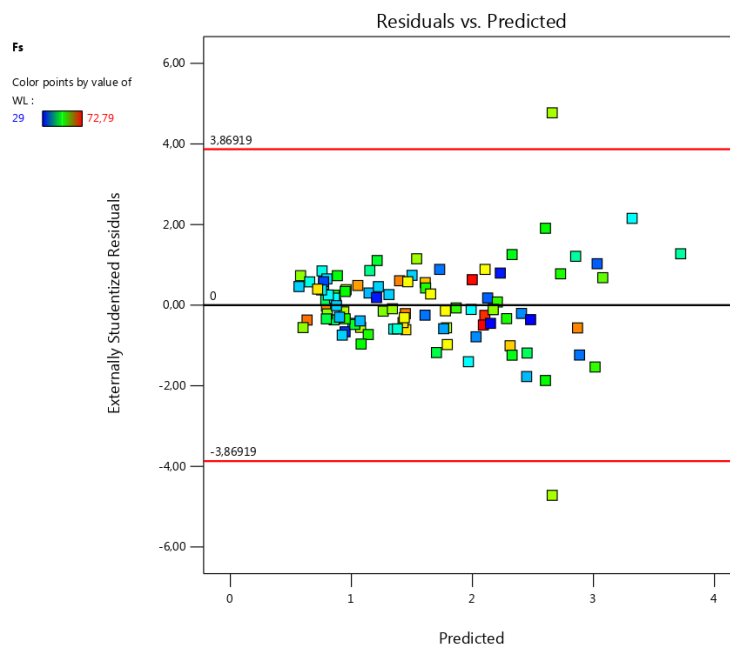


Figure IV.47: Residuals vs. Predicted Residuals Plot (Machroha02)

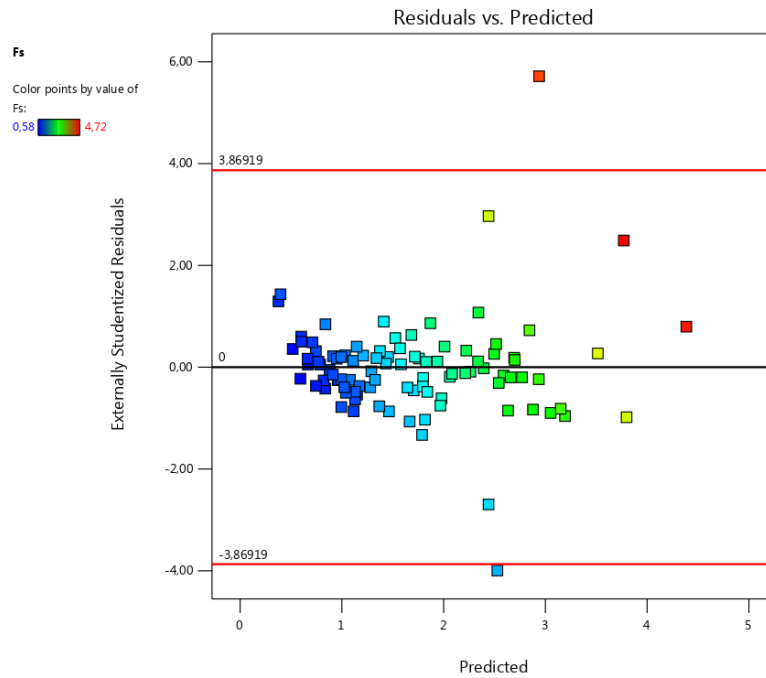


Figure IV.48: Residuals vs. Predicted Residuals Plot (Zaaroria02)

IV.8.4.5.3. Residuals vs. Run: This is a plot of the residuals versus the experimental run order. It checks for lurking variables that may have influenced the response during the experiment. The plot should show a random scatter. Trends indicate a time-related variable lurking in the background. Blocking and randomization provide insurance against trends ruining the analysis.

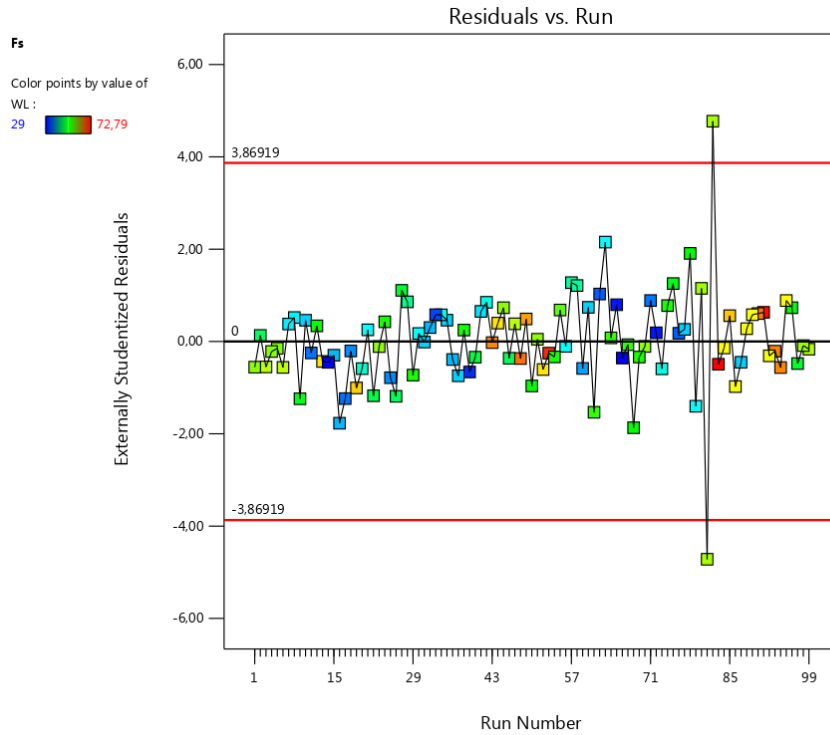


Figure IV.49: Residuals vs. Run Plot (Machroha02)

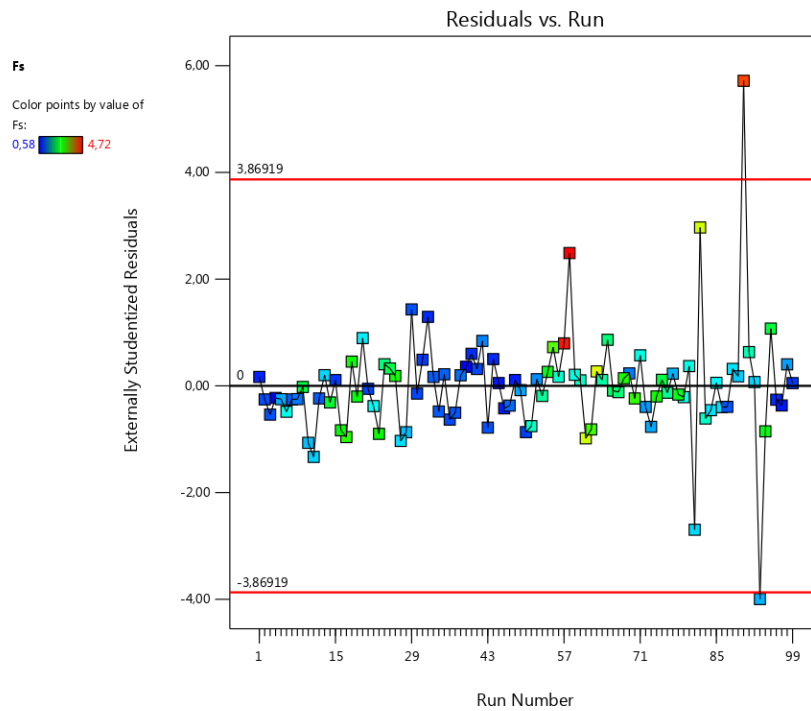


Figure IV.50: Residuals vs. Run Plot (Zaaroria02)

IV.8.4.5.4. Predicted vs. Actual: A graph of the predicted response values versus the actual response values. The purpose is to detect a value, or group of values, that are not easily predicted by the model.

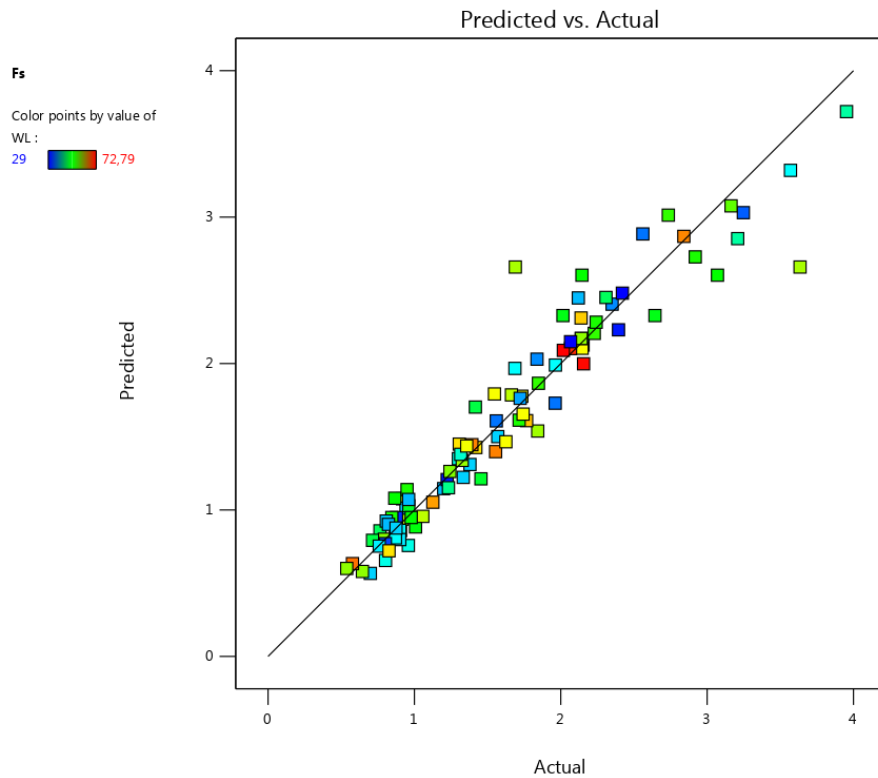


Figure IV.51: Predicted vs. Actual plot (Machroha02)

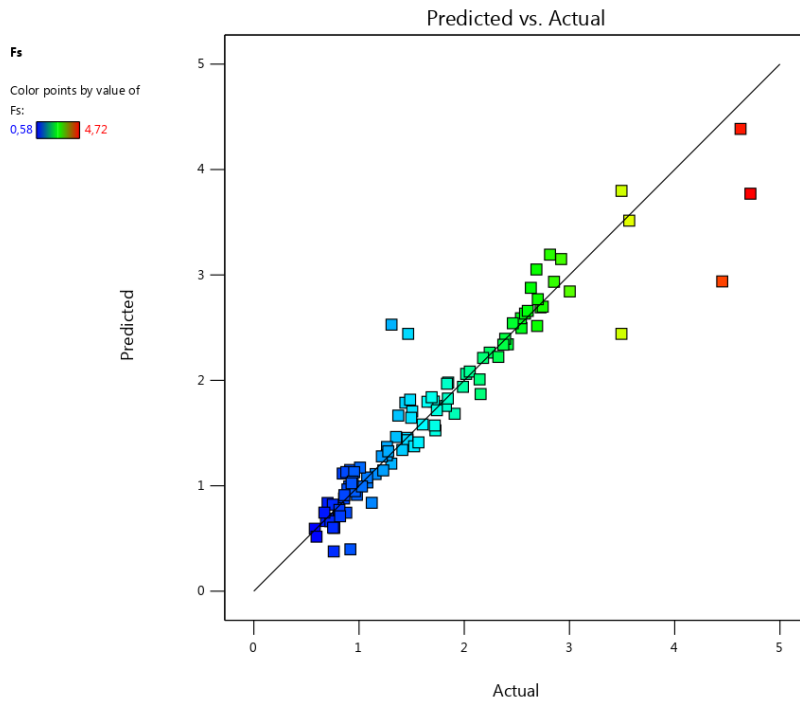


Figure IV.52: Predicted vs. Actual plot (Zaaroria02)

IV.8.4.5.5. Box-Cox Plot for Power Transforms: This plot provides a guideline for selecting the correct power law transformation. A recommended transformation is listed, based on the best lambda value, which is found at the minimum point of the curve generated by the natural log of the sum of squares of the residuals. If the 95% confidence interval around this lambda includes 1, then the software does not recommend a specific transformation. This plot is not displayed when either the logit or the arcsine square root transformation has been applied.

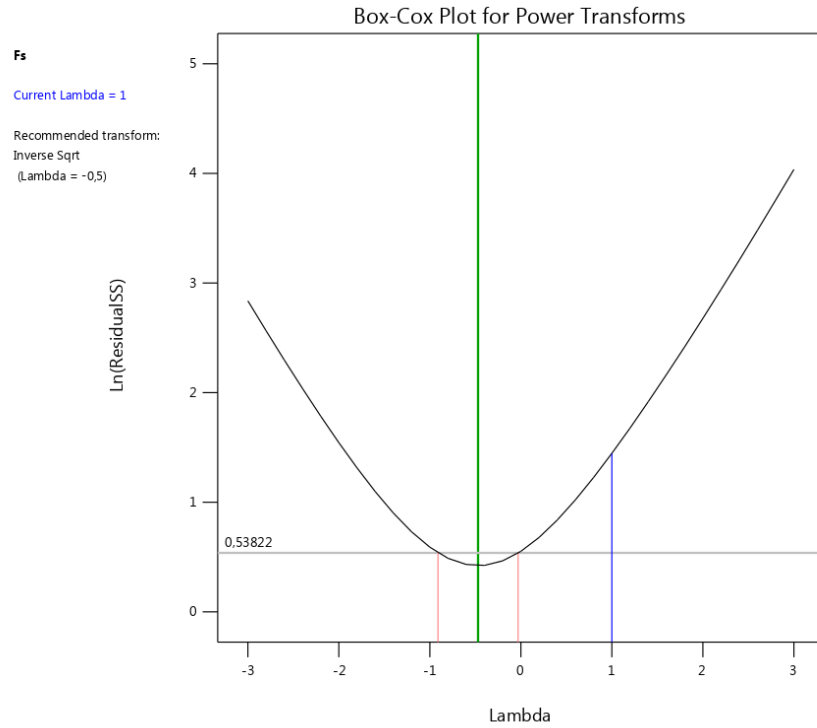


Figure IV.53: Box-Cox Plot for Power Transforms Plot (Machroha02)

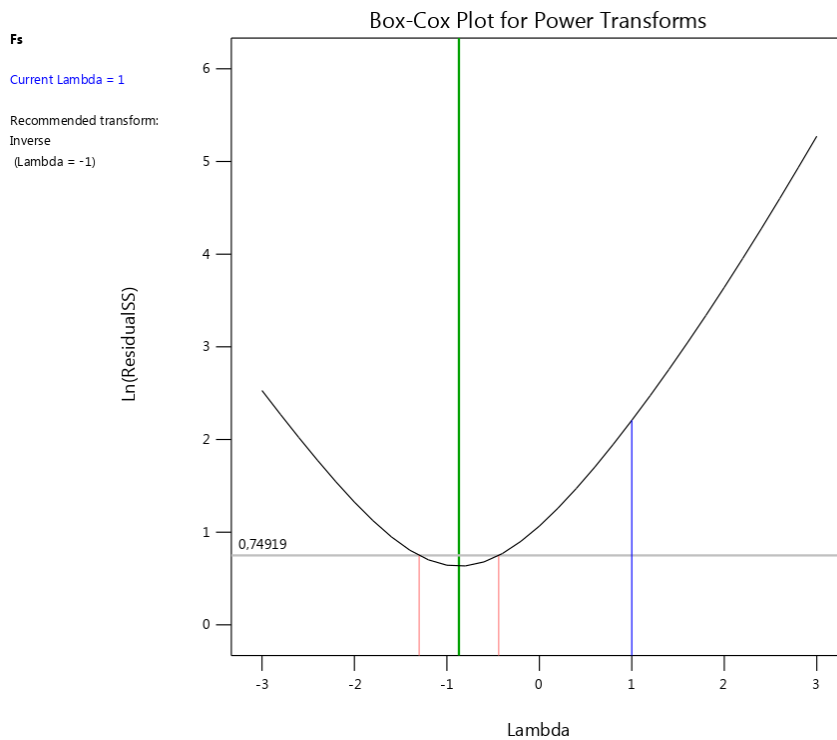


Figure IV.54: Box-Cox Plot for Power Transforms Plot (Zaaroria02)

IV.8.4.5.6. Residuals vs. Factor: This is a plot of the residuals versus any factor of your choosing. It checks whether the variance not accounted for by the model is different for different levels of a factor. If all is okay, the plot should exhibit a random scatter. Pronounced curvature may indicate a systematic contribution of the independent factor that is not accounted for by the model (Geoff Vining 2011).

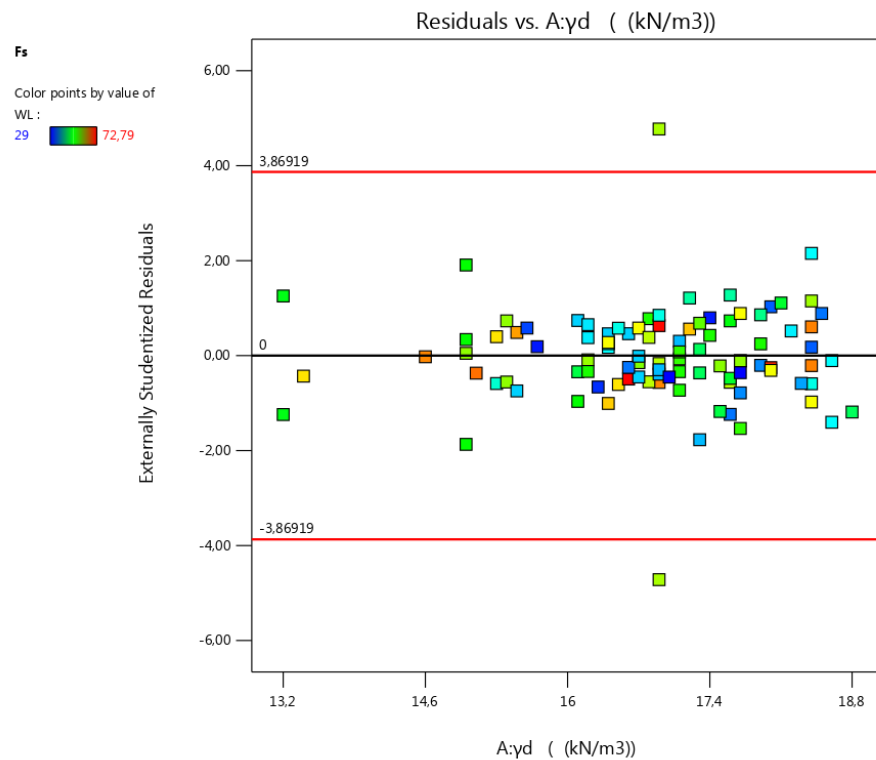


Figure IV.55: Residuals vs. Factor Plot (Machroha02)

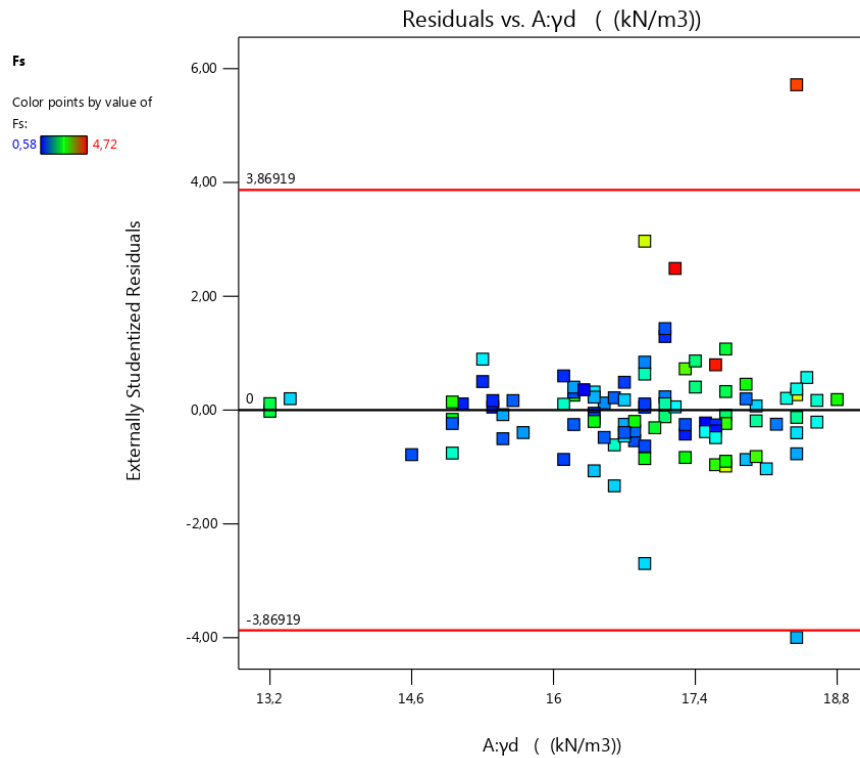


Figure IV.56: Residuals vs. Factor Plot (Zaaroria02)

IV.8.5. Modeling:

Models are used for prediction in order to generate response surface graphs and contour plots. There are significant interactions between mixture and process factors; the response surface graphs and contour plots as variation of the process conditions are shown in Figs. The unique characteristic of experimental design and modeling which is combination of response surface method (RSM) and process factors able to show statistical effects and the dynamic nature of the process knows mixture factors (geotechnical soil parameters) along with a process factor (safety factor).

Dependence on the dry and wet unit weight (kN/m^3) for this case study, Figures below show the response surfaces describing the Fs.

After that, the final equations and examples of response surfaces for the remaining measured responses are shown. The analysis was performed in analogy to the Fs.

The surface becomes 'hot' at higher response levels, the variation of Fs is between "the minimum value" blue 0,538 and "the maximum value" red above 3,953.

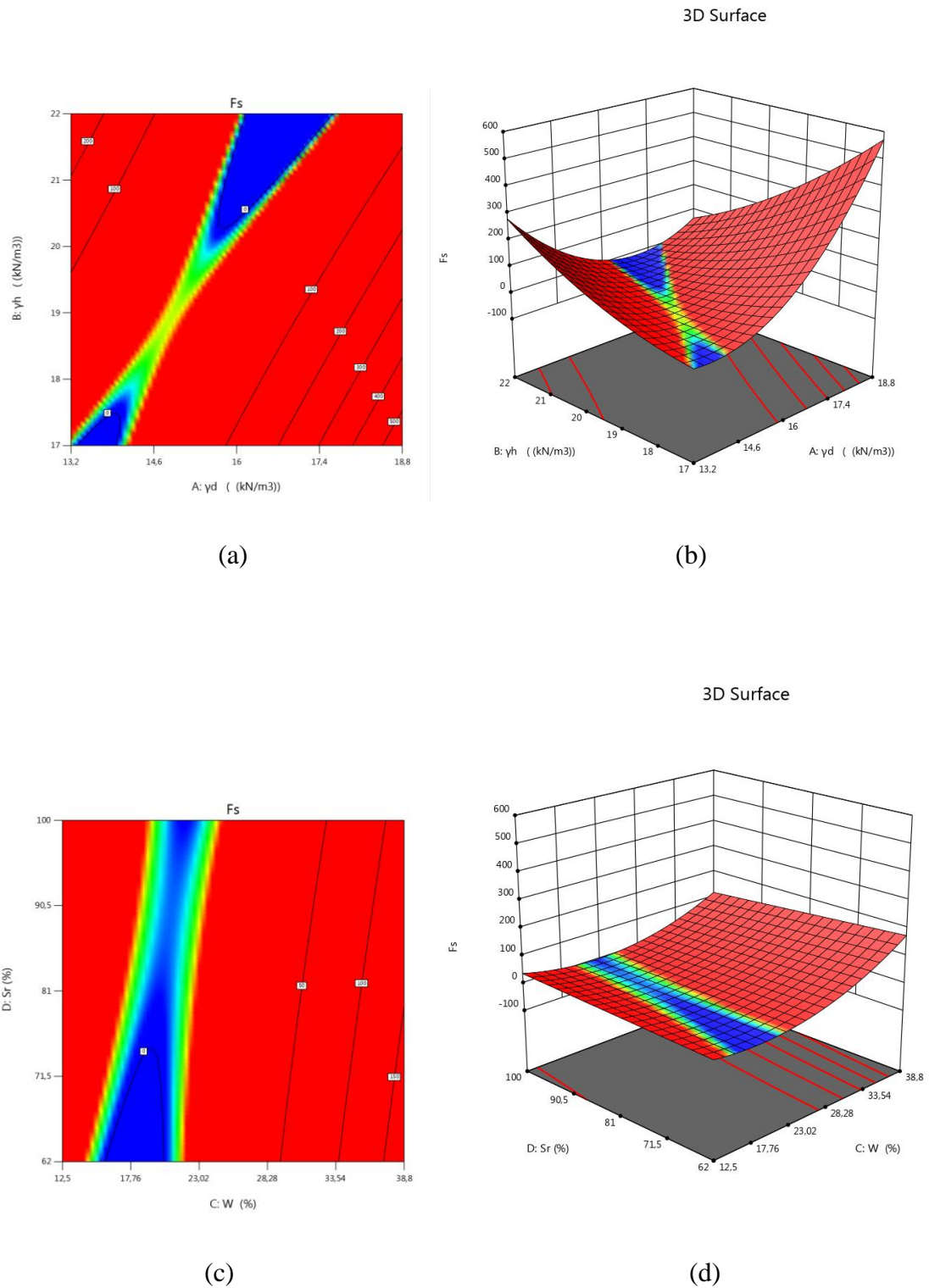


Figure IV.57: Contour and 3D plots, (a) and (b) representing the safety factor (F_s) dependence on the dry unit weight γ_d (kN/m³) and the wet unit weight γ_h (kN/m³), (c) and (d) representing the safety factor (F_s) dependence on degree of saturation S_r (%) and water content w (%) (machroha02)

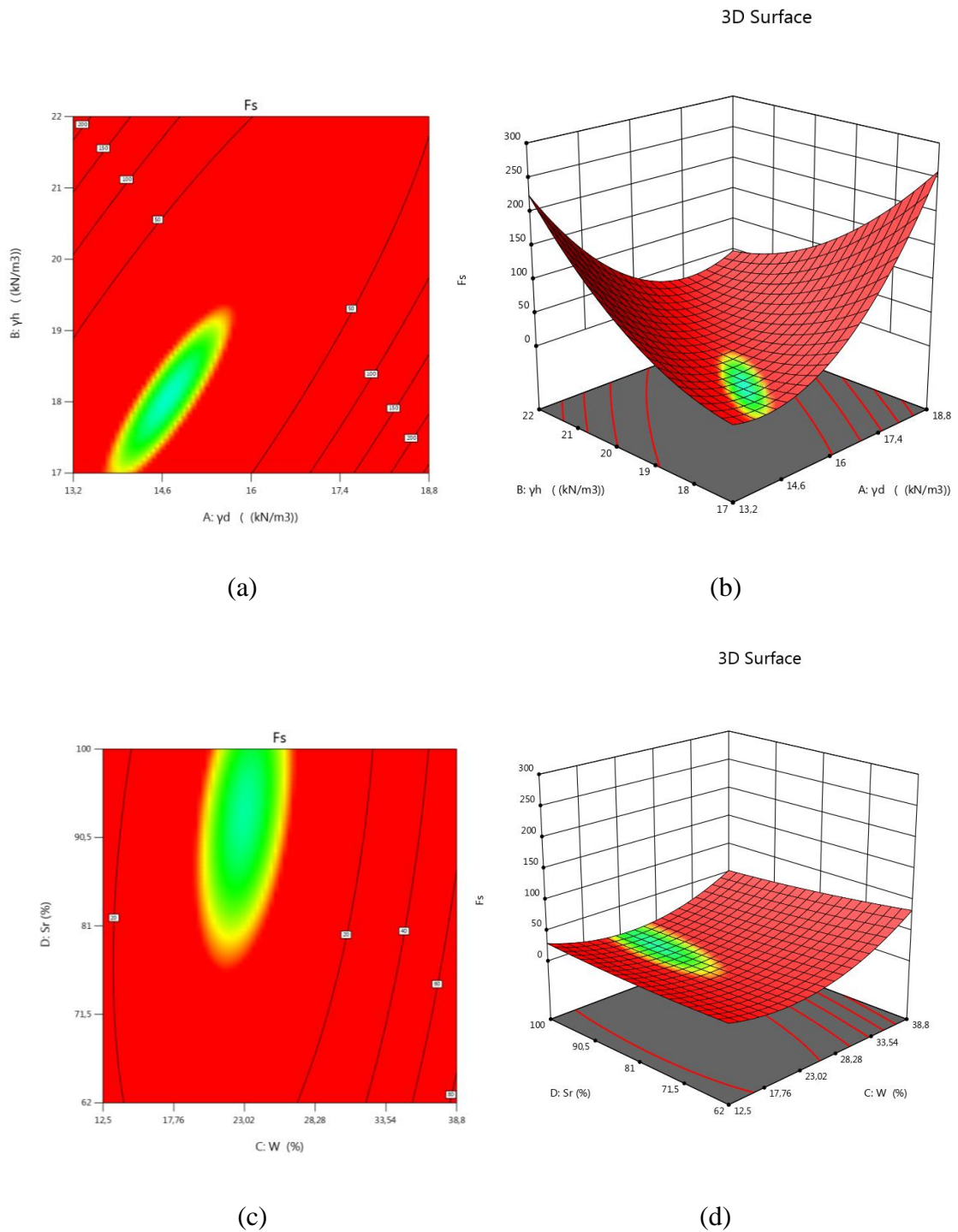


Figure IV.58: Contour and 3D plots, (a) and (b) representing the safety factor (F_s) dependence on the dry unit weight γ_d (kN/m³) and the wet unit weight γ_h (kN/m³), (c) and (d) representing the safety factor (F_s) dependence on degree of saturation S_r (%) and water content w (%) (Zaaroria02)

We chose these four variables (γ_d , γ_h , S_r , w) because we can notice their effects on (F_s) by the changing in the response surface shape and colors, they Shows the interaction

between two process variables as function of factors, while the other variables do not give as the best view of their effects on Fs.

IV.8.6. Optimization Data Analysis:

Various RSM computations for the current optimization study were performed employing Design-Expert software (Trial version 13.1.0.1). Statistical second-order model including interaction and polynomial terms was generated for all the response variables (M. K. Dhiman et al. 2008, A. Madgulkar et al. 2009). The general form of the model is represented as in the following:

$$Fs = (\gamma d. \gamma h. w. Ff. Wl. Ip. Sr. C. \varphi. \alpha)$$

We choose the desired goal for each factor and response from the menu. The possible goals are: maximize, minimize, target, within range, none (for responses only) and set to an exact value (factors only.)

A minimum and a maximum level must be provided for each parameter included. A weight can be assigned to each goal to adjust the shape of its particular desirability function. The “importance” of each goal can be changed in relation to the other goals. The default is for all goals to be equally important at a setting of 3 pluses (+++). If you want one goal to be most important, you could change it to 5 pluses (+++++).

The goals are combined into an overall desirability function. The program seeks to maximize this function. The goal seeking begins at a random starting point and proceeds up the steepest slope to a maximum. There may be two or more maximums because of curvature in the response surfaces and their combination into the desirability function. By starting from several points in the design space chances improve for finding the “best” local maximum. The default is 30 starting points. You can change this via the Options button.

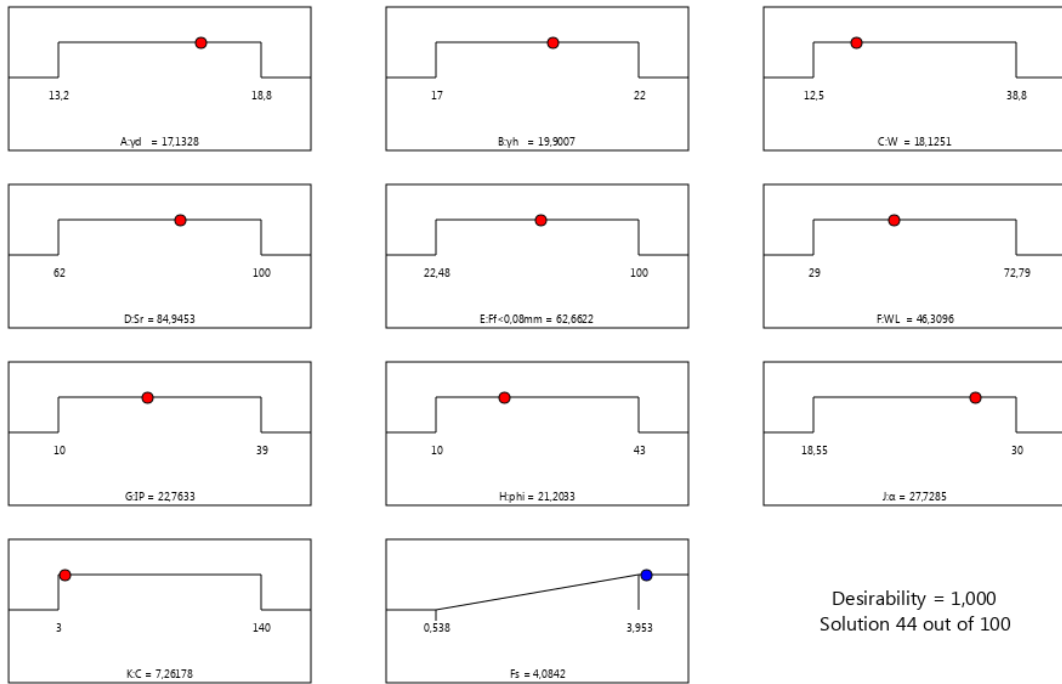
Contour, 3D surface, and perturbation plots of the desirability function at each optimum can be used to explore the function in the factor space. Also, any individual response may be graphed to show the optimum point

In this work, in the both cases, the optimization of the safety factor (F_s) in terms of the different physical parameters like wet density (γ_h), dry density (γ_d), water content (w), plasticity index (I_p), degree of saturation (S_r), the fine fraction (ff), liquidity limit (WL), cohesion strength (C), the angle of internal friction (ϕ) and the angle of the studied slope (α) (Khuri, A.I. and J.A. Cornell, 1996).

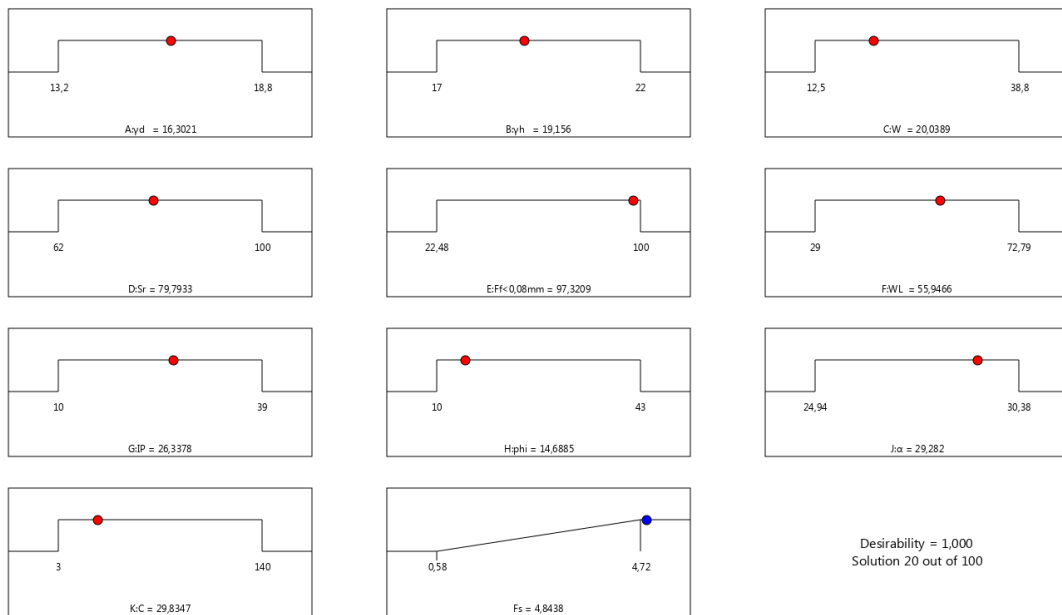
The program randomly picks a set of conditions from which to start its search for desirable results. Multiple cycles improve the odds of finding multiple local optimums, some of which are higher in desirability than others. Design-Expert then sorts the results from most desirable to least. Due to random starting conditions.

The ramp display combines individual graphs for easier interpretation. The colored dot on each ramp reflects the factor setting or response prediction for that solution. The height of the dot shows how desirable it is. View different solutions from the Solutions drop-down menu on the Factors tools; cycle through some of them and watch the dots. They may move only very slightly from one solution to the next.

The above optimal solution represents the formulation which best maximizes the safety factor and achieves a target value of 4.01 for Machroha02 and 4.84 for Zaaroria02, while at the same time finding the point with the minimum error transmitted to the responses. This should therefore represent process conditions that are robust to slight variations in factor parameters.

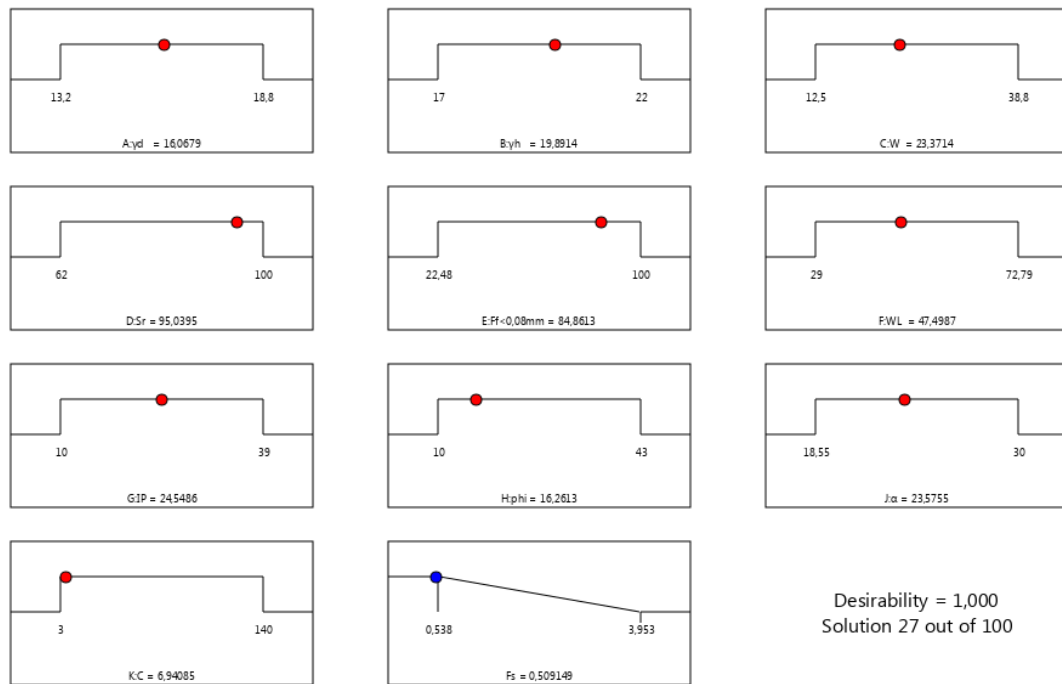


(a)

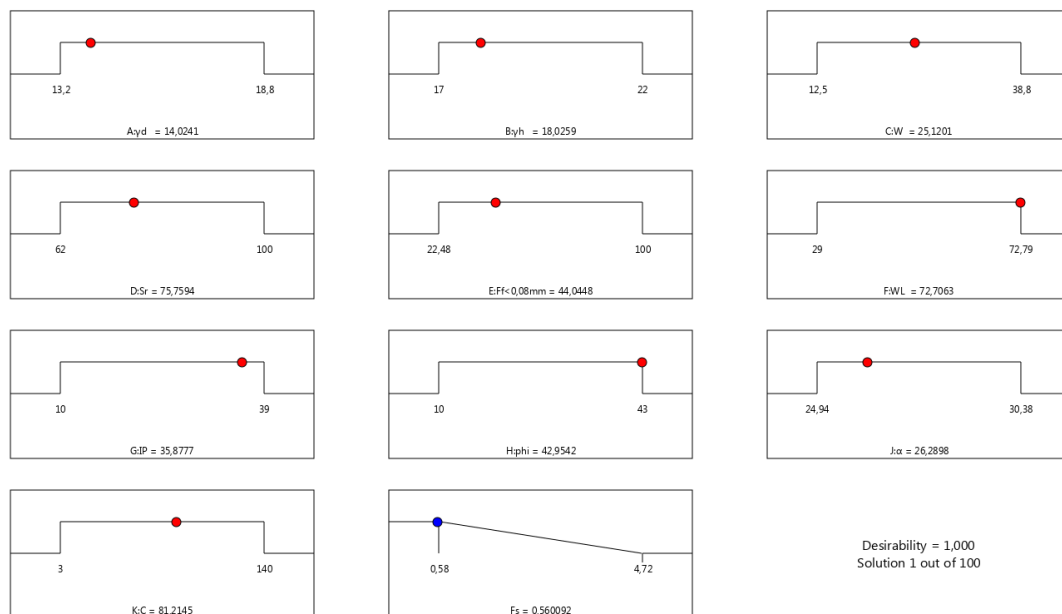


(b)

Figure IV.59: The maximization of the response (a) for Machroha02, (b) for Zaaroria02



(a)



(b)

Figure IV.60: The minimization of the response (a) for Machroha02, (b) for Zaaroria02

IV.9. Conclusion

Design–Expert offers comparative tests, screening, characterization, optimization, robust parameter design, mixture designs and combined designs. Design–Expert provides test matrices for screening up to 50 factors. Statistical significance of these factors is established with analysis of variance (ANOVA).

In this research, we reached to the final equation which correlate between 10 different variables (geotechnical soil parameters) to get the safety factor value of the studied slope, the (Fs) equation was optimized, checking the validity of the model, various relevant statistical indexes, such as F-value, coefficient of determination (R^2), Adj- R^2 and lack of fit and coefficient of variation (C.V.) were determined to be statistically adequate. Based on projected model, a highly suitable correlation as quadratic polynomial equation was developed. The desirability of obtained model was investigated.

The findings of this study suggested that the among different variables, we can get an equation to find the safety factor just by using these parameters as inputs without using special programs.

General Conclusion

General conclusion

Landslides are a serious geologic hazard common to almost in every sector Souk-Ahras region and harm economic and human life, landslides are difficult to predict because of its intensity, suddenness and dynamic nature. A view of the general conditions that characterize the studied region reveals the importance of the road network which is generally affected by slope movements. This network is traced within heterogeneous geological formations marks the influence of neotectonics on ground movements

From a seismic point of view, the wilaya of Souk Ahras is classified in zone I, which is a zone of low seismicity. The hydroclimatological condition in Souk Ahras region allows to classify the region as semi-arid climate. Rain is not homogeneous over the entire surface of the area depending on latitude and altitude participate in the intense shaping of the surface by erosion and change in the mechanical characteristics of the affected soils with considerable fine-grained content (particularly clays), which prepared to move at the simple request leads to the ground instability.

In the present study numerical modeling has been performed to investigate landslides hazard in the two sectors of Souk-Ahras region, the first is Mechrouha and the second is Zaarouria zones using equilibrium limit under the Geoslope software; the results obtained from different geological and geometrical model of safety factors (Fs) varied 0.8 to 1.7 in many hydrogeological condition, it indicates a clear unstable slope.

In this study it is focus on comparing four (04) cases of landslides hazards in Souk-Ahras region (Machroha sector 01 and 02 and Zaaroria sector 01 and 02); the slope cases have been treated and analysis to get the best correlation between the soil parameters and the safety factor, this compose the first part of the present work. In the second part, two slope cases were treated taking into account the angle of the slope α constant and variable. The obtained data base is composed of final results of the stability described by the Fs in the two cases. A second matrix data base composed of Fs as output factor and a maximum of physical and mechanical and geometrical soil parameters as input affecting stability factors such as (wet density (γ_h), dry density (γ_d), water content (w) plasticity index (I_p), degree of saturation (Sr), the fine fraction (ff) in % < 80 μ m, liquidity limit (WL), cohesive strength (C), the angle of internal friction (ϕ) and the angle of the studied slope (α)).

The data set analysis highlights the correlations between the geotechnical parameters and the calculated safety factors using Principal Component Analysis PCA combined with the Linear Regression LR to generate the best describing model of the stability.

Analysis of different geotechnical data collected from the different sectors in design of experiments (DOE) method where the response surfaces methodology (RSM) has been used to study and treat the solution by modeling and optimization parameters that affect the problems related to the landslide phenomenon. The latter allowed us to develop models by multiple regressions of the factor of safety (Fs) which presents the response in this study, the other parameters will be taken for surrogate or independent factors of input; these parameters are the dry and wet density (γ_d (t / m³), γ_h (t / m³)), the water content w (%), the plasticity and liquidity limits and the plasticity index (WL%, WP%, IP%), the percentage of fine elements F (% <0.008mm), the cohesion C (bar) and the internal friction angle Phi (°). The obtained correlations with a regression coefficient R² of 0.88 and 0.93, the model is applicable to give reliable results on landslides safety factor.

The optimization in response surface methodology and the central composite design (RSM and CCD) allow to the optimization the final DOE models by a range of desirability allows to find the accurate and sophisticate best fit models that describe the correlation of the different geotechnical parameters to the output safety factor Fs, at this level of screening it is suitable to optimize the solution by maximization or minimization the output response Fs to obtain the parameters range which describe the stability of slopes in the studied region.

Bibliography References

Bibliography References

Bibliography References

A. Guenounou, A. Malek, M. Aillerie, (2016). “Comparative performance of PV panels of different technologies over one year of exposure: Application to a coastal Mediterranean region of Algeria”, *Energy Conversion and Management*, **114**, 356-363

A. Madgulkar, M. Bhalekar, and M. Swami, (2009), “In vitro and in vivo studies on chitosan beads of losartan duolite AP143 complex, optimized by using statistical experimental design,” *AAPS PharmSciTech*, vol. 10, no. 3, pp. 743–751.

A. Zegaoui, P. Petit, M. Aillerie, J.P. Sawicki, A.W. Belarbi, M.D. Krachai, J.P. Charles, (2011). “Photovoltaic Cell/Panel/Array Characterizations and Modeling Considering both Reverse and Direct Modes”, *Energy Procedia*, 6, 695-703

Abdi, Hervé, and Lynne J. Williams, (2010). “Principal Component Analysis.” John Wiley and Sons, Inc. *WIREs Comp Stat* 2: 433–59. <http://staff.ustc.edu.cn/~zwp/teach/MVA/abdi-awPCA2010.pdf>.

Abella, C., (2008). Multi Scale Landslide Risk Assessment in Cuba. Dissertation, International Institute for Geo Information Science and Earth Observation, Enschede, The Netherlands, 273.

ABH (2005). Watershed Agency. The Medjarda-Mellegue watershed. *Les Cahiers de l'Agence*, Journal n°9. 28p.

AHMED. A, (2012). Étude numérique et confortement d'un glissement de terrain sur la RN 12. Mémoire d'ingénieur, école nationale polytechnique, El-harrach. Traitement d'un glissement de terrain et reconstruction de la chaussée avec un remblai renforcé par géosynthétique dans la wilaya de Bejaia.

Aiken LS, West SG, Pitts SC, Baraldi AN, Wurpts IC. (2012), Multiple linear regression. *Handbook of Psychology*, Second Edition. 2012 Sep 26;2

Aiken, L. S., West, S. G., Pitts, S. C., Baraldi, A. N., & Wurpts, I. C. (2012), Multiple linear regression. *Handbook of Psychology*, Second Edition, 2.

Bibliography References

Aiken, Leona S., Stephen G. West, Steven C. Pitts, Amanda N. Baraldi, and Ingrid C. Wurpts (2012), "Multiple linear regression." Handbook of Psychology, Second Edition 2.

AISSA.Mohamed Hamza, H.K., (2011), analyse et modélisation d'un glissement de terrain: p. 44-45 64-65.

Alpar. R (2003), Uygulamah çok deęişkenli istatistiksel yöntemlere giriş 1 (ikinci baskı). Ankara: Nobel Yayinlari

Anmol Sheth, Chandramohan A. Thekkath, Prakshep Mehta, Kalyan Tejaswi, Chandresh Parekh, Trilok N. Singh, Uday B. Desai, (2007), Senslide : A Distributed Landslide Prediction System, Microsoft

Anmol Sheth, Chandramohan A. Thekkath, Prakshep Mehta, Kalyan Tejaswi, Chandresh Parekh, Trilok N. Singh, Uday B. Desai, (2007). Senslide : A Distributed Landslide Prediction System, Microsoft

ANRH (1993). Pluviometric map of Northern Algeria at 1/500,000.

Arsyad, S., (1989). Konservasi Tanah dan Air. Institut Pertanian Bogor Press, Bogor.

Bendadouche.h, Lazizi.s, (2013). Glissement de terrain et confortement. Pages bleues.

Berdica, K., (2002). An introduction to road vulnerability: what has been done, is done and should be done. Transport Policy, Vol. 9, Iss. 2, pp. 117-127.

Biometrika, 28 (3-4): 321-377.

Bishop, A.W. (1955). The use of the slip circle in the stability analysis of slopes Geotechnical pp 7–1.

Bland, J.M.; Altman, D.G. (1996). "Statistics notes: measurement error". **BMJ. 312** (7047): 16541

Blayac (1912). Joseph. Esquisse géologique du Bassin de la Seybouse et de quelque régions voisines. No. 6. Adolphe Jourdan.

BLONDEAU (F). Mars (1976). – Les méthodes d'analyse de stabilité. Bull. Labo. P. et Ch., spécial, p. 56-62.

Bibliography References

- Bouroubi Y. (2009)**, Etude hydrogéologique du synclinal de la Taoura: Fonctionnement et évaluation des ressources en eaux souterraines, Université Mentouri, p25.
- Bouroubi-Ouadfel Y & Djebbar M. (2012)**. Etude hydrogéochimique et approche géothermique à la caractérisation du système karstique de Souk Ahras- Taoura. 1ier Congrès international de génie civil et d'hydraulique, 10 et 11 décembre 2012, Guelma- Algérie.
- Bouroubi-Ouadfel Y, Djebbar M. (2011)**. Apport de la géochimie à la caractérisation des écoulements du système karstique hydrothermal du synclinal de la Taoura. 9ième Colloque d'Hydrogéologie en Pays Calcaire; Besançon, France, H2 Karst. pp 74-76.
- Box, G.E.P.; Wilson, K.B. (1951)**. "On the Experimental Attainment of Optimum Conditions". Journal of the Royal Statistical Society, Series B. **13** (1): 1–45
- BULLETIN DE LIAISON N° 16**, risque info - "les mouvements de terrain", institut des risques majeurs juin 2005.
- Büyükóztürk. Ş. (2002)**. Sosyal bilimler için veri analizi el kitabı . Ankara: pegem Yayıncılık
- Carrara, A., Cardinali, M., Detti, R., Guzzetti, F., Pasqui, V., & Reichenbach, P., (1991)**. GIS Technique and Statistical Model in Evaluating Landslide Hazard. Earth Surface Processes and Landform Vol. 16 No.5 pp.427- 445.
- Cartier G., Delmas Ph., (1984)**, Les mécanismes de mouvements de terrain : nécessité de la mesure des déplacements. Colloque "Mouvements de terrain", Caen.
- CFMS. (1995)**. – Tirants d'ancrage : recommandations TA 95. 150 p., Eyrolles.
- Chakraborty, S., (2008)**. Spatio-Temporal Landslide Hazard Analysis Along a Road Corridor Based on Historical Information : Case Study from Uttarakhand India. Thesis, International Institute for Geo information Science and Earth Observation, Enschede, The Netherlands,72.
- Chouabbi, A. (1987)**. Etude geologique de la region de Hammam N'Bail (SE Guelma, Constantine, Algerie). Diss. These de doctorat de 3eme Cycle, Universite de Paul Sabatier, Toulouse, 123p.

Bibliography References

- COLAS (G.) et PILOT (G.).** –Description et classification des glissements de terrain.
- Connolly, and Szalay, and al. (1995),** Dressler, and al. 1987, Jolliffe IT. 2002, Kherif, Ferath and al 2020
- Connolly, and Szalay, et al., (1995).** “Spectral Classification of Galaxies: An Orthogonal Approach”, AJ, **110**, 1071-1082.
- Coppala, D.P., (2007).** Introduction to International Disaster Management.
- CRUDEN. DM, VARNES. DJ. (1996).** "Landslide types and processes". Chap3, InTurner, A.K. Schuster, R.L.(eds), landslide: investigation and mitigation. Transportation research Board- national research council, special report 247, Washington, D.C, national academy press, p 36-75.
- Dai, F.C., Lee, C.F., & Ngai, Y.Y, (2002).** Landslide risk assessment and management: an overview. Engineering Geology, 64(1):65-87.
- David L. (1956).** Etude géologique des monts de la haute Medjerda. Thèse Sci. Paris. Publ. Serv. Carte géol. Algérie, 1956. 304p.
- David L. (1956).** Geological Survey of the Upper Medjerda Mountains. Thesis Sci. Paris. Publ. Serv. Carte géol. Algérie, 304p.
- DHATH.G, TOUZOT.G., (1984) :** “Une présentation de la méthode des éléments finis” maloine. S.A. Editeur, paris.
- Dressler, et al., (1987).** “Spectroscopy and Photometry of Elliptical Galaxies. I. A New Distance Estimator”, ApJ, **313**, 42-58.
- Duncan, J. M. (1996),** State of the art : limit equilibrium and finite element analysis of slopes. discussion and closure. *Journal of Geotechnical Engineering.* **123(9)**, 577–596
- Durand Delga M.** Update on the structure of the Northeast of Berberia, Publ. Serv. Géol. Algérie, 39, 1969, 89-131.
- Ebta, A., (2008).** Analisis Risiko dan Mitigasi Bahaya Longsor terhadap Jaringan Jalan di Kecamatan Loano-Purworejo. Thesis, Pasca Sarjana, Gadjah Mada Universitas, Yogyakarta,118. Elsevier Inc,539.
- Elazar JP., (1982).** Multiple Regression in Behavioral Research: Explanation and Prediction. 2nd ed. New York: Holt, Rinehart and Winston.

Bibliography References

Elkhabar Newspaper 18/03/2021.

Epada, P.D.; Ganno, S.; Tabod, C.T. (2012). Geophysical and Geotechnical Investigations of a Landslide in Kekem Area. Western Cameroon. *Int. J. Geosci.*, 3, 780–789.

F. Elkhailil, (2011). “Supervision, économie et impact sur l'environnement d'un système d'énergie électrique associé à une centrale photovoltaïque”, PhD thesis, Institut des sciences et technologies, Paris (2011).

F. Hannane, H. El Mossaoui, T.V. Nguyen, P. Petit, M. Aillerie, J.P. Charles, (2013). “Forecasting the PV panel operating conditions using the Design of experiments method” *Energy Procedia*, **36**, 479-487.

F. Rabier, (2007). “Modélisation par la méthode des plans d'expériences du comportement dynamique d'un module IGBT utilisé en traction ferroviaire”, PhD thesis, Institut nationale polytechnique-Toulouse.

Fellenius, W. (1936). Calculation of the Stability of Earth Dams. Transactions, 2nd International Congress on Large Darns, International Commission on Large Dams, Washington, DC, pp 445-459.

Geoff Vining. (2011) Technical advice: residual plots to check assumptions. *Quality Engineering*, 23(1):105–110,

Graduate Admissions Dataset, 10 things about reading a regression table, A refresher on regression analysis

Haddouche O. (2003). Contribution à l'étude géologique et gîtologique des minéralisations à Pb-Zn, Fe (Ba-Sr) d'El Ouasta (Atlas saharien oriental, Algérie). Magister, Université d'Alger.

Hamasaki, E., A. Sasaki, (2004). "Study on landslide due to earthquake by using Discontinuous Deformation Analysis." *Proc. 3rd ARMS* : 1253-1256

Hamza-Cherif Riad, (2009). Mémoire Magister en Génie Civil. Thème : Etude Des Mouvements De Pentes Par Le Code De Calcul "Pfc2d". Université Abou-Bekr Belkaid (Tlemcen).

Hardiyatmo, H.C., (2006). Penanganan Tanah Longsor dan Erosi. Gadjah mada University Press, Yogyakarta,450.

Bibliography References

Highland, L.M., & Bobrowsky, P., (2008). The Landslide handbook – A Guide to Understand Landslide. US geological Survey Circular 1325, Reston, Virginia, 129p.

Homayoonfal, M., Khodaiyan, F., & Mousavi, M. (2015). Modelling and optimising of physicochemical features of walnut-oil beverage emulsions by implementation of response surface methodology: Effect of preparation conditions on emulsion stability. *Food Chemistry*, 174, 649–659.

Hotteling, H., (1936). Relation between two sets of variates.

Hungr, Oldrich, Serge Leroueil, and Luciano Picarelli, (2014). "The Varnes classification of landslide types, an update." *Landslides* 11.2 : 167-194).

Husson, Francois, Sebastien Le, and Jérôme Pagès, (2017). *Exploratory Multivariate Analysis by Example Using R*. 2nd ed. Boca Raton, Florida: Chapman; Hall/CRC. <http://factominer.free.fr/bookV2/index.html>.

J. Goupy, (1988). *La méthode des plans d'expériences Optimisation du choix des essais et de l'interprétation des résultats* (Ed. Dunod, Paris, 1988).

J. Goupy, (2013). *Introduction aux plans d'expériences avec applications* (Ed. Dunod, Paris, 2013).

J.A.B. Montevechi, A.F. De Pinho, F. Leal, F.A.S. Marins, (2007). "Application of design of experiments on the simulation of a process in an automotive industry", *Proc. of the Winter Simulation Conf.*, 1601-1609.

J.L.Durville, G.Sève : stabilité des pentes (glissement en terrain meuble), techniques de l'ingénieur.

J.P. Charles, F. Hannane, H. El Mossaoui, A. Zegaoui, T.V. Nguyen, P. Petit and M. Aillerie, (2014). "Faulty PV panel identification using the Design.

J.P. Charles, M. Aillerie, P. Petit, F. Hannane, H. El Mossaoui, (2015). "Warning of accidental shadowing of a PV generator in operation analyzed with the DoE method", *Solar Energy*, 122, 455-463.

Jaiswal, P., & Van Westen, C.J., (2009). Estimating Temporal Probability for Landslide Along Transportation Routes Based on Rainfall Threshold. *Journal Elsevier, Geomorphology*, 112: 96–105.

Bibliography References

Janbu, N. (1973). Slope Stability Computations. Embankment Dam Engineering, Casagrande Volume, pp. 47-86.

Jean, BJ (2012), "Multidisciplinary study of slope stability, UCL-Université Catholique de Louvain. P. 177-178.

JEAN-CRISTOPHE GUILIER, (2011) : "Introduction à la méthode des éléments finis". Dunod, paris.

Jibson B. Mario Parise a, Randall W. (2000). a National Research Council, Centro di Studio sulle Risorse Idriche e la Salvaguardia del Territorio, Via Orabona 4, 70125 Bari, Italy bUS Geological Survey, Box 25046, MS 966, Denver Federal Center, Denver, CO 80225, USA Received 2 November 1998; accepted for publication 7 January 2000.

Jolliffe, I.T. (2002). Principal Component Analysis. 2nd ed. New York: Springer-Verlag. <https://goo.gl/SB86SR>.

Jolliffe IT. (2002). Principal component analysis, 2nd edn. New York, NY: Springer-Verlag.

Kaiser, Henry F. (1961). "A Note on Guttman's Lower Bound for the Number of Common Factors." British Journal of Statistical Psychology 14: 1–2.

Karmoker, J.R.; Hasan, I.; Ahmed, N.; Saifuddin, M.; Reza, M.S. (2019). "Development and Optimization of Acyclovir Loaded Mucoadhesive Microspheres by Box -Behnken Design". Dhaka University Journal of Pharmaceutical Sciences. **18** (1): 1–12

Keith A., and Schuster, Robert L., (1996), Landslides—Investigation and mitigation: Transportation Research Board, National Research Council, National Academy Press

Kherif, Ferath, and Adeliya Latypova (2020). "Principal component analysis." Machine Learning. Academic Press,. 209-225.

KHERRAB. M., (2010). Mémoire de magister "Etude des structures mécaniques spatiale par la méthode des éléments finis" Constantine (2010).

Khuri, A.I. and J.A. Cornell, (1996). "Response Surfaces," 2nd edition, Marcel Dekker. New York.

Kusky, T., (2008). Landslide: Mass Wasting Soil, and Mineral hazards. Fact on File, Inc, New York,145.

Bibliography References

Lever, Jake, Martin Krzywinski, and Naomi Altman, (2017). "Points of significance: Principal component analysis."

Lindstrom, D. (2010). Schaum's Easy Outline of Statistics, Second Edition (Schaum's Easy Outlines) 2nd Edition. McGraw-Hill Education]

M. K. Dhiman, P. D. Yedurkar, and K. K. Sawant (2008), "Buccal bioadhesive delivery system of 5-fluorouracil : optimization and characterization," Drug Development and Industrial Pharmacy, vol. 34, no. 7, pp. 761–770.

M. Michaelis, C.S. Leopold, (2015). "A measurement system analysis with design of experiments: Investigation of the adhesion performance of a pressure sensitive adhesive with the probe tack test" International Journal of Pharmaceutics, 448-456

Malamud, B.D., Turcete, D.L., Guzzetti, F., & Reichenbach, P., (2004). Landslide Inventories and Their Statistical Properties. Wiley Inter science, Earth Surface Processes and Landform), 29: 687-711.

Marc-André Brideau, Nicholas J. Roberts, (2015), in Landslide Hazards, Risks and Disasters.

Martino, S.; Mazzanti, P. (2014). Integrating geomechanical surveys and remote sensing for sea cli slope stability analysis: The Mt. Pucci case study (Italy). Nat. Hazards Earth Syst. Sci., 14, 831–848.

Morgenstern, N. R. and Price, V. E. (1965). The Analysis of the Stability of general Slip Surfaces. Geotechnical, Vol. 15, No. 1 pp. 77-93.

Myers, R. H., Montgomery, D. C., & Anderson-Cook, C. M. (2016). Response surface methodology: Process and product optimization using designed experiments. John Wiley & Sons.

N. Lemonakis, A.L. Skaltsounis, A. Tsarbopoulos, E. Gikas, (2016). "Optimization of parameters affecting signal intensity in an LTQ-orbitrap in negative ion mode: a design of experiments", Talanta, **147**, 402-409.

Nayak, J., (2010). Landslide Risk Assessment Along a Major Road Corridor Based on Historical Landslide Inventory and Traffic Analysis. Thesis, International Institute for Geo Information Science and Earth Observation, Enschede, The Netherlands, 91.

Bibliography References

P. Moçotéguy, B. Ludwing, N.Y. Steiner, (2016). “Application of current steps and design of experiments methodology to the detection of water management faults in a proton exchange membrane fuel cell stack”, *Journal of Power Sources*, **303**, 126-136.

Peres-Neto, Pedro R., Donald A. Jackson, and Keith M. Somers (2005). “How Many Principal Components? Stopping Rules for Determining the Number of Non-Trivial Axes Revisited.” *British Journal of Statistical Psychology* 49: 974–97.

Plan de prévention du risque mouvements de terrain Chaville (2005) ; direction départementale de l'Équipement Hauts-de-Seine ; Atelier Urbanisme et Habitat; 13p]
Transportation research Goyallon J, Mouvement de terrain. Rapport du bureau des recherches géologiques et minières. France, 2000, 21 p

Quanhong, L., & Caili, F. (2005). Application of response surface methodology for extraction optimization of germinant pumpkin seeds protein. *Food Chemistry*, 92(4), 701–706.

RAT (M.). (1975). – Drainage. Rabattement. *Techniques de l'Ingénieur, traité Construction*, article C256.

Roth, P.L., Le, H., Oh, I.S., Van Iddekinge, C.H. and Bobko, P., (2018). Using beta coefficients to impute missing correlations in meta-analysis research: Reasons for caution. *Journal of Applied Psychology*

SCHLOSSER (F.) et UNTERREINER (Ph.), (1994). Renforcement des sols par inclusions. *Techniques de l'Ingénieur, traité Construction*, article C24.

Schmidt, Amand F., and Chris Finan (2018). "Linear regression and the normality assumption. " *Journal of clinical epidemiology* 98.

Schneider A, Hommel G, Blettner M., (2010). Linear regression analysis: Part 14 of a series on evaluation of scientific publications. *Dtsch Arztebl Int*; 107:776-82

Souk Ahras, Algeria [archive], sur www.weatherreports.com (consulté le 04 juin 2011).

Strojexport. Prospection géophysique du synclinal de Taoura-Bordj Mraou, 1977. Rapport Interne, Direction de l'Hydraulique de Souk Ahras.

Bibliography References

Thywissen, K., (2006). Components of Risk. SOURCE (Studies of the University: Research, Counsel, Education), Publication Series of UNU Institute for Environment and Human Security (UNU-EHS), Bonn, Germany,52.

University of Illinois at Urbana-Champaign, Departement of Geology.

Van westen, C. J., Alkema, D., Rusmini, M., Lubbczynska, M., Kerle, N., Deemen, M., & Woldai, T., (2009). Multi Hazard Risk Assessment, Guide Book Session 3 Hazard Assessment. International Institute for Geo Information Science and Earth Observation, Enschede, The Netherlands, 3-138.

Varnes, D.J. and IAEG, (1984). Landslide hazard zonation: a review of principles and practice. UNESCO, Darantiere, Paris, 61 pp.

Varnes, D.J., (1978). Slope movement types and processes, in Schuster, R.L., and Krizek, R.J., eds., Landslides—Analysis and control: National Research Council, Washington, D.C., Transportation Research Board, Special Report 176, p. 11–33. Turner, Keith A., and Schuster, Robert L., 1996, Landslides—Investigation and mitigation: Transportation Research Board, National Research Council, National Academy Press

Vila J M (1980). The Alpine Chain of Eastern Algeria and the Algerian-Tunisian borders. Doctorate in Science, University. P and M Curie. Paris VI. 450p.

Voicu Gh., T. Căsandroi, C. Târcolea, (2008). Testing stochastic models for simulating the seeds separation process on the sieves of a cleaning system, and a comparison with experimental data, „ACS-Agriculturae Conspectus Scientificus”, Zagreb 73(2): 95-101.

Wahono, B. F. D., (2010). Applications of Statistical and Heuristic Methods for Landslide Susceptibility Assessment (A case Study in Wadas Lintang, Wonosobo, Central Java Province, Indonesia). Thesis, International Institute for Geo Information Science and Earth Observation, Enschede, The Netherlands, 80.

Wouatong, A.S.L.; Djukem, W.D.L.; Ngague, F.; Katte, V.; Beyala, V.K.K., (2017). Influence of random inclusion of synthetic wicks fibers of hair on the behavior of clayey soils. Geotech. Geol. Eng., 35, 2637–2646.

Bibliography References

Xu, C., Pourghasemi, H. R., Jirandeh, A. G., Pradhan, B., & Gokceoglu, C. (2013). Landslide susceptibility mapping using support vector machine and GIS at the Golestan Province, Iran. *Journal of Earth System Science*, 122(2), 349-369.

Youd, T. L., Harp, E. L., Keefer, D., & Wilson, R. C. (1985). The Borah Peak, Idaho Earthquake of October 28, 1983—Liquefaction. *Earthquake spectra*, 2(1), 71-89.

Zhi-Qiang FENG, Christine RENAUD et Gregory TURBELIN (1999) : “Méthode des éléments finis”. UFR -S&T, Université d’Evry – Val d’Essonne.

Zienkiewicz, O. C., Humpheson, C. & Lewis, R. W (1975). Associated and non-associated visco-plasticity in soil mechanics. *Geotechnique*. **25**(4), 671–689 (1975).